DEPARTMENT OF CHEMISTRY IMPERIAL COLLEGE LONDON

Special Solvation Behaviour of Salts in Ionic Liquid

by

Matthew Yuk Yu Lui

Thesis submitted as partial fulfillment of the
requirements for the degree of Doctor of Philosophy
of Imperial College London

Declaration

The work described in this thesis was carried out at Imperial College London between October 2007 and December 2010. The entire body of work is my own unless expressly stated to the contrary and has not been submitted previously for a degree at this or other university.

Statement of copyright

Abstract

In a previous study[1] from the Welton Group, the reactivity resulting from mixing two different and reactive salts together was observed to be highly dependent on the type of solvent, with molecular and ionic liquids exhibiting fundamentally different reaction pathways. Ionic liquids were shown to be extremely dissociating solvents and the salts behaved as discrete reactive species. Conversely, in molecular solvents neutral ion pairs or clusters were formed.

In this thesis, further evidence of the charge screening behaviour of ionic liquids will be presented. The investigation was carried out by using Kosower's charge-transfer complex, 1-ethyl-4-(methoxycarbonyl)pyridinium iodide,[2] which is only spectroscopically active when its ions are in direct contact, hence allowing charge transfer to occur. The behaviour of this salt is therefore a good indicator of the number of pyridinium iodide contact ion pairs in solution and can be used as a probe for the amount of ion-pairing in both ionic and molecular liquids.

In the second part of the investigation, the S_N2 reaction of two reactive salts (1-butyl-1-methylpyrrolidinium bromide and dimethyl-4-nitrophenylsulfonium *bis*(trifluoromethanesulfonyl)imide) in ionic liquid/molecular liquid mixtures was studied. The aim was to examine whether complete charge screening behaviour could be achieved in ionic liquid/molecular liquid mixtures of different compositions. This research also provided some insights of general behaviour of salts in ionic liquid/molecular solvent mixtures.

Acknowledgements

I would like to show my gratitude to my supervisor Professor Tom Welton, who has been patient and supportive of me. I will always be in debt to him for the trust he granted me throughout the period spent under his supervision.

This thesis would not have been possible without the guidance of Dr. Jason Hallett and Dr. Lorna Crowhurst, who have offered me their important scientific assistance and encouragement. I would also like to thank all the members of the Welton group, past and present, who offered me their help and friendship in the last four years.

I am also grateful to Heiko Niedermeyer and Dr. Patricia Hunt for their invaluable contributions for the work of DFT calculations.

Above all I would like thank my parents for their love and understanding, and Cynthia for her encouragement and support.

Abbreviations

$[BF_4]^-$	tetrafluoroborate anion
$[C_4C_1im]^+$	1-butyl-3-methylimidazolium cation
$[C_4C_1C_1im]^+$	1-butyl-2,3-dimethylimidazolium cation
$[C_4C_1py]^+$	1-butyl-1-methypyrrolidinium cation
$[NTf_2]^-$	*bis*(trifluoromethylsulfonyl)imide anion
$[OTf]^-$	trifluoromethanesulfonate anion
$[SbF_6]^-$	hexafluoroantimonate anion
ΔE^A	activation energy
μ	dipole moment
γ^∞	infinite dilution activity coefficient
α	Kamlet-Taft's parameter for hydrogen bond donating ability
β	Kamlet-Taft's parameter for hydrogen bond accepting ability
π*	Kamlet-Taft's parameter for dipolarity/polarizability
δ_H	^{1}H chemical shift / ppm
δ_c	^{13}C chemical shift / ppm
ε_0	permittivity of free space
ε_r	dielectric constant
λ_{max}	wavelength of maximum absorption / nm
ν_{max}	frequency of maximum absorption / cm^{-1}
°C	degree Celsius
CIP	contact ion pair
cP	centipoises
DFT	density functional theory
DCM	dichloromethane
DMF	*N,N*-dimethylmethanamide
DMSO	dimethyl sulfoxide
EC_{50}	half maximal effective concentration, 50%
ESI	electrospray

$E_T(30)$	Reichardt's empirical solvent polarity scale / kcalmol^{-1}
E_T^N	normalized form of $E_T(30)$
EtOAc	ethyl acetate
F	force (Newtons)
FAB	fast-atom bombardment
g	grams
Glu	glutamate
HMPT	hexamethylphosphoric acid
J	coupling constant / Hz
K	Kelvin
k_1	first order rate constant / s^{-1}
k_2	second order rate constant / M^{-1}s^{-1}
k_{obs}	observed rate constant
LSER	linear solvation energy relationship
LSIMS	liquid secondary ion mass spectrometry
M	molar concentration
m/z	mass over charge ratio
MeCN	acetonitrile
NMR	nuclear magnetic resonance
p	para
ppm	parts per million
PTC	phase transfer catalysis
QSPR	quantitative structure-property relationship
s	singlet
S_N1	unimolecular nucleophilic substitution
S_N2	bimolecular nucleophilic substitution
SSIP	solvent-separated ion pair
t	triplet
THF	tetrahydrofuran

Thr	threonate
TMS	tetramethylsilane
UV/Vis	ultraviolet-visible
VOC	volatile organic compound
Z	Kosower's polarity parameter / $kcalmol^{-1}$

Contents

List of figures

List of tables

1 General introduction

1.1 Ionic liquids

1.1.1 General remarks

The “greening” of solvent use is one of the most important subjects in green chemistry. Many solvents are toxic and nearly all organic molecular solvents are VOCs, which are major air pollutants and can also damage soil and groundwater. However traditional organic solvents are used in very large amounts in industries, since they are almost indispensable in reactions and work-up procedures. Although these solvents are usually quite cheap to buy, the broader total costs (e.g. resource depletion) are not. During the past 20 years, scientists have attempted to limit the use of traditional organic solvents.[3] The method which stood out the most is the development of new alternative solvents that are environmentally friendly. Ionic liquids and supercritical carbon dioxide are two potential “green solvents” that have attracted most attention.[4] Supercritical carbon dioxide is “green” because it is non-toxic, on the other hand, ionic liquids have negligible vapour pressure so they do not produce air pollutants.

Of all the potential greener alternative solvents, ionic liquids seem to be the most appropriate ones for organic and inorganic synthesis. Supercritical carbon dioxide, which attracts no less attention as compared to ionic liquids, is a poor solvent for most substances.[5] Water, another “green” solvent, is reactive and also a poor solvent for many organic compounds. Conversely, ionic liquids are good solvents for both organic and inorganic materials.[6]

Ionic liquids are also attractive because of their designer solvent properties. More than a million combinations of cations and anions are potentially possible,[7] and this

diversity enables the solvent to be designed and tuned. Physical and chemical properties of ionic liquids such as viscosities, melting points, miscibilities as well as yields and selectivities of product can all be tuned simply by changing the identity of the ions.

Ionic liquids are generally defined as salts that melt below 100°C.[6] An ionic liquid is usually composed of bulky, asymmetric organic cations and weakly coordinating anions. **Figure 1** has shown some of the popular cations and anions, but in recent years some new ions for ionic liquids were synthesized (**Figure 2**).

Commonly used cations:

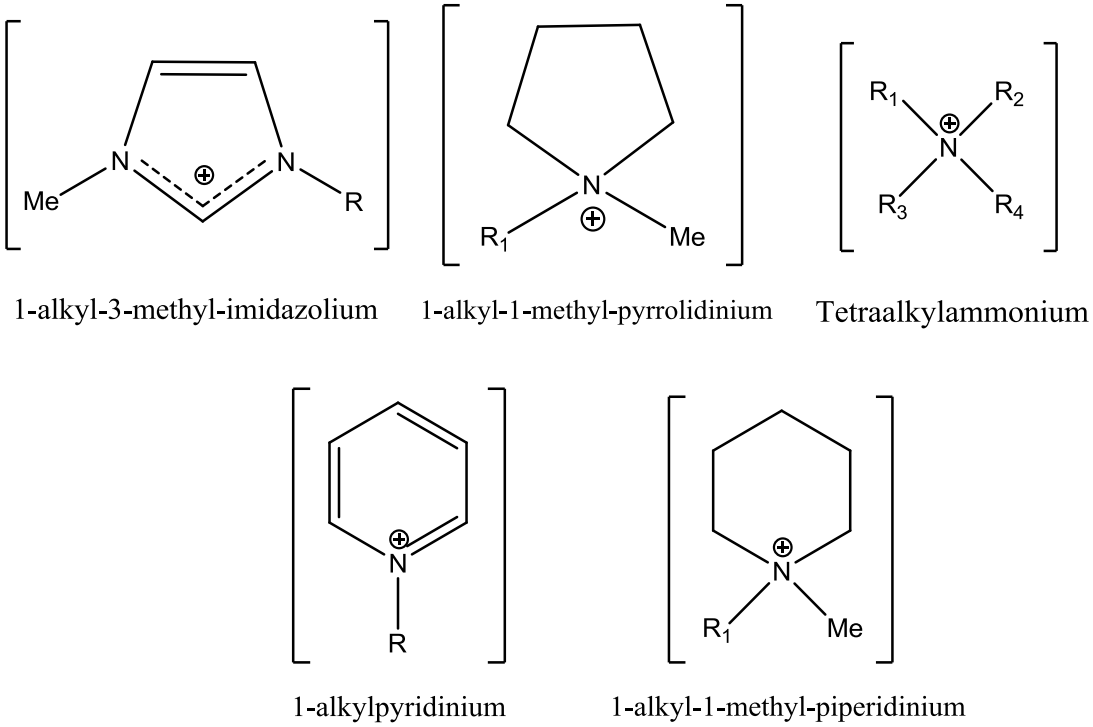

1-alkyl-3-methyl-imidazolium 1-alkyl-1-methyl-pyrrolidinium Tetraalkylammonium

1-alkylpyridinium 1-alkyl-1-methyl-piperidinium

Commonly used anions:

$[PF_6]^-$ $[BF_4]^-$ $[NTf_2]^-$ $[OTf]^-$ $[Al_2Cl_7]^-$

I^- Cl^- Br^-

$[N(Tf)_2]^- = [N(SO_2CF_3)_2]^-$

$[OTf]^- = [OSO_2CF_3]^-$

Figure 1 – Common cations and anions used in ionic liquid systems

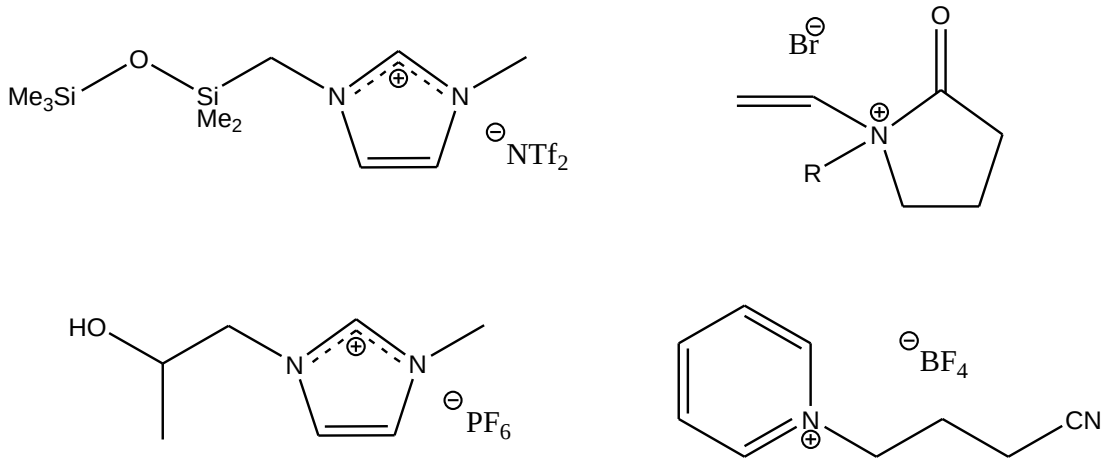

Figure 2[8-10] – Novel ionic liquids reported in the last 10 years

1.1.2 Nomenclature

Throughout this thesis a nomenclature is introduced in order to facilitate the specification of frequently used ionic liquids. The cations of the ionic liquids are enclosed by square brackets and are given first. For example 1-butyl-3-methylimidazolium *bis*(trifluoromethylsulfonyl)imide can be abbreviated as $[C_4C_1im][NTf_2]$. 'im' stands for imidazolium; another popular cation for ionic liquids, pyrrolidinium , is abbreviated as 'pyrr' throughout this report. The number subscripts after each C represents the length of the linear alkyl chain that attaches to the nitrogen atoms. For C2-substituted imidazolium cation such as 1-butyl-2,3-

dimethylimidazolium $[C_4C_1C_1im]^+$, the number subscripts after the second C represents the length of the alkyl chain at the C2 position.

1.1.3 Industrial applications

The first commercial use of ionic liquid technology was adopted by BASF in 2004 and this process is called the BASIL process.[11] BASF produces an alkoxyphenylphosphine called DEPP, by the reaction described in **Figure 3**.

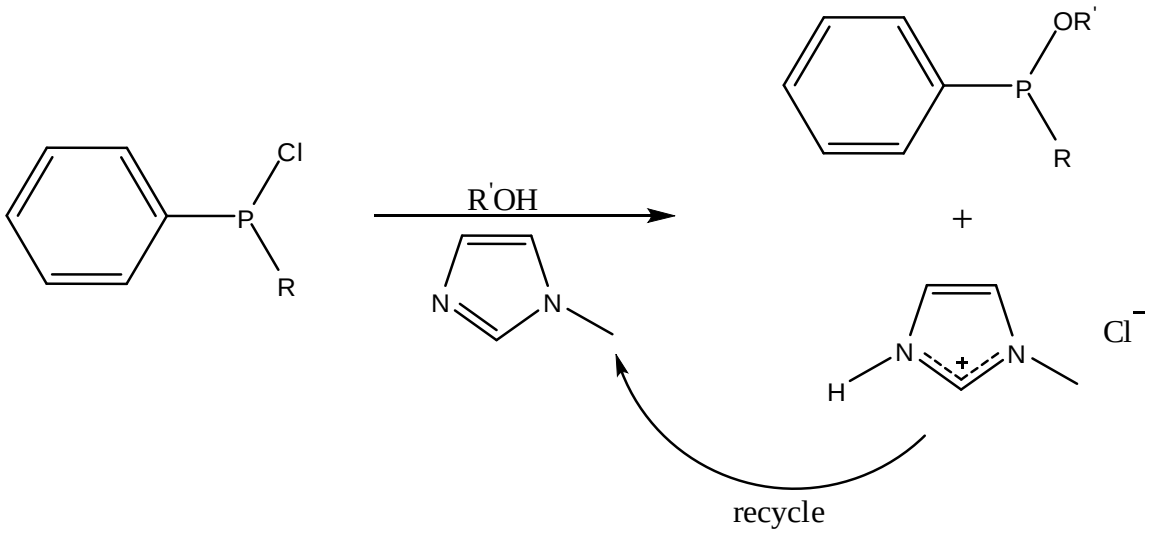

Figure 3 – The BASIL Process

A tertiary amine must be added to remove the hydrochloric acid produced by this process. 1-methylimidazole was discovered to be a good choice of amine since it reacts with HCl to form the ionic liquid $[C_1Him]Cl$, which forms a biphasic layer with the organic phase that contains the DEPP and can be removed easily compared to solid suspension. Furthermore, the 1-methylimidazole can be regenerated from the salt for recycling.

BASF has also developed another exciting application of ionic liquid that takes the $[C_1Him]Cl$ of the BASIL process to activate HCl for the following reaction that displaces hydroxyl group of 1,6-hexanediol with chloride:[12]

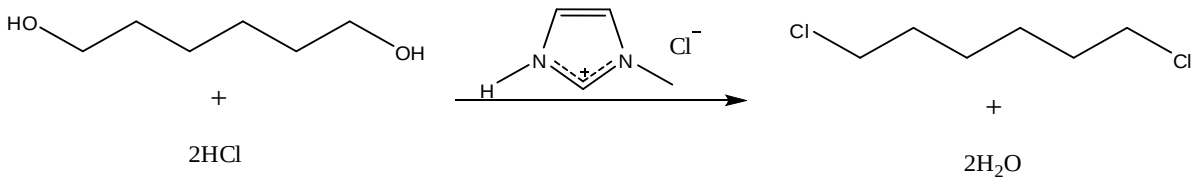

Figure 4 – The chlorination of 1,6-hexanediol

Although its exact mechanism is not yet fully understood, this reaction provides an efficient route of converting alcohols to chlorides as well as an important step for the replacements of harmful chlorinating reagents such as PCl_5, $COCl_2$ and $SOCl_2$.

Evonik Degussa is another company that develops ionic liquids on several fronts. Degussa uses ionic liquids such as $[C_4C_4C_1im][MeSO_4]$ as the immobilizers of catalysts di-µ-chloro-dichloro-(cyclohexene)diplatinum (II) (Pt-92) or hexachloroplatinic acid for hydrosilylation reactions of olefins with SiH-siloxanes.[13] The reactions are performed in a liquid-liquid biphasic system where the substrates and products are not miscible with the ionic liquid phase, which contains the catalysts. These biphasic systems minimize catalyst consumption, and clean separation of the products from the ionic solvents and catalysts can be achieved. Degussa also uses ionic liquids as additives to paints. Ionic liquids here act as secondary dispersing agents, which allow water-based pigments pastes to be used in all types of paints and coatings. This allows a reduction in the used of volatile organic solvents in paints and coatings.[13]

1.1.4 General properties of ionic liquids

1.1.4.1 Volatility of ionic liquids

Ionic liquids were originally known for their lack of vapour pressure, however in the past few years several research groups had managed to observe the evaporation of these liquids. Earle and co-workers[14] were first to distill ionic liquids under very high vacuum conditions at high temperatures (i.e. near 300 °C) and several other research groups subsequently observed similar behaviour.[14-15] In the gas phase, the ions are composed of discrete anion-cation pairs.[15]

Ionic liquids' apparent volatility does not hamper their reputations as "green solvents", since many ionic liquids show no signs of distillation below the temperature of their thermal decomposition (under atmospheric conditions) as well those of most organic processes.[15]

1.1.4.2 Flammability of ionic liquids

One of the claims for ionic liquids being "green" is that they are not flammable and easy to store. Typical organic molecular solvents, especially alkanes and alcohols, have very low flash points. Conversely, common 1,3-dialkylimidazolium and 1,2,3-trialkylimidazolium room temperature ionic liquids have very good combustion stability, as no flash points below 200 °C were detected.[16] Some of the less common functionalized ionic liquids, however, are combustible and therefore require more careful handling.[17] But overall, ionic liquids are safer than tradition solvents in terms of flammability.

1.1.4.3 Viscosity of ionic liquids

Ionic liquids are more viscous than most traditional solvents; the viscosities of ethanol, dimethyl sulfoxide and water are 1.20, 2.47 and 1.00 cP respectively (at 20 ºC) ,[18] while ionic liquids at room temperature range from around 10 cP to values in excess of 500 cP.[19] As for traditional solvents, the viscosities of ionic liquids fall as temperature increases.[19] Changing the cation and anion has strong impacts on the viscosity; generally the stronger the hydrogen bonds between the opposite ions are, the higher viscosity the ionic liquid has.[19] For example, ionic liquids of $[OTf]^-$ anion are more viscous than those of $[NTf_2]^-$, which is a weaker hydrogen bond acceptor than $[OTf]^-$. Furthermore, larger alkyl substituents on the imidazolium cation lead to more viscous ionic liquids.[19] For example, ionic liquids composed of imidazolium cations and $[NTf_2]^-$ anion exhibit an increase in viscosity from $[C_2C_1im]^+ < [C_2C_2im]^+ < [C_4C_1im]^+$.

1.1.4.4 Toxicity of ionic liquids

Although ionic liquids are widely regarded as green due to their relative involatility, the ones of $[BF_4]^-$ and $[PF_6]^-$ anions undergo very slow hydrolysis to form the toxic and corrosive HF.[20]

Ionic liquids might reduce air pollution, but they might also become pollutants of the aquatic environment due to their solubilities in water. Hence in the past five years there had been a boom in the study of ionic liquid's intrinsic toxicity. Couling and co-workers attempted to establish a quantitative structure-toxicity relationship for ionic liquids.[21] In their study, the $\log_{10} EC_{50}$ and $\log_{10} LC_{50}$ data of ionic liquids to two aquatic organisms (*Vibra fischeri* and *Daphnia magna*) were measured. According to

the results, the toxicity of ionic liquids increases with the length of alkyl chain as well as the number of nitrogen atoms in the cation ring. Conversely, the anion effect on toxicity is less important than the side chain length effect. The proposed structure effect on toxicity was later reconfirmed by another study from Matzke and co-workers.[20]

1.1.5 Thermodynamic Properties

1.1.5.1 Melting Points of Ionic Liquids

The melting point of ionic liquids is dependent on the structure and symmetry of the cations and anions. Generally, ions of greater charge delocalization can produce ionic liquids of lower melting points. The QSPR modelling approach has had some limited success in predicting the melting points of ionic liquids. Although it was concluded the deviation of calculated and predicted results was too large for accurate predictions of melting points, the QSPR approach is able to give general trends on the structural relationship of melting points. In the investigation by Eike *et al.*, it was discovered that for quaternary ammonium bromide ionic liquids asymmetry, due to one or two moderately long chains (e.g. octyl) with two or three shorter chains (*e.g.* butyl), gives lower melting points.[22] The same study also suggested branching on the longer chains leads to lower melting points.

1.1.5.2 Decomposition Points of Ionic Liquids

The upper operating limit of an ionic liquid is given by its thermal decomposition. The decomposition points for ionic liquids are difficult to predict, because thermal decomposition is a chemical rather than physical phenomenon. Quantum chemical

calculations have been used to calculate activation energies in order to predict decomposition mechanisms and rates. For ionic liquids with sufficiently nucleophilic anions, their main decomposition pathway is the S_N2 dealkylation of the cation by the anion (**Figure 5**).[23]

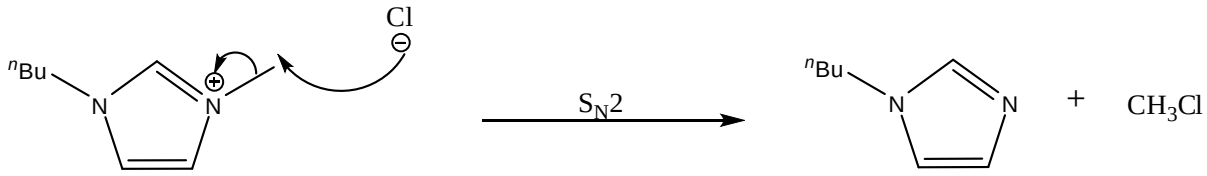

Figure 5 – Thermal decomposition of $[C_4C_1im]Cl$ into methyl chloride and 1-butylimidazole (ΔE^A = 127 kJ/mol)[23]

For ionic liquids with the $[NTf_2]^-$ anion, another decomposition pathway was observed. These ionic liquids can be decomposed *via* the elimination of SO_2 from the anion, at higher activation energy (**Figure 6**).

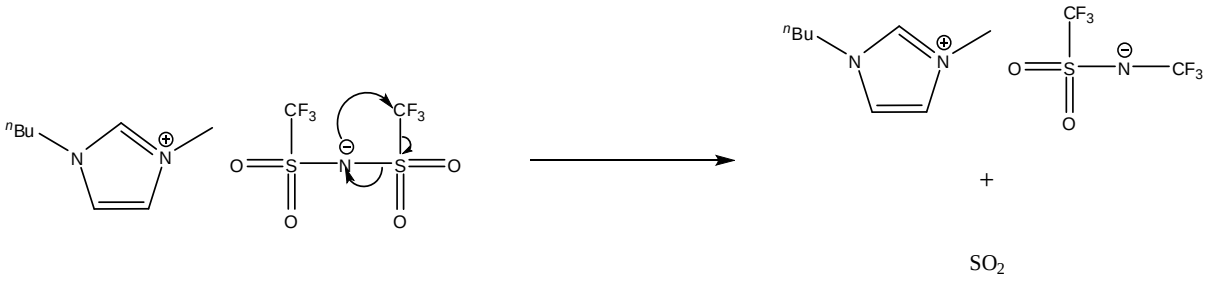

Figure 6 – Thermal decomposition of $[C_4C_1im][NTf_2]$ (ΔE^A = 255 kJ/mol)[23]

1.1.6 Miscibility with other types of liquids

Many chemical processes involving ionic liquids that were reported employ the use of molecular solvents or water as co-solvents.[24] The viscous nature of ionic liquid introduces engineering issues, such as uneven concentration and temperature distributions, as results of poor mass and energy transfer within chemical reactors.[25] This is one of the reasons why there have been much on-going research looking at

fundamental properties and reactions in ionic liquid/molecular solvent mixtures, which have lower viscosities than a pure ionic liquid. Mancini *et al.* have recently characterised the microscopic properties of some 1,3-diakylimidazolium ionic liquid/molecular solvent mixtures using Kamlet-Taft parameters, and investigated the reactivity of a nucleophilic aromatic substitution in MeCN or DMF/ionic liquid mixtures.[24] Kim *et al.* also studied the rates of a nucleophilic substitution reaction in ionic liquid/MeCN mixtures.[25]

On the other hand, ionic liquids are immiscible with “non-polar” solvents and many of them do not mix with water. The immicibility of these can be employed in biphasic catalysis applications, as described earlier. Ionic liquids that immobilize transition metal complexes provide good recycling for these catalysts.

1.1.6.1 Miscibility with water

For the common $[C_nC_1im]X$ ionic liquids, the rule of thumb is that the miscibility with water decreases as the alkyl chain length increases. This was shown in the investigation carried out by Holbrey, in which water miscibility and the hygroscopic nature of the $[C_nC_1im]BF_4$ ionic liquids decreases markedly with increasing alkyl chain length.[26] In addition, hydrogen bonding to the anion is a significant contribution to the hydrophilicity of the ionic liquid. The octanol-water partition coefficients (K_{OW}), which quantify the hydrophobicity of a compound, were measured for a number of $[C_4C_1im]^+$ ionic liquids by Ropel and co-workers.[27] The K_{OW} was found to increase in the order $[OTf]^- < [BF_4]^- < Br^- < [NO_3]^- < Cl^- < [PF_6]^- < [NTf_2]^-$.

1.1.6.2 Miscibility with organic solvents

Common ionic liquids are generally immiscible with typical “non-polar” organic solvents (i.e. $\varepsilon_r \leq 7$), but mix well with the “polar” ones (i.e. $\varepsilon_r \geq 7$). The infinite dilution activity coefficients (γ^{∞}), which measure solute-solvent interactions, were measured for a number of ionic/molecular liquid mixtures (**Table 1**).[28] $\gamma^{\infty} > 1$ indicates that solvent-solute interactions are less favourable than the solvent-solvent interactions, and the larger the value, the more unfavourable these interactions are. When γ^{∞} is greater than 10, the two liquids of concern are usually not miscible. $\gamma^{\infty} < 1$ indicates that the solvent-solute interactions are *more* favourable than the solvent-solvent interactions, and the smaller the value, the more favourable these interactions are. This situation is typical when there are very strong specific interactions present, such as hydrogen bonding (e.g. DMSO dissolved in water has a $\gamma^{\infty} = 0.09$)[29]. $\gamma^{\infty} = 1$ represents an ideal solution where solute-solvent interactions are about as favourable as solute-solvent interactions (e.g. heptanes dissolved in hexane has a $\gamma^{\infty} = 1.05$)[30].

Ionic Liquid	Co-solvent	γ^{∞}
$[C_2C_1im][NTf_2]$	Ethanol	1.525
$[C_2C_1im][NTf_2]$	1-Hexanol	5.254
$[C_2C_1im][NTf_2]$	DCM	0.891
$[C_2C_1im][NTf_2]$	Hexane	25.346
$[C_2C_1C_1im][NTf_2]$	Ethanol	2.043
$[C_2C_1C_1im][NTf_2]$	1-hexanol	5.790
$[C_2C_1C_1im][NTf_2]$	DCM	0.909
$[C_2C_1C_1im][NTf_2]$	Hexane	25.267

Table 1[28] – Experimental Activity Coefficients γ∞ at Infinite Dilution at 313 K

Generally, as shown in **Table 1**, ionic liquids are miscible with “polar” solvents such as ethanol and dichloromethane, but they are immiscible with “non-polar” liquids like hexanes. Activity coefficients for ionic/molecular liquid mixtures are only approximates of their miscibilities, as delocalized compounds such as benzene and toluene, which have small γ^{∞}, are not miscible with ionic liquids.

1.1.7 Polarity of ionic liquids

Beside physical properties such as boiling and flashing points, polarity is another important attribute that characterizes a solvent. Many researchers have looked into the polarity of ionic liquids; in recent year Weingärtner has measured the dielectric constant with dielectric spectroscopy for a number of typical ionic liquids (**Table 2**).[31-32]

Ionic Liquid	ε_r
$[C_2C_1im]OTf$	15.1
$[C_4C_1im]OTf$	13.2
$[C_2C_1im]NTf_2$	12.3
$[C_4C_1pyrr]NTf_2$	11.9
$[C_4C_1im]BF_4$	11.7
$[C_4C_1C_1im]NTf_2$	11.6
$[C_4C_1im]NTf_2$	11.6
$[C_4C_1im]PF_6$	11.4

Table 2[31-32] – Dielectric constants of ionic liquids

The dielectric constants of typical ionic liquids were measured to be around the region of 11-16, which is somewhere between the values of *n*-butanol (ε_r = 17.8) and 1,2-dichloroethane (ε_r = 10.3). One should remember that dielectric constant is a bulk physical property instead of a chemical one. Dielectic constant is inadequate to capture the complex and specific solvent-solute interactions at molecular levels. The

inability of dielectric constants to provide adequate correlations with many experimental data has led to the development of empirical solvent polarity scales.

1.1.7.1 Empirical polarity parameters

A number of empirical solvent polarity scales were developed to encompass the specific solvation interactions; the scales as such were formed by the use of solvent-sensitive reference processes such as reaction rates, equilibria or spectral absorptions. Winstein's Y-values measures solvents' polarity in terms of their influence on the rates of the ionization reaction of a number of alkyl halides.[33]

The more widely used empirical scales are based on solvatochromism. The $E_T(30)$ scale developed by Reichardt[34] is one of the most often mentioned of such scales. The $E_T(30)$ scale is based on the wavelength of the intramolecular $\pi \rightarrow \pi^*$ transition of a pyridinium-*N*-phenoxide betaine dye, better known as Reichardt's dye (**Figure 7**):

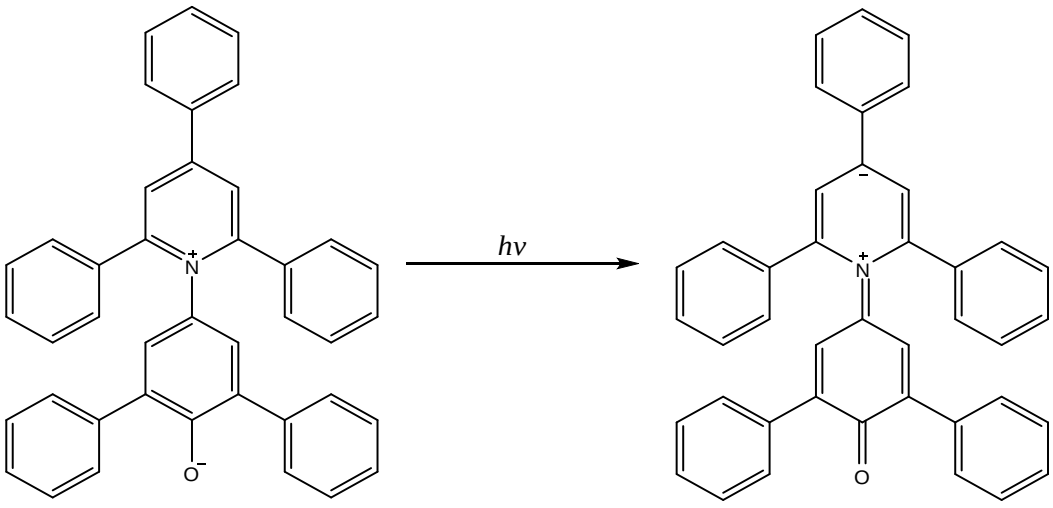

Figure 7 – Reichardt's dye and $E_T(30)$ ($E_T(30) = 28592 / \lambda_{max}$)

For convenience, the $E_T(30)$ values are usually normalized to give the E_T^N scale, which avoids the use of non-SI units and ranges from 0 (TMS) to 1 (water).

$E_T^N = (E_T \text{ (solvent)} - E_T \text{ (TMS)}) / (E_T \text{ (water)} - E_T \text{ (TMS)}) = (E_T \text{ (solvent)} - 30.7) / 32.4$

Ionic/Molecular Liquid	E_T^N
Methanol	0.762[35]
$[C_4C_1im]BF_4$	0.672
$[C_4C_1im]SbF_6$	0.670
$[C_4C_1im]OTf$	0.655
Ethanol	0.654[14]
$[C_4C_1im]NTf_2$	0.649
$[C_4C_1C_1im]NTf_2$	0.548
$[C_4C_1pyrr]NTf_2$	0.544
Acetonitrile	0.460[35]
Toluene	0.100[35]

Table 3 – E_T^N of some ionic and molecular liquids

The Reichardt's betaine dye is sensitive to both the hydrogen bond donor ability (through the negative charged oxygen) and dipolar and polarization interactions (through the positive charge on the nitrogen and the delocalization of this charge) of solvents; hence it is not suitable for observing one particular solvent-solute interactions. Ionic liquids of strong hydrogen bond acidity (i.e. those contain $[C_4C_1im]^+$ cations) usually have higher E_T^N values than those with weaker hydrogen bond donating ability i.e. those contain $[C_4C_1im]^+$ and $[C_4C_1C_1im]^+$ cations (**Table 3**). In terms of E_T^N values, ionic liquids can be considered as polar solvents; their numbers are in the range between methanol (a polar protic solvent) and acetonitrile (a polar aprotic solvent).

1.1.7.2 Kamlet-Taft Solvatochromic Polarity Parameters

The single-parameter approach of E_T^N scale cannot be considered as a universal solvent polarity scale since it responds to a combination of non-specific and specific interactions, but not them separately. On the other hand, it is not capable of interacting specifically with electron pair donor solvents. A multi-parameter approach where individual parameters evaluate different types of interactions would be a better approach. The Kamlet-Taft's solvatochromic comparison method is one such approach.[36-38] Kamlet-Taft's method measures separately the hydrogen bond donating ability of the solvent (parameter α), hydrogen bond accepting ability of the solvent (parameter β) and solvent's polarizability/dipolarity (parameter π*). The three solvatochromic parameters of solvents are determined by the energies of the longest UV/Vis wavelength absorption peaks of certain carefully selected probe solutes. The three parameters can be gathered in a multiparameter equation to form linear solvation energy relationship (LSER) which can rationalize solvent effects on many chemical and physical properties (e.g. reaction stereoselectivity[39], dipole moment[40], redox properties[41]).

$$XYZ = (XYZ)_0 + \mathbf{s}\pi^* + \mathbf{a}\alpha + \mathbf{b}\beta \qquad (\textbf{Equation 1})$$

1.1.7.2.1 Dipolarity/Polarizability – π*

A solvatochromic dye that has sufficient non-specific interactions with the solvent, but negligible hydrogen bonding is used to derive the π* scale. In the original investigation by Kamlet and Taft, seven solvatochromic probes that have strong and symmetric solvatochromic maxima in an attempt to average out any undesirable specific interactions of any one probe molecule.[38] The data used to calculate π*

scale was then expanded; in total, 47 dyes were used to give π* values to 70 solvents. While this increased amount of data used could screen out anomalies in the original set of dyes, it makes the measurement of solvent polarity impractical when new ionic liquids are made. Hence in this investigation, a single probe *N,N*-diethyl-4-nitroaniline (**Figure 8**) was used to measure π* values of ionic liquids.

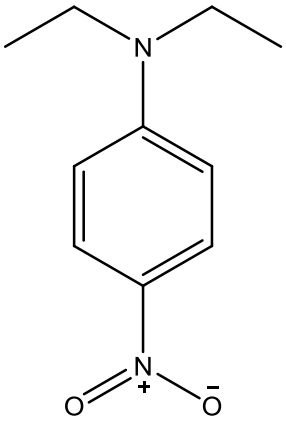

Figure 8 – *N,N*-diethyl-4-nitroaniline

The general expression to calculate the π* parameter can be obtained from **Equation 1**. In this case XYZ is the v_{max} for a particular probe in a given solvent. Assuming no hydrogen bonding interactions take place between solvent and probe (α = β = 0), the expression becomes:

$$v_{max} = v_0 + s\pi^* \qquad \textbf{(Equation 2)}$$

where *s* is a solvent independent coefficient that depends on the probe selected, v_{max} and v_0 are the longest wavelength intensity of the spectral absorption in kilokeyser units (1 kilokeyser = 10^{-3} cm^{-1}) of the solvent to study and cyclohexane respectively. The π* scale takes as solvent reference cyclohexane (π* = 0) and normalizes the scale in such a way that DMSO has a assigned π* value of 1. For *N,N*-diethyl-4-nitroaniline, the expression for π* is:

$\nu_{max} = 27.52 + 3.182\pi^*$ (**Equation 3**)

All ionic liquids that have been investigated are high in π* values (**Table 4**). The π* values result from measuring the ability of the ionic liquids to induce a dipole in the probe solute and should be expected to incorporate the effect of Coulombic interactions from the ions as well as dipole and polarizability effects.

Ionic / molecular liquid	π*
$[C_4C_1im]BF_4]$	1.05
$[C_4C_1im][SbF_6]$	1.04
$[C_4C_1C_1im][NTf_2]$	1.02
$[C_4C_1im][OTf]$	1.00
$[C_4C_1im][NTf_2]$	0.99
$[C_4C_1pyrr][NTf_2]$	0.96
MeCN	0.80[35]
Methanol	0.73[35]
Ethanol	0.54[42]
Toluene	0.53[35]

Table 4 – π* of some ionic and molecular liquids

1.1.7.2.2 Hydrogen bond basicity – β

As described above, β describes the solvent's ability to donate electron density to form a hydrogen bond with acidic hydrogen atoms. The β scale is normalized to β = 1 for hexamethylphosphoric acid triamide (HMPT) and for non-hydrogen bond acidic solvents reaches values close or equal to zero. The β values are derived by comparing the spectra of closely related pairs of probes;[36] in this investigation the pair 4-nitroaniline/*N,N*-diethyl-4-nitroaniline (**Figure 9**) was used to measure the β values of a number of ionic liquids. The shifts of the longest wavelength π to π* absorption bands of the two dyes are compared for each solvent. The two probes

employed in this investigation (4-nitroaniline and *N,N*-diethyl-4-nitroaniline) are both capable to act as hydrogen bond accepting (HBA) substrates in hydrogen bond donating (HBD) solvents, but only 4-nitroaniline can act as a HBD substrate in HBA solvents at the same time. The effect of non-specific interactions were subtracted with the use of the π* parameter i.e. *N,N*-diethyl-4-nitroaniline.

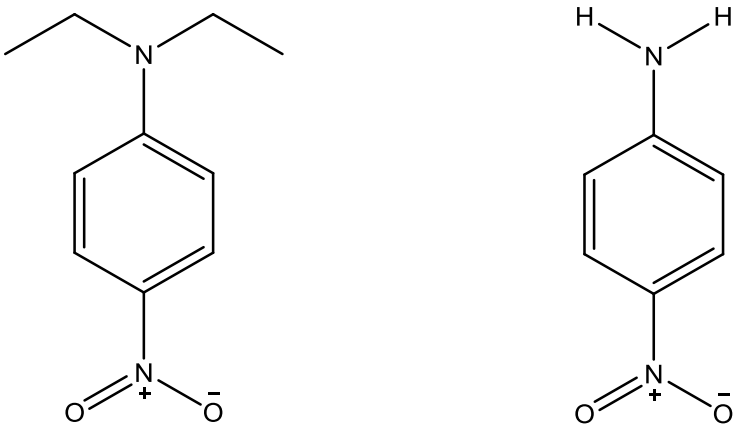

Figure 9 – *N,N*-diethyl-4-nitroaniline and 4-nitroaniline

Ionic/Molecular Liquid	β
Ethanol	0.77[42]
Methanol	0.61[35]
$[C_4C_1im][OTf]$	0.49
$[C_4C_1im][BF_4]$	0.37
MeCN	0.37[35]
$[C_4C_1pyrr][NTf_2]$	0.29
$[C_4C_1C_1im][NTf_2]$	0.26
$[C_4C_1im][NTf_2]$	0.23
$[C_4C_1im][SbF_6]$	0.15
Toluene	0.077[35]

Table 5 – β values of some ionic and molecular liquids

The normalized equation used to obtain the β value is:

$$\beta = 0.358(31.10 - \nu_{4\text{-nitroaniline}}) - 1.125\pi^* \quad \textbf{(Equation 4)}$$

Crowhurst *et al.* demonstrated that the β values of ionic liquids were largely dominated by the identity of the anion.[35] The β values of some ionic liquids and molecular solvents are shown in **Table 5**.

1.1.7.2.3 Hydrogen bond acidity – α

The α scale is normalized to α = 1 for methanol and takes values close to zero for non-hydrogen bond donor solvents. The probes used to measure α are *N,N*-diethyl-4-nitroaniline and Reichardt's betaine dye. Both probes measure the polarizability / dipolarity effects of the solvent, but Reichardt's dye is also sensitive to the hydrogen bond donor ability of solvent. The α parameter is formed by subtracting the polarizability / dipolarity effects (π*) from the Reichardt's $E_T(30)$ scale. The normalized equation to obtain α value is:

$$\alpha = 0.0649E_T(30) - 2.03 - 0.72\pi^* \quad \textbf{(Equation 5)}$$

The α values of ionic liquids are largely determined by the identity of the cation,[35] and are generally moderate (**Table 6**). Ionic liquids of $[C_4C_1im]^+$ and $[C_4C_1py]^+$ cations have higher α than aprotic molecular solvents (e.g. toluene and MeCN) and lower α than protic molecular solvents (e.g. methanol and ethanol).

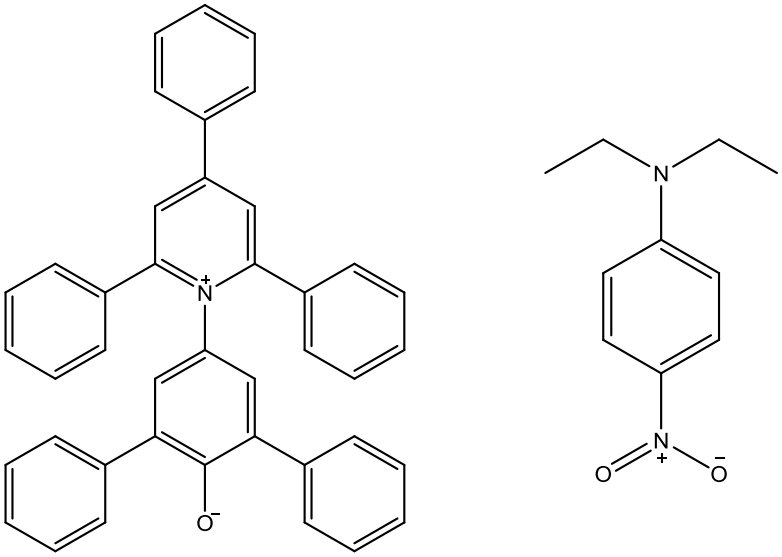

Figure 10 – Reichardt's dye and *N,N*-diethyl-4-nitroaniline

Ionic/Molecular Liquid	α
Methanol	1.05[35]
Ethanol	0.83[42]
$[C_4C_1im][SbF_6]$	0.62
$[C_4C_1im][BF_4]$	0.62
$[C_4C_1im][OTf]$	0.62
$[C_4C_1im][NTf_2]$	0.61
$[C_4C_1pyrr][NTf_2]$	0.42
$[C_4C_1C_1im][NTf_2]$	0.38
MeCN	0.35[35]
Toluene	-0.21[35]

Table 6 – α of some ionic and molecular liquids

1.2 Solvent effects on rate of reaction

Most chemical processes are carried out in solution and the choice of the solvent for a particular reaction can significantly affect both its rate and its mechanism.[42] The mode rate of reaction is affected by the solvent can be explained on the basis of the transition state theory, which assumes a quasi-equilibrium is present between the

reactant and the activated complex. In essence, the reaction rates are influenced by differential solvation of the reactant and transition state by the solvent. If the transition state is stabilized by the solvent to a greater extent than the starting material then the Gibbs energy of activation is smaller and the reaction proceeds faster (**Figure 11**). Conversely, if the transition state is stabilized by the solvent to a lesser extent than the starting material then the Gibbs energy of activation is bigger and the reaction proceeds more slowly (**Figure 11**).

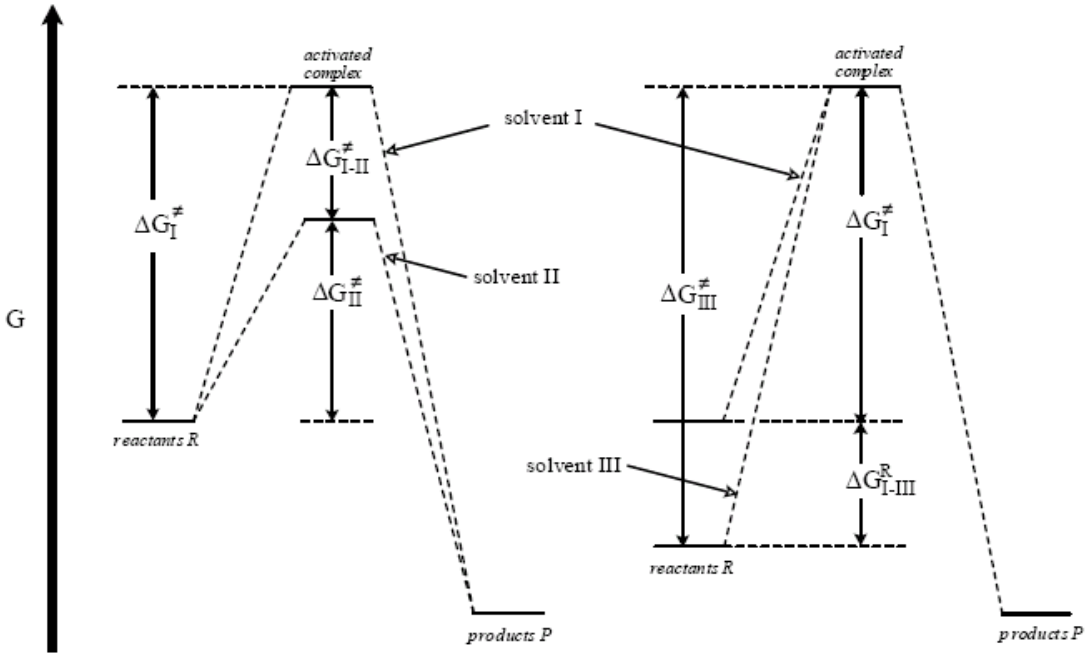

Figure 11[42] – Gibbs energy diagram for a chemical reaction in three different solvents. On the left: reaction with less stabilized (solvent I) and more stabilized (solvent II) transition state; on the right: reaction with less stabilized (solvent I) and more stabilized (solvent III) reactants.

Therefore, understanding how each species is stabilized and how the reaction rate can be manipulated by the choice of solvent is fundamental, as it can reduce time and cost especially for large scale chemical processes.

1.2.1 Solvent effects on rate of nucleophilic substitution

Nucleophilic substitution is one of the most common classes of organic chemical processes. Well-established reactions such as Kolbe nitrile synthesis[25] and organic reductions with hydrides[43] are just some of the examples of nucleophilic substitution reactions. Solvent effects on the rate of aliphatic nucleophilic substitution have been widely investigated, starting with the qualitative studies by Hughes and Ingold.[42, 44] They rationalized such solvent effects by considering the differences in electrostatic interactions between solvent and solute molecules of initial and transition states, finding the following:

a) An increase in solvent polarity results in an increase in the rates of those reactions in which the charge density is greater in the activated complex than in the initial reactant molecule(s).

b) An increase in solvent polarity results in a decrease in the rates of those reactions in which the charge density is lower in the activated complex than in the initial reactant molecule(s).

c) A change in solvent polarity will have a negligible effect on the rates of those reactions that involve little or no change in the charge density on going from reactant(s) to the activated complex.

Using these Hughes-Ingold rules, qualitative predictions about the effect of solvent polarity on the reaction rates of nucleophilic substitutions can be made (**Table 7**):

Reaction type	Reactant	Activated complex	Charge alteration during activation	Effect of increased solvent polarity on rate
(a) S_N1	R-X	$R^{\delta+}\ldots X^{\delta-}$	Separation of unlike charges	Large increase
(b) S_N1	$R\text{-}X^+$	$R^{\delta+}\ldots X^{\delta+}$	Dispersion of charge	Small decrease
(c) S_N2	Y + R-X	$Y^{\delta+}\ldots R\ldots X^{\delta-}$	Separation of unlike charges	Large increase
(d) S_N2	Y^- + R-X	$Y^{\delta-}\ldots R\ldots X^{\delta-}$	Dispersion of charge	Small decrease
(e) S_N2	$Y + R\text{-}X^+$	$Y^{\delta+}\ldots R\ldots X^{\delta+}$	Dispersion of charge	Small decrease
(f) S_N2	$Y^- + R\text{-}X^+$	$Y^{\delta-}\ldots R\ldots X^{\delta+}$	Destruction of charge	Large decrease

Table 7 – Hughes-Ingold predictions of solvent effect on the rates of nucleophilic substitutions

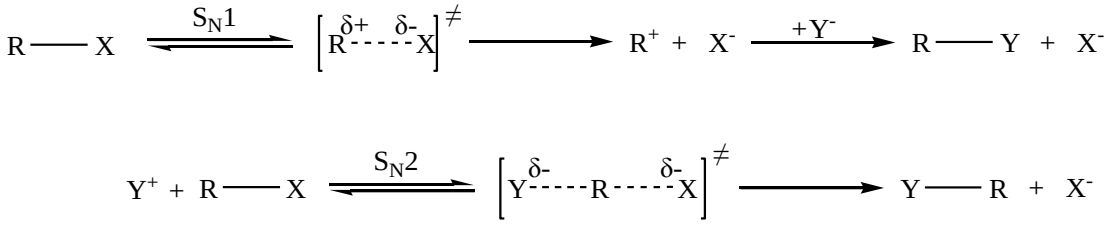

Figure 12 – Mechanisms of S_N1 and S_N2 reactions

An experimental example is the alkaline hydrolysis of the trimethylsulfonium ion, which is a type (f) reaction[45] (**Figure 13**):

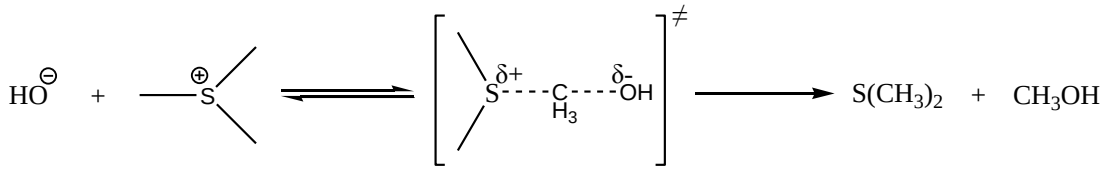

Figure 13 – Alkaline hydrolysis of trimethylsulfonium ion

The authors measured the rate of this reaction in a number of aqueous ethanoic solvent mixture. When the concentration of the less polar ethanol increases in the solvent mixture, the rate increases significantly; this is in accordance to the Hughes-Ingold rules.

1.2.1.1 Limitations of Hughes-Ingold rules

Although of great utility, Hughes-Ingold rules cannot be considered as a universal guideline for the prediction of solvent effect on the rate of nucleophilic substitution. This is because the Hughes-Ingold rules treat solvents as a dielectric continuum, characterized by, for examples, by bulk physical properties such as its dielectric constant ε_r and dipole moment μ; while in reality solvent molecules can also interact with solutes through specific interactions, such as hydrogen bonding.[42]

The compound *p*-methoxyneophyl toluenesulfonate undergoes anchimerically assisted solvolysis in the type (a) S_N1 fashion (**Figure 14**),[46] which Hughes-Ingold rules would predict an increase in rate with increasing solvent polarity. However, in spite of this, the reaction rate for this reaction in solvents of relatively high permittivity, such as MeCN (ε_r = 37.5) and DMSO (ε_r = 47.2), are slower than protic solvents of low permittivity, such as ethanol (ε_r = 24.3) and methanol (ε_r = 33.0). This result demonstrates that polarity scale based on dielectric constants is often not sufficient to rationalize the solvent effect on reaction rates, as specific interactions between solvent and solute may also be important.

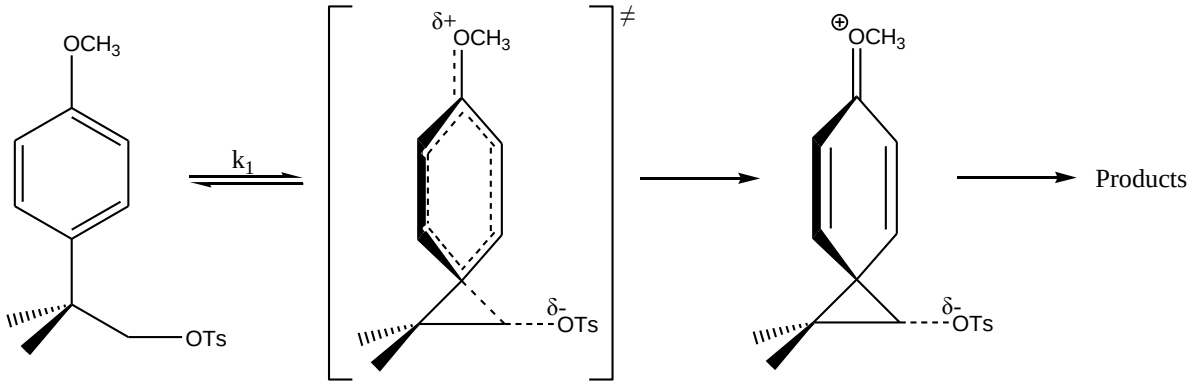

Figure 14 – Solvolysis of p-methoxyneophyl toluenesulfonate

Consideration of specific solvations (e.g. hydrogen bonding) of the starting materials and activated complexes can contribute to a better understanding of solvent effect on organic reactions.

1.2.2 Nucleophilic substitutions in ionic liquids

Ionic liquids can operate as both solvents and catalysts for nucleophilic reactions. One of the earliest advances in the field of nucleophilic substitutions in ionic liquids was reported by Wheeler *et al.*, who demonstrated that ionic liquids can be used as catalytic, environmentally benign solvents for cyanide displacement on benzyl chloride.[47] Nucleophilic substitution reactions of those using a salt reactant as a nucleophile are often carried out using phase-transfer catalysis (PTC). The phase-transfer catalyst, usually a tetraalkylammonium salt, acts as a shuttle for the reaction anion, carrying it between a polar phase (e.g. aqueous) that contains the salt reactant and a non-polar organic phase that contains the organic reactant.[48] Since ionic liquids are also comprised of bulky organic cations, they can be suitable dual action catalysts and solvents for reactions in which the PTC is effective. Wheeler and co-workers found this is the case for ionic liquid $[C_4C_1im][PF_6]$, which acted as both the transfer catalyst and solvent for the reaction between potassium cyanide and

benzyl chloride.[47] This new approach replaces the water/organic biphasic system and thus eliminating the need for a volatile organic solvent, without a large penalty in rate. This process is still considered to be biphasic since the cyanide salt is only soluble in the ionic liquid and formed a suspension.

In a separate study, Lourenço and co-workers again demonstrated that $[C_4C_1im][PF_6]$ is an efficient transfer phase catalyst and solvent for several nucleophilic substitution reactions (e.g. alkylation of Schiff bases, azide/halogen exchange), this time under aqueous/ionic liquid phase transfer conditions.[49]

Since the turn of the century there have been an abundance of publications which view ionic liquids acting solely as solvents in nucleophilic substitution reactions. Much of this work has reported exciting results, such as increases in reactivity and selectivity.[50]

Yadav *et al.* successfully devised an efficient and clean method for the synthesis of β-amino alcohols with ionic liquids $[C_4C_1im][BF_4]$ and $[C_4C_1im][PF_6]$ as the solvent.[51] In this reaction, epoxides underwent smooth ring-opening with aryl amines in ionic liquids, under mild and neutral conditions to afford the corresponding β-amino alcohols in good yields with high regioselectivity (**Figure 15**).

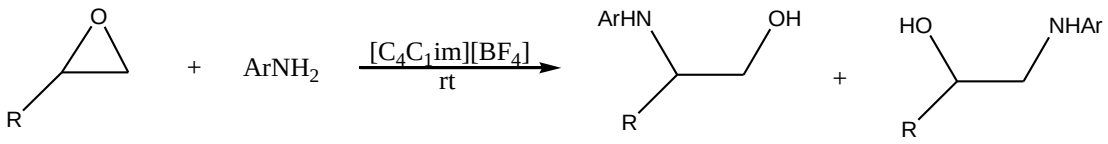

Figure 15 – Formation of β-amino alcohols in ionic liquids

Liu and co-workers then discovered that ionic liquids can be utilized to increase the nucleophilicity of potassium salts of aromatic acids toward α-aryloxy ketone synthesis (**Figure 16**).[52]

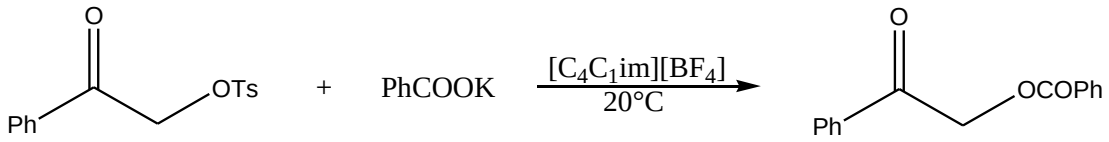

Figure 16 – Nucleophilic substitution of α-aryloxy ketone with potassium salts of aromatic acids in ionic liquids

Even at lower temperatures, the reactions in $[C_4C_1im][BF_4]$ and $[C_4C_1im][PF_6]$ were much faster than those carried out in ethanol and MeCN, and improved product yields were obtained. Separation of products from the ionic liquid was also proved to be straightforward.

Although the findings of these researchers were often exceptional, few attempted to answer fundamental questions regarding the source of the effect of ionic liquids on these nucleophilic substitutions.

Lancaster *et al.* carried out some of the earliest quantitative kinetic studies of nucleophilic substitution reactions in ionic liquids. The rates of reaction between nucleophilic halides and methyl-*p*-nitrobenzenesulfonate were first measured in $[C_4C_1im][BF_4]$ (**Figure 17**),[53] and subsequently in three other ionic liquids ($[C_4C_1im][NTf_2]$, $[C_4C_1C_1im][NTf_2]$ and $[C_4C_1py][NTf_2]$) and two molecular solvents (DCM and hexafluoropropan-2-ol).[54] In their second investigation, the authors concluded that there is no unique “ionic liquid effect” on this reaction, as in the three ionic liquids the rates for this reaction are found to be within the range observed for the same reaction in molecular solvents.[54] It was found that reaction rates were highest in DCM and lowest in the highly ionizing hexafluoropropan-2-ol. Using the Hughes-Ingold rules for the type (d) reaction in **Table 7**, the authors concluded that ionic liquids are more polar than DCM, but less polar than hexafluoropropan-2-ol.

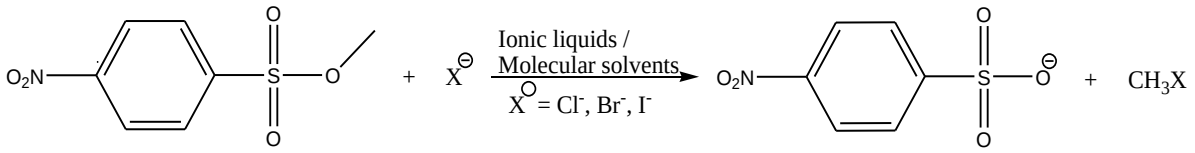

Figure 17 – Nucleophilic substitution of methyl-p-nitrobenzenesulfonate with halides

For the past ten years, the Welton group has carried out quantitative kinetic studies on many types of S_N2 reactions (types (c) to (f) as described in **Table 7**),[1, 53-58] and employed an extended approach of the Hughes-Ingold rules to analyze the kinetic data. In these investigations, it has been shown that although common ionic liquids have similar dielectric constant and π*, the rates of many reactions in these solvents are often very different. This is again because the traditional Hughes-Ingold rules assume the solvent and solute interact *via* electrostatics alone, while in reality many other supramolecular interactions exist between the two. Ionic liquids of different ions have different hydrogen-bond acceptor and donor abilities. For that reason, the Welton group incorporated Kamlet-Taft parameters (for hydrogen bond acidity and basicity) in analyzing the kinetic results. For instance, the rates of reaction between halides and methyl- *p*-nitrobenzenesulfonate were correlated with Kamlet-Taft parameters of a number of ionic and molecular liquids.[56] The Kamlet-Taft LSER approach to kinetic data demonstrate that the rates of these reactions were negatively dependent on the hydrogen bond acidity (α) of solvents. These correlations can be explained in terms of the solvent donating a hydrogen bond to the anion; hence reducing the latter's capacity to attack the electrophile methyl- *p*-nitrobenzenesulfonate.

For most S_N2 reactions, ionic liquids behaved the same as polar molecular solvents by comparing data.[53-58] The Welton group had, however, discovered that the S_N2

reaction of the trifluoromethanesulfonate and *bis*(trifluoromethanesulfonyl)imide salts of dimethyl-4-nitrophenylsulfonium ($[p\text{-}NO_2PhS(CH_3)_2]^+[X]^-$; $[X]^- = [OTf]^-, [NTf_2]^-$) with halide ion (type f)) in ionic liquids, follow a fundamentally different pathway to the same salts in molecular solvents.[1] For this reaction, no Kamlet-Taft LSER of ionic and molecular liquids could be obtained as there were no second order rate constants for molecular solvents. It was concluded that the lack of solute ion-pairing in ionic liquid was the cause of this interesting behaviour.[1] The results of this investigation arguably provided the first demonstration of a special "ionic liquid effect". Further discussions of these results will be made in **Section 4.1.6**.

1.2.3 Nucleophilic substitutions in ionic liquid/molecular solvent mixtures

Chemical reactions in mixed solvent systems are not new to synthetic chemists, as in some cases they have been shown to be beneficial in terms of improving reaction rate.[59] Mixing ionic liquids with molecular solvents may be useful for chemical and physical reasons, since the viscous nature of ionic liquid introduces engineering issues, such as uneven concentration and temperature distributions, as a result of poor mass and energy transfer within chemical reactors.[60] Mixing an ionic liquid with molecular co-solvent can dramatically lower the viscosity of the solution and improve their use in processes.[61-63]

Many reported chemical processes involving ionic liquids employed the use of molecular solvents or water as co-solvents. The Chi group was particularly interested in studying nucleophilic substitutions in ionic liquid / molecular solvent mixtures.[60, 64-65] His group demonstrated that the addition of ionic liquids to the typical reaction mixtures can have a profound effect on reaction rates. The traditional method to introduce a fluoride atom into aliphatic organic compounds is by nucleophilic

displacement of various sulfonates and halides by fluoride,[66] and alkali metal fluorides are the conventional reagents for the introduction of fluorine ions into the system.[64] However, these fluoride salts have limited solubilities and low nucleophilicities in traditional solvents. The Chi group showed that ionic liquids significantly enhance the solubility and reactivity of the metal salts in the fluorinations of compounds such as 2-(3-methanesulfonyloxypropoxy)naphthalene and 2-(3-methanesulfonyloxypropyl)naphthalene.[60, 64]

The Chi group also demonstrated that the reactivities of water and methanol as nucleophilic oxygen sources where greatly enhanced in ionic liquid, in the nucleophilic substitutions of a number of haloalkanes.[65] These displacement reactions did not proceed in pure ionic liquids, since the non-polar haloalkanes were insoluble. Hence the less polar molecular co-solvents (e.g. acetone, 1,4-dioxane) were required in these reactions.[65]

Despite all this work, quantitative kinetic studies on nucleophilic substitution reactions in ionic liquid / molecular solvent mixtures are not easy to find. One of the rare examples was carried out by Harifi-Mood and co-workers, who studied the solvent kinetic effects on the aromatic nucleophilic substitution between 2-chloro-3,5-dinitropyridine and aniline in $[C_4C_1im][BF_4]$/alcohols mixtures (**Figure 18**).[67]

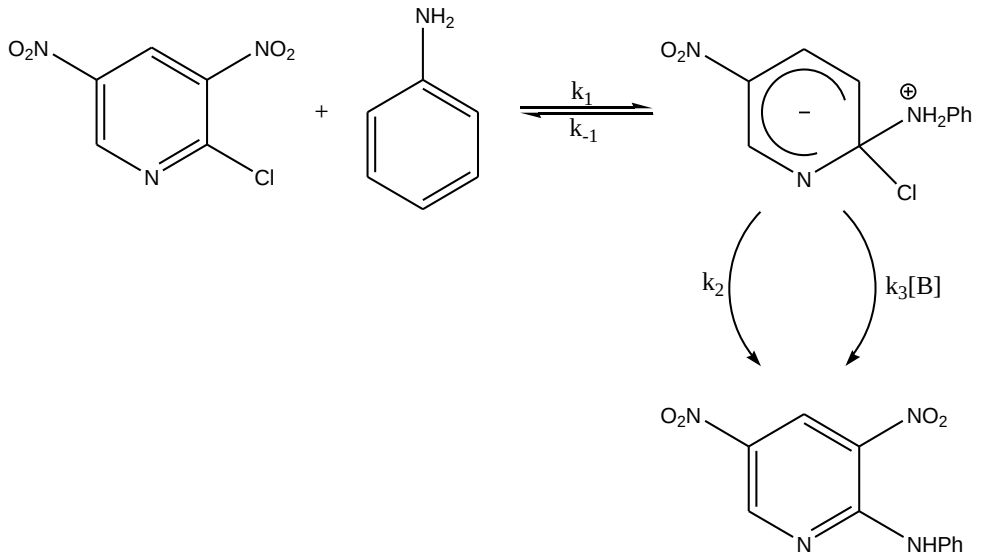

Figure 18 – Nucleophilic substitution of dinitropyridine with aniline in [C_4C_1im][BF_4]/alcohols mixtures

In this investigation, the reaction rates were found to decrease with increasing concentration of [C_4C_1im][BF_4]. The rate-step of the reaction was the formation of a zwitterionic intermediate, which is stabilized by hydrogen bonding interactions by the solvents.[67] The authors concluded that increasing amount of [C_4C_1im][BF_4] decreased α and β of the ionic liquid / alcohols mixtures, resulting in a less stabilized intermediate.[67]

In summary, the reaction rates of organic reactions are dependent upon the relative stabilization / destabilization of reactants and transition state by the solvent. The solvent effect on the rate of nucleophilic substitutions can be estimated by Hughes-Ingold rules (**Section 1.2.1**). However, Hughes-Ingold rules are not always adequate – they consider pure electrostatic interactions between ions or dipolar molecules and solvents in initial and transition states, and discount the fact specific forces such as hydrogen bonding are also involved in solvent-solute interactions. Therefore, one must consider all kinds of solvent-solute interactions in analyzing the kinetic effect on nucleophilic substitution reactions. The Welton group successfully used Kamlet-Taft

parameters, which encompassed specific (α and β) and non-specific interactions (π*), to analyze many types of nucleophilic substitution reactions in pure ionic liquids and molecular solvents.[53-58] On the other hand, quantitative study of nucleophilic substitution reactions in ionic liquid / molecular solvent mixtures is rare.

1.3 Ion pairs

An ion pair is a pair of oppositely charged ions that are held together by Coulombic interaction without formation of a covalent bond. Experimentally, ion pairs behave as one unit in determining electric conductivity, kinetic and thermodynamic properties.[42] Ion pairs have a life time of around or above 1 ns, and can be considered to be at chemical equilibrium with the free ions in solution.[68-69] The electrostatic energy to be gained by ion association will favour enormously the ion pair over free ions in the gas phase, but to a lesser extent in solution as solvation is competitive with ion pair formation.

It was difficult for scientists to come up with a universal quantitative definition of an ion pair because one needs to impose an arbitrary upper limit for the distance of separation to be permitted. Bjerrum was the first person who defined what an ion pair is.[70] The electrostatic work required to separate the two ions (i and j) with charges z_i and z_j is $W_{ij}(r) = -z_i z_j e^2/\varepsilon_r r$, where e is the unit charge, ε_r is the dielectric costant of medium and r is the distance between the two ions.[68] Bjerrum then calculated the probability of ion i to be at distance r from the ion j. For ions of opposite charges, the probability would have a minimum at a certain distance (**Equation 6**):

$$q = z_i z_j e^2/\varepsilon_r k_B T \qquad \textbf{(Equation 6)}$$

where k_B is the Boltzmann constant and T is the temperature in Kelvin. The “Bjerrum ion pairs” was defined as opposite charged ions with their centres closer together than a distance *q*.

The ion pair concept then further developed and different types of ion pair were revealed. First, contact ion pairs are formed when no solvent molecules intervene between the two oppositely charged ions that are in closes contact. The contact ion pair has only one common primary solvation shell.[42] Second, solvent-shared ion pairs are formed when the two oppositely charged ions are separated by the thickness of only one solvent molecule.[42] In solvent-separated ion pairs, the two ions have their own primary solvation shells which however interpenetrate each other. On the other hand, the primary solvation shells of both ions can be in contact, so that there is some overlap of secondary and further solvation shell takes place. When this occurs solvent-separated ion pairs are formed.[71] However, a clear experimental distinction between solvent-separated and solvent-shared ion pairs is not easily obtainable. Therefore, the designations solvent-separated and solvent-shared ion pairs are interchangeable.[42]

Grunwald was the first to visualize the existence of two distinct ion pair species in solutions (contact ion pair and solvent-separated ion pair).[72] Winstein and Robinson then used this concept to account for their results in the solvolysis of some arene sulfonates.[73] But it was Hogen-Esch and Smid who provided the first convincing evidence for the existence of contact and solvent-separated ion pairs.[74-75] They measured the absorption spectra of sodium fluorenide salt in THF at different temperatures (i.e. 25 °C and below -50 °C). A sharp absorption peak at 355 nm was observed at room temperature; but on cooling, a new peak developed at 373 nm while the peak at 355 nm decreased. Eventually only the peak at 373 nm remained

below -50 °C.[74-75] The reversibility of this process and the existence of two separate bands indicate the presence of a new entity at low temperatures in equilibrium with that existing at room temperature. The bathochromic shift was caused by the lost of influence of the sodium cation on the π-electron system of the carbanion, due to penetration of THF molecules between the ion pair couples. However, conductivity studies indicated only a few percent of free ions were present under the conditions of electronic spectroscopy experiments.[74] The authors therefore suggested the entity formed at low temperatures was a solvent-separated ion pair, which was spectroscopically indistinguishable with free ions.

In molecular solvents, ionic compounds can exist as ion aggregates, contact ion pairs, solvent-separated ion pairs, solvent-shared ion pairs or solvated free ions, but in each case the cation and anion require each other's proximity in order to preserve charge neutrality.

1.3.1 Experimental evidence of ion pairs

The traditional technique of measuring amount of ion pairs in solution is conductivity measurement. In a solution containing ions, a fraction of ions associated to form neutral ion pairs or aggregates. These neutral entities do not take part in conduction, hence the measured conductivity would decrease with increasing amount of ion pairs in solution. The classic study was carried out by Fuoss and Krauss, who studied the electrical conductivities of tetra-iso-amylammonium nitrate in some dioxane and water mixtures.[76] Using mathematical models linking the ion dissociation constant and conductance, they demonstrated that the ion dissociation increased with increasing water concentration in the binary solvent mixtures.

Spectroscopic measurement is also popular in determining whether ion is associated or dissociated in solution. Apart from UV/Vis spectroscopy that was mentioned previously (**Section 1.3**), infrared and Ramen spectroscopy have both been employed extensively. The vibration frequency of ion is shifted when the ion is solvated by solvent molecules; this proves the ion is dissociated from its opposite ion. Conversely, when the peak for an ion in solution is the same as the one in the solid state, the ion is likely to be paired with another ion(s). The intensity of the bands also indicates the amount of each entity in the solution. As well as using conductivity method, Guha and workers employed IR spectroscopy in measuring ion association of thiocyanate and nitrate salts in 2-methoxyethanol.[77] They demonstrated in $NaNO_3$ and NH_4NO_3 solutions the concentrations of contact ion pairs were negligibly small and that a preponderant proportion of ion pairs were a solvent-separated form.

High resolution ESR spectroscopy is also useful in proofing the presence of ion pairs in solution. Atherton and Weissman demonstrated pairing of sodium and naphthalenide ion would cause additional hyperfine splitting in the ESR spectrum, due to the coupling between the radical napthanlenide ion's electrons and the nucleus of sodium ion.[78] Subsequent ESR studies of Hirota revealed the presence of more than two types of ion pairs in this system, by interpreting the temperature dependence of the alkali metal splittings and the line widths of the hyperfine splittings.[79] The studies also determined the association constants of the ion-pairing processes.

1.4 Preferential solvation of ions

In this investigation, the kinetics of a S_N2 reaction was studied in some binary solvent mixtures. From studies of the solvation of ions in binary mixtures it was found that the ratio of the solvent components in the solvation shell may be different from that in the bulk solution.[80-82] The observation that the solvation shell has a composition other than macroscopic ratio it termed preferential solvation. A solute always surrounds itself preferably by the component of solvent mixture that leads to the more negative Gibbs energy of solvation. Preferential solvation leads to large deviation from the ideal behaviour, where each solvent component in the binary mixtures has the equal physical and chemical effects on the solute. In general, the composition that the solute “sees” is different from the bulk composition of the mixed solvents, in other words a solute is more or less preferentially solvated in most binary solution.[80] Preferential solvation studies can be carried out with thermodynamic, spectroscopic and kinetic techniques.[80]

Preferential solvation of ions in mixed solvents have been observed in many studies.[83] However, experimental results reported on preferential solvation of ions in non-aqueous liquid mixtures are rather limited.[83] This is partly because many of the ions under investigation are common electrolytes (i.e. metal salts) which are hardly soluble in organic solvents.

In the early 1990s, Bagchi *et al.* began studying the preferential solvation of some pyridinium iodides, which are soluble in “non-polar” solvents like THF, in mixed solvents using UV/Vis spectroscopy.[84-87] These pyridinium iodides exhibited solvatochromic behaviour, and the positions of the UV/Vis absorption band was followed to measure the extent of preferential solvation of pyridinium iodides in

different binary solvent mixtures (e.g. ethanol and acetone). Bagchi concluded that size effect of solvents and solvent-solvent interactions paid an important role in preferential solvation.[85, 87]

Ghoneim investigated the preferential solvation behaviour of several zwitterionic betaine dyes in a number of mixed binary solvents.[88] He demonstrated that protic solvent (methanol) replaced preferentially the aprotic solvent (DCM) molecules in the solvation shell of the dyes. This behaviour was observed because protic solvents could form favourable hydrogen bonds to phenolate oxygen atom of the betaine dyes. Groneim therefore concluded that preferential solvation of these zwitterions is largely dependent upon hydrogen bond formation.[88]

Brennecke carried out Reichardt's dye measurements in some ionic liquid/organic solvent mixtures.[89] It was found that small amount of ionic liquids were enough to induce very large shifts of the absorption bands for ionic liquid/aprotic molecular solvent mixtures, indicating that ionic liquids preferentially solvated the betaine dye in these solutions. Conversely, the dye was preferentially solvated by the very protic 2,2,2-trifluoroethanol in $[C_6C_1im][NTf_2]$/ 2,2,2-trifluoroethanol mixtures,[89] indicated again that the specific hydrogen bonding interaction between the negative charged phenolate and alcohol can cause preferential solvation by the latter.

Beside UV/Vis spectroscopy, another useful technique to probe preferential solvation of ions in binary solvent mixtures is NMR spectroscopy.[42] This is to measure chemical shift of metal ions in the solvent mixtures.[42, 90] Measurements are based on the assumption that the chemical shift of the solute ion is determined in an additive fashion by the solvent molecules comprising the solvation shell.

There were numerous studies on the preferential solvation of halide ions in binary solvent, mostly organic/aqueous mixtures. The more extreme example of these was the theoretical study by Krienke and co-workers, who investigated the solvation behaviour of sodium and chloride ions in mixtures of water and 1,4-dioxane, each of which have very different polarity.[91] This investigation demonstrated that only water appeared in the solvation shell of the chloride ion, therefore exhibited selective solvation behaviour (i.e. complete preferential solvation).

An example of showing how preferential solvation effect chemical kinetics in mixed solvents can be found in the study carried out by Humeres and co-workers, who studied the S_N2 reaction of sodium 4-nitrophenoxide and iodomethane in acetone/water mixtures.[92] The reaction was fastest in pure acetone, but the addition of water to the solution caused the reaction to slow down considerably. The authors concluded that the heavy slowing of reaction was due to the preferential solvation of the phenoxide ion by the hydrogen bond donating solvent i.e. water.[92]

Overall, the normally “polar” ions are usually preferentially solvated by the more polar solvent in binary mixtures.[91] But once again one must notes that “polarity” includes non-specific and specific interactions, and the latter play an important role in determining the extents of preferential solvation. For instance, anions form energetically favourable hydrogen bond with protic solvents,[93-94] hence is preferentially solvated by the latter in protic/aprotic polar solvent mixtures.[89, 93] Polarity of solvent is not the only factor determining the extent of preferential solvation of ions, however, as other factors like solvent size are also important. [85, 87, 95]

1.5 Aim of the project

The objective of this project was to see whether ion pairs exist in ionic liquids and binary ionic liquid/molecular solvent mixtures.

Building on from the study of Ranieri,[1, 137] the ion association/dissociation behaviour of solute ions in pure ionic liquids and molecular solvents was investigated through the study of the UV/Vis spectra of Kosower's charge-transfer complex, 1-ethyl-4-(methoxycarbonyl)pyridinium iodide, in a range of ionic and organic molecular liquids.

To understand the ion pairing behaviour of solute ions in binary ionic liquid/molecular solvent mixtures, the chemical kinetics of a S_N2 reaction of two salts (1-butyl-1-methylpyrrolidinium bromide and dimethyl-4-nitrophenylsulfonium *bis*(trifluoromethanesulfonyl)imide) were studied in some binary ionic liquid/molecular liquid mixtures.

2 Preparation and purification ionic liquids and organic salts

2.1 Typical synthesis of ionic liquids – metathesis

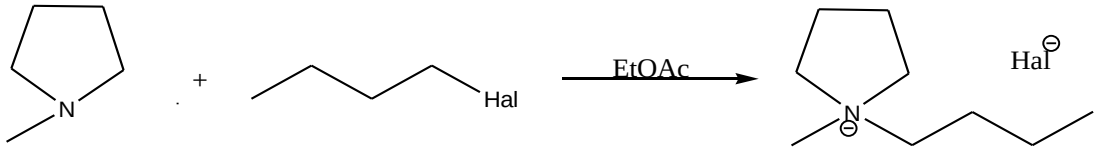

Figure 19 – Formation of ammonium halide precursor

Typically, the first step of synthesis of ionic liquids involves the quarternization of a trialkyl amine with alkyl halide to form an ammonium halide precursor (**Figure 19**). The reactants and solvents were distilled from suitable drying agents before use, as the products are extremely hygroscopic. The reaction itself is an exothermic reaction, and it may cause overheating of the reaction solution; this in turn leads to colorization of the ionic liquid. These reactions are carried out in weakly polar solvents, such as ethyl acetate and toluene; although an example by Schleicher and Scurto demonstrated that the reaction to form $[C_6C_1im]Br$ is fastest in aprotic polar solvents (e.g. DMSO and MeCN).[96] The white solid product is purified by washing with dry ethyl acetate or recrystallizing from acetonitrile/ethyl acetate mixtures under inert atmosphere. The formation of the bromide and iodide salts are generally faster than that of the chloride salts, due to the weaker C-Br and C-I bonds. Chloride salts are however easier to purify as they are more amorphous, making trapped starting materials are more difficult to remove. Iodide salts are also readily colorized due to the oxidation of iodide ion to form iodine.

Solvent-free conditions for the quarternization reaction had been investigated by other researchers. Namboodiri and Varma reported the uses of microwave heating in the reaction.[97] This method avoided the use of solvents and allowed reactions to be

conducted very quickly, but its reaction conditions are difficult to control; “hot spots” are easily generated, leading to variable quality of products.[50] Namboodiri and Varma also reported the uses of ultrasound at this stage of the synthesis.[98] The use of ultrasound allowed excellent yield being reached more quickly and at lower temperatures than with conventional heating and stirring.[98] The purity of products prepared *via* sonication was also found to be greater than before. This method seems attractive but it is not well developed yet, as a result the conventional method with the use of solvents was employed in this investigation.

The second step was an anion exchange reaction of the precursor with alkali salts such as lithium *bis*(trifluoromethansulfonyl)imide where the formation of the lithium halide by-product is the driving force of the reaction (**Figure 20**).

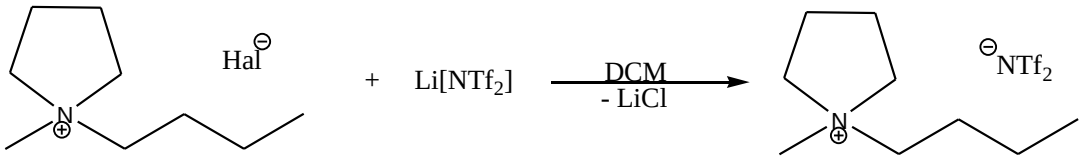

Figure 20 – Anion exchange reaction of the halide precursor with Li[NTf_2]

The alkali halide salts have low solubility in DCM, whilst the product salt and starting materials are, so the ionic liquid is easily filtered. To increase overall yield, the alkali salts are further washed with DCM. Halide impurities remaining in the combined organic solution are removed by extraction with distilled water. To determine if the ionic liquid is halide free, the aqueous washings are tested using aqueous silver nitrate. If halide is present, it combines with an Ag(I) ion to form silver(I) halide which precipitates out of the aqueous solution due to its extremely low solubility in water.[99] The ionic liquid/DCM solution is washed a further times more after a negative silver nitrate test is obtained.

Ionic liquids of weakly basic anions, such as $[NTf_2]^-$, $[PF_6]^-$ and $[SbF_6]^-$, are generally insoluble in water and so the halide impurities can be removed relatively easily. Conversely, ionic liquids of $[BF_4]^-$ and $[OTf]^-$ are soluble in water, hence the washing becomes more tricky for these liquids: The $[BF_4]^-$ and $[OTf]^-$ ionic liquids are dissolved in plenty of DCM (e.g. 800 mL for 50 mL of ionic liquid) and are extracted with only a small amount of water each time (e.g. ~1 mL). It may take more than 50 washings to make the ionic liquid completely halide free.

The typical two-step synthesis of quarter-ammonium ionic liquids is not perfect. It involves heavy use of DCM, which is a harmful, volatile liquid. Secondly, halide contaminants are reactive and corrosive to reactors. New work has been conducted to look at potential methods to make ionic liquids more efficiently and cleanly.

2.2 Other synthetic methods

Another method to synthesize ionic liquids is by direct combination of tertiary amines with alkylating agents, such as alkyl triflate and alkyl sulphate (**Figure 21**).[100] The procedure for these routes are much shorter than for metathesis. However, great care is needed when using these direct alkylation routes, since the reactions are highly exothermic; overheating of the reaction mixture can cause the formation of coloured or otherwise impure ionic liquids. Furthermore, a lot of these alkylating agents are water sensitive and can be hydrolyzed to form acids which are then difficult to remove from ionic liquids.

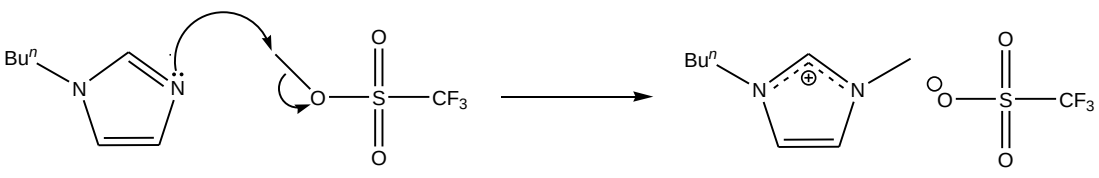

Figure 21 – Direct combination of a tertiary amine with an alkylating agent

The preparation of ionic liquids *via* simple, novel processes that result in formation of the desired salts and easily separated by-products (e.g. water) has been investigated by several researchers. Ohno and co-workers reported the synthesis of ionic liquids by neutralizing hydroxide precursors (e.g. $[C_2C_1im]OH$ and $[(C_4)_4P]OH$) with appropriate Brønsted acids.[101-103] In this synthesis a halide precursor, such as $[C_2C_1im]Br$, was prepared by the typical quarternization of an amine/phosphine with a haloalkane. An aqueous solution of the halide precursor was then passed down a column of AMBERLITE IRA400OH resin to generate a dilute aqueous hydroxide solution (e.g. $[C_2C_1im]OH$), which was neutralized with an aqueous solution of the Brønsted acid (**Figure 22**).[101] Using this method, the Ohno group synthesized ionic liquids from a series of amino acids (e.g. $[C_2C_1im][Glu]$ and $[C_2C_1im][Thr]$),[101] and those based on azole type ions (**Figure 22**).[103]

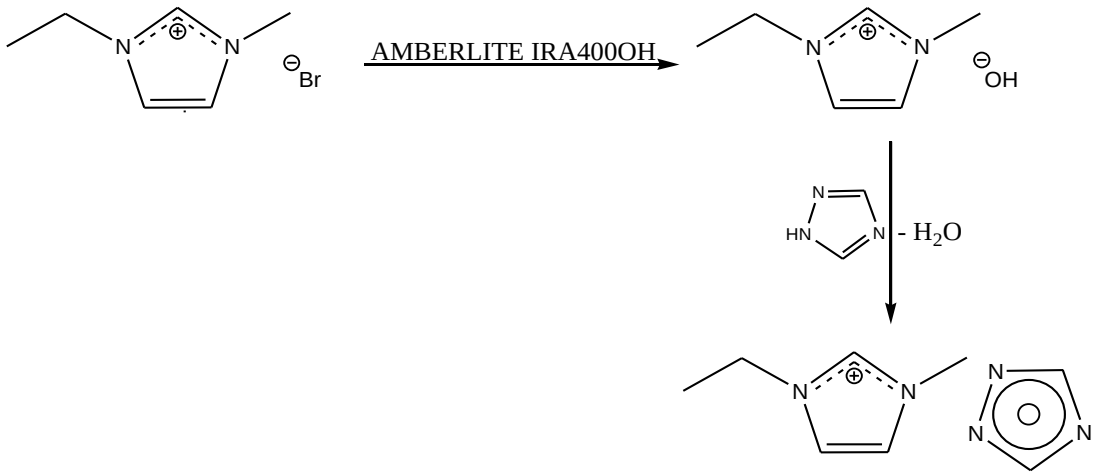

Figure 22 – Ohno's method to synthesize a triazole ionic liquid

Rogers *et al*. reported the synthesis of two hydrogen carbonate ionic liquid precursors, 1,2,3-trimethylimidazolium and *N*,*N*-dimethylpyrrolidinium hydrogen carbonate salts (**Figure 23**).[104] These salts can be converted to ionic liquids by a

simple, acid–base reaction of virtually any acid (inorganic, organic carboxylic, and organic noncarboxylic) with a pK_a less than that of $[HCO_3]^-$.[105-106] The by-products of the second step are water and carbon dioxide, both of which are harmless and straightforward to remove. In the route to make imidazolium hydrogen carbonates, a side reaction usually occurs to form the zwitterionic carboxylate precursors, such as 1,2,3-trimethylimidazolium-4-carboxylate (**Figure 23**). The addition of a strongly polar aprotic solvent (e.g. DMSO), in the presence of water and carbon dioxide, can lead to the decarboxylation of these zwitterions to form the desired hydrogen carbonate precursors (**Figure 23**).[104-107] Ionic liquid synthesis based on the $[HCO_3]^-$ salts is efficient, halide free and environmentally benign. Although this method is promising, it needs further development in order to be broadly applicable (optimization of reaction conditions). Disadvantages of this route include; harsh reaction conditions (very high pressure and temperature)[108] and the use of Brønsted acids, which are difficult to remove from ionic liquids.

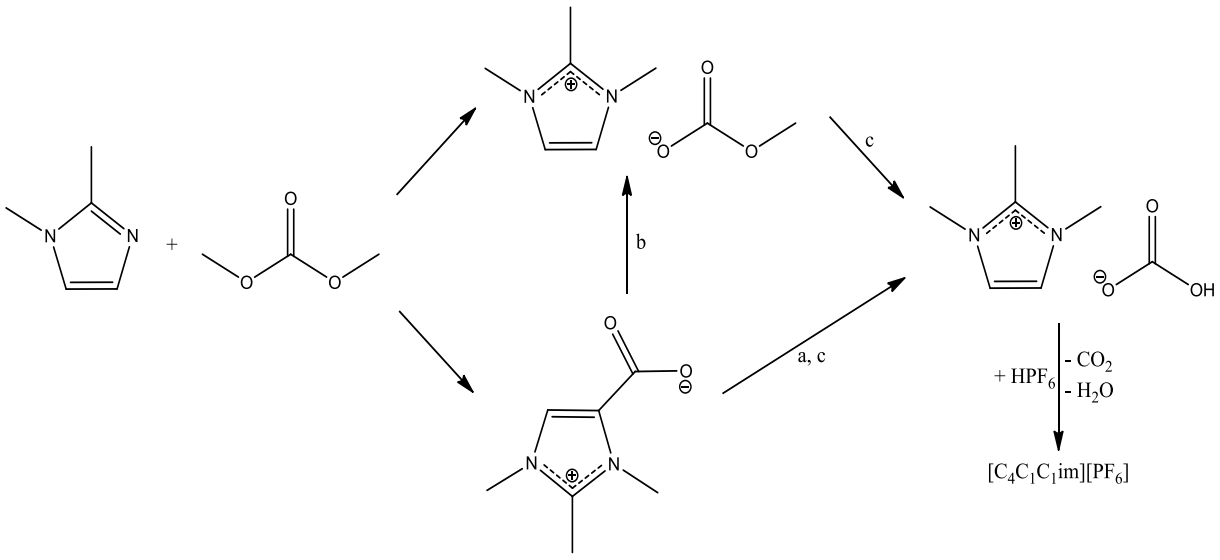

Figure 23 – Rogers's method to synthesize ionic liquids, *via* hydrogen carbonate precursors

Overall, although some of these novel synthesis methods appeared to be attractive, namely for the reasons that they are easier to carry out and their by-products are easier to remove, the typical synthesis method of metathesis was still preferred in this investigation. It is simply more difficult to make sure ionic liquids produced from the new methods are pure.

2.3 Decolorization of ionic liquids

Often, the ionic liquids produced by these routes are coloured by synthetic impurities, although the identity of the impurity/impurities is not completely known. Suggestions for the colourant include unreacted starting materials,[50] and side products caused by excessive heating in the alkylation reactions when the halide precursors are made.[109-110] Although the coloured impurities are at a very low concentrations in ionic liquids (probably in the region of parts per billion) [110], they have very high molar extinction coefficients.[110] The ionic liquids must be decolorized before experiments involving electronic visible region absorption spectroscopy. Commonly this is achieved by the use of sorbents. A small amount of activated charcoal is stirred with the coloured ionic liquid overnight, after which the charcoal has absorbed most of the colourant. The mixture is then passed through a column containing alumina or silica, both of which trap charcoal particles and remove any remaining imidazole or other amine precursors.[110]

Unsurprisingly, the simplest method to determine optical purity of ionic liquids is *via* UV/Vis spectroscopy. Spectra should be obtained using a neat sample of ionic liquid before the main experiments, with optically pure samples having if no absorbance above 300 nm.

2.4 Experimental

2.4.1 Instrumental

^{1}H-NMR and ^{13}C-NMR were recorded on a JEOL 400 MHz spectrometer. Chemical shifts are reported in ppm (versus tetramethylsilane) and coupling constants in Hz.

ESI and FAB mass spectra were recorded on a VG AutoSpec-Q mass spectrometer.

All UV/Vis spectra were recorded using a double beam Perkin-Elmer LAMBDA 650 UV/Vis spectrometer. All spectra were obtained at 25 °C using quartz cuvettes of 1, 5, and 10 mm pathlength.

2.4.2 Chemicals and reagents

All organic starting materials were purchased from Sigma Aldrich. Sodium tetrafluoroborate and sodium hexafluoroantimonate were also purchased from Sigma Aldrich. Lithium *bis*(trifluoromethylsulfonyl)imide and lithium trifluoromethanesulfonate were purchased from Apollo Scientific.

All solvents were purified from standard drying agents. 1-methylimidazole, 1-methylpyrrolidine and methyl isonicotinate were distilled from potassium hydroxide before use. 1-chlorobutane, 1-bromobutane, 1-iodobutane, bromoethane and iodoethane were all distilled from phosphorus pentoxide before use.

2.4.3 Synthesis of 1-butyl-1-methylpyrrolidium chloride, [C_4C_1pyrr]Cl

In a two-necked round-bottom flask, 1-chlorobutane (221 mL, 2.05 mol, 1.07 eqv.) was added to slowly, to 1-methylpyrrolidine (220 mL, 1.92 mol) in ethyl acetate (200 mL). The mixture was then stirred for 96 hours at 45 °C and white crystals of

[C_4C_1pyrr]Cl precipitated. The colourless solution was removed by cannula filtration and the crystals were washed with ethyl acetate (3 × 50 mL). Afterwards, the crystals were recrystallized from EtOAc/MeCN mixture and dried in *vacuo* to yield pure [C_4C_1pyrr]Cl.

δ_H (400 MHz, DMSO-d^6)/ppm 3.49 (4H, m, N(C$\underline{H}_2$)$_2$), 3.39 (2H, m, NC$\underline{H}_2$(CH$_2$)$_2$CH$_3$), 3.02 (3H, s, NC$\underline{H}_3$), 2.06 (4H, s, NCH$_2$(C$\underline{H}_2$)$_2$), 1.66 (2H, quintet, $^3J_{H\text{-}H}$=7.2 Hz, NCH$_2$C$\underline{H}_2$CH$_2$CH$_3$), 1.29 (2H, sextet, $^3J_{H\text{-}H}$=7.0 Hz, N(CH$_2$)$_2$C$\underline{H}_2$CH$_3$), 0.91 (3H, t, $^3J_{H\text{-}H}$=7.0 Hz, N(CH$_2$)$_3$C$\underline{H}_3$).

δ_C (400 MHz, DMSO-d^6)/ppm 62.8 (2C, s, N($\underline{C}$H$_2$)$_2$), 62.1 (2C, s, N(CH$_2$)$_2$($\underline{C}$H$_2$)$_2$), 47.0 (1C, s, N$\underline{C}$H$_3$), 24.9 (1C, s, N$\underline{C}$H$_2$(CH$_2$)$_2$CH$_3$), 20.8 (1C, s, NCH$_2$$\underline{C}H_2CH_2CH_3$), 19.2 (1C, s, N(CH$_2$)$_2$$\underline{C}H_2CH_3$), 13.4 (1C, s, N(CH$_2$)$_3$$\underline{C}H_3$).

m/z (ESI$^+$) 319 ([(C_4C_1pyrr)$_2$Cl]$^+$, 17%), 142 ([C_4C_1pyrr]$^+$, 100%); m/z (ESI$^-$) 212 ([(C_4C_1py)Cl$_2$]$^-$, 100%), 35 (Cl$^-$, 52%).

2.4.4 Synthesis of 1-butyl-1-methylpyrrolidium bromide, [C_4C_1pyrr]Br

The same procedure was used as indicated for [C_4C_1pyrr]Cl with the exception that the use of 1-bromobutane was used instead of 1-chlorobutane. 1-bromobutane (160 mL, 1.48 mol, 1.03 eqv.) was added slowly to 1-methylpyrrolidine (150 mL, 1.44 mol) in ethyl acetate (150 ml) and stirred for 24 hours at room temperature to give a white solid. The colourless solution was removed by cannula filtration and the crystals were washed by ethyl acetate (3 × 100 mL). Afterwards, the crystals were recrystallized from EtOAc/MeCN and dried in *vacuo* to yield pure [C_4C_1pyrr]Br.

δ_H (400 MHz, DMSO-d^6)/ppm 3.49 (4H, m, N(C$\underline{H}_2$)$_2$), 3.35 (2H, m, NC$\underline{H}_2$(CH$_2$)$_2$CH$_3$), 3.01 (3H, s, NC$\underline{H}_3$), 2.07 (4H, s, NCH$_2$(C$\underline{H}_2$)$_2$), 1.67 (2H, quintet, $^3J_{H\text{-}H}$=7.3 Hz, NCH$_2$C$\underline{H}_2$CH$_2$CH$_3$), 1.31 (2H, sextet, $^3J_{H\text{-}H}$=7.2 Hz, N(CH$_2$)$_2$C$\underline{H}_2$CH$_3$), 0.92 (3H, t, $^3J_{H\text{-}H}$=7.2 Hz, N(CH$_2$)$_3$C$\underline{H}_3$).

δ_C (400 MHz, DMSO-d^6)/ppm 63.8 (2C, s, N($\underline{C}H_2)_2$), 63.2 (2C, s, $N(CH_2)_2(\underline{C}H_2)_2$), 47.9 (1C, s, $N\underline{C}H_3$), 25.4 (1C, s, $N\underline{C}H_2(CH_2)_2CH_3$), 21.5 (1C, s, $NCH_2\underline{C}H_2CH_2CH_3$), 19.8 (1C, s, $N(CH_2)_2\underline{C}H_2CH_3$), 14.0 (1C, s, $N(CH_2)_3\underline{C}H_3$).

m/z (FAB^+) 364 ($[(C_4C_1pyrr)_2Br]^+$, 15%), 142 ($[C_4C_1pyrr]^+$, 100%); m/z (FAB^-) 302 ($[(C_4C_1pyrr)Br_2]$-, 100%), 79 (Br^-, 10%).

Found (%): C, 48.81; H, 9.15; N, 6.37; Calc. (%) for $C_9H_{20}NBr$: C, 48.66; H, 9.07; N, 6.30.

2.4.5 Synthesis of 1-butyl-3-methylimidazolium chloride, $[C_4C_1im]Cl$

In a three-necked round-bottom flask, 1-chlorobutane (150 mL, 1.44 mol, 1.15 eqv.) was added slowly to a stirred solution of 1-methylimidazole (100 mL, 1.25 mol) in toluene (100 mL). The mixture was heated (45 °C) for 96 hours. After cooling to room temperature, the upper phase was removed by cannula filtration and the lower phase was allowed to crystallize in a freezer (-22 °C). The product was then recrystallized from MeCN (50 mL) and washed with ethyl acetate (3 x 50 mL). Finally, the product was dried in *vacuo* to give white crystals of $[C_4C_1im]Cl$.

δ_H (400 MHz, DMSO-d^6)/ppm 9.33 (1H, s, $N_2C\underline{H}$), 7.81 and 7.73 (2H, 2s, $2NC\underline{H}$), 4.23 (2H, t, $^3J_{H\text{-}H}$=7.2 Hz, $NC\underline{H}_2(CH_2)_2CH_3$), 3.87 (3H, s, $NC\underline{H}_3$), 1.72(2H, quintet, $^3J_{H\text{-}H}$=7.4 Hz, $NCH_2C\underline{H}_2CH_3$), 1.16 (2H, sextet, $^3J_{H\text{-}H}$=7.3 Hz, $NCH_2CH_2C\underline{H}_2CH_3$), 0.85 (3H, t, $^3J_{H\text{-}H}$=7.4 Hz, $N(CH_2)_3C\underline{H}_3$).

δ_C (400 MHz, DMSO-d^6)/ppm 137.8 (1C, s, $N_2\underline{C}$), 124.6 and 122.0 (2C, s, $2N\underline{C}H$), 48.0 (1C, s, $N\underline{C}H_2(CH_2)_2CH_3$), 35.7 (1C, s, $N\underline{C}H_3$), 31.2 (1C, s, $NCH_2\underline{C}H_2CH_2CH_3$), 19.1 (1C, s, $N(CH_2)_2\underline{C}H_2CH_3$), 13.2 (1C, s, $N(CH_2)_3\underline{C}H_3$).

m/z (FAB^+) 313 ($[(C_4C_1im)_2Cl]^+$, 20%), 139 ($[C_4C_1im]^+$, 100%) ; m/z (FAB^-) 209 ($[(C_4C_1im)Cl_2]^-$, 100%), 35 (Cl^-, 55%).

Found (%): C, 54.88; H, 8.71; N, 15.90; Calc. (%) for $C_8H_{15}N_2Cl$: C, 55.01; H, 8.66; N, 16.04.

2.4.6 Synthesis of 1-butyl-3-methylimidazolium bromide, [C_4C_1im]Br

In a three-necked round-bottom flask, 1-bromobutane (110 mL, 1.02 mol, 1.01 eqv.) was added very slowly to a stirring solution of 1-methylimidazole (80 mL, 1.01 mol) in ethyl acetate (200 mL) for 24 hours at room temperature. After cooling to room temperature, the upper phase was removed by cannula filtration and the lower phase was allowed to crystallize in a freezer (-22 °C). The product was then recrystallized from MeCN (70 mL) and washed with ethyl acetate (2 x 100 mL). Finally, the product was dried in *vacuo* to give white crystals of [C_4C_1im]Br.

δ_H (400 MHz, DMSO-d^6)/ppm 9.32 (1H, s, $N_2C\underline{H}$), 7.85 and 7.77 (2H, 2s, 2NC$\underline{H}$), 4.19 (2H, t, $^3J_{H\text{-}H}$=6.0 Hz, NC$\underline{H}_2(CH_2)_2CH_3$), 3.87 (3H, s, NC$\underline{H}_3$), 1.76 (2H, quintet, $^3J_{H\text{-}H}$=7.2 Hz, $NCH_2C\underline{H}_2CH_3$), 1.24 (2H, sextet, $^3J_{H\text{-}H}$= 8.0 Hz, $NCH_2CH_2C\underline{H}_2CH_3$), 0.88 (3H, t, $^3J_{H\text{-}H}$= 8.0 Hz, $N(CH_2)_3C\underline{H}_3$).

δ_C (400 MHz, DMSO-d^6)/ppm 137.0 (1C, s, $N_2\underline{C}$), 124.0 and 122.7 (2C, s, 2N$\underline{C}$H), 48.9 (1C, s, N$\underline{C}H_2(CH_2)_2CH_3$), 36.2 (1C, s, N$\underline{C}H_3$), 31.8 (1C, s, $NCH_2\underline{C}H_2CH_2CH_3$), 19.2 (1C, s, $N(CH_2)_2\underline{C}H_2CH_3$), 13.8 (1C, s, $N(CH_2)_3\underline{C}H_3$).

m/z (FAB$^+$) 359 ([$(C_4C_1im)_2{}^{81}Br]^+$, 10%), 357 ([$(C_4C_1im)_2{}^{79}Br]^+$, 10%), 139 ([$C_4C_1im]^+$, 100%); m/z (LSIMS$^-$) 301 ([$(C_4C_1im)^{81}Br_2]^-$, 47%) 299 ([$(C_4C_1im)^{79}Br^{81}Br]^-$, 100%), 297 ([$(C_4C_1im)^{79}Br_2]^-$, 49%), 81 ($^{81}Br^-$, 68%), 79 ($^{79}Br^-$, 70%).

Found (%): C, 43.94; H, 7.04; N, 12.93; Calc. (%) for $C_8H_{15}N_2Br$: C, 43.85; H, 6.90; N, 12.78.

2.4.7 Synthesis of 1-butyl-2,3-dimethylimidazolium bis(trifluoromethylsulfonyl)imide, [$C_4C_1C_1$im][NTf_2]

In a two-necked round-bottom flask, lithium *bis*(trifluoromethylsulfonyl)imide (92.4 g, 0.32 mol) and [$C_4C_1C_1$im]Cl (60.2 g, 0.32 mol) were mixed and stirred in DCM (250 mL) for 24 hours and filtered. The residual LiCl was washed with DCM (2 x 50 mL).

The combined organic extracts were washed with distilled water until the aqueous free (by silver nitrate test). The DCM was then removed in rotary evaporator, and the resulting liquid was filtered through a pad of acidic alumina and charcoal to give the colourless ionic liquid $[C_4C_1C_1im][NTf_2]$.

δ_H (400 MHz, DMSO-d^6)/ppm 7.61 and 7.64 (2H, 2s, 2NC<u>H</u>), 4.11 (2H, t, $^3J_{H-H}$=8.0 Hz, NC<u>H</u>$_2$(CH$_2$)$_2$CH$_3$), 3.75 (3H, s, NC<u>H</u>$_3$), 2.58 (3H, s, N$_2$CC<u>H</u>$_3$), 1.69 (2H, quintet, $^3J_{H-H}$=8.0 Hz, NCH$_2$C<u>H</u>$_2$CH$_2$CH$_3$), 1.29 (2H, sextet, $^3J_{H-H}$=8.0 Hz, CH$_2$CH$_2$C<u>H</u>$_2$CH$_3$), 0.91 (3H, t, $^3J_{H-H}$=8.0 Hz, N(CH$_2$)$_3$C<u>H</u>$_3$).

δ_C (400 MHz, DMSO-d^6)/ppm 144.67 (1C, s, N$_2$<u>C</u>), 122.75 and 121.31 (2C, s, 2N<u>C</u>H), 119.94 (2C, quartet, $^1J_{C-F}$=319.1 Hz), 47.74 (1C, s, N<u>C</u>H$_2$(CH$_2$)$_2$CH$_3$), 35.08 (1C, s, N<u>C</u>H$_3$), 31.63 (1C, s, NCH$_2$<u>C</u>H$_2$CH$_2$CH$_3$), 19.32 (1C, s, N(CH$_2$)$_2$<u>C</u>H$_2$CH$_3$), 13.78 (1C, s, N(CH$_2$)$_3$<u>C</u>H$_3$), 9.53 (1C, s, N$_2$C<u>C</u>H$_3$).

m/z (FAB$^+$) 586 ([(C$_4$C$_1$C$_1$im)$_2$NTf$_2$]$^+$, 50%), 153 ([C$_4$C$_1$C$_1$im]$^+$, 100%); m/z (FAB$^-$) 280 ([N(SO$_2$CF$_3$)$_2$]$^-$, 100%).

Found (%): C, 30.58; H, 3.85; N, 9.58; Calc. (%) for $C_{11}H_{17}N_3O_4S_2F_6$: C, 30.48; H, 3.95; N, 9.70.

2.4.8 Synthesis of 1-butyl-3-methylimidazolium hexafluoroantimonate, $[C_4C_1im][SbF_6]$

In a two-necked round-bottom flask, sodium hexafluoroantimonate (35.1 g, 0.14 mol) and $[C_4C_1im]Br$ (28.1 g, 0.13 mol) were mixed and stirred in DCM (250 mL) for 72 hours and filtered. The residual NaBr salt was washed with DCM (2 x 50 mL). The combined DCM extracts were washed with water until the aqueous phase was halide free (by silver nitrate test), after which the DCM was removed in rotary evaporator. The liquid was filtered through a pad of acidic alumina and charcoal to give $[C_4C_1im][SbF_6]$ as a colourless liquid.

δ_H (400 MHz, DMSO-d^6)/ppm 9.10 (1H, s, $N_2C\underline{H}$), 7.76 and 7.69 (2H, 2s, 2NC$\underline{H}$), 4.16 (2H, t, $^3J_{H\text{-}H}$=8.0 Hz, NC$\underline{H}_2(CH_2)_2CH_3$), 3.85 (3H, s, NC$\underline{H}_3$), 1.77 (2H, quintet, $^3J_{H\text{-}H}$=7.0 Hz, $NCH_2C\underline{H}_2CH_2CH_3$), 1.26 (2H, sextet, $^3J_{H\text{-}H}$=7.2 Hz, $CH_2CH_2C\underline{H}_2CH_3$), 0.91 (3H, t, $^3J_{H\text{-}H}$=8.0 Hz, $N(CH_2)_3C\underline{H}_3$).

δ_C (400 MHz, DMSO-d^6)/ppm 136.96 (1C, s, $N_2\underline{C}$), 124.07 and 122.72 (2C, s, 2N$\underline{C}$H), 48.96 (1C, s, N$\underline{C}H_2(CH_2)_2CH_3$), 36.18 (1C, s, N$\underline{C}H_3$), 31.80 (1C, s, $NCH_2\underline{C}H_2CH_2CH_3$), 19.23 (1C, s, $N(CH_2)_2\underline{C}H_2CH_3$), 13.70 (1C, s, $N(CH_2)_3\underline{C}H_3$).

m/z (FAB^+) 513 ($[(C_4C_1im)_2SbF_6]^+$, 67%), 139 ($[C_4C_1im]^+$, 100%); m/z (FAB^-) 235 ($[SbF_6]^-$, 100%).

Found (%): C, 25.72; H, 3.96; N, 7.38; Calc. (%) for $C_8H_{15}N_2SbF_6$: C, 25.63; H, 4.03; N, 7.47.

2.4.9 Synthesis of 1-butyl-3-methylimidazolium trifluoromethanesulfonate, [C_4C_1im][OTf]

In a two-necked round-bottom flask, lithium trifluoromethanesulfonate (33.5 g, 0.33 mol) and [C_4C_1im]Cl (55.7 g, 0.33 mol) were stirred in DCM (60 mL) for 24 hours, and then filtered. The residual LiCl salt was washed with DCM (2 × 50 mL). The combined DCM extracts were washed with water until the aqueous phase was halide free (by silver nitrate test), after which the DCM was removed in rotary evaporator. The liquid was filtered through a pad of acidic alumina and charcoal to give the colourless liquid [C_4C_1im][OTf].

δ_H (400 MHz, DMSO-d^6)/ppm 9.10 (1H, s, $N_2C\underline{H}$), 7.77 and 7.70 (2H, 2s, 2NC$\underline{H}$), 4.16 (2H, t, $^3J_{H\text{-}H}$=7.2 Hz, NC$\underline{H}_2(CH_2)_2CH_3$), 3.85 (3H, s, NC$\underline{H}_3$), 1.76 (2H, quintet, $^3J_{H\text{-}H}$=7.4 Hz, $NCH_2C\underline{H}_2CH_2CH_3$), 1.27 (2H, sextet, $^3J_{H\text{-}H}$=7.4 Hz, $CH_2CH_2C\underline{H}_2CH_3$), 0.90 (3H, t, $^3J_{H\text{-}H}$=7.4 Hz, $N(CH_2)_3C\underline{H}_3$).

δ_C (400 MHz, DMSO-d^6)/ppm 136.95 (1C, s, $N_2\underline{C}$), 124.97 and 122.72 (2C, s, 2N$\underline{C}$H), 119.53 (1C, quartet, $^1J_{C\text{-}F}$ = 325.0 Hz, $[OSO_2\underline{C}F_3]^-$), 48.96 (1C, s,

N<u>C</u>H$_2$(CH$_2$)$_2$CH$_3$), 36.19 (1C, s, N<u>C</u>H$_3$), 31.80 (1C, s, NCH$_2$<u>C</u>H$_2$CH$_2$CH$_3$), 19.22 (1C, s, N(CH$_2$)$_2$<u>C</u>H$_2$CH$_3$), 13.70 (1C, s, N(CH$_2$)$_3$<u>C</u>H$_3$).

m/z (FAB$^+$) 427 ([(C$_4$C$_1$im)$_2$OTf]$^+$, 100%), 139 ([C$_4$C$_1$im]$^+$, 91%); m/z (FAB$^-$) 437 ([C$_4$C$_1$im(OTf)$_2$]$^-$, 96%), 149 ([O(SO$_2$CF$_3$)]$^-$, 100%).

Found (%): C, 37.65; H, 5.34; N, 6.64; Calc. (%) for C$_9$H$_{15}$N$_2$O$_3$SF$_3$: C, 37.50; H, 5.24; N, 9.75.

2.4.10 Synthesis of 1-butyl-1-methylpyrrolidinium bis(trifluoromethylsulfonyl)imide, [C$_4$C$_1$pyrr][NTf$_2$]

In a two-necked round-bottom flask, lithium *bis*(trifluoromethylsulfonyl)imide (94.0 g, 0.33 mol) was added to a solution of [C$_4$C$_1$pyrr]Br (72.7 g, 0.33 mol) in DCM (150 mL). The resulting mixture was stirred for 72 hours, and then filtered. The residual LiBr salt was washed with DCM (2 × 50 mL). Then the combined organic extracts were washed with water until the aqueous phase was halide free (by silver nitrate test), after which the DCM was removed in rotary evaporator. The resulting liquid was filtered through a pad of acidic alumina and charcoal to give the colourless liquid [C$_4$C$_1$pyrr][NTf$_2$].

δ_H (400 MHz, DMSO-*d*^{6})/ppm 3.44 (4H, m, N(C<u>H</u>$_2$)$_2$), 3.28 (2H, m, NC<u>H</u>$_2$(CH$_2$)$_2$CH$_3$), 2.97 (3H, s, NC<u>H</u>$_3$), 2.08 (4H, s, NCH$_2$(C<u>H</u>$_2$)$_2$), 1.68 (2H, quintet, $^3J_{H\text{-}H}$=7.4 Hz, NCH$_2$C<u>H</u>$_2$CH$_2$CH$_3$), 1.32 (2H, sextet, $^3J_{H\text{-}H}$=7.2 Hz, N(CH$_2$)$_2$C<u>H</u>$_2$CH$_3$), 0.94 (3H, t, $^3J_{H\text{-}H}$=7.2 Hz, N(CH$_2$)$_3$C<u>H</u>$_3$).

δ_C (400 MHz, DMSO-*d*^{6})/ppm 119.95 (2C, quartet, $^1J_{C\text{-}F}$=320.3 Hz, [N(SO$_2$<u>C</u>F$_3$)$_2$]$^-$) 63.86 (2C, s, N(<u>C</u>H$_2$)$_2$), 63.38 (2C, s, N(CH$_2$)$_2$(<u>C</u>H$_2$)$_2$), 47.94 (1C, s, N<u>C</u>H$_3$), 25.38 (1C, s, N<u>C</u>H$_2$(CH$_2$)$_2$CH$_3$), 21.52 (1C, s, NCH$_2$<u>C</u>H$_2$CH$_2$CH$_3$), 19.76 (1C, s, N(CH$_2$)$_2$<u>C</u>H$_2$CH$_3$), 13.90 (1C, s, N(CH$_2$)$_3$<u>C</u>H$_3$).

m/z (ESI$^+$) 142 ([C$_4$C$_1$pyrr]$^+$, 100%); m/z (ESI$^-$) 280 ([N(SO$_2$CF$_3$)]$^-$, 100%).

Found (%): C, 31.39; H, 4.61; N, 6.64; Calc. (%) for $C_{11}H_{20}N_2O_4S_2F_6$: C, 31.28; H, 4.77; N, 6.63.

2.4.11 Synthesis of 1-butyl-3-dimethylimidazolium bis(trifluoromethylsulfonyl)imide, $[C_4C_1im][NTf_2]$

In a two-necked round-bottom flask, lithium *bis*(trifluoromethylsulfonyl)imide (122.6 g, 0.43 mol) and $[C_4C_1im]Br$ (91.6 g, 0.42 mol) were mixed and stirred in DCM (350 mL) for 72 hours and filtered. The residual LiBr was washed with DCM (2 x 80 mL). The combined organic extracts were washed with distilled water until the aqueous free (by silver nitrate test). The DCM was then removed in rotary evaporator, and the resulting liquid was filtered through a pad of acidic alumina and charcoal to give the colourless ionic liquid $[C_4C_1im][NTf_2]$.

δ_H (400 MHz, DMSO-d^6)/ppm 9.12 (1H, s, $N_2C\underline{H}$), 7.77 and 7.70 (2H, 2s, $2NC\underline{H}$), 4.23 (2H, t, $^3J_{H\text{-}H}$=7.8 Hz, $NC\underline{H}_2(CH_2)_2CH_3$), 3.87 (3H, s, $NC\underline{H}_3$), 1.72 (2H, quintet, $^3J_{H\text{-}H}$=8.0 Hz, $NCH_2C\underline{H}_2CH_3$), 1.20 (2H, sextet, $^3J_{H\text{-}H}$=7.3 Hz, $NCH_2CH_2C\underline{H}_2CH_3$), 0.88 (3H, t, $^3J_{H\text{-}H}$=7.0 Hz, $N(CH_2)_3C\underline{H}_3$).

δ_C (400 MHz, DMSO-d^6)/ppm 136.85 (1C, s, $N_2\underline{C}$), 126.62 and 122.12 (2C, s, $2N\underline{C}H$), 119.85 (2C, quartet, $^1J_{C\text{-}F}$=319.5 Hz), 48.70 (1C, s, $N\underline{C}H_2(CH_2)_2CH_3$), 35.79 (1C, s, $N\underline{C}H_3$), 31.29 (1C, s, $NCH_2\underline{C}H_2CH_2CH_3$), 18.78 (1C, s, $N(CH_2)_2\underline{C}H_2CH_3$), 13.04 (1C, s, $N(CH_2)_3\underline{C}H_3$).

m/z (FAB^+) 564 ($[(C_4C_1im)_2NTf_2]^+$, 66%), 142 ($[C_4C_1im]^+$, 100%); m/z (FAB^-) 280 ($[N(SO_2CF_3)]^-$, 100%).

Found (%): C, 28.55; H, 3.67; N, 10.15; Calc. (%) for $C_{10}H_{15}N_3O_4S_2F_6$: C, 28.64; H, 3.61; N, 10.02.

2.4.12 Synthesis of 1-butyl-3-methylimidazolium tetrafluoroborate, $[C_4C_1im][BF_4]$

In a two-necked round-bottom flask, sodium tetrafluoroborate (35.9 g, 0.14 mol) and $[C_4C_1im]Cl$ (23.8 g, 0.14 mol) were mixed and stirred in DCM (230 mL) for 24 hours, and then filtered. The residual NaCl was washed with DCM (2 x 50 mL). The combined organic extracts were washed with distilled water until the aqueous free (by silver nitrate test). The DCM was then removed in rotary evaporator, and the resultant liquid was filtered through a pad of acid alumina and charcoal to give the colourless ionic liquid $[C_4C_1im][BF_4]$.

δ_H (400 MHz, DMSO-*d*^{6})/ppm 9.04 (1H, s, $N_2C\underline{H}$), 7.74 and 7.68 (2H, 2s, $2NC\underline{H}$), 4.15 (2H, t, $^3J_{H\text{-}H}$=7.4 Hz, $NC\underline{H}_2(CH_2)_2CH_3$), 3.85 (3H, s, $NC\underline{H}_3$), 1.74 (2H, quintet, $^3J_{H\text{-}H}$=7.4 Hz, $NCH_2C\underline{H}_2CH_3$), 1.28 (2H, sextet, $^3J_{H\text{-}H}$=7.3 Hz, $NCH_2CH_2C\underline{H}_2CH_3$), 0.90 (3H, t, $^3J_{H\text{-}H}$=7.4 Hz, $N(CH_2)_3C\underline{H}_3$).

δ_C (400 MHz, DMSO-*d*^{6})/ppm 136.60 (1C, s, $N_2\underline{C}$), 123.95 and 122.07 (2C, s, $2N\underline{C}H$), 48.60 (1C, s, $N\underline{C}H_2(CH_2)_2CH_3$), 35.88 (1C, s, $N\underline{C}H_3$), 31.60 (1C, s, $NCH_2\underline{C}H_2CH_2CH_3$), 19.11 (1C, s, $N(CH_2)_2\underline{C}H_2CH_3$), 13.65 (1C, s, $N(CH_2)_3\underline{C}H_3$).

m/z (FAB^+) 365 ($[(C_4C_1im)_2BF_4]^+$, 67%), 139 ($[C_4C_1im]^+$, 100%); m/z (FAB^-) 313 ($[C_4C_1im(BF_4)_2]^+$, 55%), 87 ($[BF_4]^-$, 100%).

Found (%): C, 42.53; H, 6.57; N, 12.24; Calc. (%) for $C_8H_{15}N_2BF_4$: C, 42.51; H, 6.69; N, 12.39.

2.4.13 Synthesis of 1-ethyl-4-methoxycarbonylpyridinium bis(trifluoromethylsulfonyl)imide

In a two-necked round-bottom flask, methyl isonicotinate (35 mL, 0.30 mol) and bromoethane (110 mL, 1.47 mol, 4.97 eqv.) were mixed and heated to reflux (50 °C) for about 80 hours. The white-yellow solid was filtered and washed with ethyl acetate

(3 × 30 mL). and dried in *vacuo* to give 1-ethyl-4-methoxycarbonylpyridinium bromide.

Then in a two-necked round-bottom flask, 1-ethyl-4-methoxycarbonylpyridinium bromide (20.7 g, 84.1 mmol) and lithium *bis*(trifluoromethylsulfonyl)imide (24.1 g , 84.1 mmol) were stirred in DCM (50 mL) for 80 hours to give 1-ethyl-4-methoxycarbonylpyridinium *bis*(trifluoromethylsulfonyl)imide as a brown liquid.

δ_H (400 MHz, DMSO-*d*^{6})/ppm 9.29 and 8.52 (4H, AB quartet, $^3J_{AB}$=6.0 Hz, Ar-H), 4.73 (2H, quartet, $^3J_{HH}$=6.7 Hz, $CH_3C\underline{H}_2N^+$), 4.00 (3H, s, $C\underline{H}_3O$), 1.57 (3H, t, $^3J_{HH}$=6.0 Hz, $C\underline{H}_3CH_2N^+$).

δ_C (400 MHz, DMSO-*d*^{6})/ppm 163.08 (1C, s, $\underline{C}CO_2CH_3$), 146.53 (2C, s, $\underline{C}HNCH_2CH_3$), 144.16 (2C, s, $\underline{C}HCCO_2CH_3$), 127.68 (1C, s, $\underline{C}O_2CH_3$), 119.94 (1C, quartet, $^1J_{C\text{-}F}$=1279 Hz, $[N(SO_2\underline{C}F_3)]^-$), 57.39 (1C, s, $CH_3\underline{C}H_2N^+$), 54.23 (1C, s, $\underline{C}H_3O$), 16.94 (1C, s, $\underline{C}H_3CH_2N^+$).

m/z (ESI$^+$) 166 ([*p*-$CH_3CO_2PyC_2H_5]^+$, 100%); m/z (ESI$^-$) 280 ($[N(SO_2CF_3)]^-$, 100%).

2.4.14 Synthesis of 1-butyl-1-methylpyrrolidinium iodide, [C_4C_1pyrr]I

In a two-necked round-bottom flask, 1-methylpyrrolidine (25.0 mL, 0.24 mol) was added slowly to an ethyl acetate (50 mL) solution containing 1-iodobutane (27.5 mL, 0.24 mol) and the mixture was stirred for 24 hours. The resulting white precipitate was filtered and recrystallized from MeCN (50 mL) to form the white crystalline 1-butyl-1-methylpyrrolidinium iodide.

δ_H (400 MHz, DMSO-*d*^{6})/ppm 3.47 (4H, m, $N(C\underline{H}_2)_2$), 3.34 (2H, m, $NC\underline{H}_2(CH_2)_2CH_3$), 3.00 (3H, s, $NC\underline{H}_3$), 2.09 (4H, s, $NCH_2(C\underline{H}_2)_2$), 1.68 (2H, m, $NCH_2C\underline{H}_2CH_2CH_3$), 1.32 (2H, sextet, $^3J_{H\text{-}H}$=7.2 Hz, $N(CH_2)_2C\underline{H}_2CH_3$), 0.93 (3H, t, $^3J_{H\text{-}H}$=8.0 Hz, $N(CH_2)_3C\underline{H}_3$).

δ_C (400 MHz, DMSO-d^6)/ppm 63.88 (2C, s, N($\underline{C}H_2)_2$), 63.26 (2C, s, $N(CH_2)_2(\underline{C}H_2)_2$), 48.04 (1C, s, $N\underline{C}H_3$), 25.42 (1C, s, $N\underline{C}H_2(CH_2)_2CH_3$), 21.54 (1C, s, $NCH_2\underline{C}H_2CH_2CH_3$), 19.76 (1C, s, $N(CH_2)_2\underline{C}H_2CH_3$), 14.01 (1C, s, $N(CH_2)_3\underline{C}H_3$).

m/z (FAB^+) 411 ($[(C_4C_1py)_2I]^+$, 22%), 142 ($[C_4C_1py]^+$, 100%); m/z (FAB^-) 396 ($[(C_4C_1py)I_2]^+$, 82%), 127 (I^-, 100%).

Found (%): C, 40.30; H, 7.40; N, 5.24; Calc. (%) for $C_9H_{20}NI$: C, 40.16; H, 7.49; N, 5.20.

2.4.15 Synthesis of 1-ethyl-4-(methoxycarbonyl)pyridinium iodide (Kosower's salt)

Methyl isonicotinate (75 ml, 635 mmol) and iodoethane (220 ml, 2.75 mol) were heated at 40°C for 24 hours. The resulting bright orange solid was washed several times with cold acetone and EtOAc. The solid was then recrystallized from acetone to give bright orange crystals.

m.p. 111.6-111.8°C (lit. 111-112°C)[2]

δ_H (400 MHz, DMSO-d^6)/ppm 9.35 and 8.52 (4H, AB quartet, $^3J_{AB}$=6.4 Hz, Py-$\underline{H}$), 4.75 (2H, quartet, $^3J_{H\text{-}H}$=7.3 Hz, $C\underline{H}_2CH_3$), 3.99 (3H, s, $CO_2C\underline{H}_3$), 1.58 (3H, t, $^3J_{H\text{-}H}$=7.2 Hz, $CH_2C\underline{H}_3$).

δ_C (400 MHz, DMSO-d^6)/ppm 163.1 (1C, s, $\underline{C}O_2CH_3$), 146.55 (2C, s, $\underline{C}HNCH_2CH_3$), 144.02 (1C, s, $\underline{C}CO_2CH_3$), 127.64 (2C, s, $\underline{C}HCCO_2CH_3$), 57.40 (1C, s, $N\underline{C}H_2CH_3$), 54.37 (1C, s, $CO_2\underline{C}H_3$), 16.73 (1C, s, $CH_2\underline{C}H_3$).

m/z (ESI^+) 166 ($[C_9H_{12}NO_2]^+$, 100%); (ESI^-) 420 ($[C_9H_{12}NO_2]I_2^-$, 20%), 127 (I^-, 100%)

Found (%): C, 36.86; H, 4.09; N, 4.69; Calc. (%) for $C_9H_{12}NO_2I$: C, 36.88; H, 4.13; N, 4.78.

2.4.16 Synthesis of dimethyl-4-nitrophenylsulfonium methylsulfate, [*p*-$NO_2PhS(CH_3)_2$][CH_3OSO_3]

4-Nitrothioanisole (4.10 g, 24.2 mmol) and dimethylsulfate (10.0 mL, 0.11 mol, ~4.5 eqv.) were stirred for two hours at 100 °C. After cooling to room temperature the resulting white solid was filtered and recrystallized twice from minimum amount of methanol. The product was dried in *vacuo* to give the white crystals [*p*-$NO_2PhS(CH_3)_2$][CH_3OSO_3].

δ_H (400 MHz, DMSO-d^6)/ppm 8.52 and 8.34 (4H, AB quartet, $^3J_{AB}$=8.2 Hz, Ar-H), 3.38 (3H, s, [C$\underline{H}_3OSO_3]^-$), 3.34 (6H, s, $CS^+(C\underline{H}_3)_2$).

δ_C (400 MHz, DMSO-d^6)/ppm 150.70 (1C, s, $\underline{C}S^+(CH_3)_2$), 134.63 (1C, s, $\underline{C}NO_2$), 131.97 (2C, s, $\underline{C}HCNO_2$), 125.36 (2C, s, $\underline{C}HCS^+(CH_3)_2$), 53.28 (1C, s, [$\underline{C}H_3OSO_3]^-$), 28.46 (2C, s, $CS^+(\underline{C}H_3)_2$).

m/z (ESI^+) 184 ([*p*-$NO_2PhS(CH_3)_2]^+$, 100%); m/z (ESI^-) 406 (([*p*-$NO_2PhS(CH_3)_2$][$CH_3OSO_3]_2)^-$, 100%), 111 ([$CH_3OSO_3]^-$, 75%).

Found (%): C, 36.69; H, 4.54; N, 4.64; Calc. (%) for $C_9H_{13}NO_6S_2$: C, 36.60; H, 4.44; N, 4.74.

2.4.17 Synthesis of dmethyl-4-nitrophenylsulfonium *bis*(trifluoromethylsulfonyl)imide, [*p*-$NO_2PhS(CH_3)_2$][NTf_2]

[*p*-$NO_2PhS(CH_3)_2$][CH_3OSO_3] (3.23 g, 10.9 mmol) and lithium *bis*(trifluoromethylsulfonyl)imide (3.14 g, 10.9 mmol) were stirred overnight in water (10 mL) at room temperature. A yellow liquid was separated from water (10 mL) and filtered. The liquid was then further washed with water and dried under *vacuo* to give the product [*p*-$NO_2PhS(CH_3)_2$][NTf_2].

δ_H (400 MHz, DMSO-d^6)/ppm 8.53 and 8.34 (4H, AB quartet, $^3J_{AB}$=8.2 Hz, Ar-H), 3.34 (6H, s, $CS^+(C\underline{H}_3)_2$).

δ_C (400 MHz, DMSO-d^6)/ppm 150.69 (1C, s, $\underline{C}S^+(CH_3)_2$), 134.60 (1C, s, $\underline{C}NO_2$), 131.95 (2C, s, $\underline{C}HCNO_2$), 125.37 (2C, s, $\underline{C}HCS^+(CH_3)_2$), 119.93 (2C, quartet, $^1J_{C\text{-}F}$=1279 Hz, $[N(SO_2\underline{C}F_3)_2]^-$), 28.47 (2C, s, $CS^+(\underline{C}H_3)_2$).

m/z (ESI^+) 184 ($[p\text{-}NO_2PhS(CH_3)_2]^+$, 100%); m/z ($ESI^-$) 280 ($[N(SO_2CF_3)_2]^-$, 100%).

Found (%): C, 25.92; H, 2.11; N, 5.91; Calc. (%) for $C_{10}H_{10}N_2O_6S_3F_6$: C, 25.87; H, 2.17; N, 6.03.

3 Solvation behaviour of salts in ionic liquids

3.1 Introduction

Since the birth of modern ionic liquids, researchers have tried to demonstrate special physical and chemical properties which are unique to ionic liquids. The idea of ionic liquids being not distillable was one of those, but it was disproved by many examples[15, 111] which showed ionic liquids are distillable under very high vacuum conditions at high temperatures (i.e. near 300 °C). Another investigation carried by Earle and co-workers demonstrated that the choice of which ionic liquid to use in a reaction of toluene and nitric acid can have a dramatic effect on the outcome of the reaction (forming different products).[112] Unfortunately, the authors did not provide with us enough fundamental insights on what causes the selection to happen. Beside the few exceptional cases, no special “Ionic Liquid effect” was discovered in the earlier studies of ionic liquids; earlier investigation of reaction rates and spectra of solute species indicated ionic liquids behave similarly to polar molecular liquids, and no special “Ionic Liquid effect” was discovered in these experiments.[35, 53-58]

However, the Welton group had proposed recently that the reactivity resulting from mixing two different and reactive salts (i.e. charged electrophiles and nucleophiles) together is highly dependent on the type of solvent, with molecular and ionic liquids displaying fundamentally different reaction pathways. In this report, it was suggested the salts behaved as dissociated reactive species, whereas in molecular solvents neutral ion-pairs and clusters are formed as the reactive species.[1] This hypothesis of the lack of ion-pairing of solute salts in ionic liquids was subsequently supported by a theoretical carried out by Lynden-Bell.[113]

Beside these two studies, there have been many mentions of ion association/dissociation in ionic liquids in the literature, but to my knowledge none of them concerns about *solute* ion association/dissociation behaviour in ionic liquids; MacFarlane[114-115] and Watanabe[116-119] studied the conductivities of ionic liquids and both suggested that there were ion associations (pairing and aggregation) in these liquids. However, their findings were aimed at association behaviour of ions in the ionic liquid itself, not that of ion solutes in a binary salt mixture. Thus these results have limited relevance to the research carried out of this thesis.

Together with Reichardt's E_T^N, Kosower's Z scale was one of the early successful empirical polarity scales and is based on the position of the absorption maximum of the longest wavelength charge-transfer band of 1-ethyl-4-(methoxycarbonyl)pyridinium iodide (**Figure 24**).[2, 120] The pyridinium iodide complex is only spectroscopically active when the salt exists as a contact ion pair, so allowing charge transfer (**Figure 24**). The intensity of this band is therefore a good indication of the amount of contact ion pairs in solution.

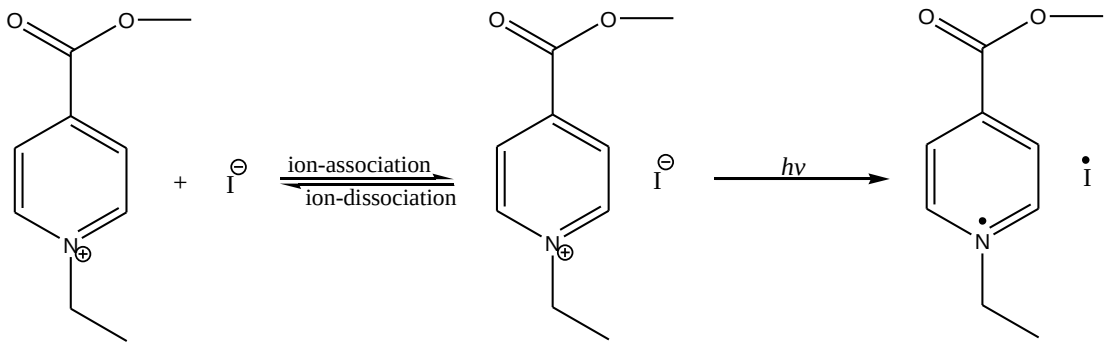

Figure 24 – Ion association/dissociation equilibrium of 1-ethyl-4-(methoxycarbonyl)pyridinium iodide

The amount of ion pairs in solution is mainly dependent on the following factors:

1. Hydrogen bonding accepting and donating abilities of solvents. Solvents such as

water and methanol are able to (a) stabilize and solvate individual cations with the lone pairs on their electronegative oxygen atom and (b) stabilize and solvate individual anions with their electropositive hydrogen atom:

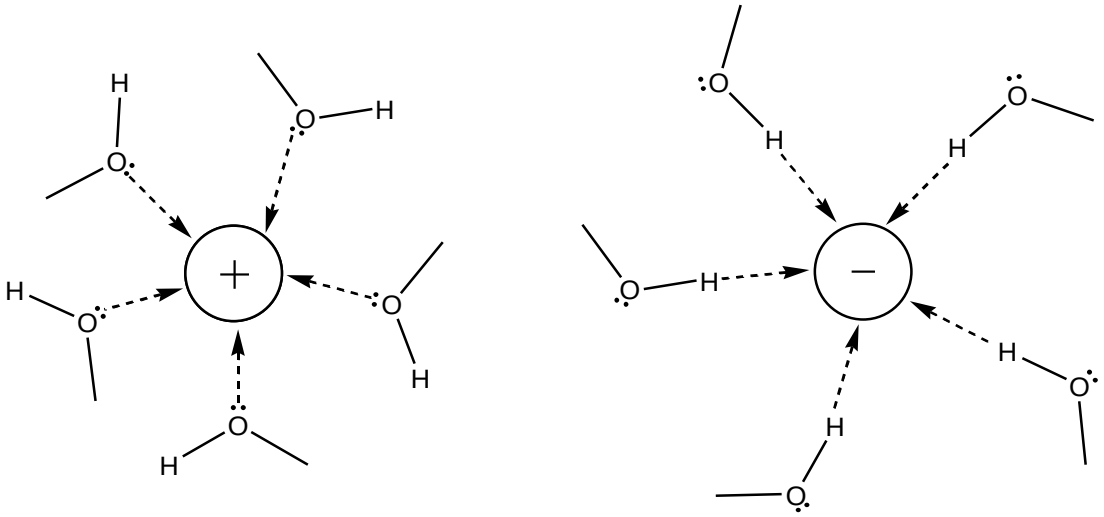

Figure 25 – Methanol clustering around the ions

2. According to the Coulomb's Law (**Equation 7**), the magnitude of electrostatic interaction between the two opposite charged ions is directly proportional to their charges and inversely proportional to the square of their separation as well as the dielectric constant of the medium (i.e. solvent). Hence, the amount of ion pairs in solution increases with (a) the charge-to-size ratio of ions, (b) dielectric constant of solvent.

$$F = Q_1Q_2/\pi\varepsilon_0\varepsilon_r r^2 \qquad \textbf{(Equation 7)}$$

where F is the electrostatic force (in Newtons), Q_1 and Q_2 are the charges of the cation and the anion respectively, ε_0 is permittivity of free space, ε_r is the dielectric constant of the medium and r is the separation of two ions.

The attraction of ion pairs is dominated by the Coulombic forces and is inversely proportional to the dielectric constant of the solvents. Solvents of high dielectric constants are capable of reducing the strong electrostatic interactions between oppositely charged ions to an extent that ion pairs can dissociate into free ions. These solvents are described as “dissociated solvents”. Conversely, in solvents of dielectric constants less than 10 (i.e. chloroform, 1,4-dioxane) practically no free ions are found.[42]

In accordance with ionic liquids’ dielectic constants measured by Weingärtner (ε_r = 10-15)[31-32], it would be expected that the degree of ion pair dissociation in the ionic liquids would be less than polar solvents such as 1-butanol (ε_r = 17.8) and MeCN (ε_r = 37.5). The Welton group’s earlier kinetic study, however, shows that this is not the case. The aims of my investigation is to resolve these two contradictory sets of results and to further understand the ion association/dissociation behaviour in ionic liquids, using the charge transfer complex 1-ethyl-4-(methoxycarbonyl)pyridinium iodide. The amount of pyridinium iodide ion pairs in solution is proportional to their UV/Vis absorbance.

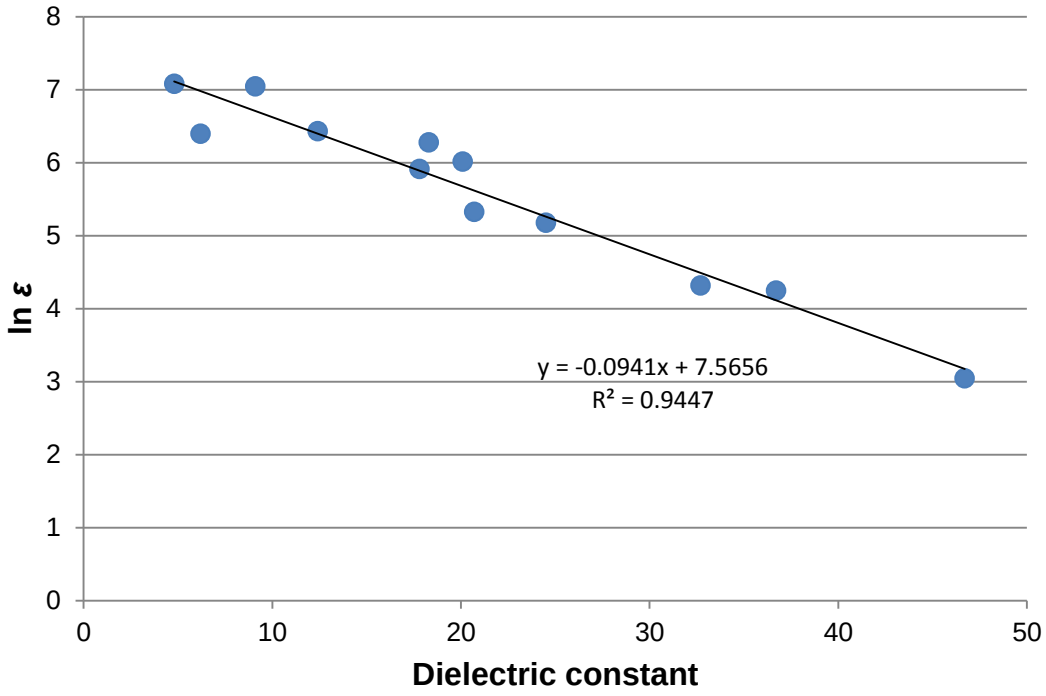

Figure 26 – Relationship between natural logarithm of molar extinction coefficient (*ε*) of Kosower's salt (from Kosower's data[2]) and dielectric constant of a selection of molecular solvents

Using data recorded by Kosower,[2] the natural logarithm of molar extinction coefficient (*ε*) of 1-ethyl-4-(methoxycarbonyl)pyridinium iodide in different molecular solvents (at similar concentration) are plotted against these solvents' dielectric constant (**Figure 26**). The resulting graph clearly shows that there is an inverse relationship between the amount of ion pairs in solution and dielectric constant of the solvent involved.

Additional to the two factors mentioned, the stability of an ion pair also diminishes with increasing temperature and pressure.[121]

3.1.1 UV/Vis spectroscopic measurements

All spectra were recorded using a double beam Perkin-Elmer LAMBDA 650 UV/Vis spectrometer. All spectra were obtained at 25 °C using quartz cuvettes of 1, 5, and 10 mm pathlength.

A stock solution of the Kosower's salt was prepared under N_2 by dissolving a certain amount of 1-ethyl-4-(methoxycarbonyl)pyridinium iodide in 5 mL of freshly distilled dichloromethane. The solution obtained showed a dark orange colour. Then, an equal amount of this solution and previously dried ionic liquid were added under N_2 to a 5 mL round-bottom flask. With continuous stirring, the DCM was removed under vacuum.

The solution of the salt mixture was then transferred under N_2 to a cuvette to record the UV/Vis spectrum.

3.2 Preliminary studies

The Kosower's 1-ethyl-4-(methoxycarbonyl)pyridinium iodide initially used in this investigation was bought from Sigma-Aldrich. The amount of ion pairs in solution is quantified by the molar extinction coefficient $\boldsymbol{\varepsilon}$, which is calculated according to the Beer-Lambert Law:

$$\mathbf{A = \varepsilon C_0 l} \qquad \textbf{(Equation 8)}$$

in which A is the absorbance, C_0 is the total concentration of the Kosower's complex added and l is the pathlength of the spectrophotometric cell. All the measurement of spectra was carried out at fixed temperature (25 °C) in this investigation.

A trial experiment was carried out whereby the UV/Vis spectra of Kosower's salt in $[C_4C_1im][NTf_2]$ were recorded. The λ_{max} of its peak is at around 362 nm. Initially, it was found that the intensity of this peak fluctuated with respect to time. For example:

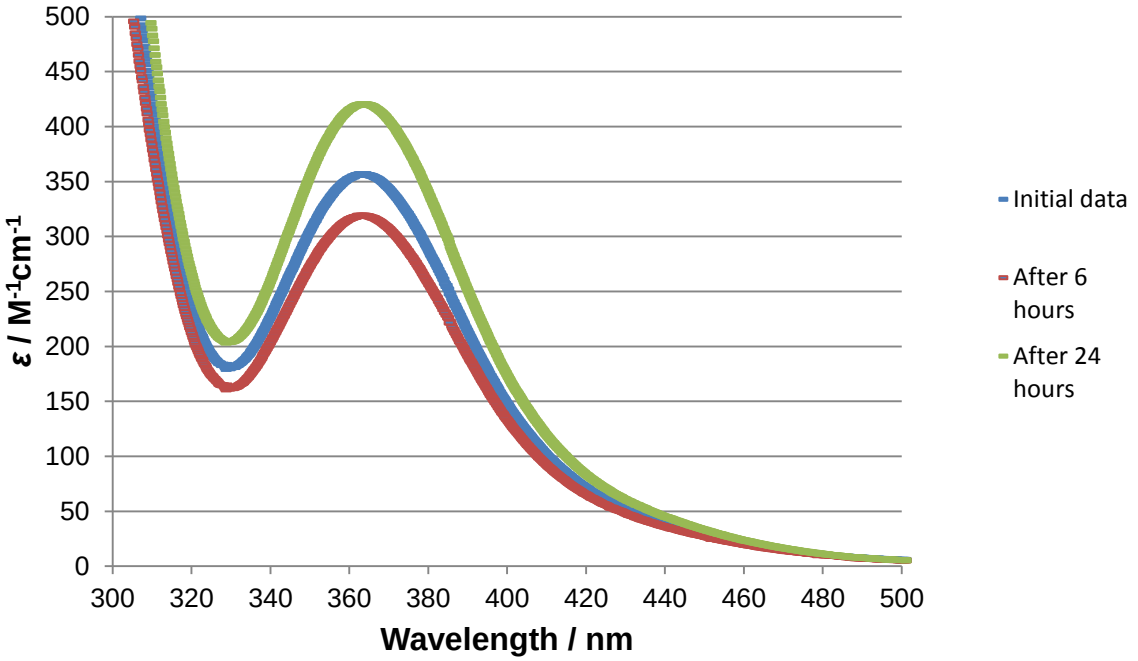

Figure 27 – Intensity fluctuating for Kosower's salt in $[C_4C_1im][NTf_2]$

The decrease in intensity was thought to be due to poor mixing of the complex with the ionic liquid. Ionic liquids have high viscosities and hence are poor mass transfer media. As time went by, and as the mixing had become more complete, the pyridinium and iodide ions of Kosower's salt become more "dissociated" (by the ionic liquid). Consequently the charge transfer band of iodide anions to the pyridinium cations reduced. At this stage of the investigation, the reason for the increase in intensity of the charge transfer band was not yet fully understood. To solve the mixing problem, rather than directly mixing the pyridinium complex and ionic liquid together, a new method was devised to prepare the solution.

3.2.1 New method to prepare ionic solution

A stock solution of Kosower's salt in DCM was prepared. Then, the solution was added to a pure ionic liquid, and the resulting mixture was stirred. The mixing of Kosower's salt in ionic liquid/molecular solvent mixtures is much faster than the direct mixing of the dye in pure ionic liquids, since ionic liquid/molecular solvent mixtures have lower viscosities than unmixed ionic liquids. After about 3 minutes of stirring, the DCM was evaporated from the mixture by vacuum (at room temperature), leaving a pure solution of Kosower's salt in ionic liquid.

The charge-transfer complex was dissolved in some ionic liquids and their molar extinction coefficients at different concentrations were recorded and summarized in **Figure 28 – 30**. All of the bands observed have λ_{max} of around 362 nm and molar extinction coefficient of 300 $M^{-1}cm^{-1}$:

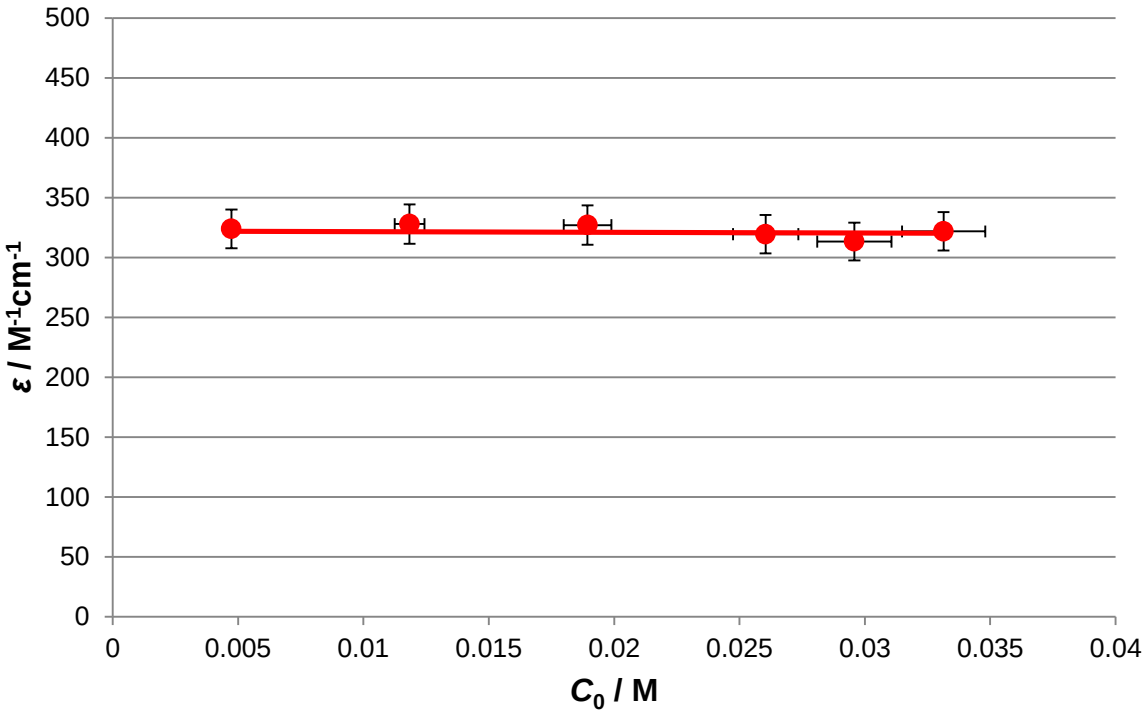

Figure 28 – Molar extinction coefficient versus concentrations of Kosower's salt in $[C_4C_1pyrr][NTf_2]$

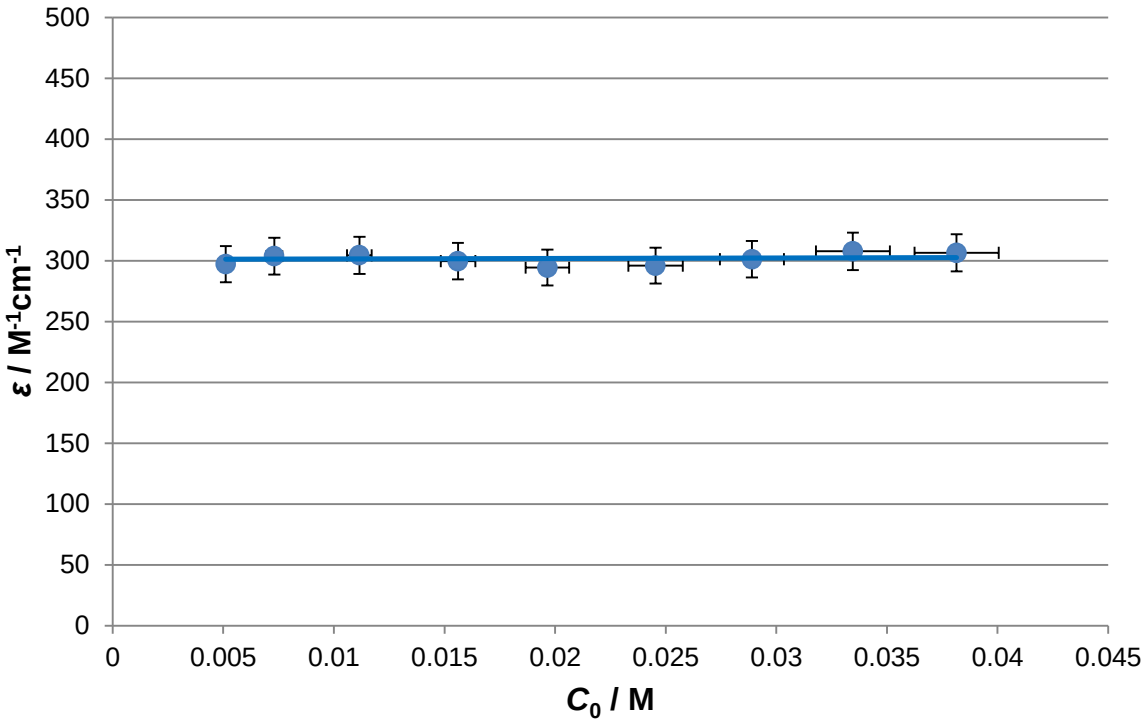

Figure 29 – Molar extinction coefficient versus concentrations of Kosower's salt in $[C_4C_1im][OTf]$

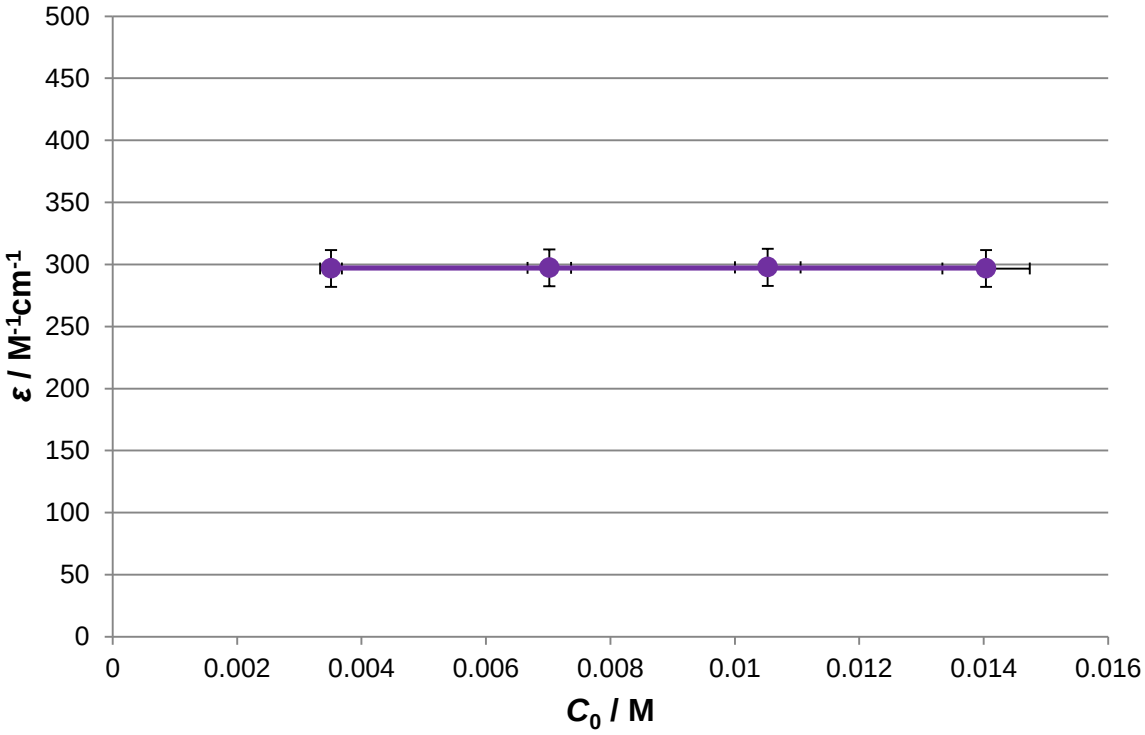

Figure 30 – Molar extinction coefficient versus concentrations of Kosower's salt in $[C_4C_1im][NTf_2]$

Considering the equilibrium of complex formation of pyridinium and iodide ions (**Figure 24**), for solvents of relatively low polarity such as DCM, the molar extinction coefficient should increases with concentration since the number of associated ion pair increases. For ionic liquids, the molar extinction coefficient stayed constant with respect to concentration (see **Figure 28 – 30**). Initially, it was thought that this behaviour occurred because the pyridinium and iodine ions were completely dissociated. However, if the ions were so far apart from each other, there shouldn't be any charge-transfer at all. We became suspicious over the identity of the peaks we saw in the spectra: were they really the charge transfer bands of the iodide anion to the pyridinium cation? Can they be the charge transfer bands of $[NTf_2]^-$ or $[OTf]^-$ (of $[C_4C_1im][NTf_2]$, $[C_4C_1pyrr][NTf_2]$ or $[C_4C_1im][OTf]$) to the pyridinium cation. To answer this question, the salt 1-ethyl-4-(methoxycarbonyl)pyridinium *bis*(trifluoromethylsulfonyl)imide was synthesized by the following route (**Figure 31**):

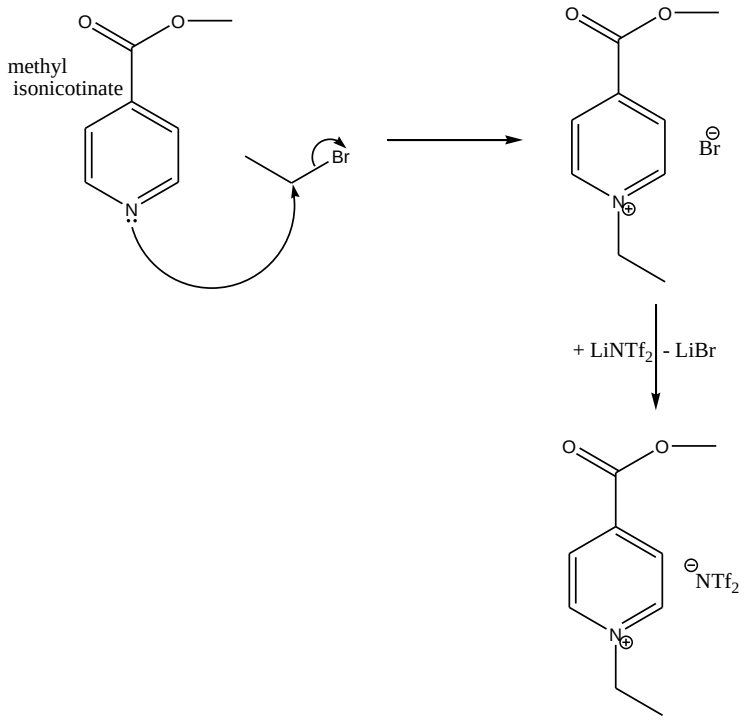

Figure 31 – Synthesis route to make 1-ethyl-4-(methoxycarbonyl)pyridinium *bis*(trifluoromethylsulfonyl)imide

Several synthesis attempts of this compound were made, but purification proved to be difficult. The starting material methyl isonicotinate (see **Figure 31**) degraded easily to form a dark-coloured residue, which was difficult to separate from the product. Although the product had this deep brown impurity, no charge-transfer band was observed in the UV/Vis spectrum when this was added to $[C_4C_1pyrr][NTf_2]$ at 0.04 M concentration (similar to the concentrations of Kosower's complex added in the earlier experiments) (**Figure 32**). Hence the ionic liquids' anions such as $[NTf_2]^-$ do not charge transfer to the pyridinium ion and were not responsible for the band at about 362 nm. A small amount of $[C_4C_1pyrr]I$ (0.03 M), which was prepared by the direct alkylation of 1-methylpyrrolidine with 1-iodobutane, was then added to this solution of 1-ethyl-4-(methoxycarbonyl)pyridinium *bis*(trifluoromethylsulfonyl)imide in $[C_4C_1pyrr][NTf_2]$. The charge transfer band at around 365 nm appeared as a result (**Figure 32**), but its extinction coefficient (26 $M^{-1}cm^{-1}$) was much lower than the 300 $M^{-1}cm^{-1}$ value observed previously. This experiment demonstrated that although ionic liquids were previously described as "super-dissociating" solvents, the pyridinium and iodide ions could still charge-transfer in ionic liquids.

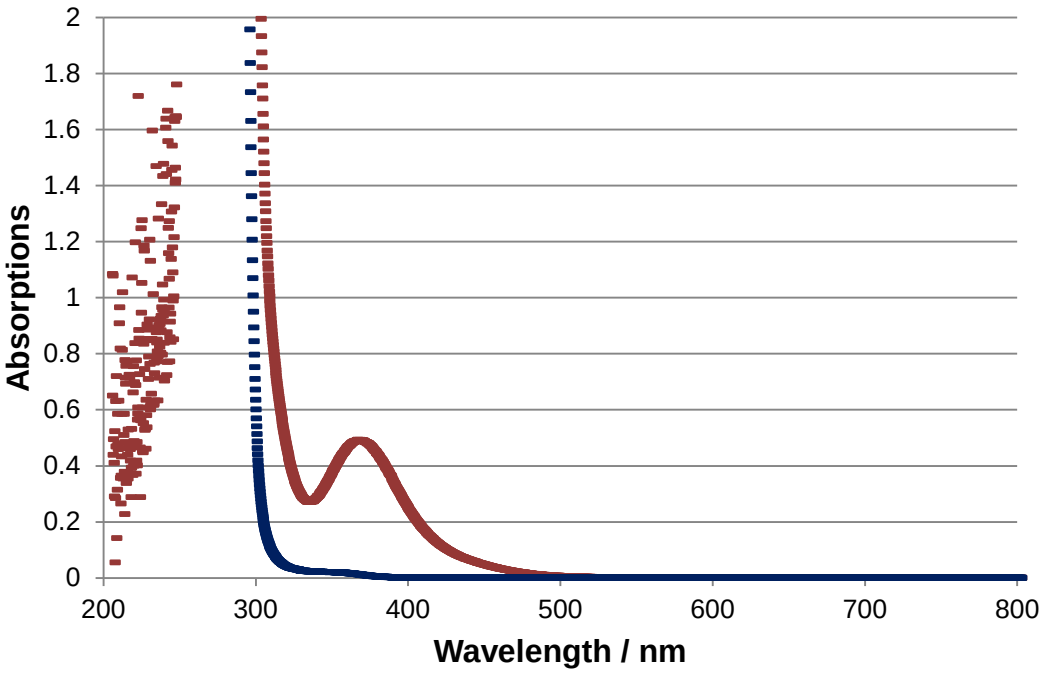

Figure 32 – Dark blue graph: 1-ethyl-4-(methoxycarbonyl)pyridinium bis(trifluoromethylsulfonyl)imide (0.04 M) in [C_4C_1pyrr][NTf_2]; Red graph: addition of [C_4C_1pyrr]I (0.03 M) to the prior solution

One possible explanation for the appearance of charge-transfer band for ionic liquid solution is that a high concentration of Kosower's salt was actually needed to obtain a signal in the UV/Vis spectrometer, since the salt has very low extinction coefficients, compared to common solvatochromic dyes. Because of this high concentration of Kosower's salt in solution, the chance of the pyridinium and iodide to "meet" randomly in this fully ionic solution is high, and since the timescale of electronic transition is much faster than that of ion migration (Franck-Condon Principle), the pyridinium cations and iodide anions might be able to charge transfer without being intimate ion pairs. The highest extinction coefficient ever recorded in literature for Kosower's salt was 1410 (chloroform, C_0 = 54.8 mM).[2] The molar extinction coefficients for the same compound in polar solvents were even lower; for instance, the molar extinction coefficient for Kosower's salt in methanol (concentration of complex 10.2 mM) was 129.[2] Conversely, solvatochromic dyes

such as *N*,*N*-dimethyl-4-nitroaniline, 4-nitroaniline and Brooker's merocyanines[122-123] all have molar extinction coefficients of higher than 10000 M^{-1} cm^{-1}.

If the above explanation was true, there were still several important questions which needed to be answered: firstly, why was there such a big difference in the molar extinction coefficients for Kosower's salt/$[C_4C_1pyrr][NTf_2]$ and 1-ethyl-4-(methoxycarbonyl)pyridinium *bis*(trifluoromethylsulfonyl)imide/$[C_4C_1pyrr]I$ / $[C_4C_1pyrr][NTf_2]$ mixtures when the compositions and conditions were almost identical? Secondly, if the occurrence of charge-transfer between the pyridinium and iodide ions was predominantly due to their random encounters rather than ion-associations, then the "apparent" ion contacts between the two in the solution, and hence intensity of the charge-transfer band, would be dependent upon the concentration-based statistical probability of them coming into contact. This probability should in turn be dependent upon the concentrations of the two species (pyridinium and iodide ions) accountable for the charge transfer. Yet using the same data as revealed in **Figures 28 – 30** to rearrange and plot **Figures 33 – 35** (A vs C_0I where slope = ε) one could see that the absorbance is first order with respect to concentration (i.e. absorbance is proportional to concentration), therefore the absorbance is dependent upon one species instead of two:

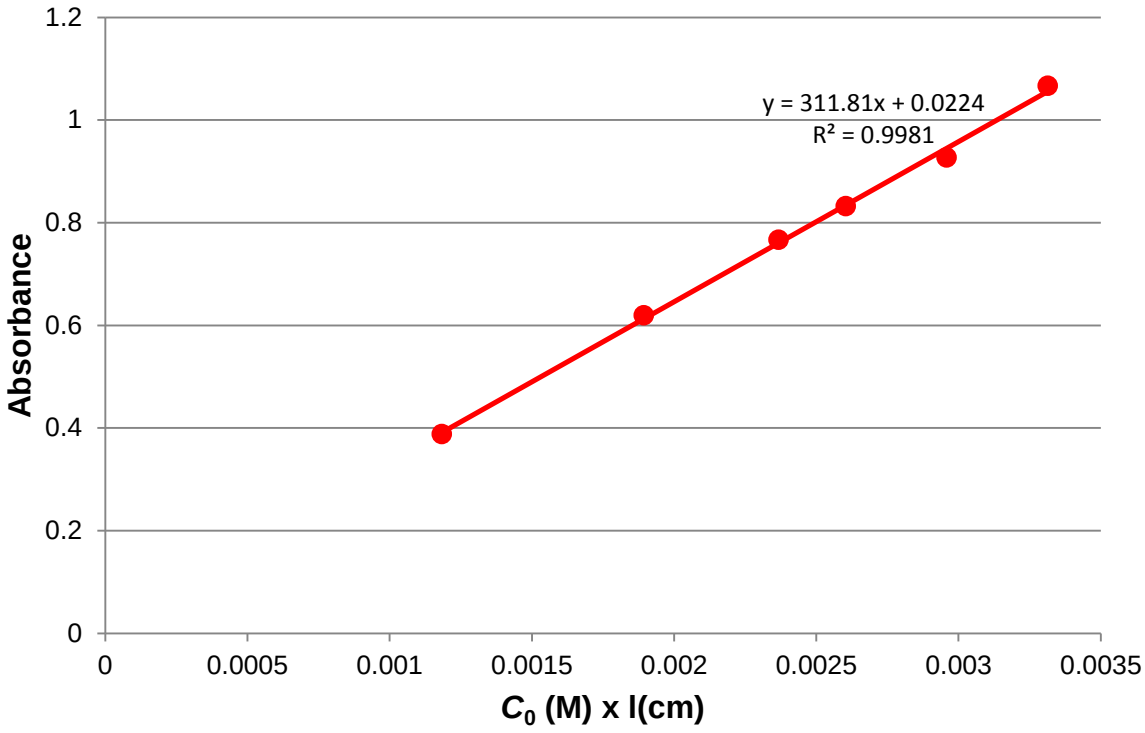

Figure 33 – Absorbance versus concentrations of Kosower's salt in $[C_4C_1pyrr][NTf_2]$ x pathlength

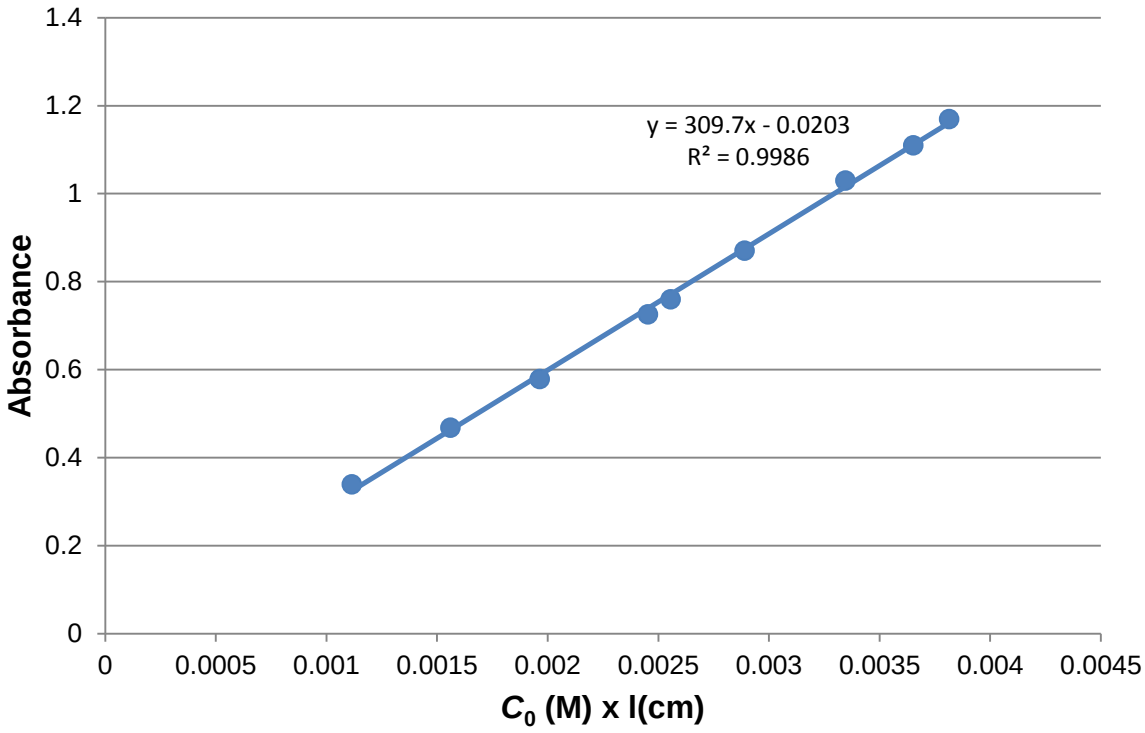

Figure 34 – Absorbance versus concentrations of Kosower's salt in $[C_4C_1im][OTf]$ x pathlength

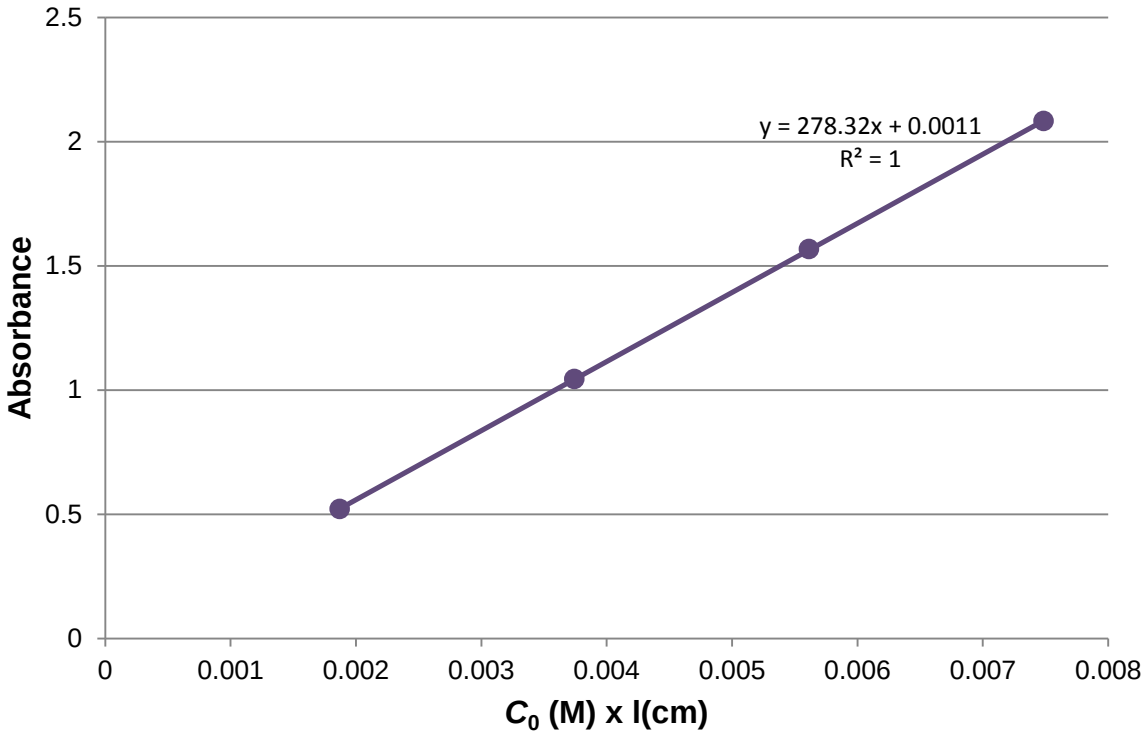

Figure 35 – Absorbance versus concentrations of Kosower's salt in $[C_4C_1im][NTf_2]$ x pathlength

These contradictory and puzzling results led us to decide to study the fundamental aspects, such as the characteristics of the Kosower's salt itself. The instability of the salt's precursor methyl isonicotinate, possibly due to the fact its ester functional group might be susceptible to nucleophilic attack by the pyridinyl-nitrogen, which caused us to believe that some impurities might be formed in the salt and this absorbed light at the visible region. It was decided the Kosower's salt should be self-synthesized and preserved under very inert conditions. The salt was synthesized by the direct alkylation of methyl isonicotinate with ethyl iodide (**Figure 36**). Since both of these reagents are unstable and turned brown over short period of time, they were quickly mixed in ethyl acetate in the dark after purification. The resulting complex was recrystallized twice before further experiment.

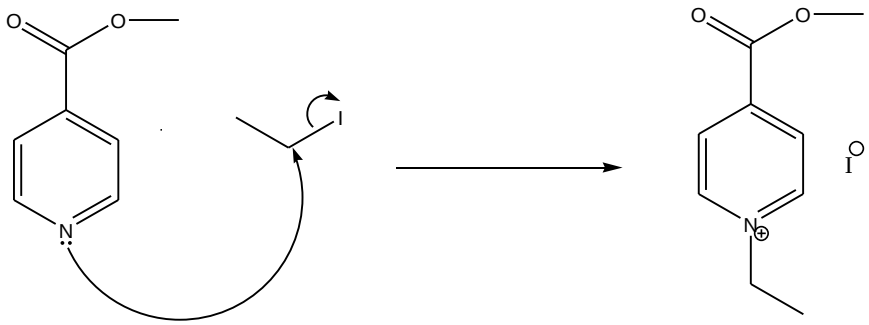

Figure 36 – Synthesis of 1-ethyl-4-(methoxycarbonyl)pyridinium iodide

When this charge-transfer complex was added to $[C_4C_1im][NTf_2]$ at concentrations (about 0.01 M) similar to those in the kinetic experiments previously reported[1], no charge-transfer band was observed. The charge-transfer band did appear, however, when the concentration of the complex was higher. On the other hand, the absorption band at 362 nm no longer appeared on the UV/Vis spectrum.

The most likely impurity that caused the absorption band at about 362 nm was the triiodide complex ion I_3^-. The iodide ion of the charge-transfer complex could undergo light-induced redox reaction to form iodine I_2, which associated with another iodide ion to form complex ion I_3^-.[124] The occurrence of this reaction could also explain why the intensity increased over time (see **Figure 33**) when exposed to light.

The charge-transfer band was not observed earlier because the intensity of the I_3^- peak was so much greater than the one of the charge transfer band. And since the positions of the charge-transfer band and I_3^- band were so similar one could not observed the charge transfer band which was hidden under the I_3^- band. Previous spectroscopic studies demonstrated that I_3^- absorbed at about 353-365 nm,[124-126] consistent with my result.

To prevent photochemical degradation of iodide ions from occurring, light was avoided during storage of the complex as well as during preparation of the solution.

3.3 Measurements with new complex

The absorbance of the charge-transfer band at various concentrations of the complex were recorded in six ionic liquids: ([C_4C_1im][NTf_2], [C_4C_1im][OTf], [C_4C_1im][BF_4], [C_4C_1im][SbF_6], [C_4C_1pyrr][NTf_2] and [$C_4C_1C_1$im][NTf_2]. These data are shown displayed in **Tables 8 – 13** and **Figures 37 – 42**:

Kosower's salt in $[C_4C_1im][NTf_2]$:

Concentration / M	Molar extinction coefficient / $M^{-1}cm^{-1}$	Slope	y-intercept	R^2
0.0290	26.18	823.12 (10.88)	3.44 (1.25)	0.9993
0.0437	38.90			
0.0882	77.93			
0.118	102.04			
0.149	125.56			
0.180	150.17			

Table 8 – Molar extinction coefficient versus concentrations of new Kosower's salt in $[C_4C_1im][NTf_2]$

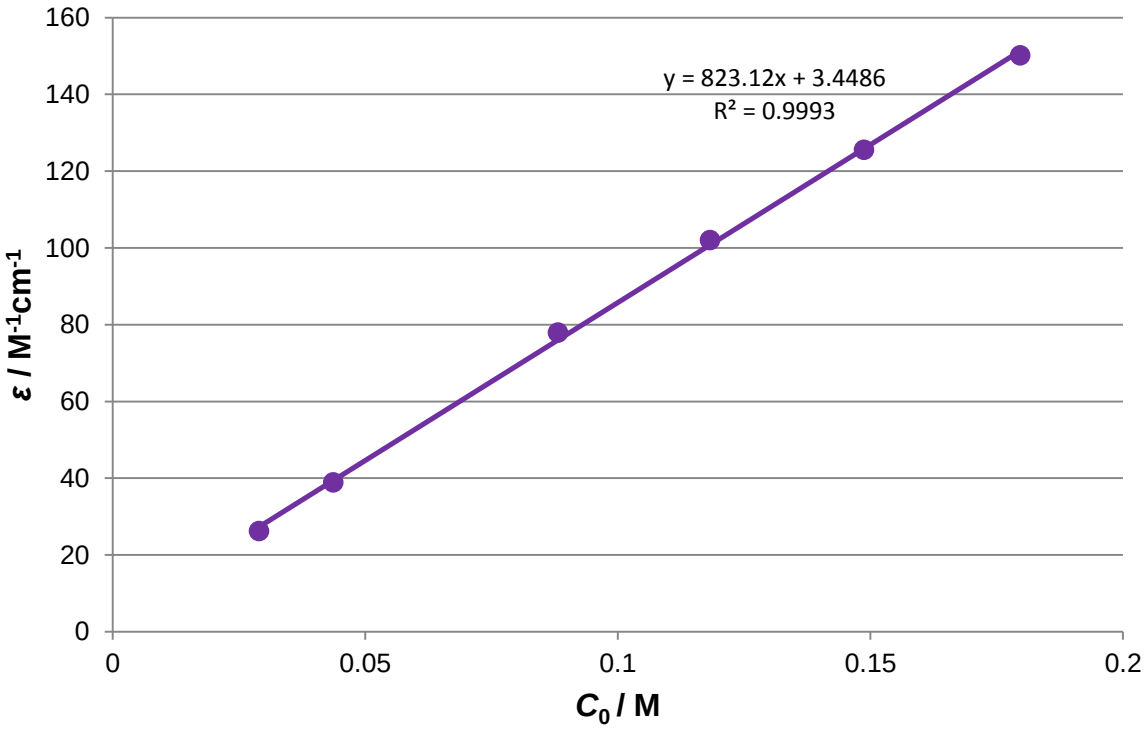

Figure 37 – Molar extinction coefficient versus concentrations of new Kosower's salt in $[C_4C_1im][NTf_2]$

Kosower's salt in $[C_4C_1im][OTf]$:

Concentration / M	Molar extinction coefficient / $M^{-1}cm^{-1}$	Slope	y-intercept	R^2
0.0252	23.01	681.75 (6.55)	6.15 (0.66)	0.9996
0.0507	40.64			
0.0765	58.14			
0.103	76.84			
0.130	94.78			
0.156	111.38			

Table 9 – Molar extinction coefficient versus concentrations of new Kosower's salt in $[C_4C_1im][OTf]$

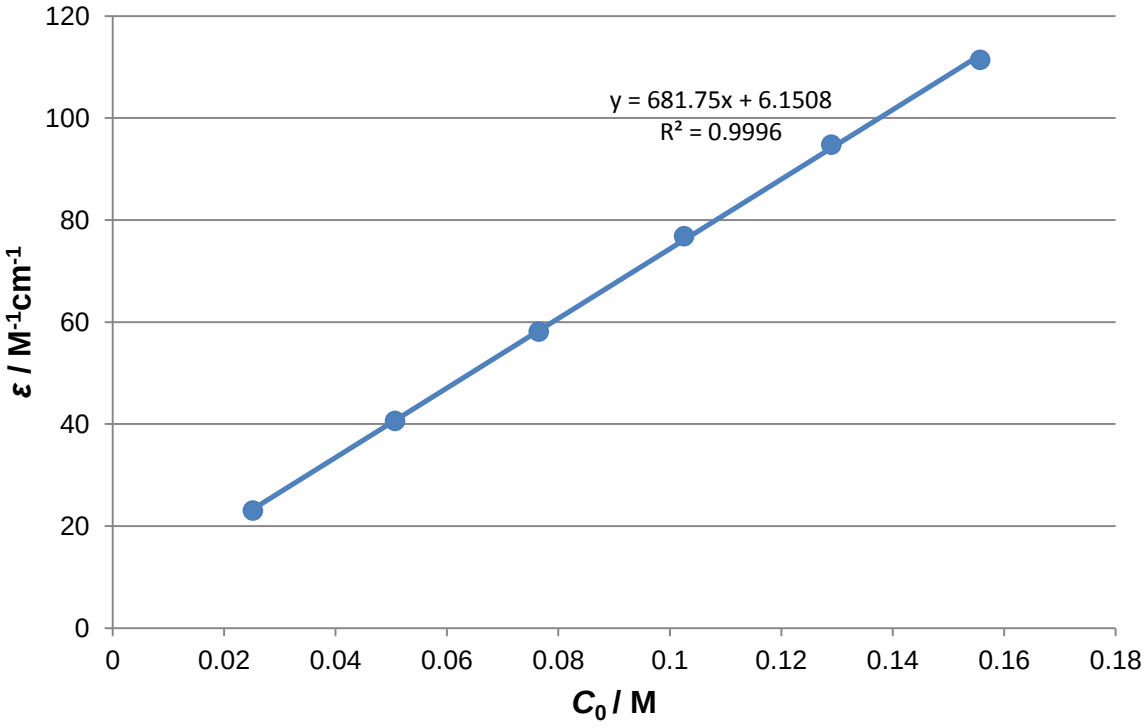

Figure 38 – Molar extinction coefficient versus concentrations of new Kosower's salt in $[C_4C_1im][OTf]$

Kosower's salt in $[C_4C_1im][BF_4]$:

Concentration / M	Molar extinction coefficient / $M^{-1}cm^{-1}$	Slope	y-intercept	R^2
0.0301	20.25	585.15 (9.14)	3.31 (1.01)	0.9990
0.0556	35.81			
0.0840	53.10			
0.113	69.55			
0.142	87.81			
0.172	102.41			

Table 10 – Molar extinction coefficient versus concentrations of new Kosower's salt in $[C_4C_1im][BF_4]$

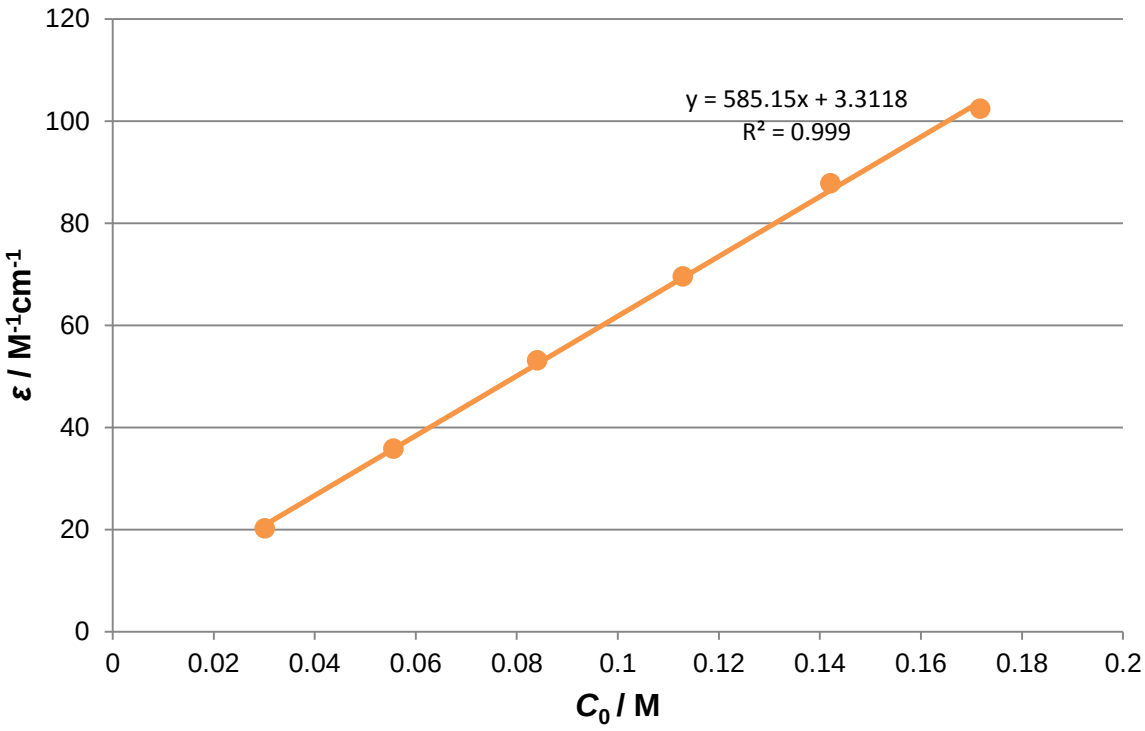

Figure 39 – Molar extinction coefficient versus concentrations of new Kosower's salt in $[C_4C_1im][BF_4]$

Kosower's salt in $[C_4C_1im][SbF_6]$:

Concentration / M	Molar extinction coefficient / $M^{-1}cm^{-1}$	Slope	y-intercept	R^2
0.0307	24.72	705.00 (8.66)	3.67 (0.97)	0.9994
0.0565	43.12			
0.0852	64.10			
0.115	86.08			
0.143	104.85			
0.173	124.55			

Table 11 – Molar extinction coefficient versus concentrations of new Kosower's salt in $[C_4C_1im][SbF_6]$

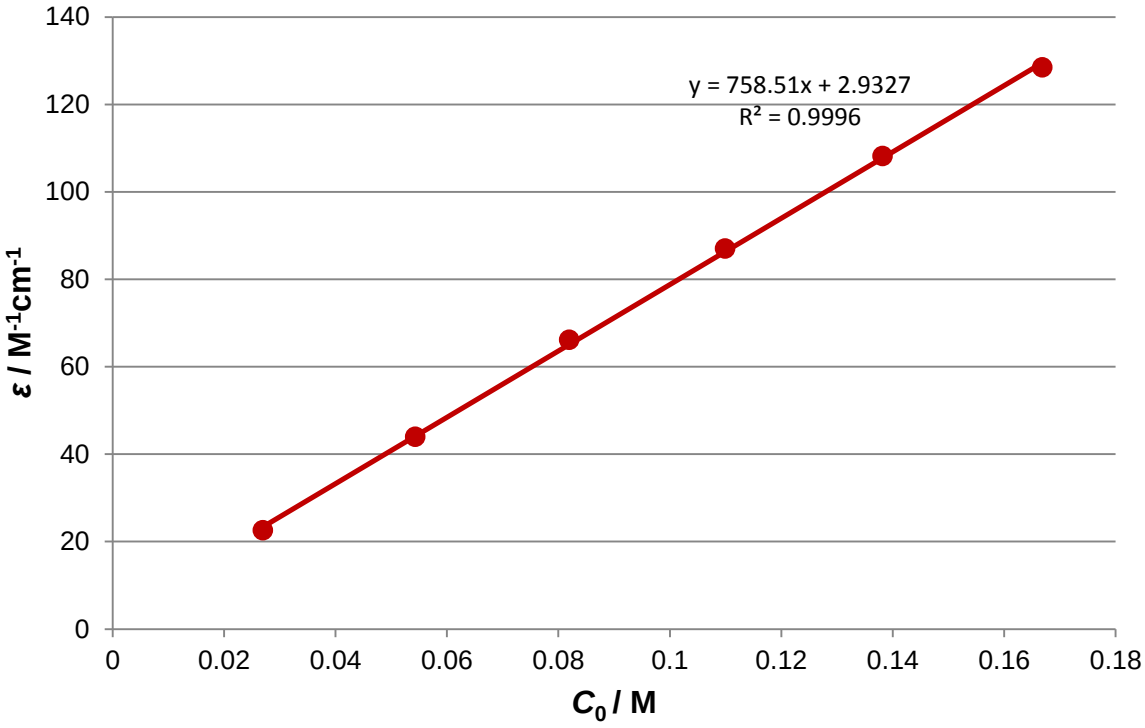

Figure 40 – Molar extinction coefficient versus concentrations of new Kosower's salt in $[C_4C_1im][SbF_6]$

Kosower's salt in $[C_4C_1pyrr][NTf_2]$:

Concentration / M	Molar extinction coefficient / $M^{-1}cm^{-1}$	Slope	y-intercept	R^2
0.0270	22.57	758.51 (7.97)	2.93 (0.86)	0.9996
0.0543	43.97			
0.0819	66.09			
0.110	86.98			
0.138	108.15			
0.167	128.43			

Table 12 – Molar extinction coefficient versus concentrations of new Kosower's salt in $[C_4C_1pyrr][NTf_2]$

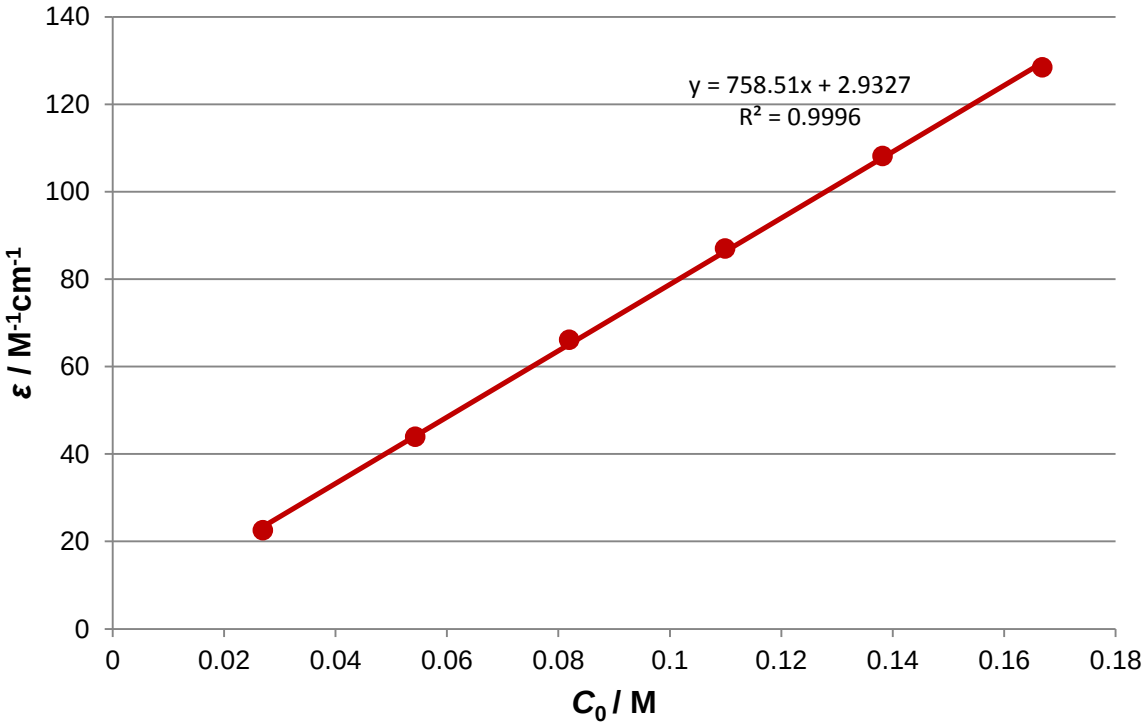

Figure 41– Molar extinction coefficient versus concentrations of new Kosower's salt in $[C_4C_1pyrr][NTf_2]$

Kosower's salt in $[C_4C_1C_1im][NTf_2]$:

Concentration / M	Molar extinction coefficient / $M^{-1}cm^{-1}$	Slope	y-intercept	R^2
0.0271	25.07	848.62 (10.05)	3.52 (1.09)	0.9994
0.0543	50.36			
0.0823	73.94			
0.110	98.16			
0.139	121.55			
0.168	144.46			

Table 13 – Molar extinction coefficient versus concentrations of self-prepared Kosower's salt in $[C_4C_1C_1im][NTf_2]$

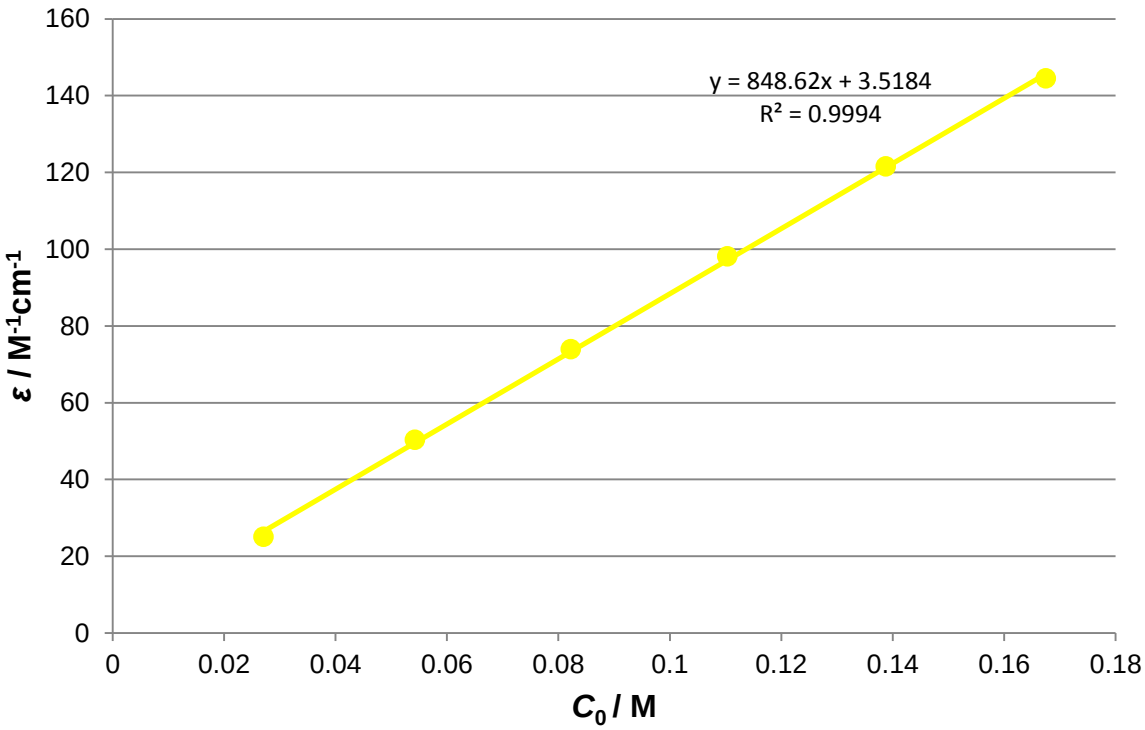

Figure 42 – Molar extinction coefficient versus concentrations of self-prepared Kosower's salt in $[C_4C_1C_1im][NTf_2]$

For every ionic liquid, the molar extinction coefficient is linearly dependent upon the concentration of salt in solution. Each of the y-intercepts was close to zero and the slopes increased roughly in order of increasing ionic liquid molar volume (**Table 14**).

Ionic Liquid	Slope	y-intercept	Molar Volume / cm^3mol^{-1}
$[C_4C_1im][N(Tf)_2]$	823.12 (10.88)	3.44 (1.25)	0.291[127]
$[C_4C_1im][OTf]$	681.75 (6.55)	6.15 (0.66)	0.211[127]
$[C_4C_1im][BF_4]$	585.15 (9.14)	3.31 (1.01)	0.190[127]
$[C_4C_1im][SbF_6]$	705.00 (8.66)	3.67 (0.97)	0.223
$[C_4C_1pyrr][NTf_2]$	758.51 (7.97)	2.93 (0.86)	0.300[128]
$[C_4C_1C_1im][NTf_2]$	848.62 (10.05)	3.52 (1.09)	0.302

Table 14 – Slopes, y-intercepts of the plots and molar volume of ionic liquids

For comparisons, the molar extinction coefficients at various concentrations of complex in several molecular liquids: 1,2-dichloroethane, 1-butanol and MeCN were measured. In these molecular liquids, the molar extinction coefficient varies non-linearly with concentration, due to the existence of ion pair formation equilibria. This behaviour differs drastically from the results obtained for the complex dissolved in ionic liquids. To rationalize these results, an equilibrium model was created.

3.4 Equilibrium Model

For the following equilibrium (**Scheme 1**):

$$Py^+ + I^- \underset{}{\overset{K_A}{\rightleftharpoons}} PyI$$

Free ions CIP

(**Scheme 1**)

The relationship of the concentration of the contact ion pairs (CIP), the only charge transfer species in the model, and the ion association constant K_A, can be described as:

$K_A = [CIP]/[Py^+][I^-]$ (**Equation 9**)

Assuming all pyridiniums and iodides were added as 1-ethyl-4-(methoxycarbonyl)pyridinium iodide, $[Py^+] = [I^-]$, the mass balance equation becomes:

$$C_0 = [Py^+] + [CIP] \quad \textbf{(Equation 10)}$$

Rearranging **Equation 9** and **10** gives

$$K_A = [CIP]/(C_0 - [CIP])^2 \quad \textbf{(Equation 11)}$$

$$K_A[CIP]^2 + (-2K_AC_0 - 1)[CIP] + K_AC_0^2 = 0 \quad \textbf{(Equation 12)}$$

Equation 12 is then put into the quadratic formula, in which only the negative root is physically meaningful, to yield:

$$[CIP] = (C_0 - 0.5/K_A) - 0.5(4C_0/K_A + 1/K_A^2)^{0.5} \quad \textbf{(Equation 13)}$$

[CIP] is directly proportional to the absorbance, A, of the charge-transfer band. The relationship between the observed molar extinction coefficient (ε) and the total concentration of charge-transfer complex added (C_0) is displayed in **Figure 43** for several values of K_A, assuming 1410 $M^{-1}cm^{-1}$ is the molar extinction coefficient for a 100 % ion-paired solution (1410 $M^{-1}cm^{-1}$ was the highest ε ever recorded by Kosower, for 54.8 mM of complex in chloroform)[2].

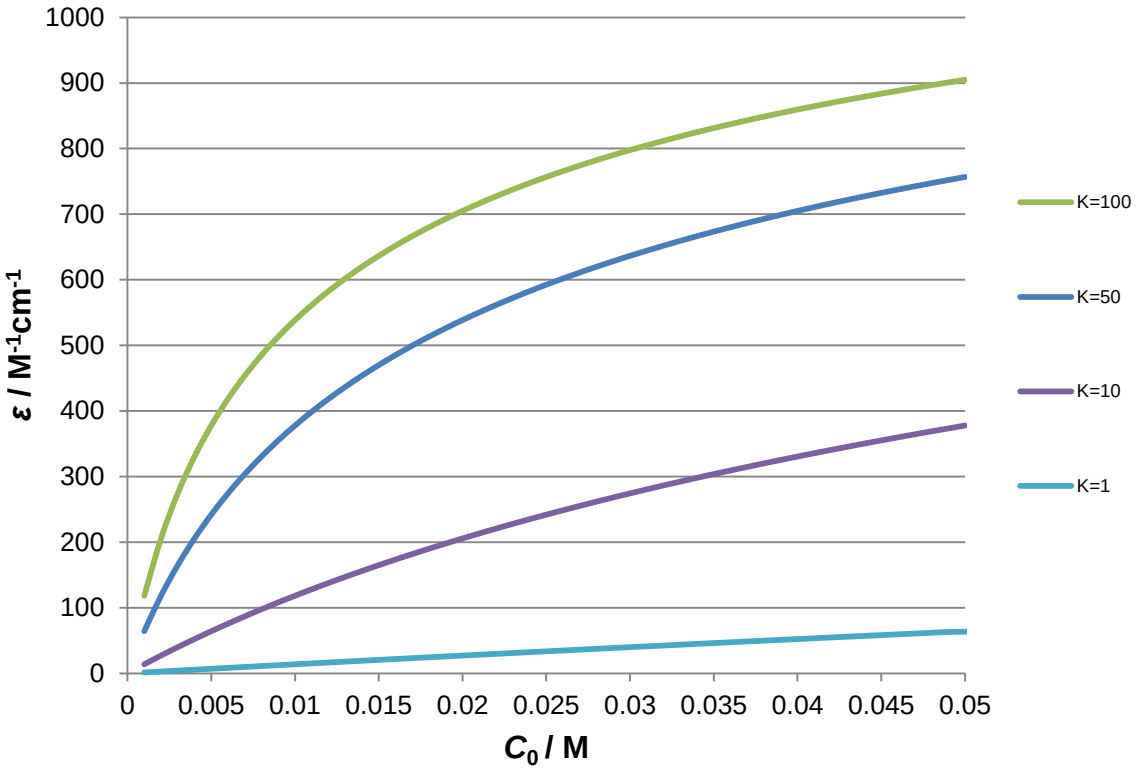

Figure 43 – Theoretical molar extinction coefficient as a function of total concentration of charge-transfer complex, C_0, based on Equation 13

As indicated in **Figure 43**, at low concentration range the only condition under which this generates a near-straight line is when $K_A = 1$. According to this equilibrium model, the results showed that there was no preference in either direction in the ionic liquids for the pyridinium and iodide ions to be associated or dissociated. The occurrence of charge-transfer for these systems was not due to ion-pairing, but because at any instant some pyridinium and iodide ions just happen to be next to each other in this totally ionic solution. Electronic transitions are essentially instantaneous compared with the time scale of ions' motions; therefore charge transfer occurred even if the pyridinium and iodide ions were not held together as intimate ion pairs.

Although the equilibrium model seemed to approximate the experimental data reasonably well, it was realized that this was not a good representation of the ionic

liquid mixtures. In reality neither species (free ions and contact ion pairs) in the above equilibrium (**Scheme 1**) were present in these solutions. In these ionic liquid solutions, an iodide was in contact with a pyridinium ion or a cation of the ionic liquid all the time. Unlike in typical polar molecular solvents, the pyridinium and iodide ions are never “free” in these totally ionic solutions. Therefore, a novel “bulk”, statistical approach was employed to model the ionic liquid mixtures.

3.5 Liquid *pseudo*-lattice model

If the ionic contacts inside these totally ionic solutions are independent of the ions involved, then the number of “apparent” contact ion pairs for the charge transfer complex will be strictly dependent upon the concentration-based probability of the pyridinium and iodide ions coming into contact. These totally ionic solutions can be approximated using a lattice-type model with zero site exchange energy, at any given concentration the statistical probability for the pyridinium and iodide ions being located on adjacent lattice sites can be calculated. Our solution was therefore modelled as a non-discriminating ionic lattice structure. Given that *n* is the ratio of the total number of possible anion sites in the cybotactic shell of each pyridinium cation to the number of sites that give rise to an absorption, where m_I is the number of iodide ions in the solution and m_T is the total number of anions in the solution (calculated from the pure ionic liquid molar volume), then the probability that any given anion in the solvation shell of a pyridinium cation is *not* an iodide would be:

$$(m_T - m_I)/m_T \qquad \textbf{(Equation 14)}$$

The probability that *none* of the *n* anions in the solvation shell of a pyridinium cation are an iodide would be:

$[(m_T - m_I)/m_T]^n$ (**Equation 15**)

Therefore, the probability of having at least one iodide anion in the solvation shell, $P_{[Py]I}$, is:

$P_{[Py]I} = 1 - [(m_T - m_I)/m_T]^n$ (**Equation 16**)

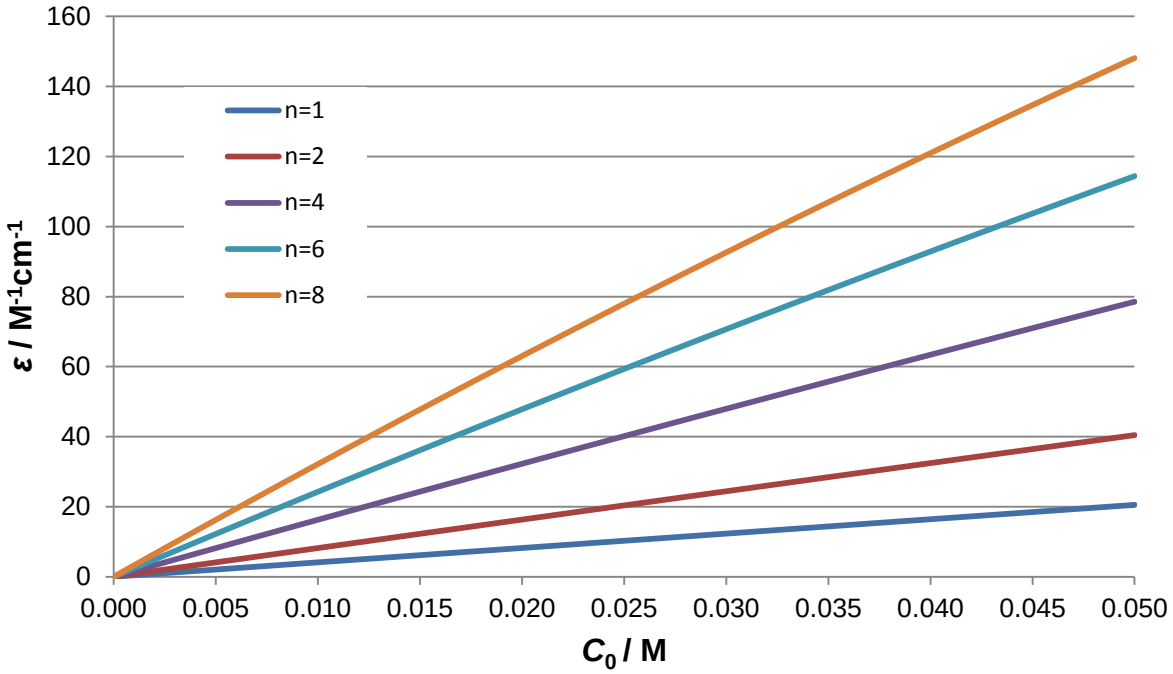

Figure 44 –Theoretical molar extinction coefficient as a function of total concentration of charge-transfer complex, C_0, based on Equation 16

The absorbance will now be proportional to $P_{[Py]I}$. The curves for the concentration-dependence of the molar extinction coefficient for various numbers, *n*, of ions in the cybotactic shell of the pyridinium ion were calculated and are shown in **Figure 44**. At low concentration range (e.g. 0 – 0.2 M), all the graphs are linear. Hence, this *pseudo*-lattice model is consistent with the experimental results.

The slopes of these lines are expected to be proportional to the molar volume of the ionic liquid, with ionic liquids of larger ions yielding bigger slopes. This is also consistent with our experimental findings. Using the value of this slope, as well as

the estimated molar extinction coefficient for 100 % ion-paired solution (1410 $M^{-1}cm^{-1}$),[2] it is possible to approximate the number of anions in the cybotactic region of the pyridinium cation. After correcting for the molar volume of the ionic liquids used in this investigation, the slopes quoted above all collapse to a single value of $n \approx 2$ (**Table 15**). This demonstrates that there were probably two ions around a charge transfer site. Given that it has been shown that there are two sites around the pyridinium cation in which the iodide can give charge transfer (one above and one below the pyridinium)[2], there were probably four ions around each pyridinium.

Ionic Liquid	**Molar Volume / cm^3mol^{-1}**	***n***
$[C_4C_1im][NTf_2]$	0.291[127]	2.036
$[C_4C_1im][OTf]$	0.211[127]	2.323
$[C_4C_1im][BF_4]$	0.190[127]	2.209
$[C_4C_1im][SbF_6]$	0.223	2.272
$[C_4C_1pyrr][NTf_2]$	0.300[128]	1.815
$[C_4C_1C_1im][NTf_2]$	0.302	2.026

Table 15 – Molar volume of ionic liquid and *n* (number of anions in the cybotactic region of a pyridinium cation)

The fact that the charge-transfer behaviour in ionic liquids followed this *pseudo*-lattice model indicates that in these mixtures, the interactions of the different ionic species with their immediate surroundings have very similar energies. Therefore, site exchange energies between ions are near zero and the “solute-solute”, “solute-solvent” and “solvent-solvent” interactions are indistinguishable. In ionic liquid solvents, solute ions are neither held together in classical solvated contact ion pairs nor kept apart as solvated free ions. The results showed that an unique solvation behaviour can exist for salts dissolved in an ionic solvent – the solute behaves as two distinct species, a cation and an anion, completely screened from each other

and interact independently with solvent ions or other solute ions. Thus, the ionic liquid solvents appear to form ideal mixtures with the dissolved Kosower's salt. Although the 6 ionic liquids employed in this investigation have different polarity profiles i.e. they have considerable different hydrogen bond acidities and basicities (α and β), they behaved identically when mixed with Kosower's salt, as no signs of *solute* ion-pairing discovered in these seemingly ideal mixtures. In these mixtures, the strong electrostatic forces dominated solvation; other "supramolecular" interactions had negligible capacity to affect the solvation of Kosower salt in ionic liquids.

3.6 Energy of the metathesis reaction

In this ideal mixture of ions there should be no energy change upon site exchanage. This implies that any ion metathesis taking place within the mixed ions solution will not result in a change to the overall energy of the solution. To further affirm the experimental findings, the energy of the metathesis reaction between Kosower's complex and ionic liquid $[C_4C_1im][OTf]$ (**Scheme 2**) was approximated by theoretical DFT calculations, carried out by Heiko Niedermeyer:[129]

$$[Py]I + [C_4C_1im][OTf] \rightleftharpoons [Py][OTf] + [C_4C_1im]I \qquad \text{(Scheme 2)}$$

The site exchange (**Figure 45**) in this ionic liquid solution can be simplified to the metathesis reaction because: a) the pyridinium iodide salt was not very concentrated (about 0.5 – 5 mol% Kosower's salt in ionic liquids) in these solutions, it can be assumed that at most one of the anions present in the solvation shell of any cation is an iodide. b) we can ignore interactions common to both sides and assuming that any changes on metathesis are symmetrical. If the hypothesis given by the results of

the absorptivity experiment is correct, the energy for the metathesis reaction should be or close to zero.

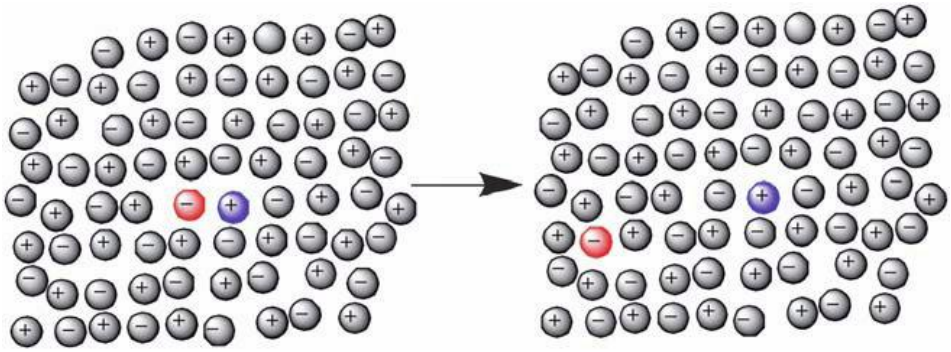

Figure 45 – Site exchange of a liquid *pseudo*-lattice

The results from the DFT calculations demonstrated that there is no particular preferential interaction between two specific opposite ions. The Gibbs free energy of the ion exchange reaction is close to zero (-0.69 $kJmol^{-1}$), which according to the following relationship: $\Delta G^{ex} = -RTlnK^{ex} \approx 0$, $K^{ex} \approx 1$. The result $K^{ex} \approx 1$ is consistent with the results given by the *pseudo*-lattice model.

3.7 Double equilibrium model for molecular solvents

It should be noted that closer examination of the results of measurements of ion association of molecular liquids (1,2-dichloroethane, 1-butanol and MeCN) show that the molar extinction coefficients obtained in these molecular liquids (**Table 16 – 18**) clearly do not fit the single equilibrium model (**Section 3.4, Equation 13**) that was initially used to characterize the ionic liquid data (see **Figure 46**).

Concentration / M	Molar extinction coefficient / $M^{-1}cm^{-1}$
$1.83 \cdot 10^{-4}$	696
$2.19 \cdot 10^{-4}$	695
$3.95 \cdot 10^{-4}$	738
$4.58 \cdot 10^{-4}$	825
$5.48 \cdot 10^{-4}$	804
0.00115	893
0.00224	882
0.00229	912
0.00458	913
0.00460	900
0.00897	965
0.00984	926
0.0183	973
0.0196	966

Table 16 – Molar extinction coefficient versus concentrationsof Kosower's salt in 1,2-dichloroethane

Concentration / M	Molar extinction coefficient / $M^{-1}cm^{-1}$
$5.23 \cdot 10^{-4}$	233
$8.76 \cdot 10^{-4}$	294
0.00162	320
0.00365	385
0.00392	398
0.00486	425
0.00652	441
0.00936	462
0.0110	510
0.0130	491
0.0145	517
0.0259	551
0.0295	580
0.0387	598
0.0437	626

Table 17 – Molar extinction coefficient versus concentrations of Kosower's salt in 1-butanol

Concentration / M	Molar extinction coefficient / $M^{-1}cm^{-1}$
0.00582	74
0.0116	115
0.0232	180
0.0346	213
0.0466	251
0.0594	290

Table 18 – Molar extinction coefficient versus concentrations of Kosower's salt in MeCN

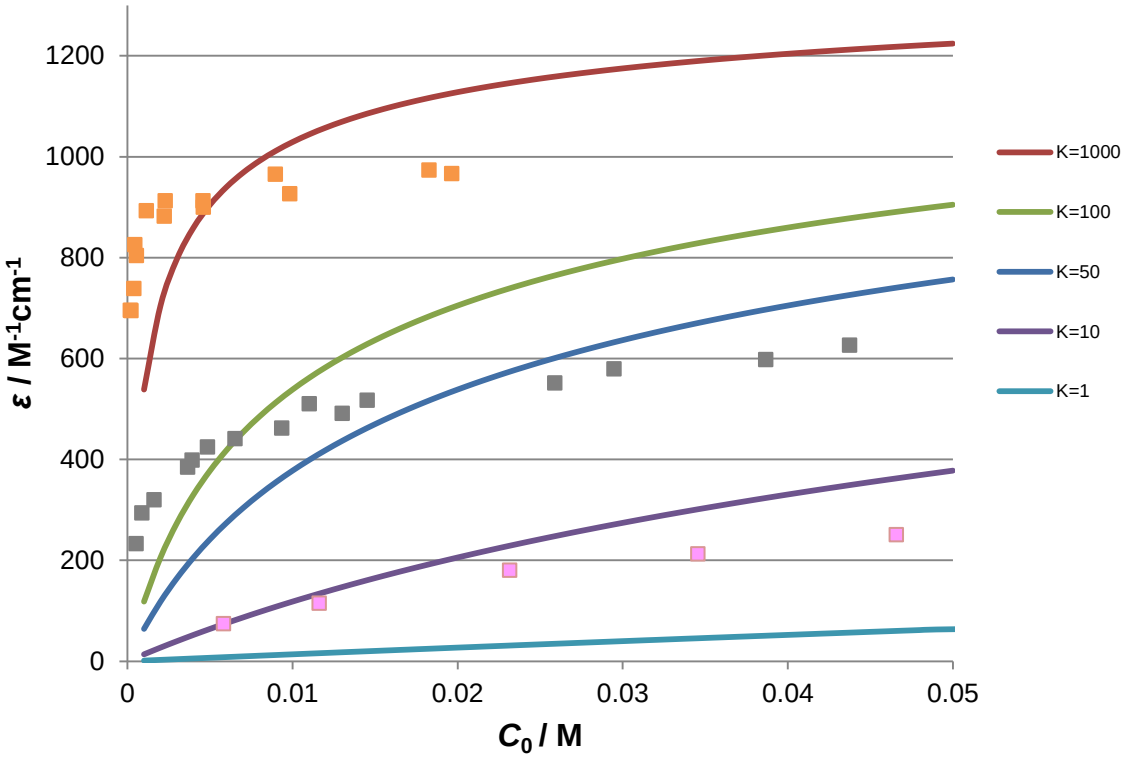

Figure 46 – Experimental data of Kosower's salt in 1,2-dichloroethane (orange), 1-butanol (grey) and MeCN (pink) overlap with the theoretically predicted curves generated by Equation 13

This is because the single equilibrium model assumes only two types of species (free ions and contact ion pairs) are present in solution, ignoring the possibility of the existence of other species (e.g. solvent separated ion pairs, quadrupolar ion pairs and higher aggregates) in molecular solutions. Bagchi[130] and Hemmes and co-workers[131-132] both reported evidence for the presence of solvent-separated ion pairs

(SSIP) in the molecular solutions of *N*-alkylpyridinium iodide. Binder *et al*. also suggested the presence of solvent-separated ion pairs in solutions of 1-alkyl-4-(cyanopyridinium) iodide.[126] An alternative model based upon the following two step mechanism (**Scheme 3**)[42, 126] was thus used to characterize the data for molecular liquids:

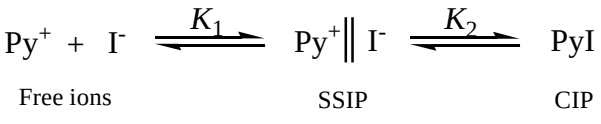

(**Scheme 3)**

$K_1 = [SSIP]/[Py^+][I^-]$ (**Equation 17**)

$K_2 = [CIP]/[SSIP]$ (**Equation 18**)

Assuming all pyridiniums and iodides were added as Kosower's complex, $[Py^+] = [I^-]$:

$C_0 = [Py^+] + [SSIP] + [CIP]$ (**Equation 19**)

$K_1[Py^+]^2 = [SSIP]$ (**Equation 20**)

$K_2[SSIP] = [CIP]$ (**Equation 21**)

$K_1^{-1}[SSIP] = [Py^+]^2$ (**Equation 22**)

$K_1^{-1}K_2^{-1}[CIP] = [Py^+]^2$ (**Equation 23**)

$[Py^+] = K_1^{-0.5}K_2^{-0.5}[CIP]^{-0.5}$ (**Equation 24**)

Rearranging **Equations 19**, **21** and **24** gives

$C_0 = K_1^{-0.5}K_2^{-0.5}[CIP]^{-0.5} + K_2^{-1}[CIP] + [CIP]$ (**Equation 25**)

$(1 + K_2^{-1})[CIP] + K_1^{-0.5}K_2^{-0.5}[CIP]^{-0.5} - C_0 = 0$ (**Equation 26**)

This new model (**Equation 26**) has two variables, K_1 and K_2. With the use of iteration, the best fit for this model to the molecular solvent data is presented as **Figure 47** and the equilibrium constants obtained are included as **Table 19**. Again, the ε of 100% ion-paired solution is 1410 $M^{-1}cm^{-1}$.

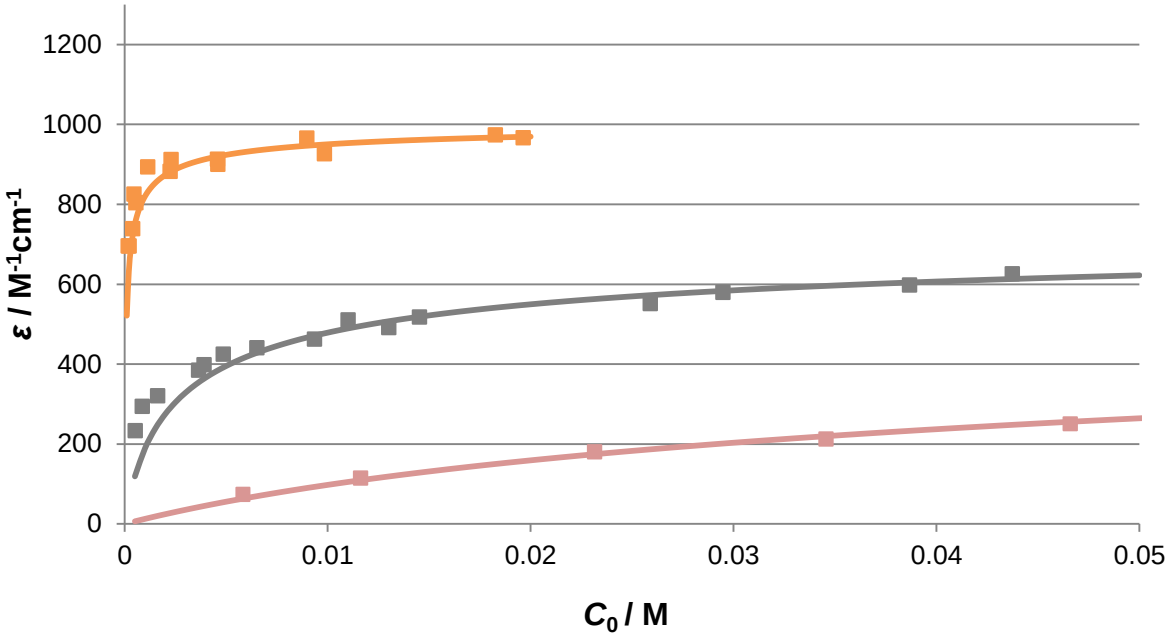

Figure 47 – Double equilibrium model fitting for 1,2-dichloroethane (orange), 1-butanol (grey) and MeCN (pink)

Solvent	K_1	K_2
1,2-dichloroethane	5990	2.59
1-butanol	195	1.21
MeCN	8.63	1.07

Table 19 – K_1 and K_2 for molecular solvents

Our results for molecular liquids confirm the Coulomb's law, as both K_1 and K_2 decrease with increasing dielectric constant. For example, K_1 decreases from a value of **5990** in 1,2-dichloroethane (ε_r = 10.7) to **8.63** in MeCN (ε_r = 36). Meanwhile K_2 decreases from **2.59** to **1.07**. These results were in accordance with the

Coulomb's law, demonstrated that the extent of ion association/dissociation depended strongly on the permittivity of solvent. Note that in the double equilibrium model the equilibrium of clustering of single CIPs was not included, since this model was sufficient to fit my data.

These results demonstrated that SSIPs and CIPs were both present in molecular solvents. On the other hand, the charges of opposite ions are effectively screened in ionic liquid solutions; therefore neither SSIPs nor CIPs were present in ionic liquids.

3.8 Z values of ionic liquids

In molecular liquids, the Z value depends somewhat upon the Kosower's salt concentration - the lower the Z, the greater its sensitivity to the complex concentration.[2]

For instance, a substantial change was observed in 1,2-dichloroethane in which the Z values went from 63.3 $kcalmol^{-1}$ at 0.2 mM to 65.1 $kcalmol^{-1}$ at 20 mM (**Figure 48**).

Polarity increases with concentration simply because these solutions become more "ionic" as more complex is added. On the other hand, no or small effects were found in more polar liquids (e.g. in 1-butanol and MeCN). As the concentrations of Kosower's salt proved to play such a significant part in determining the position of the charge transfer band, polarity comparison with Z values is not simple for solvents. The ideal scenario would be when there is a simple direct proportional relationship between complex concentrations and Z values so that Z values of pure solvents can be determined by extrapolation to $C_0 = 0$. **Figure 48** illustrates how Z values change with complex concentrations in 1,2-dichloroethane and the two variables do not form a direct proportional relationship as we would like.

Consequently, comparisons of *Z*-values for different solvents were made at a fixed concentration. It is simply not possible to measure Z for less polar solvents (such as dichloroethane) correctly since Z changes so much with concentration of Kosower's salt in these solutions.

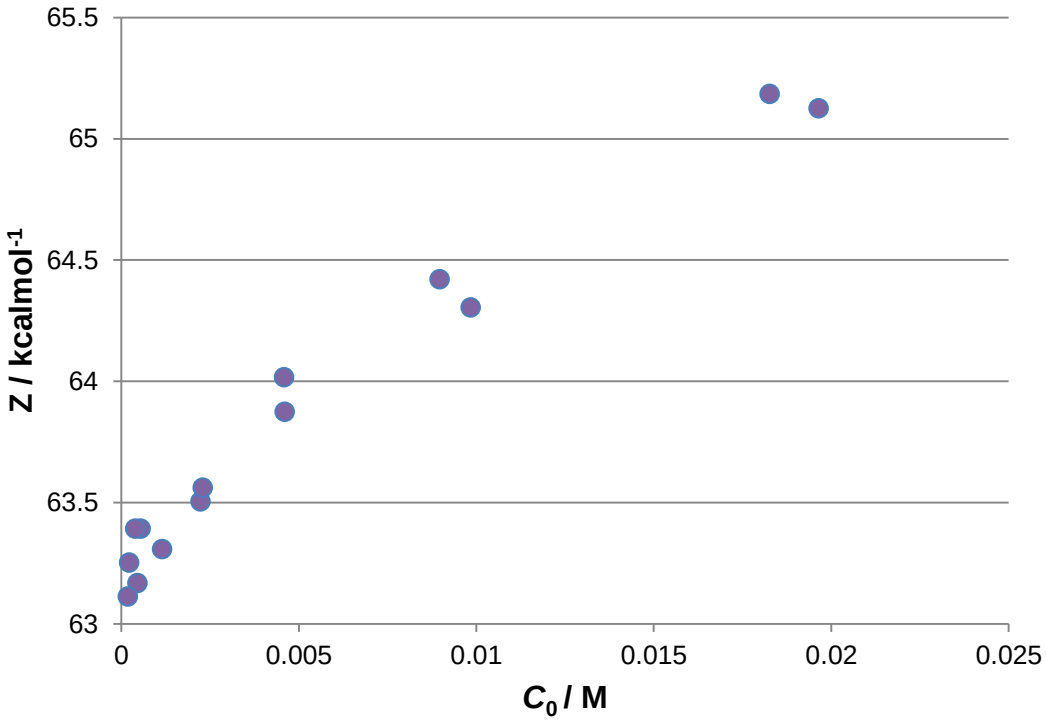

Figure 48 – Z versus Concentration of Kosower's salt in 1,2-dichloroethane

Our common ionic liquids have *Z*-values in the range of 72.7-76.5 kcalmol^{-1} (see **Table 20**), which is generally lower than those of polar protic liquids (*e.g*. 1-butanol) and higher than polar non-hydrogen-bonding liquids (*e.g*. MeCN).

Liquid	Z / kcalmol^{-1}	α	β	π*
Water	94.6[133]	1.16[35]	0.50[35]	1.13[35]
Methanol	83.6[133]	1.05[35]	0.61[35]	0.73[35]
Ethanol	79.6[133]	0.86[133]	0.75[133]	0.54[133]
Acetic acid	79.2[133]	1.12[133]	0.45[133]	0.64[133]
1-butanol	78.6	0.84[133]	0.84[133]	0.47[133]
$[C_4C_1im][BF_4]$	76.5	0.62	0.37	1.05
$[C_4C_1im][OTf]$	76.0	0.62	0.49	1.00
$[C_4C_1im][SbF_6]$	75.8	0.62	0.15	1.04
$[C_4C_1im][NTf_2]$	74.3	0.61	0.23	0.99
$[C_4C_1pyrr][NTf_2]$	73.3	0.42	0.26	0.96
$[C_4C_1C_1im][NTf_2]$	72.7	0.38	0.26	1.02
Propylene carbonate	72.4[133]	0.00[133]	0.40[133]	0.83[133]
MeCN	71.3[133]	0.35[35]	0.37[35]	0.80[35]
DMSO	70.2[133]	0.00[133]	0.76[133]	1.00
1,2-dichloroethane	65.2	0.00[133]	0.10[133]	0.81[133]

Table 20 – Z values and Kamlet-Taft parameters for various molecular solvents and ionic liquids (unmarked are experimental data)

The Z values of ionic liquids $[C_4C_1im][OTf]$ and $[C_4C_1im][BF_4]$ vary strongly with concentrations (**Figure 49**), but the direction of the change is opposite to that of 1,2-dichloroethane (see **Figure 48**). The two ionic liquids are less polar when more complex is added; this behaviour has never been seen for molecular liquids. This unfamiliar behaviour is caused by the fact concentrations of Kosower's salt used in these ionic liquid experiments are so high (about 0.5 – 5 mol% Kosower's salt in ionic liquids) that it is possible to have two or more iodide anions around the pyridinium cations at the same moment. As concentration of the complex increases, more iodide anions would be adjacent to the pyridinium cations; at the same time, there would be less $[BF_4]^-$ or $[OTf]^-$ ions around the pyridinium ions. The decrease in the number of the more polar $[BF_4]^-/[OTf]^-$ as well as the increase in the number of the less polar I^- around the cybotactic region of pyridinium cause an overall decrease

in polarity (i.e. Z) of that region. On the other hand, $[NTf_2]^-$/$[SbF_6]^-$and I^- are much more similar in terms of polarity; therefore, concentration of Kosower's salt has much less effect on the Z measured in $[C_4C_1im][NTf_2]$, $[C_4C_1pyrr][NTf_2]$, $[C_4C_1C_1im][NTf_2]$ and $[C_4C_1im][SbF_6]$.

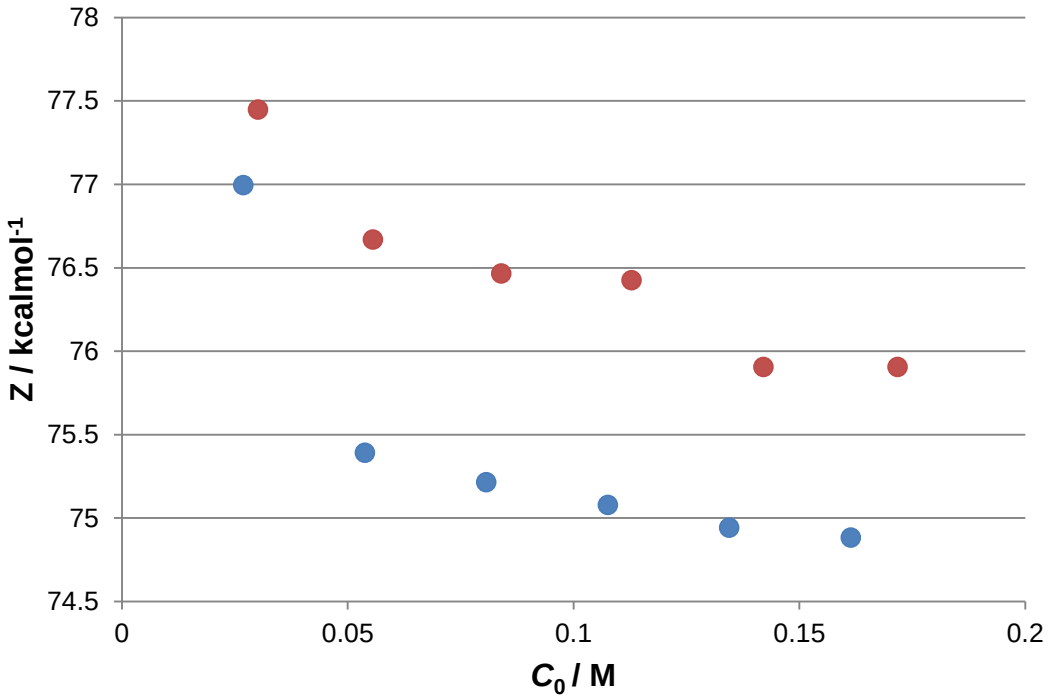

Figure 49 – Z versus Concentration of Kosower's salt in $[C_4C_1im][OTf]$ (Blue graph) and $[C_4C_1im][BF_4]$ (Red graph)

3.8.1 Z's relationships with Kamlet-Taft parameters

The single-parameter approach of Z scale cannot be considered as a universal polarity scale. 1-ethyl-4-(methoxycarbonyl)pyridinium iodide is sensitive to a combination of non-specific and specific interactions, but not them separately. Using molecular solvents' Z values and Kamlet-Taft parameters reported elsewhere,[133] a regression analysis was carried out between Z and different Kamlet-Taft parameters. It was found that Z correlates best with α and π* (**Figure 50**); that means like Reichardt's dye, Kosower's salt is sensitive to both the hydrogen bond acidity and

polarity of solvents. Common ionic liquids have lower α than polar protic liquids but higher α than polar aprotic liquids, hence their Z-values of ionic liquids are in between the numbers for polar protic solvents and those for polar aprotic solvents.

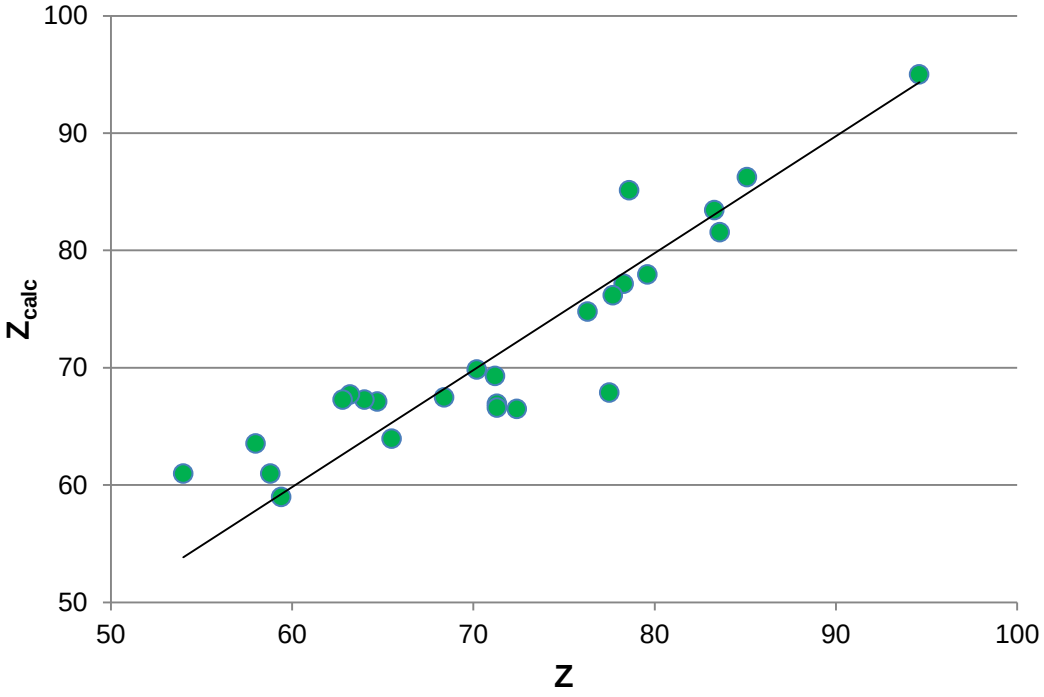

Figure 50 – Z_{calc} (Z_{calc} = 50.10 + 19.75π* + 19.99α) versus Z (empirical data measured in molecular solvents by Kosower[2])

3.9 Resolving the "contradictory results"

The apparent ideal ionic liquid mixtures in this investigation contradict with common observations: salts like alkali metal halides i.e. the by-products of ionic liquid synthesis do not mix with typical ionic liquids. These results also contrasted with the one from Seddon,[134] who reported the phenomenon of immiscible ionic liquids – non-ideal ionic liquids mixing behaviour. The non-ideal behaviour observed elsewhere arose mainly because of poor size matching. For example in NaCl, the sizes of Na^+ and Cl^- ions are similar and are much smaller than those of ionic liquids. The similarity in sizes enables the ions to occupy lattice sites of approximately the same

size, thus forming very favourable lattice energies. This does not point toward preferential ion-pairing in the *ionic liquid solution*, rather the formation of crystallized solid is entropically more favourable. Seddon's investigation also involved ionic liquids of ions of significantly different sizes. His group attempted to mix the large $[P(C_6H_{13})_3(C_{14}H_{29})]Cl$ ionic liquid with the much smaller $[C_nC_1im]Cl$ ($n < 6$) and found the two immiscible.[134] The mixing of $[C_2C_1im][C_1SO_3]$ and $[P(C_6H_{13})_3(C_{14}H_{29})][NTf_2]$ was also attempted by the same group,[134] and again two phases were formed. The small $[C_2C_1im]^+$ cation preferred to associate with the small $[C_1SO_3]^-$ and the larger $[P(C_6H_{13})_3(C_{14}H_{29})]^+$ and $[NTf_2]^-$ ions associate with each other in the upper phase.[134] Once more, there was preferential ion association *between phases*, but not *within each phase*. These examples demonstrated systems where ion association between multiple phases is entropically driven with no illustration of enthalpic association (ion-pairing) within the phases. Seddon reported that for the mixing of $[C_nC_1im]Cl$ ($n = 2$-5) and $[P(C_6H_{13})_3(C_{14}H_{29})]Cl$, ΔH of mixing was negligible (between -2 and +2 kJ mol^{-1}) while the $T\Delta S$ of mixing was dominant (-4.5 and -12 kJ mol^{-1}).[134] These results further indicated that mismatched ion size (i.e. entropy) is responsible for the biphasic behaviour.

As this and previous results[1] have suggested, ionic liquids are liquids that should have very high apparent dielectric constants. On the other hand, Weingärtner's microwave dielectric spectroscopy measurements indicate that ionic liquids are solvents of only moderate polarity (i.e. higher than 1,2-dichloroethane, lower than 1-butanol and MeCN).[31-32] However, this difference does not mean one of these results is necessarily wrong. In fact, any model that involves the movement of molecules or ions necessarily implies the importance of timescales. The absorptivity (molar extinction coefficient) measurements are concentration-based equilibrium

measurements that are in longer timescale, which allows ion motion to dominate solvation. In addition, according to the Hole Theory, the diffusion rate of ions inside the ionic liquids is very slow due to their large sizes;[135] that means the time for the different ions to reorganize and reach their equilibrium positions is much longer than the time for electron excitation. For example, the self-diffusion coefficient of $[C_4C_1im][NTf_2]$ is 3.83×10^{-11} m^2/s.[117] Conversely, the dielectric spectroscopy measurements by Weingärtner resulted from measurement of a rapid dielectric polarization. The timescale of the dielectric spectroscopy measurements (region of 10^{-9} to 10^{-12} s) are much shorter than the one of my absorptivity measurements (time for the ions to reach their equilibrium positions). It can be thought as that the dielectric spectroscopy "freezes out" ionic movement and the "snapshot" of the ionic liquid that is obtained ostensibly appeared less polar. Therefore, these experimental findings did not automatically disprove Weingärtner's results; and the question of how polar are ionic liquids very likely depends upon when you ask. Ionic liquids can be thought as very polar species on long timescale, and moderately polar species on short timescale.

3.10 Conclusion

In this investigation, the results showed that the ionic charge transfer complex 1-ethyl-4-(methoxycarbonyl)pyridinium iodide, does not form preferential ion pairs in room temperature ionic liquids, but rather ideal solutions. Ionic liquids can completely separate the solute cations and anions from each other in these totally ionic solution. However, this does not mean that the solute cations and anions are never in contact, just that this contact is random. In these ionic ideal mixtures, the identity of individual ions does not seem to matter; the solute ions are so separated as to be made into

completely unrelated species. In other words, ion solutes are neither “associated” nor “dissociated” in the classical sense; on the contrary, the sum of ionic contacts between the solutes in an ionic liquid is simply given by a concentration-based statistical distribution. However, one must note that these results are based upon observations of 1-ethyl-4-(methoxycarbonyl)pyridinium iodide in 6 different ionic liquids. These are mixtures of salts composed of similar ions, particularly in terms of relative sizes. It is possible that mixtures of more dissimilar salts would deviate from this kind of ideal behaviour, as Arce and co-workers had demonstrated that trihexyltetradecylphosphonium chloride and 1-alkyl-3-methylimidazolium chloride (where the alkyl group is shorter than hexyl) are mutually immiscible.[134]

In molecular solvents such as 1,2-dichloroethane and MeCN, ionic compounds exist as solvated free ions, solvent-separated ion pairs and contact ion pairs; in each case the solute cation and anion require each other’s proximity in order to preserve charge neutrality. Ionic liquids, conversely, can solvate individual solute ions completely as the ionic liquid itself is capable of preserving charge neutrality.

The results of this investigation did not necessarily contradict with Weingärtner’s permittivity measurements, which suggested ionic liquids as moderately polar solvents.[31-32] The absorptivity measurements in this investigation involved a longer timescale, allowing ion movement to dominate solvation, yielding a very high polarity for ionic liquids. While Weingärtner’s measurements recorded “snapshots” of the ionic liquid, “froze out” ionic movement and so the ionic liquid appeared less polar.

4 Nucleophilic reactions of ionic reactants in ionic liquid/molecular solvent mixtures

4.1 Introduction

Much of the interest in ionic liquids has been in their potential application as solvents for chemical synthesis and catalysis.[50] Many of the works published in the area have been carried out in a way of "trial and error", as fundamental solvent kinetic and thermodynamic effects of ionic liquids on typical organic and inorganic reactions have only been investigated by small number of research groups.[1, 52-58, 136] The kinetic and thermodynamic studies showed us that for most organic reactions, the mechanisms found in ionic liquids are similar to those in polar molecular solvents.

As described earlier, the search of a unique "ionic liquid effect" was accomplished two years ago when the Welton group discovered that the S_N2 reaction of a charged electrophile with halide ion in ionic liquids followed a fundamentally different pathway as compared to the same salts reacting in molecular solvents.[1] It was reported that the reactions of charged nucleophiles and charged electrophiles in molecular liquid solutions proceed *via* ion pairs, while in ionic liquids the same reaction proceed *via* "free" solvated ions as ionic liquids are "super-dissociating" solvents towards solute salts.[1]

The viscous nature of ionic liquids introduces engineering issues, such as uneven concentration and temperature distributions, as results of poor mass and energy transfer within chemical reactors. This is one of the reasons why there have been many on-going studies looking at fundamental properties and reactions in ionic liquid/molecular solvent mixtures, which have lower viscosities than a pure ionic liquid.[59-60]

In this investigation, the rates of the nucleophilic substitution of electrophilic dimethyl-4-nitrophenylsulfonium salt with nucleophilic halide ion in ionic liquid/molecular solvent mixtures were investigated. The results would give us an understanding of behaviour of reactions of charged nucleophiles and charged electrophiles in ionic liquid/molecular liquid mixtures.

4.1.1 Choice of ionic liquid

Due to time constraints, it was not possible to investigate the solvent effects of mixtures of many ionic liquids. Hence only ionic liquid/molecular solvent mixtures of one ionic liquid were tested in this investigation, and this ionic liquid was $[C_4C_1pyrr][NTf_2]$. $[C_4C_1pyrr][NTf_2]$ was the choice of ionic liquid because it has relatively low hydrogen bonding capabilities compared to other popular ionic liquids; pyrrolidinium's hydrogen bond acidity is weaker than imidazolium's and protic cations',[35] and out of all the stable common anions (e.g. ions which do not undergo hydrolysis) for ionic liquids, $[NTf_2]^-$ has the weakest hydrogen bond accepting ability. Hence for $[C_4C_1pyrr][NTf_2]$, the hydrogen bonding contribution to the ionic liquid's overall polarity is relatively low compared to other common ionic liquids. The "purer" ionic nature of $[C_4C_1pyrr][NTf_2]$ renders it a good representative for all ionic liquids.

4.1.2 Choice of co-solvents

The aim was to investigate the kinetic effect of the reaction $[p\text{-}NO_2PhS(CH_3)_2][NTf_2]$ and bromide in mixtures of $[C_4C_1pyrr][NTf_2]$ and different types of molecular solvents. Ionic liquids are not miscible with non-polar solvents (i.e. $\varepsilon_r \leq 7$ and low π^*), hence the kinetic studies can only be carried out in ionic liquid/polar solvent mixtures. It was decided to include solvents of different hydrogen bonding capabilities; therefore a

solvent of high α and high β, a solvent of high α and low β, a solvent of low α and high β, a solvent of low α and low β were chosen for the investigation.

The choices of solvents are summarized in the following table (**Table 21**):

α	β	π*	Solvent examples	Remark
High	High	High	Methanol, 1-butanol	**Benzyl alcohol** was selected
High	High	Low	*Unavailable*	
High	Low	High	Trifluoroethanol, hexafluoro-2-propanol	Reactions in solvents of this category were found to be too slow to monitor
High	Low	Low	*Unavailable*	
Low	High	High	MeCN, DMSO	**MeCN** was selected
Low	High	Low	*Unavailable*	
Low	Low	High	DCM, 1,2-dichloroethane	**1,2-dichloroethane** was selected
Low	Low	Low	Hexane	Not miscible with ionic liquids

Table 21 – Choice of co-solvents in this investigation

4.1.3 Choice of electrophile and nucleophile

The salt dimethyl-4-nitrophenylsulfonium *bis*(trifluoromethanesulfonyl)imide ([*p*-$NO_2PhS(CH_3)_2$][NTf_2]) was selected as the standard electrophile of this experiment. The anion of this salt is the same as the one of ionic liquid chosen for this investigation; therefore confusion could be avoided. [C_4C_1pyrr]Br was selected as the standard nucleophile for similar reason; the cation of the salt is the same as that of ionic liquid. [C_4C_1pyrr]Br was chosen ahead of [C_4C_1pyrr]Cl simply because the

former is less hygroscopic and leads to more accurate measurements. The two reactants would react to form the demethylated product (**Figure 51**):

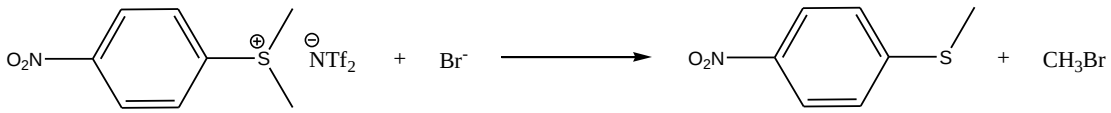

Figure 51 – Reaction of [*p*-$NO_2PhS(CH_3)_2$][NTf_2] with bromide ion

4.1.4 Synthesis of starting materials

The nucleophile [C_4C_1pyrr]Br was synthesized as described in **Section 2.4.2**.

The electrophile dimethyl-4-nitrophenylsulfonium *bis*(trifluoromethanesulfonyl)imide was produced in a two-step synthesis (**Figure 52**). First, the readily available *p*-nitrothioanisole was methylated by reacting dimethylsulfate, forming dimethyl-4-nitrophenylsulfonium methyl sulfate. This salt then underwent an ion exchange reaction with lithium *bis*(trifluoromethanesulfonyl)imide to form the desired product.

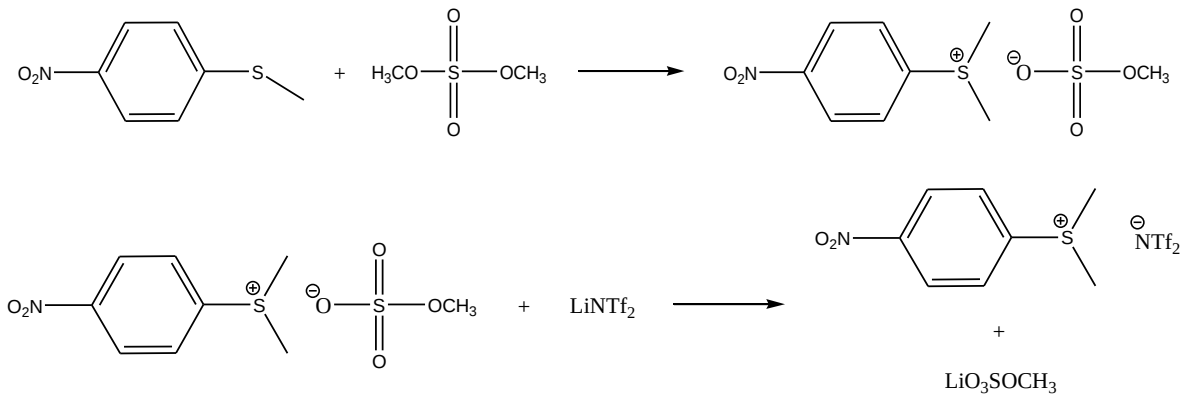

Figure 52 – Synthesis of [*p*-$NO_2PhS(CH_3)_2$][NTf_2]

4.1.5 Kinetic methodology

For conventional reactions, methods to determine rates usually involve measuring concentrations as a function of time. However, it is normally necessary only to

monitor some physical property of the system (e.g. conductance for ionic reagents, optical rotation for chiral molecules) which indicates the extent of reaction. For instance, UV/Vis spectroscopy enabled continuous and rapid measurement of the electronic transitions of reactants/products as a function of time. According to the Beer-Lambert law, the absorbance and the concentration are directly proportional; hence it is perfectly applicable to measure rates of reactions with UV/Vis spectroscopy.

The integrated rate equations and hence the treatment of kinetic data becomes more complex as the reaction order increases. It is easier to generate *pseudo*-first order conditions, which simplify a kinetic study of a reaction. For our bimolecular, second-order reaction, the nucleophile Br^- ion was used in large excess (i.e. >100 times excess), so that its concentration remains effectively constant. Thus we only need to consider the change in absorptions of the electrophile [*p*-$NO_2PhS(CH_3)_2$][$N(Tf)_2$] or the demethylated product *p*-NO_2PhSCH_3 with respect to time.

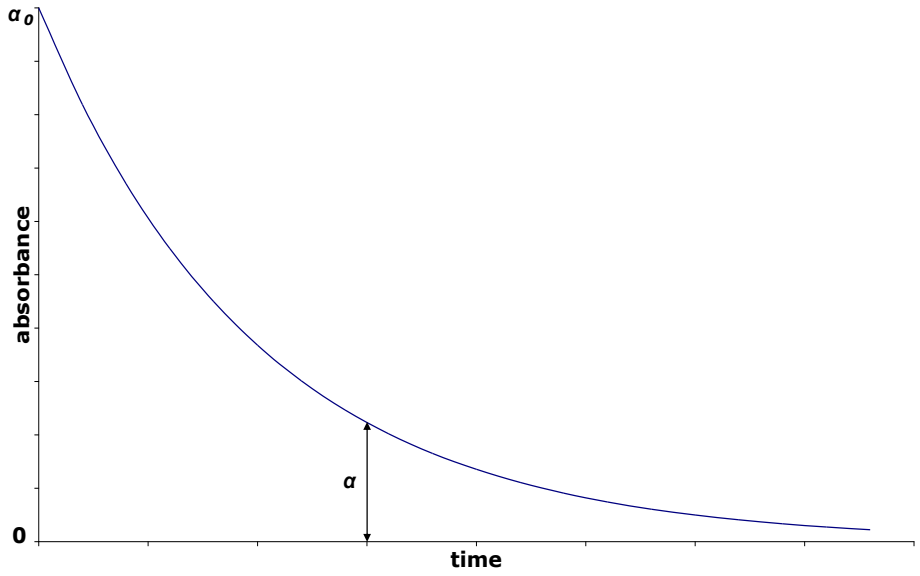

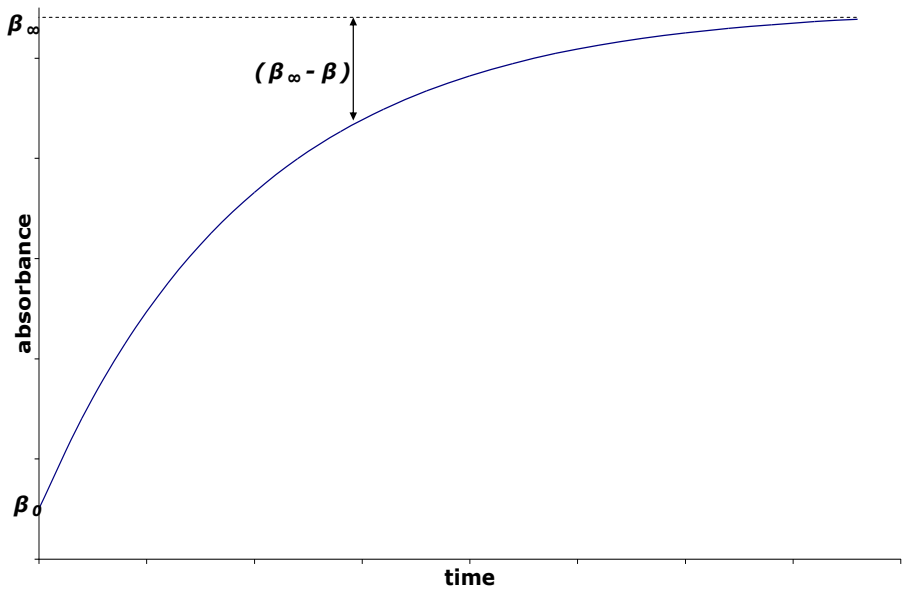

Figure 53 – The course of a first order reaction is accompanied by a decrease reactant's absorbance α, and an increase in product's β

The reactions were carried out using *pseudo*-first order conditions; hence the use of a first order kinetic analysis was appropriate. Since the absorbance varies linearly with the extent of reaction, the absolute concentrations of the reactants or products need not to be known. The course of the reaction is accompanied by a decrease of reactant's absorbance α, and an increase in product's absorbance β (**Figure 53**). α is directly related to the concentration of reactant A.

$A_0 = C(\beta_\infty - \beta_0)$ (**Equation 27**)

$A = C(\beta_\infty - \beta)$ (**Equation 28**)

Where C is proportionality constant related to the absorption coefficients of reactants and products. Substitution of these equations into the integrated first-order rate equation, gives the corresponding equations expressed in terms of the solution absorbance:

$\ln(\beta_\infty - \beta) = -kt + \ln(\beta_\infty - \beta_0)$ (**Equation 29**)

This shows that the absorbance approaches the value at the end of the reaction (infinity value) with the same rate constant, k, as that for the reaction expressed in terms of the reactant concentration. The rate constant can be obtained directly from the slope of a plot of $\ln(\beta_\infty - \beta)$ versus time.

In the situation when the final absorptions of a reaction are unknown (e.g. for very slow reactions), the following method was applied. The reaction again can be followed by observing the increase in absorbance. If time t_1, t_2, t_3, ..., absorptions B_1, B_2, B_3, …, and times $t_1 + \Delta$, $t_2 + \Delta$, $t_3 + \Delta$, …., absorptions $B_1 + \Delta$, $B_2 + \Delta$, $B_3 + \Delta$, …., are selected, where Δ is a constant time interval (**Figure 54**), it follows that:

$$B_\infty - B_t = (B_\infty - B_0)e^{-kt} \qquad \textbf{(Equation 30)}$$

$$B_\infty - B_{t+\Delta} = (B_\infty - B_0)e^{-k(t+\Delta)} \qquad \textbf{(Equation 31)}$$

Subtracting **Equation 30** from **31** gives

$$B_{t+\Delta} - B_t = (B_\infty - B_0)e^{-kt}(1-e^{-k\Delta}) \qquad \textbf{(Equation 32)}$$

$$\ln(B_{t+\Delta} - B_t) = -kt + \ln(B_\infty - B_0)(1- e^{-k\Delta}) \qquad \textbf{(Equation 33)}$$

$$\ln(B_{t+\Delta} - B_t) = -kt + c \qquad \textbf{(Equation 34)}$$

where $c = \ln(B_\infty - B_0)(1- e^{-k\Delta})$ is a constant. Thus a plot of $\ln((B_{t+\Delta} - B_t)$ against time should be linear with a slope equal to –k. For good accuracy the time interval between the two series of readings, Δ, should be at least two times the half-life.

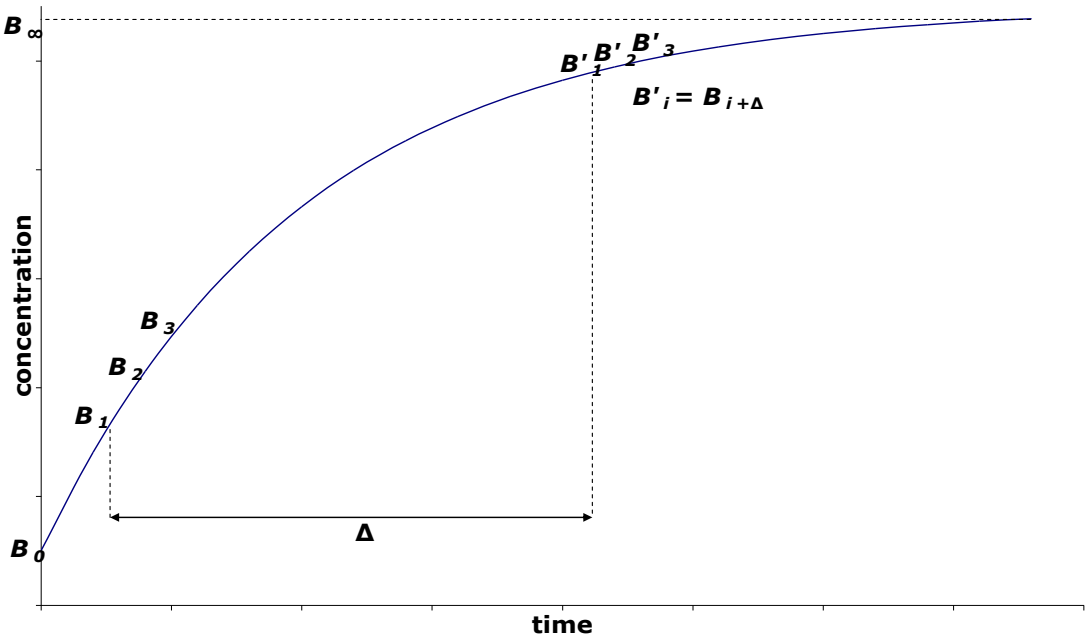

Figure 54 – The second method of determining k_{obs}

The second-order rate constant (k_2) for the reaction can be extrapolated by means of linear regression (*pseudo*-first order rate constant $k_{obs} = k_2[Br^-]_0$).

4.1.6 Background of the reaction[1, 137]

In the previous investigation carried out by Ranieri *et al.*, the rates of reaction of the trifluoromethanesulfonate and *bis*(trifluoromethanesulfonyl)imide salts of dimethyl-4-nitrophenylsulfonium ($[p\text{-}NO_2PhS(CH_3)_2]^+[X]^-$; $[X]^- = [OTf]^-, [N(Tf)_2]^-$) with halide ion were measured in pure ionic liquids and molecular liquids.[1, 137] The rate of this bimolecular reaction was quantified by using large excess of one reagent to give *pseudo*-first order kinetic behaviour, which is linear dependence of k_{obs} upon nucleophile (chloride ion) concentration. This linearity was observed when the reaction was performed in an ionic liquid (**Figure 55**).

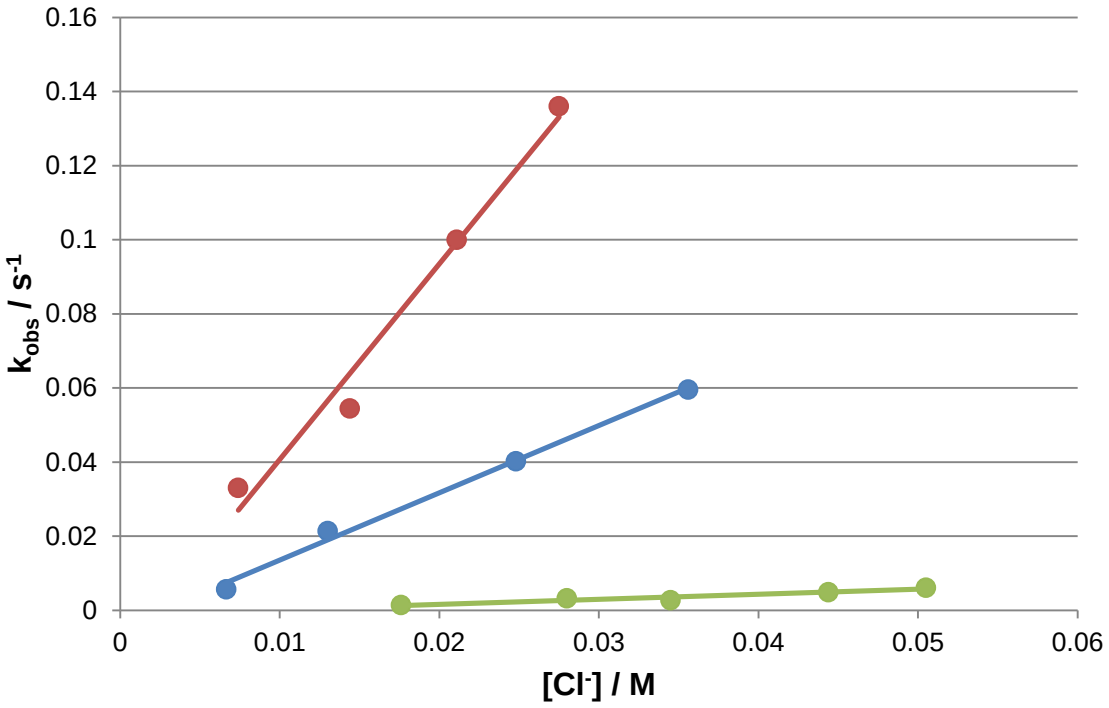

Figure 55[137] – Kinetic results of the reaction between dimethyl-4-nitrophenylsulfonium salt and chloride in ionic liquids. The acidic proton of [C4Him][OTf], which could neutralize and completely deactivate the chloride anion, might also have an effect on the reaction rates. (Red line: [C_4C_1pyrr][OTf]; blue line: [C_4C_1im][NTf_2]; green line: [C_4Him][OTf])

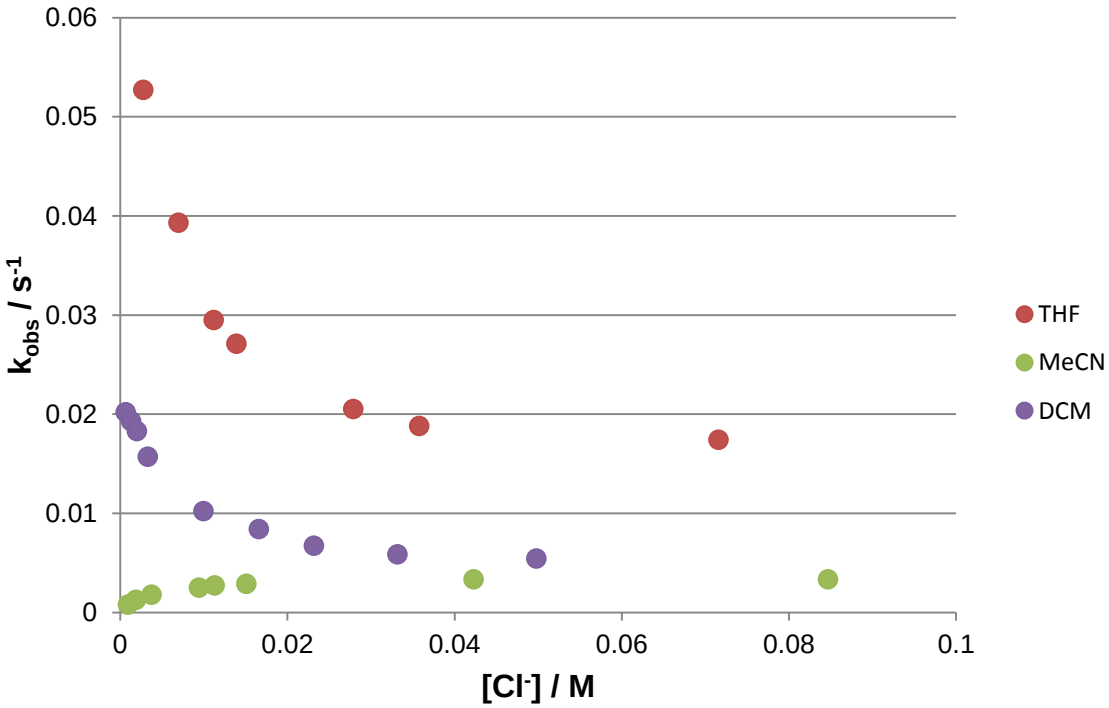

Figure 56[1, 137] – Kinetic results of the reaction between dimethyl-4-nitrophenylsulfonium salt and chloride in in molecular solvents

Conversely, when a molecular solvent was used non-linear partial-order (for polar solvents like MeCN) or negative-order kinetics (for non-polar solvents like DCM) were observed (**Figure 56**). In molecular solvents, an ion metathesis reaction occurs to give dimethyl-4-nitrophenylsulfonium chloride (**Figure 57**).

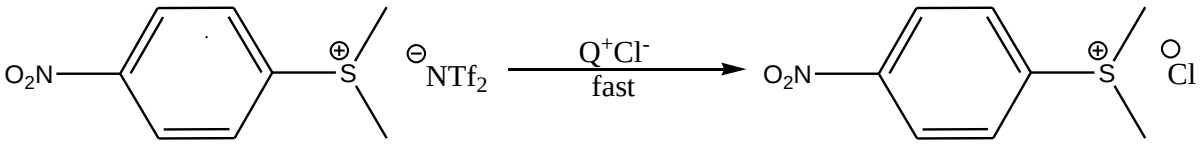

Figure 57 – Ion metathesis reaction of dimethyl-4-nitrophenylsulfonium *bis*(trifluoromethanesulfonyl)imide to give dimethyl-4-nitrophenylsulfonium chloride (Q^+ refers to the quaternary cation originally associated with the chloride ion)

This salt exists as reactive ion pairs in solution for polar solvents or precipitates for non-polar solvents (**Figure 58**):

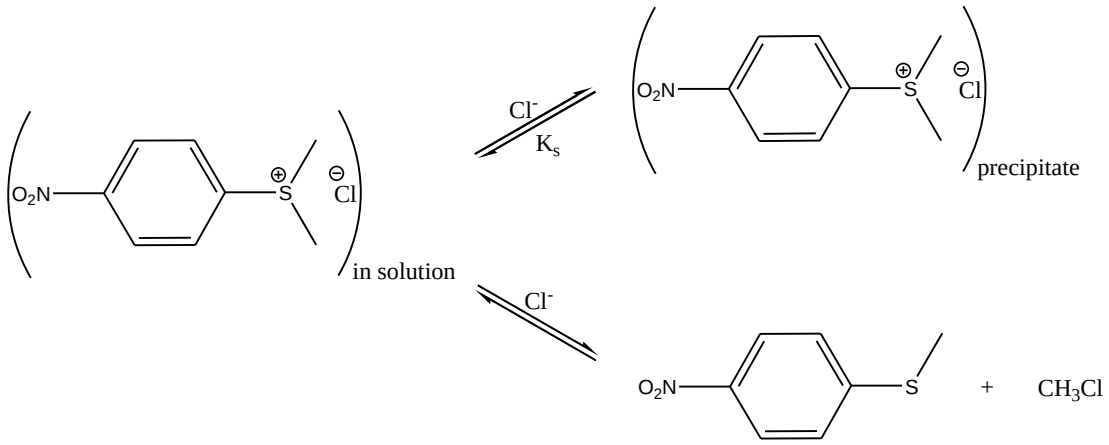

Figure 58 – Formation of precipitates and product from ion pairs in solution

For reactions in non-polar molecular solvents such as DCM, THF and acetone, as the concentration of tetrahexylammonium chloride (Q^+Cl^-) is increased, the equilibrium for the metathesis (**Figure 58**) leads to the greater formation of dimethyl-4-nitrophenylsulfonoium chloride. The low solubility of dimethyl-4-nitrophenylsulfonoium chloride in non-polar solvents guides to the greater depletion

of electrophile in solution as well as slowing of reaction rate upon increasing bromide concentration. Hence apparent negative order of the reaction was observed in non-polar solvents (**Figure 56**).[1, 137] When there was sufficient tetrahexylammonium chloride to complete formation of dimethyl-4-nitrophenylsulfonoium chloride, the effect of increasing chloride concentration on rate of reaction becomes zero. This leads to the "levelling off" of the k_{obs} (**Figure 56**).

When the same reaction is carried out in polar molecular solvents like MeCN and DMSO, the ion pair dimethyl-4-nitrophenylsulfonoium chloride is soluble and is the reactive species that forms the demethylated product *p*-NO_2PhSCH_3. The reaction mechanism for polar liquids can be hypothesized in the following manner. First, the initial metathesis leads to the formation dimethyl-4-nitrophenylsulfonium chloride, which can also exists as quaternary ion pairs in solution (**Figure 59**):

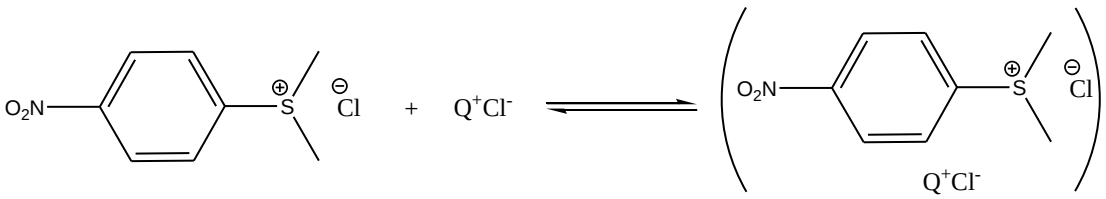

Figure 59 – Formation of ion pairs in polar molecular solvents such as MeCN

As discussed before, the ion pair is the reactive species in the solution (**Figure 60**). Increasing the amount of bromide would lead to the greater formation of the reactive ion pair, and hence the rate of reaction.

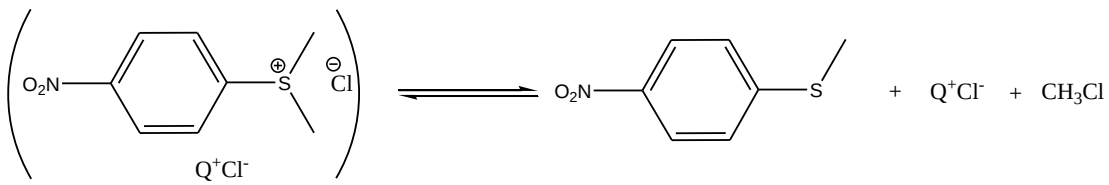

Figure 60 – The formation of product from the quadrupolar ion pair

Alternatively, the ion pairs can redistribute in the following equilibrium (**Figure 61**):

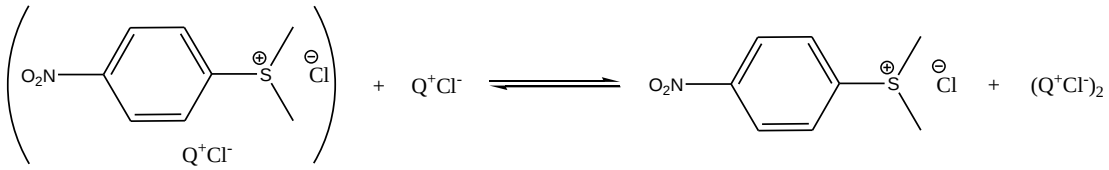

Figure 61 – Redistribution of the ion pair

The di-quarternary ammonium quadrupolar ion pair can also undergo a monomer-dimer equilibrium shift to complete the reaction cycle (**Figure 62**):

$$\left(Q^+Cl^-\right)_2 \rightleftharpoons 2Q^+Cl^-$$

Figure 62 – Monomer-dimer equilibrium

An overall reaction scheme can be produced by following the above hypotheses (**Figure 63**):

$$E^+Cl^- + Q^+Cl^- \underset{k_{-1}}{\overset{k_1}{\rightleftharpoons}} \left(E^+Cl^- \ Q^+Cl^-\right)$$

$$\left(E^+Cl^- \ Q^+Cl^-\right) \xrightarrow{k_2} \text{Products}$$

$$\left(E^+Cl^- \ Q^+Cl^-\right) + Q^+Cl^- \xrightarrow{k_3} E^+Cl^- + \left(Q^+Cl^-\right)_2$$

$$\left(Q^+Cl^-\right)_2 \overset{\text{rapid}}{\rightleftharpoons} 2Q^+Cl^-$$

Figure 63 – The simplified kinetic scheme for formation of demethylated product from reactive ion pair (E^+ = the electrophilic dimethyl-4-nitrophenylsulfonium cation); Q^+ = quaternary cation originally associated with the chloride ion)

The corresponding rate law can be written as:

$$\frac{d[\text{Products}]}{dt} = k_2[(E^+Cl^-\ \ Q^+Cl^-)] \qquad \textbf{(Equation 35)}$$

From the kinetic scheme (**Equation 35**) the following expression can be derived:

$$\frac{d[(E^+Cl^-\ \ Q^+Cl^-)]}{dt} = k_1[E^+Cl^-][Q^+Cl^-] - k_{-1}[(E^+Cl^-\ \ Q^+Cl^-)] - k_2[(E^+Cl^-\ \ Q^+Cl^-)] - k_3[(E^+Cl^-\ \ Q^+Cl^-)]\,[Q^+Cl^-]$$

(Equation 36)

A steady state approximation for $[(E^+Cl^-\ Q^+Cl^-)]$ leads to:

$$\frac{d[(E^+Cl^-\ \ Q^+Cl^-)]}{dt} \approx 0 \approx k_1[E^+Cl^-][Q^+Cl^-] - k_{-1}[(E^+Cl^-\ \ Q^+Cl^-)] - k_2[(E^+Cl^-\ \ Q^+Cl^-)] - k_3[(E^+Cl^-\ \ Q^+Cl^-)]\,[Q^+Cl^-] \rightarrow$$

$$[(E^+Cl^-\ \ Q^+Cl^-)] = \frac{k_1[E^+Cl^-][Q^+Cl^-]}{k_{-1} + k_2 + k_3[Q^+Cl^-]} \qquad \textbf{(Equation 37)}$$

Rearranging **Equation 35** and **37** gives

$$\frac{d[\text{Products}]}{dt} = \frac{k_1k_2[E^+Cl^-][Q^+Cl^-]}{k_{-1} + k_2 + k_3[Q^+Cl^-]} \qquad \textbf{(Equation 38)}$$

Since an excess of Q^+Cl^- was used in the reactions **Equation 37** becomes:

$$\frac{d[\text{Products}]}{dt} = k_{obs}[E^+Cl^-]$$

$$\text{where } k_{obs} = \frac{k_1k_2[Q^+Cl^-]}{k_{-1} + k_2 + k_3[Q^+Cl^-]} \text{ is a constant} \qquad \textbf{(Equation 39)}$$

There was enough experimental evidence to support the validity of **Equation 39** as well as the predicted mechanism; in “polar” molecular solvents, increasing the concentration of the halide nucleophile would increase the reaction rate, but not in the linear fashion such as in experiments for ionic liquids (i.e. partial order kinetics). In ionic liquid, all the ionic solutes react as “free” solvated ions; while in dissociating

molecular solvents (e.g. MeCN), the solutes can be free ions and ion pairs. The ion-paired sulfonium halides are more reactive than the “free” solvated halide ions in solution.

4.1.6.1 Viscosity effects of ionic liquids

The high viscosity of ionic liquids may cause huge reduction of rates in diffusion-controlled reactions. But according to Ranieri,[137] viscosity would not be a key factor in affecting the kinetics of this reaction, since one should witnessed a dramatic decrease of reactivity passing from molecular solvents (of different ionizing abilities) to the ionic liquids, which did not happen at all. Diffusion-controlled reactions usually occur when the general reaction rates are very fast, i.e. as quickly as the reactants encounter, they react. The reaction between dimethyl-4-nitrophenylsulfonoium cations and halides is not a fast reaction.

4.1.7 UV/Vis spectroscopic measurements

The electrophile sulfonium salt was found to be unreactive in the solvents mentioned as no change in absorbance was observed in the absence of nucleophile within 24 hours.

The nucleophile [C_4C_1pyrr]Br was weighed in a volumetric flask. Then the solvent or solvent mixture was added under anaerobic conditions, to complete the volume. This was used as a batch solution of nucleophile in order to prepare solutions of different concentrations. For example, a certain portion of the batch solution was added into the 0.5 cm path length quartz cuvette under anaerobic conditions. Dilution with a

certain amount of pure solvent/solvent mixture gave the actual concentration of the nucleophile in the cuvette.

Then the nucleophile solution was transferred to the spectrometer, thermostatted (at 25 °C) for >5 minutes. An aliquot of the electrophile [*p*-$NO_2PhS(CH_3)_2$][NTf_2] in the same solvent/solvent mixture was added, UV/Vis spectra were then recorded at regular intervals.

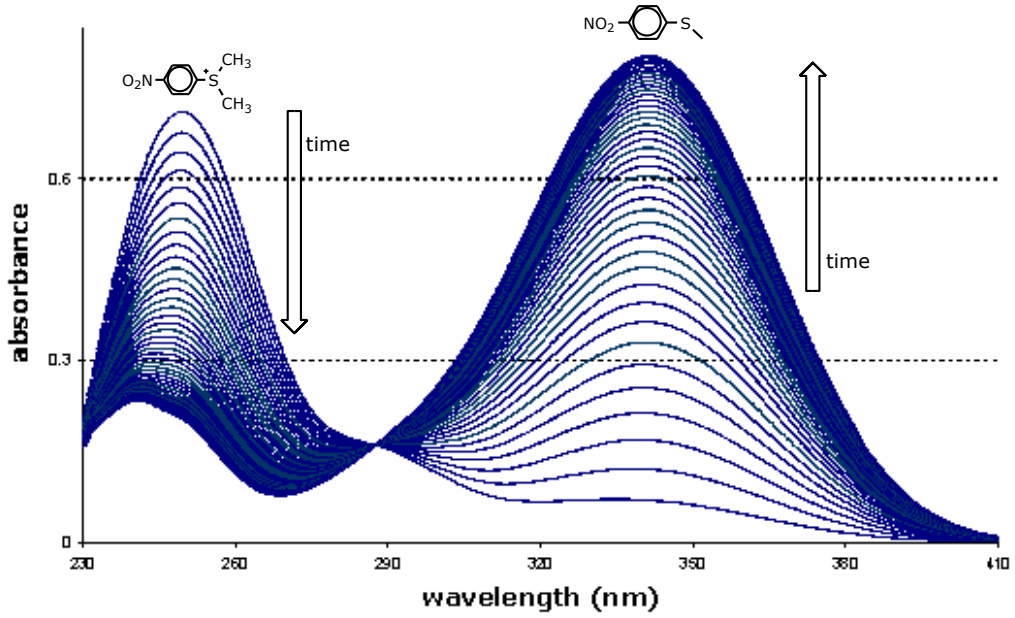

Figure 64[1] – the formation of the demethylated product as observed on the UV/Vis spectrometer

The demethylated product *p*-NO_2PhSCH_3 absorbed at 345 nm (**Figure 64**) and the absorbance values at this wavelength were recorded for kinetic analysis. The large (90 nm) difference between λ_{max} of reactant and product made the absorbance measurements simple. The downside of this method was that the absorption bands of products and reactants shifted as the absorbance increased (due to formation and deformation of clusters. Hence, large amount of time was spent on making sure that the absorbance of the actual λ_{max} was recorded for each interval.

4.2 Preliminary Study

Firstly, the *pseudo*-first order rate constants k_{obs} in 100% MeCN were measured. Previous experiment of the same solvent reported by Ranieri was carried out at the concentration (of chloride anion) range of 0 – 0.09 M (**Figure 65**).[1, 137]

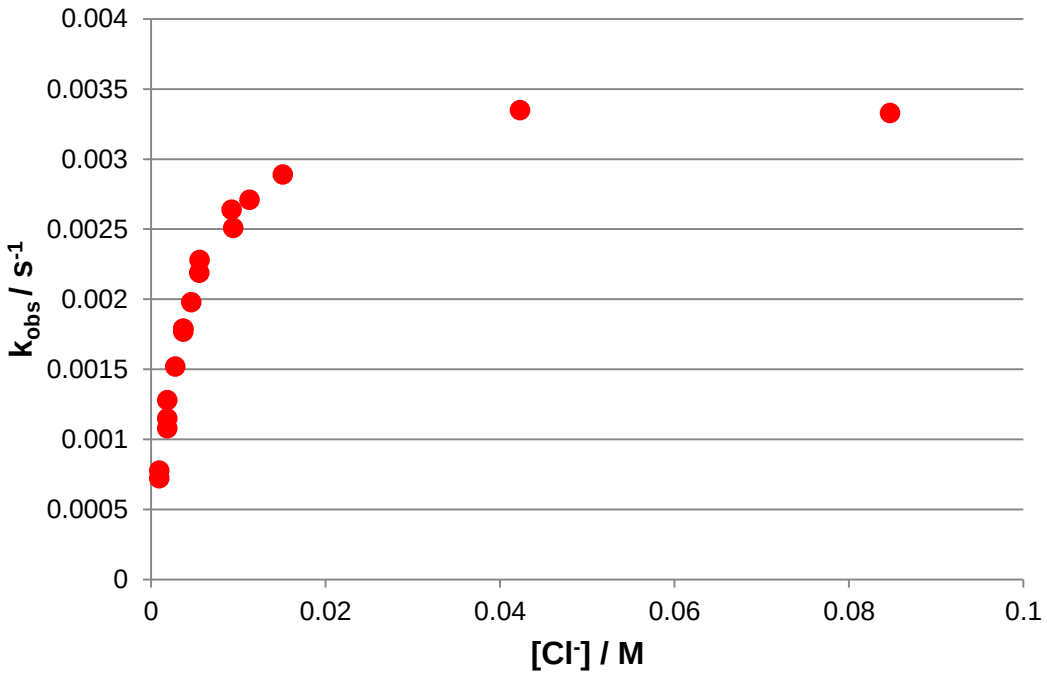

Figure 65[137] – The dependence of k_{obs} on the chloride concentration for the reactions with [*p*-$NO_2PhS(CH_3)_2$][X] ([X]$^-$ = [NTf_2]$^-$ /[OTf]$^-$) in MeCN

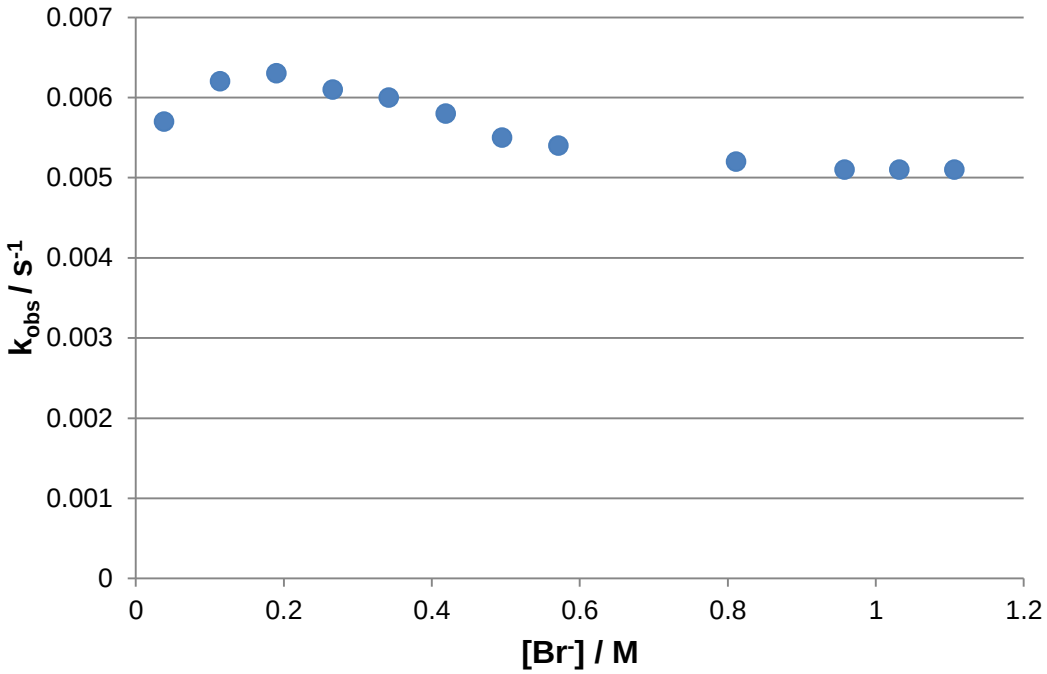

Figure 66 – The dependence of k_{obs} on the bromide concentration for the reactions [*p*-$NO_2PhS(CH_3)_2$][NTf_2] in MeCN

In that experiment, non-linear partial-order kinetics was observed as described earlier; k_{obs} increases with respect to the halide concentrations, but the slope decreases at the same time. It was found that when the bromide concentration reached a certain point (~0.2 M), the graph would arrive at a maximum and went back down again (**Figure 66**). This may be because the higher bromide concentration caused the ion exchanges to take place more rapidly, leading to the formation of higher number of dimethyl-4-nitrophenylsulfonoium bromide, which started to precipitate from solution (**Figure 67**). The plateau of this graph can be regarded as the "solubility limit" of the dimethyl-4-nitrophenylsulfonoium bromide in MeCN. After reaching the "solubility" limit the excess amount of bromide causes more dimethyl-4-nitrophenylsulfonoium bromide to precipitate out of solution. When the bromide concentration is so high that the formation of the sulfonium bromide is complete, there would be no further effect of increased bromide concentration on the reaction rate. This is observed as the flattening off of the k_{obs}. The kinetic behaviour

past the “solubility limit” of this reaction is similar to that of the reaction carried out by Ranieri in “non-polar” solvents (e.g. DCM and THF).

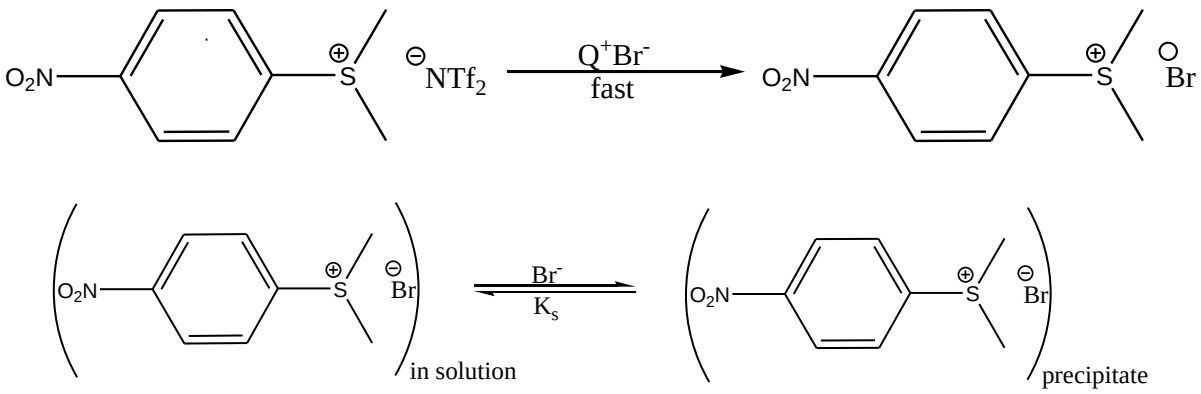

Figure 67 – Formation of sulfonium bromide ion pair and its precipitate (at ~0.2M bromide concentration) in MeCN

After looking at kinetic behaviour in pure MeCN, the *pseudo*-first order rate constants k_{obs} in 100% 1,2-dichloroethane were measured. The results are displayed in **Figure 68**.

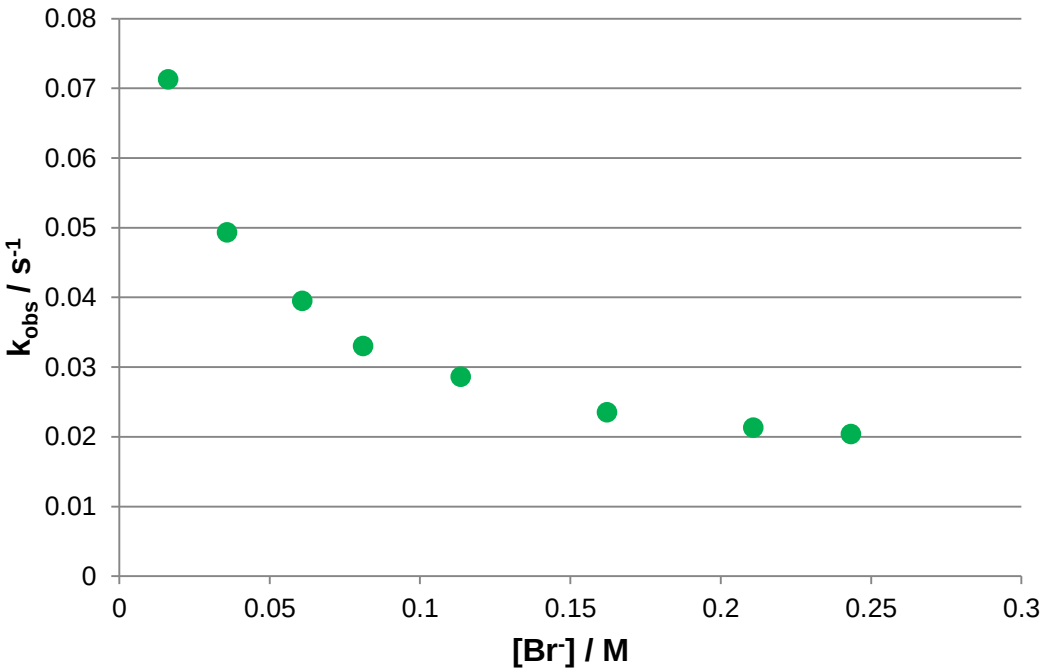

Figure 68 – The dependence of k_{obs} on the bromide concentration for the reactions with [*p*-$NO_2PhS(CH_3)_2$][NTf_2] in 1,2-dichloroethane

Since the solubility of [C_4C_1pyrr]Br in 1,2-dichloroethane is lower than in MeCN, the kinetic study for pure 1,2-dichloroethane was carried out at lower bromide concentrations (0 – 0.25 M). The kinetic behaviour of the reaction between the sulfonium salt and bromide ion in pure 1,2-dichloroethane was similar to that of the reaction between the sulfonium salt and chloride ion in "non-polar" solvents as reported by Ranieri;[1, 137] the low solubility of the ion pair dimethyl-4-nitrophenylsulfonium bromide in 1,2-dichloroethane led to the depletion of electrophile (**Figure 68**) and slowing of reaction rate upon increasing chloride concentration i.e. negative order kinetics. The complete formation of dimethyl-4-nitrophenylsulfonoium bromide led to the "levelling off" of k_{obs}.

4.2.1 Second order rate constants for reaction in 1,2-dichloroethane and MeCN

The best approach to study solvent effects on the kinetic behaviour of this bimolecular reaction is by measuring and comparing second order rate constant k_2 for different solvents and solvent mixtures.

As discussed earlier, *pseudo*-first order approximation was used because it simplifies the measurement of second order rate constant; but since no linearity can be formed between k_{obs} and bromide concentration, k_2 cannot be measured using *pseudo*-first order conditions for reaction in molecular solvents. In the earlier experiments, large excess amount of bromide was employed in the reactions, and it caused large amount of dimethyl-4-nitrophenylsulfonoium ion pairs to present in solution. This ion association prevented us from calculating k_2. In a further attempt to obtain k_2, a direct measurement of this was carried out for reaction in 1,2-dichloroethane and MeCN. This direct measurement of k_2 can be carried out at low

mole ratio of electrophile and nucleophile (i.e. no large excess amount of nucleophile is needed), hence it may be able to largely limit amount of ion pairs in solution. The second order reaction rate law is demonstrated below (**Section 4.2.2.1**).

4.2.1.1 Second order reaction rate law

It is convenient to use the decrease in concentration, x, of one reactant as the reaction variable. As the two reactants are consumed equal amounts, $A = A_0 - x$ and $B = B_0 - x$, therefore:

$dx/dt = k(A_0 - x)(B_0 - x)$ (**Equation 40**)

Integration of **Equation 40** from t = 0, x = 0 to give **Equation 41**:

$$\int_0^x \frac{dx}{(A_0 - x)(B_0 - x)} = \int_0^t k\,dt$$

$$\frac{1}{(A_0 - B_0)} \left(\ln \frac{(A_0 - x)}{A_0} - \ln \frac{(B_0 - x)}{B_0} \right) = kt \quad \text{(Equation 41)}$$

Equation 41 can be simplified by combining the two logarithms and noting that $A = A_0 - x$, $B = B_0 - x$ to give **Equation 42**:

$$\frac{1}{(A_0 - B_0)} \ln \frac{B_0}{A_0} \frac{A}{B} = kt \quad \text{(Equation 42)}$$

The second order rate constant k can be determined from the plot of ln A/B versus t, which should be linear with the slope equal to $(A_0 - B_0)k$. A and B can be determined by the absorbance of UV/Vis spectra.

4.2.1.1 Results

An attempt to directly measure the second order rate constant of a reaction in 1,2-dichloroethane was carried out. It was a difficult experiment because some these reactions were too fast to follow (i.e. complete in a few seconds), especially at the bromide concentration range of 4 x 10^{-4} to 0.005 M. The reactions were carried out in 1,2-dichloroethane at very low bromide concentrations (about 6 x 10^{-5} to 4 x 10^{-4} M), and the concentration of the sulfonium salt used was kept approximately constant (~3·10^{-4} M). From **Figure 69** one could see that even at small concentrations k_2 are not constant, therefore the second order rate constants measured cannot be considered as genuine.

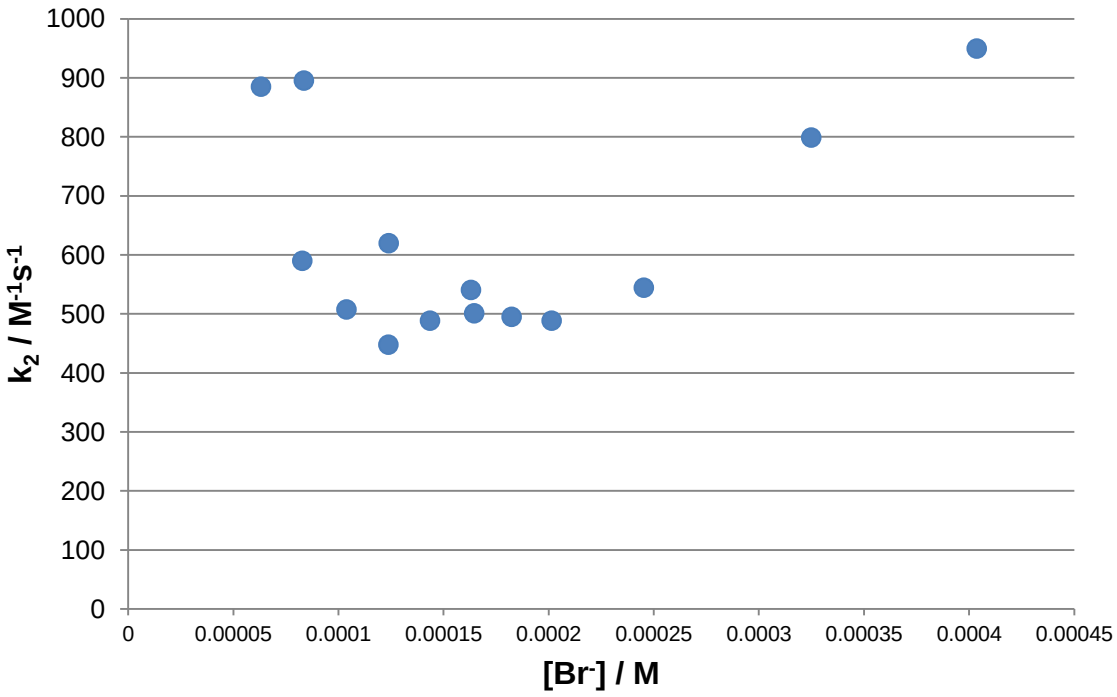

Figure 69 – The dependence of k_2 on the bromide concentration for the reactions with [*p*-$NO_2PhS(CH_3)_2$][NTf_2] in 1,2-dichloroethane

A similar experiment was carried out in MeCN, but the attempt to find a genuine second order rate constant for MeCN was not successful. Even at this very low concentration range of bromide (about 5 x 10^{-5} to 0.0015 M), where the mole ratio of

bromide and the sulfonium salt (~$3 \cdot 10^{-4}$ M) is around 0.3:1 - 5:1, the k_2 decreased upon increasing bromide concentration (**Figure 70**). The results from both 1,2-dichloroethane and MeCN demonstrated that significant extent of ion association might still occur at low bromide concentration.

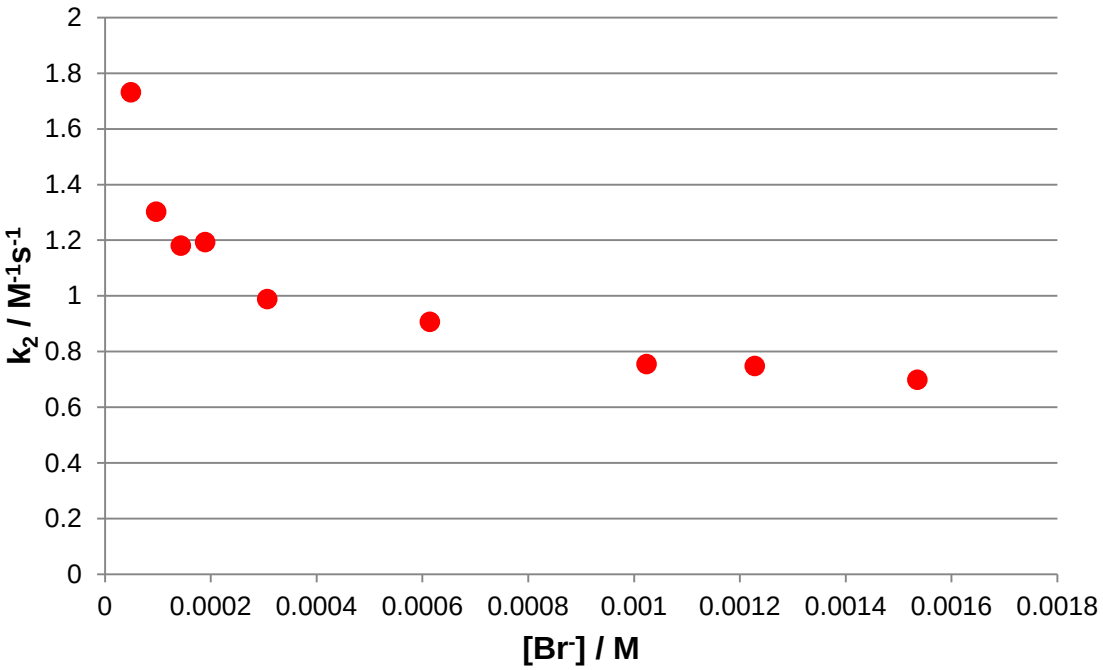

Figure 70 – The dependence of k_2 on the bromide concentration for the reactions with [*p*-$NO_2PhS(CH_3)_2$][NTf_2] in MeCN

4.3 *Pseudo*-first order kinetics of reactions in [C_4C_1pyrr][NTf_2]/1,2-dichloroethane mixtures

Since it was not possible to measure k_2 of the reaction in molecular solvents, the only way to examine the kinetic behaviour of various ionic liquid/molecular solvent mixtures is by comparing the k_{obs} of these mixtures across different bromide concentrations. For that reason the k_{obs} were measured in mixtures of [C_4C_1pyrr][NTf_2] and co-solvents of several different compositions, at different concentrations between 0 – 0.25 M.

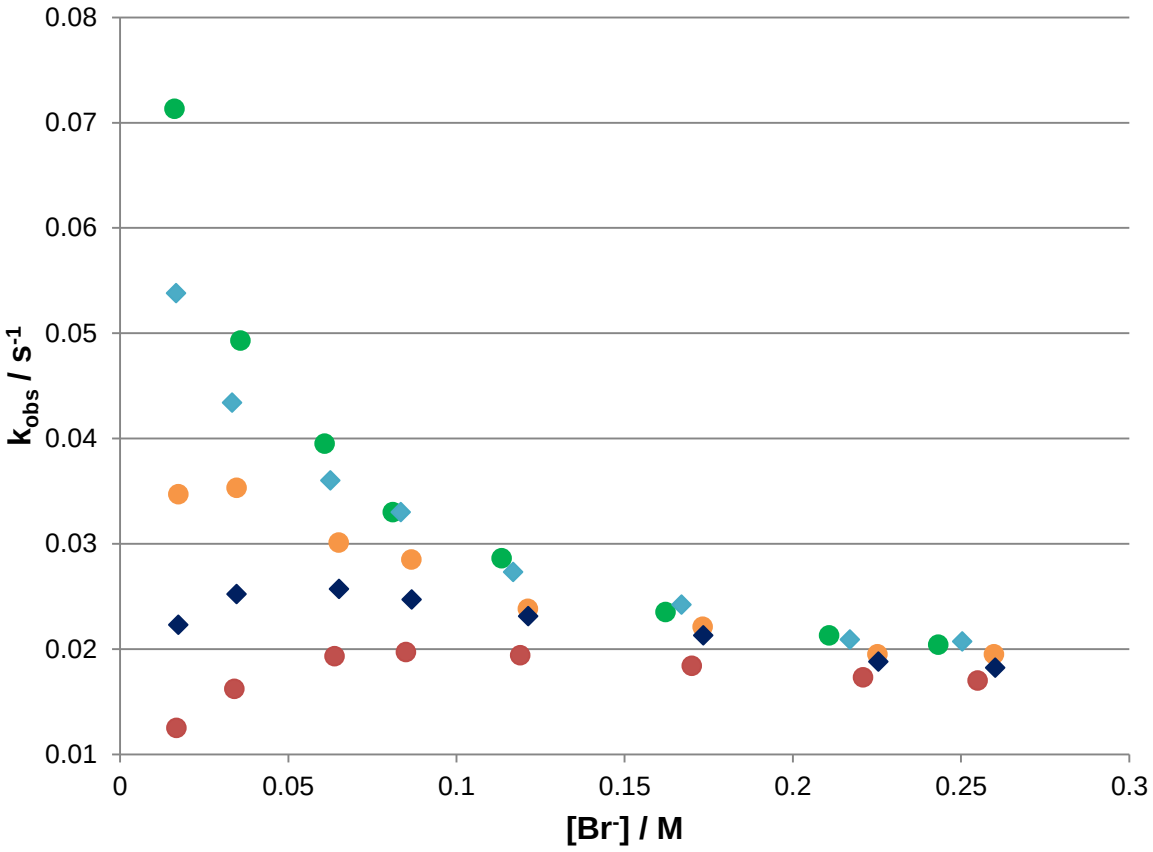

Figure 71 – The dependence of k_{obs} on the bromide concentration for the reactions with [*p*-$NO_2PhS(CH_3)_2$][NTf_2] in mixtures of [C_4C_1pyrr][NTf_2]/1,2-dichloroethane (Green: 100% 1,2-dichloroethane; light blue: 0.21 mol% [C_4C_1pyrr][NTf_2]; orange: 0.54 mol% [C_4C_1pyrr][NTf_2]; dark blue: 1.09 mol% [C_4C_1pyrr][NTf_2]; red: 2.00 mol% [C_4C_1pyrr][NTf_2])

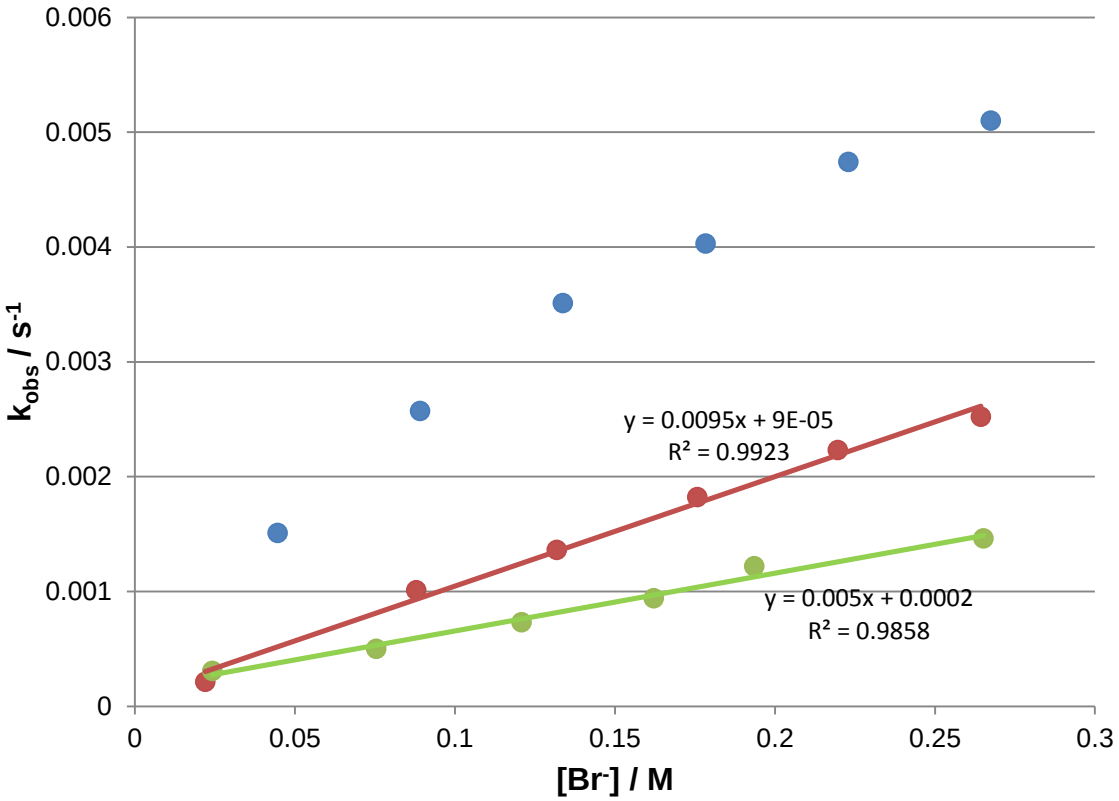

Figure 72 – The dependence of k_{obs} on the bromide concentration for the reactions with [*p*-$NO_2PhS(CH_3)_2$][NTf_2] in mixtures of [C_4C_1pyrr][NTf_2]/1,2-dichloroethane (Blue: 19.8 mol% [C_4C_1pyrr][NTf_2]; red: 50.0 mol% [C_4C_1pyrr][NTf_2]; light green: 100% [C_4C_1pyrr][NTf_2])

First, the *pseudo*-first order rate constants for [C_4C_1pyrr][NTf_2]/1,2-dichloroethane solvent mixtures were measured (**Figures 71 – 72**). The k_{obs} of reactions in pure 1,2-dichloroethane are generally higher than those in pure [C_4C_1pyrr][NTf_2]; and as expected the k_{obs} values for the [C_4C_1pyrr][NTf_2]/1,2-dichloroethane mixtures are in between the numbers for the pure solvents. The results demonstrated that non-ideal reaction solvent mixtures were formed, as a small amount of ionic liquids is enough to heavily slow down the reaction. These kinetic results can be explained in terms of preferential solvation. As described in **Section 1.4**, in binary solvent mixtures, the ratio of the solvent components in the solvation shell may be different from that in the bulk solution, since solute likes to surround itself preferably by one type of solvent that leads to more stabilization. In this experiment, it was likely that the

$[C_4C_1pyrr][NTf_2]$ preferentially solvated and stabilized one of the starting materials, led to the increase in activation energy. The effective concentrations of ionic liquids in these mixtures were therefore much higher than the actual amounts added. To quantify the non-ideal behaviour the calculation of "rate retardation factor" was proposed. "Rate retardation factors" are the ratios between the actual ionic liquid concentrations (in **mol%**) in the solvent mixtures and the effective ionic liquid concentrations (in **mol%**). The effective ionic liquid concentration is calculated by:

Effective $[C_4C_1pyrr][NTf_2]$ concentration (**mol%**) = 100 x (k_{obs}([C_4C_1pyrr][NTf_2]/co-solvent mixture) – k_{obs}(100% Co-solvent)) / (k_{obs}(100% [C_4C_1pyrr][NTf_2]) – k_{obs}(100% co-solvent)) (**Equation 43**)

With the effective ionic liquid concentration value from **Equation 43**, the "rate retardation factor" can be calculated:

"Rate retardation factor" = Effective $[C_4C_1pyrr][NTf_2]$ concentration (**mol%**) / Initial $[C_4C_1pyrr][NTf_2]$ concentration (**mol%**) (**Equation 44**)

It was decided comparisons would be made at the following bromide concentration points 0.017 M, 0.034 M, 0.065 M, 0.085 M, 0.12 M, 0.17 M and 0.22 M. It was extremely difficult to add precisely and same amount of $[C_4C_1pyrr]Br$ into the reaction system for every experiment. As a result, the amount of $[C_4C_1pyrr]Br$ added was slightly different for the various kinetic experiments. Therefore, linear interpolation (and occasionally extrapolation) was employed to bring all the k_{obs} data to the same bromide concentration points. For example, for concentration value X in the interval X_1 to X_2 (**Figure 73**), the k_{obs} value y along the "linear interpolant" is given by the following equation **Equation 45**:

$$y = y_1 + (X – X_1)(y_2 – y_1)/(X_2 – X_1) \quad \textbf{(Equation 45)}$$

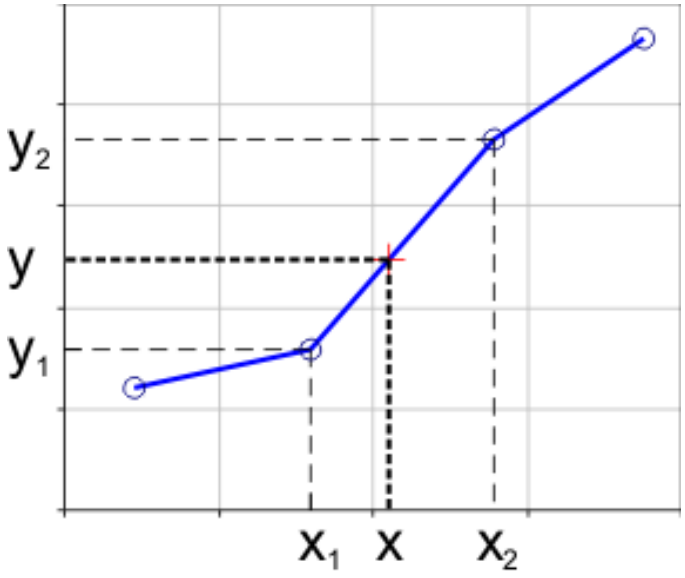

Figure 73[138] – Diagram illustrating how to predict the corresponding y for X by linear interpolating X_1,y_1 and X_2,y_2

Using **Equation 43 – 45** and k_{obs} results in **Section 4.9.1**, the solvent mixtures' effective ionic liquid concentrations of reactions and "rate retardation factors" were calculated for bromide concentrations stated before (**Tables 22 – 28**).

Mole% of $[C_4C_1pyrr][NTf_2]$ in mixtures	Predicted k_{obs} / s^{-1}	Effective $[C_4C_1pyrr][NTf_2]$ concentration / mol%	Rate retardation factor
0 (0 M)	0.0704		
0.21 (0.027 M)	0.0536	24.0	114
0.54 (0.066 M)	0.0347	50.9	94.3
1.09 (0.134 M)	0.0222	68.6	63.0
2.00 (0.240 M)	0.0125	82.5	41.2
19.8 (1.61 M)	$5.76 \cdot 10^{-4}$	99.5	5.03
50.0 (2.64 M)	$2.55 \cdot 10^{-4}$	100.0	2.00
100 (3.34 M)	$2.40 \cdot 10^{-4}$		

Table 22 – Predicted k_{obs}, effective $[C_4C_1pyrr][NTf_2]$ concentrations and "rate retardation factor" at $[Br^-]$ = 0.017 M

Mole% of $[C_4C_1pyrr][NTf_2]$ in mixtures	Predicted k_{obs} / s^{-1}	Effective $[C_4C_1pyrr][NTf_2]$ concentration / mol%	Rate retardation factor
0 (0 M)	0.0514		
0.21 (0.027 M)	0.0432	15.9	75.8
0.54 (0.066 M)	0.0354	31.3	57.9
1.09 (0.134 M)	0.0251	51.5	47.2
2.00 (0.240 M)	0.0162	68.9	34.4
19.8 (1.61 M)	0.00119	98.3	4.97
50.0 (2.64 M)	$4.17 \cdot 10^{-4}$	99.8	2.00
100 (3.34 M)	$3.25 \cdot 10^{-4}$		

Table 23 – Predicted k_{obs}, effective $[C_4C_1pyrr][NTf_2]$ concentrations and "rate retardation factor" at $[Br^-] = 0.034$ M

Mole% of $[C_4C_1pyrr][NTf_2]$ in mixtures	Predicted k_{obs} / s^{-1}	Effective $[C_4C_1pyrr][NTf_2]$ concentration / mol%	Rate retardation factor
0 (0 M)	0.0382		
0.21 (0.027 M)	0.0357	6.68	31.8
0.54 (0.066 M)	0.0301	21.4	39.6
1.09 (0.134 M)	0.0257	33.1	30.4
2.00 (0.240 M)	0.0193	50.0	25.0
19.8 (1.61 M)	0.00197	96.0	4.85
50.0 (2.64 M)	$7.13 \cdot 10^{-4}$	99.4	1.99
100 (3.34 M)	$4.81 \cdot 10^{-4}$		

Table 24 – Predicted k_{obs}, effective $[C_4C_1pyrr][NTf_2]$ concentrations and "rate retardation factor" at $[Br^-] = 0.065$ M

Mole% of $[C_4C_1pyrr][NTf_2]$ in mixtures	Predicted k_{obs} / s^{-1}	Effective $[C_4C_1pyrr][NTf_2]$ concentration / mol%	Rate retardation factor
0 (0 M)	0.0325		
0.21 (0.027 M)	0.0327	-0.847	-4.03
0.54 (0.066 M)	0.0287	11.8	21.8
1.09 (0.134 M)	0.0248	24.1	22.1
2.00 (0.240 M)	0.0197	40.0	20.0
19.8 (1.61 M)	0.00247	94.1	4.75
50.0 (2.64 M)	$9.03 \cdot 10^{-4}$	99.0	1.98
100 (3.34 M)	$5.82 \cdot 10^{-4}$		

Table 25 – Predicted k_{obs}, effective $[C_4C_1pyrr][NTf_2]$ concentrations and "rate retardation factor" at $[Br^-]$ = 0.085 M

Mole% of $[C_4C_1pyrr][NTf_2]$ in mixtures	Predicted k_{obs} / s^{-1}	Effective $[C_4C_1pyrr][NTf_2]$ concentration / mol%	Rate retardation factor
0 (0 M)	0.0279		
0.21 (0.027 M)	0.0271	3.00	14.3
0.54 (0.066 M)	0.0240	14.5	26.9
1.09 (0.134 M)	0.0232	17.5	16.1
2.00 (0.240 M)	0.0194	31.4	15.7
19.8 (1.61 M)	0.00322	90.9	4.59
50.0 (2.64 M)	0.00124	98.2	1.96
100 (3.34 M)	$7.58 \cdot 10^{-4}$		

Table 26 – Predicted k_{obs}, effective $[C_4C_1pyrr][NTf_2]$ concentrations and "rate retardation factor" at $[Br^-]$ = 0.12 M

Mole% of $[C_4C_1pyrr][NTf_2]$ in mixtures	Predicted k_{obs} / s^{-1}	Effective $[C_4C_1pyrr][NTf_2]$ concentration / mol%	Rate retardation factor
0 (0 M)	0.0231		
0.21 (0.027 M)	0.0240	-3.85	-18.3
0.54 (0.066 M)	0.0222	4.25	7.86
1.09 (0.134 M)	0.0214	7.80	7.16
2.00 (0.240 M)	0.0184	21.4	10.7
19.8 (1.61 M)	0.00393	86.8	4.38
50.0 (2.64 M)	0.00176	96.8	1.94
100 (3.34 M)	0.00101		

Table 27 – Predicted k_{obs}, effective $[C_4C_1pyrr][NTf_2]$ concentrations and "rate retardation factor" at $[Br^-]$ = 0.17 M

Mole% of $[C_4C_1pyrr][NTf_2]$ in mixtures	Predicted k_{obs} / s^{-1}	Effective $[C_4C_1pyrr][NTf_2]$ concentration / mol%	Rate retardation factor
0 (0 M)	0.0210		
0.21 (0.027 M)	0.0209	0.822	3.92
0.54 (0.066 M)	0.0198	6.50	12.0
1.09 (0.134 M)	0.0191	10.0	9.19
2.00 (0.240 M)	0.0173	18.8	9.41
19.8 (1.61 M)	0.00469	82.7	4.17
50.0 (2.64 M)	0.00219	95.3	1.91
100 (3.34 M)	0.00126		

Table 28 – Predicted k_{obs}, effective $[C_4C_1pyrr][NTf_2]$ concentrations and "rate retardation factor" at $[Br^-]$ = 0.22 M

As shown in **Tables 22** – **24**, the calculated "rate retardation factors" for $[C_4C_1pyrr][NTf_2]$/1,2-dichloroethane mixtures at $[Br^-]$ = 0.017, 0.034 and 0.065 M were high. Very small amounts of $[C_4C_1pyrr][NTf_2]$ (e.g. 0.21, 0.54, 1.09 and 2.00 mol%) were enough to slow down the reaction in 1,2-dichloroethane to a great extent. For example, for solvent mixture 0.21 mol% $[C_4C_1pyrr][NTf_2]$ / 99.79 mol% 1,2-dichloroethane, the "rate retardation factor" was 114 (**Table 22**) when the

bromide concentration was 0.017 M; this meant the effective concentration of ionic liquid was 114 times the actual concentration. The value of 114 was also the highest number recorded for experiments in $[C_4C_1pyrr][NTf_2]$/1,2-dichloroethane mixtures.

When the reactions were carried out using higher bromide concentrations (i.e. 0.085, 0.12, 0.17 and 0.22 M), "rate retardation factors" for ionic liquid/1,2-dichloroethane mixtures were still observed but the extents of them were not as high as when lower bromide concentrations were reacted (**Tables 25 – 28**). Generally, the "rate retardation factors" decrease upon increasing bromide concentrations, for all $[C_4C_1pyrr][NTf_2]$/1,2-dichloroethane mixtures.

Finally, as shown in **Figures 71** and **72**, all the binary solvent mixtures except 50.0 mol% $[C_4C_1pyrr][NTf_2]$ / 50.0 mol% 1,2-dichloroethane generated non-linear k_{obs} vs $[Br^-]$ plots. The plots indicated strong preferential solute ion-pairing occurred in these binary mixtures. Conversely, the plot for 50.0 mol% $[C_4C_1pyrr][NTf_2]$ / 50.0 mol% 1,2-dichloroethane is linear, pointed toward the lack of preferential solute ion-pairing in solution. With this linear plot second order rate constant for 50.0 mol% $[C_4C_1pyrr][NTf_2]$ / 50.0 mol% 1,2-dichloroethane could be measured (k_2 = 0.00953 $M^{-1}s^1$). The k_2 of 100% $[C_4C_1pyrr][NTf_2]$ of the reaction was measured to be 0.00503 $M^{-1}s^1$ (see **Figure 72**).

4.4 *Pseudo*-first order kinetics of reactions in $[C_4C_1pyrr][NTf_2]$/MeCN mixtures

After seeing the heavy slowing of reactions by the ionic liquid in $[C_4C_1pyrr][NTf_2]$/1,2-dichloroethane mixtures, the *pseudo*-first order rate constants were also measured in $[C_4C_1pyrr][NTf_2]$/MeCN mixtures (at similar bromide concentration range), to see whether a similar kinetic behavior could be seen. The results are displayed in

Figures 74 and **75**. The plot for 50.4 mol% $[C_4C_1pyrr][NTf_2]$ / 49.6 mol% MeCN is basically linear, hence in this solvent mixture solute ion-pairing is negligible. The k_2 for this mixture 0.00560 $M^{-1}s^{-1}$. Plots for other solvent mixtures are non-linear, pointed toward the presence of solute ion-pairing.

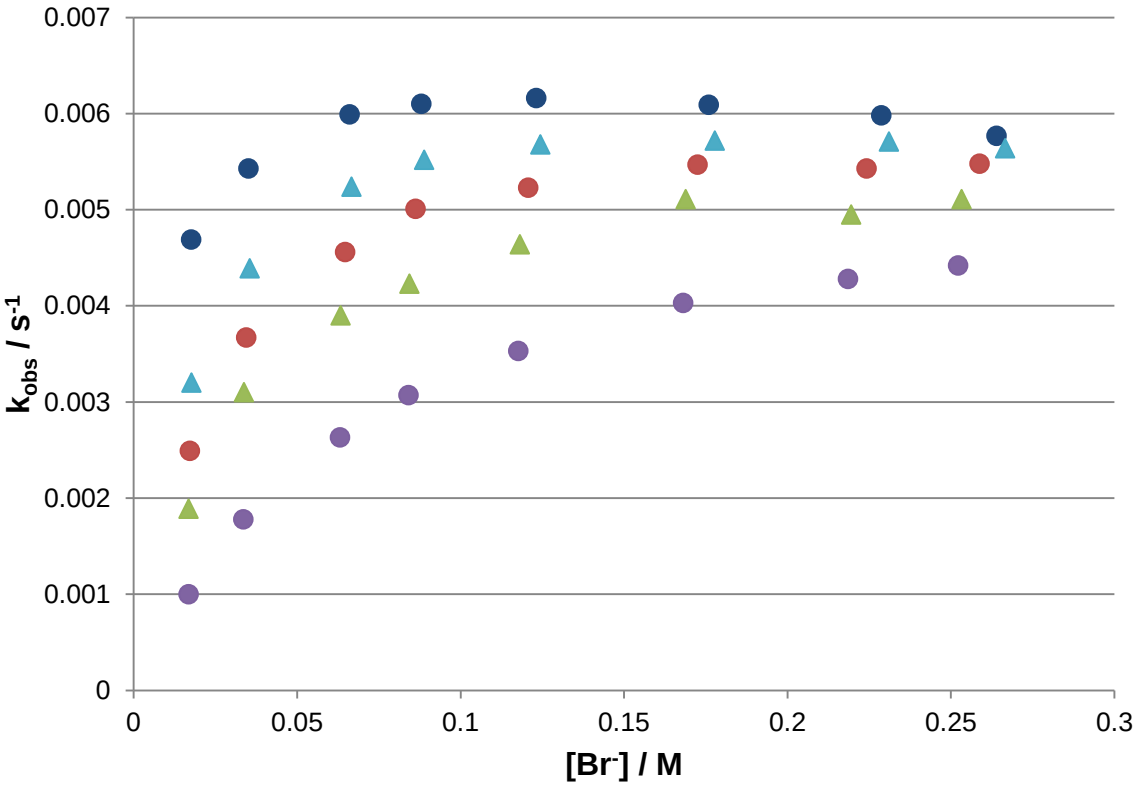

Figure 74 – The dependence of k_{obs} on the bromide concentration for the reactions with [*p*-$NO_2PhS(CH_3)_2$][NTf_2] in mixtures of [C_4C_1pyrr][NTf_2]/MeCN (Dark blue: 100% MeCN; light blue: 0.21 mol% [C_4C_1pyrr][NTf_2]; red: 0.50 mol% [C_4C_1pyrr][NTf_2]; light green: 1.03 mol% [C_4C_1pyrr][NTf_2]; purple: 2.17 mol% [C_4C_1pyrr][NTf_2])

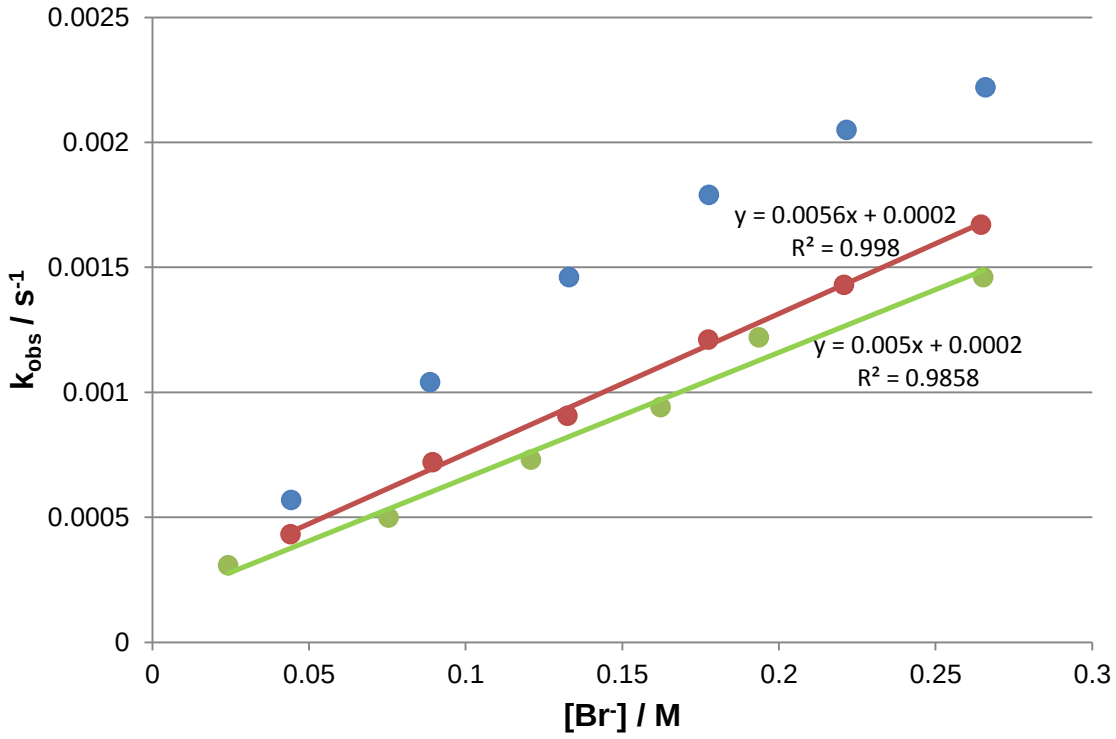

Figure 75 – The dependence of k_{obs} on the bromide concentration for the reactions with [*p*-$NO_2PhS(CH_3)_2$][NTf_2] in mixtures of [C_4C_1pyrr][NTf_2]/MeCN (Light blue: 18.8 mol% [C_4C_1pyrr][NTf_2]; red: 50.4 mol% [C_4C_1pyrr][NTf_2]; light green: 100% [C_4C_1pyrr][NTf_2])

Once again, a non-ideal solvent effect was observed as tiny amount of ionic liquid was enough to slow down the reactions significantly. **Equations 43 – 45** and k_{obs} results (**Section 4.9.2**) were used to calculate the "rate retardation factors" (**Table 29 – 35**).

Mole% of $[C_4C_1pyrr][NTf_2]$ in mixtures	Predicted k_{obs} / s^{-1}	Effective $[C_4C_1pyrr][NTf_2]$ concentration / mol%	Rate retardation factor
0 (0 M)	0.00466		
0.21 (0.040 M)	0.00315	34.3	163
0.50 (0.093 M)	0.00247	49.5	99.1
1.03 (0.186 M)	0.00190	62.5	60.7
2.17 (0.374 M)	0.00101	82.7	38.1
18.8 (1.89 M)	$2.18 \cdot 10^{-4}$	100.5	5.35
50.4 (2.84 M)	$2.90 \cdot 10^{-4}$	98.9	1.96
100 (3.34 M)	$2.40 \cdot 10^{-4}$		

Table 29 – Predicted k_{obs}, effective $[C_4C_1pyrr][NTf_2]$ concentrations and "rate retardation factor" at $[Br^-]$ = 0.0017 M

Mole% of $[C_4C_1pyrr][NTf_2]$ in mixtures	Predicted k_{obs} / s^{-1}	Effective $[C_4C_1pyrr][NTf_2]$ concentration / mol%	Rate retardation factor
0 (0 M)	0.00538		
0.21 (0.040 M)	0.00429	21.7	103
0.50 (0.093 M)	0.00364	34.5	69.1
1.03 (0.186 M)	0.00311	45.0	43.7
2.17 (0.374 M)	0.00179	71.1	32.8
18.8 (1.89 M)	$4.36 \cdot 10^{-4}$	97.9	5.21
50.4 (2.84 M)	$3.85 \cdot 10^{-4}$	98.9	1.96
100 (3.34 M)	$3.30 \cdot 10^{-4}$		

Table 30 – Predicted k_{obs}, effective $[C_4C_1pyrr][NTf_2]$ concentrations and "rate retardation factor" at $[Br^-]$ = 0.034 M

Mole% of $[C_4C_1pyrr][NTf_2]$ in mixtures	Predicted k_{obs} / s^{-1}	Effective $[C_4C_1pyrr][NTf_2]$ concentration / mol%	Rate retardation factor
0 (0 M)	0.00597		
0.21 (0.040 M)	0.00519	14.2	67.6
0.50 (0.093 M)	0.00456	25.6	51.3
1.03 (0.186 M)	0.00392	37.3	36.2
2.17 (0.374 M)	0.00267	60.2	27.7
18.8 (1.89 M)	$7.89 \cdot 10^{-4}$	94.5	5.03
50.4 (2.84 M)	$5.59 \cdot 10^{-4}$	98.7	1.96
100 (3.34 M)	$4.86 \cdot 10^{-4}$		

Table 31 – Predicted k_{obs}, effective $[C_4C_1pyrr][NTf_2]$ concentrations and "rate retardation factor" at $[Br^-]$ = 0.065 M

Mole% of $[C_4C_1pyrr][NTf_2]$ in mixtures	Predicted k_{obs} / s^{-1}	Effective $[C_4C_1pyrr][NTf_2]$ concentration / mol%	Rate retardation factor
0 (0 M)	0.00608		
0.21 (0.040 M)	0.00547	11.2	53.2
0.50 (0.093 M)	0.00498	20.0	40.0
1.03 (0.186 M)	0.00424	33.6	32.6
2.17 (0.374 M)	0.00308	54.6	25.1
18.8 (1.89 M)	0.00100	92.4	4.91
50.4 (2.84 M)	$6.71 \cdot 10^{-4}$	98.4	1.95
100 (3.34 M)	$5.82 \cdot 10^{-4}$		

Table 32 – Predicted k_{obs}, effective $[C_4C_1pyrr][NTf_2]$ concentrations and "rate retardation factor" at $[Br^-]$ = 0.085 M

Mole% of $[C_4C_1pyrr][NTf_2]$ in mixtures	Predicted k_{obs} / s^{-1}	Effective $[C_4C_1pyrr][NTf_2]$ concentration / mol%	Rate retardation factor
0 (0 M)	0.00615		
0.21 (0.040 M)	0.00566	9.17	43.6
0.50 (0.093 M)	0.00523	17.2	34.4
1.03 (0.186 M)	0.00466	27.8	27.0
2.17 (0.374 M)	0.00355	48.2	22.2
18.8 (1.89 M)	0.00130	89.9	4.78
50.4 (2.84 M)	$8.67 \cdot 10^{-4}$	98.0	1.94
100 (3.34 M)	$7.58 \cdot 10^{-4}$		

Table 33 – Predicted k_{obs}, effective $[C_4C_1pyrr][NTf_2]$ concentrations and "rate retardation factor" at $[Br^-]$ = 0.12 M

Mole% of $[C_4C_1pyrr][NTf_2]$ in mixtures	Predicted k_{obs} / s^{-1}	Effective $[C_4C_1pyrr][NTf_2]$ concentration / mol%	Rate retardation factor
0 (0 M)	0.00610		
0.21 (0.040 M)	0.00571	7.54	35.9
0.50 (0.093 M)	0.00546	12.6	25.1
1.03 (0.186 M)	0.00511	19.5	18.9
2.17 (0.374 M)	0.00404	40.5	18.6
18.8 (1.89 M)	0.00173	85.8	4.56
50.4 (2.84 M)	0.00115	97.3	1.93
100 (3.34 M)	0.00101		

Table 34 – Predicted k_{obs}, effective $[C_4C_1pyrr][NTf_2]$ concentrations and "rate retardation factor" at $[Br^-]$ = 0.17 M

Mole% of $[C_4C_1pyrr][NTf_2]$ in mixtures	Predicted k_{obs} / s^{-1}	Effective $[C_4C_1pyrr][NTf_2]$ concentration / mol%	Rate retardation factor
0 (0 M)	0.00600		
0.21 (0.040 M)	0.00571	6.04	28.8
0.50 (0.093 M)	0.00543	11.9	23.9
1.03 (0.186 M)	0.00495	22.1	21.4
2.17 (0.374 M)	0.00429	36.2	16.7
18.8 (1.89 M)	0.00204	83.5	4.44
50.4 (2.84 M)	0.00143	96.5	1.91
100 (3.34 M)	0.00126		

Table 35 – Predicted k_{obs}, effective $[C_4C_1pyrr][NTf_2]$ concentrations and "rate retardation factor" at $[Br^-]$ = 0.22 M

Similar to those in $[C_4C_1pyrr][NTf_2]$/1,2-dichloroethane mixtures, the "rate retardation factors" for $[C_4C_1pyrr][NTf_2]$/MeCN mixtures were high at low bromide concentrations i.e. 0.017, 0.034 and 0.065 M (**Table 29 – 31**). The highest "rate retardation factor" recorded was 163, for reaction in 0.21 mol% $[C_4C_1pyrr][NTf_2]$/99.79 mol% MeCN and where $[Br^-]$ = 0.017 M (**Table 29**). The "rate retardation factors" generally decrease upon increasing bromide concentrations, for all $[C_4C_1pyrr][NTf_2]$/MeCN mixtures.

Obviously, the heavy slowing by the ionic liquid in $[C_4C_1pyrr][NTf_2]$/MeCN and $[C_4C_1pyrr][NTf_2]$/1,2-dichloroethane mixtures means that the activation energy of reaction increased upon increasing amount of $[C_4C_1pyrr][NTf_2]$ in the solvent mixtures. As discussed earlier, the size of Gibbs energy of activation is influenced by the differential solvation of the reactant and transition state by the solvent. If the starting material is stabilized by the solvent to a greater extent than the transition state, and/or the transition state is destabilized by the solvent to a greater extent than the starting material, the Gibbs energy of activation would be bigger. It was likely that one of the starting materials was preferentially stabilized by the ionic liquid.

The objective at this point was to find out the major reason for the strong rate retardation. The hypothesis is that the starting material bromide anion was strongly stabilized by the pyrrolidinium cation through hydrogen bonding, therefore raising the energy threshold for reaction upon increasing ionic liquid concentration (**Section 4.5**).

4.5 Hydrogen bonding effect

For a S_N2 reaction of anionic nucleophile, it is well established that the attacking nucleophile can be specifically solvated by protic solvents, so that its reactivity, and therefore the rate of the reaction will be diminished.[42, 139-141]

In the kinetic study of reaction of trifluoromethanesulfonate and *bis*(trifluoromethanesulfonyl)imide salts of dimethyl-4-nitrophenylsulfonium with chloride ion, Ranieri was able to obtain second order rate constant k_2 of reaction in ionic liquids due to the fact the observed *pseudo*-first order rate constants were proportional to the chloride concentrations (**Table 36**).[137]

Ionic liquid	k_2 / $M^{-1}s^{-1}$	*α*	*β*	*π**
$[C_4C_1C_1im][NTf_2]$	0.0039 (0.0008)	0.38	0.24	1.01
$[HC_4im][OTf]$	0.00014 (0.00005)	0.95	0.44	1.03
$[C_4C_1pyrr][NTf_2]$	0.0048 (0.0004)	0.43	0.25	0.95
$[C_4C_1im][NTf_2]$	0.0018 (0.0001)	0.62	0.24	0.98
$[C_4C_1pyrr][OTf]$	0.0053 (0.0006)	0.40	0.46	1.02
$[C_4C_1im][OTf]$	0.00116 (0.00009)	0.62	0.46	1.01

Table 36[137] – k_2 values and Kamlet-Taft values recorded by Ranieri

The Hughes-Ingold rule[44-45] predicts that an increase in solvent polarity would largely decrease the reaction rate of this reaction. The solvent effects on this reaction were examined using a linear solvation energy relationship based on the Kamlet-Taft solvent scales (α, β, and π^*) It must be said that such analysis was made difficult due to the restricted range of π^* values, as most common ionic liquids have π^* of around 1.

Table 37 displays the results of the correlation between the rate constants and the Kamlet-Taft solvent parameters.

Parameters	LSER Equation	*p*-values	R^2
α, β, π^*	$\ln k_2 = 5.11 – 6.01\alpha + 0.87\beta – 8.36\pi^*$	XYZ_0: 0.48 α: 0.012 β: 0.65 π^*: 0.32	0.98

Table 37[112] – LSER between k_2 and α, β, π*

The error associated with each parameter was appraised in terms of the *p*-value, and any terms found to be statistically insignificant (~0.05) were eliminated. The LSER of the natural logarithm of rate constants with all three Kamlet-Taft parameters showed that β and π^* are not significant. For this reason a new LSER was conducted, which omits β and π^* (**Table 38 and Figure 76**).

Parameter	LSER Equation	*p*-values	R^2
α	$\ln k_2 = -2.80 - 6.28\alpha$	XYZ_0: 0.0015 α: 0.0048	0.96

Table 38[137] – LSER between k_2 and α

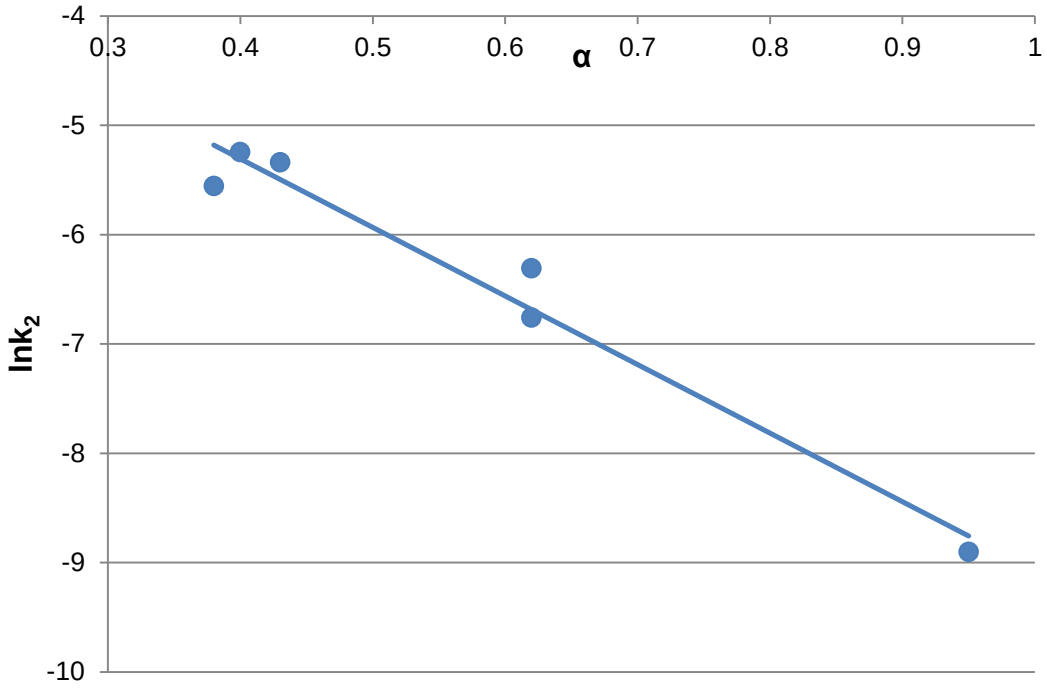

Figure 76 – $\ln k_2$ vs α

The rate constant is shown to be governed by the hydrogen bond acidity of the solvent (α), with a large negative coefficient in the LSER. The kinetic results reveal that the Hughes-Ingold prediction of solvent's effects on rates is accurate if one

considers α is the only relevant polarity descriptor, as higher values of α will produce a large decrease k_2. The large negative α dependence can be explained by the strong hydrogen-bond interaction between the cation, which contributes most of the α effect of an ionic liquid, and the lone pair of electrons on the halide. The strong hydrogen bonding interaction deactivates the nucleophilicity of the halide, hence making the reaction slower in solvents of higher α values.

This result in turn can explain the strong retarding effect by the ionic liquid in ionic/molecular liquid mixtures described above. $[C_4C_1pyrr]^+$ and other common cations for ionic liquids are much better hydrogen bond donor than aprotic solvents such as 1,2-dichloroethane (α = 0.00)[133] and MeCN (α = 0.19)[35]; hence the halide nucleophile preferentially interacts with the cation of the ionic liquid through hydrogen bonding, in the ionic liquid/molecular solvent mixture. The strong hydrogen bonding interaction of the halide and the cation deactivates the reactivity of the former and thereby decreases the rate significantly. Since a small amount of ionic liquid is enough to attract much of the halide anions in aprotic solvent solutions, hence a strong rate retardation effect can be seen with mixtures of low ionic liquid concentrations.

4.6 *Pseudo*-first order kinetics of reactions in 1,2-dichloroethane/1-butanol and 1,2-dichloroethane/benzyl alcohol mixtures

To reaffirm the hypothesis that the huge slowing effect was caused by hydrogen bonding, the rates of reaction in 1,2-dichloroethane/1-butanol were measured. The rates were expected to slow down enormously due to the deactivation of bromide anion by hydroxyl group of benzyl alcohol, which have an α value of 0.60[133]. The *pseudo*-first order rate constants of reactions in one 2.15 mol% benzyl alcohol /

97.85 mol% 1,2-dichloroethane mixture was measured at the concentration range of 0 – 0.255 M (**Figure 77**).

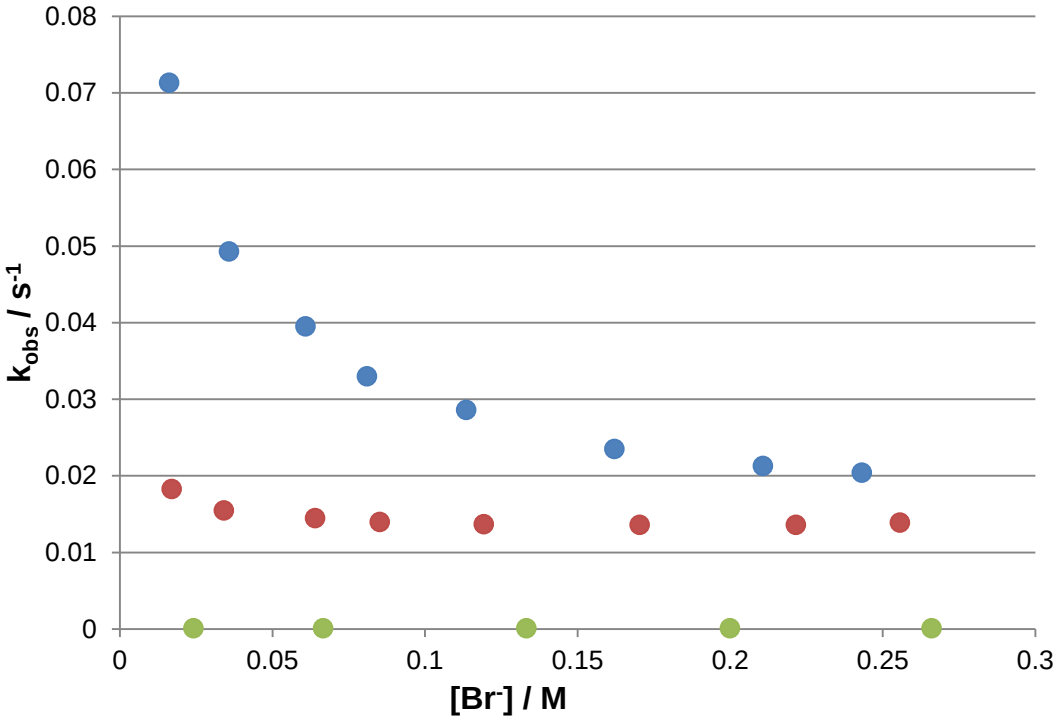

Figure 77 – The dependence of k_{obs} on the bromide concentration for the reactions with [*p*-$NO_2PhS(CH_3)_2$][NTf_2] in 100% 1,2-dichloroethane (blue), benzyl alcohol (light green) and 2.15 mol% benzyl alcohol / 97.85 mol% 1,2-dichloroethane (red)

Using the k_{obs} values (see **Section 4.9.3**), the effective benzyl alcohol concentrations and "rate retardation factors" for the solvent mixtures were calculated. The data were summarized in **Table 39**.

Bromide concentration / M	Predicted k_{obs} / s^{-1}	Effective benzyl alcohol concentration / mol%	Rate retardation factors
0.017	0.0183	74.1	34.5
0.034	0.0155	70.0	32.5
0.065	0.0145	62.2	28.9
0.085	0.0140	57.0	26.5
0.12	0.0137	51.1	23.8
0.17	0.0136	41.4	19.3
0.22	0.0136	35.5	16.5

Table 39 – Predicted k_{obs}, effective benzyl alcohol concentrations and "rate retardation factors" for 2.15 mol% benzyl alcohol / 97.85 mol% dichloroethane mixture

It was observed that like $[C_4C_1pyrr][NTf_2]$, benzyl alcohol could also slow down the reaction in 1,2-dichloroethane significantly. Even when the concentration of benzyl alcohol was relatively small (2.15 mol%), the alcohol reduced the reaction rate of 1,2-dichloroethane by up to 74.1 %. The calculated "rate retardation factors" for benzyl alcohol/1,2-dichloroethane mixture ranges from 16.5-34.5, which are similar to the ones of $[C_4C_1pyrr][NTf_2]$ in 2.00 mol% $[C_4C_1pyrr][NTf_2]$/1,2-dichloroethane mixture (**Table 22 – 28**). Also similar to what was observed in experiments $[C_4C_1pyrr][NTf_2]$/1,2-dichloroethane and $[C_4C_1pyrr][NTf_2]$/MeCN mixtures, the "rate retardation factor" for benzyl alcohol/1,2-dichloroethane mixture generally decreases with increasing bromide concentration.

The *pseudo*-first order rate constants of reactions in 2.07 mol% 1-butanol / 97.93 mol% 1,2-dichloroethane solvent mixture were also measured (**Figure 78**). Like $[C_4C_1pyrr][NTf_2]$ and benzyl alcohol, 1-butanol could greatly reduce the rate of reaction in 1,2-dichloroethane. The "rate retardation factor" for 2.07 mol% 1-butanol / 97.93 mol% 1,2-dichloroethane mixture ranges from 13.7-25.6 (**Table 40**). As before,

the “rate retardation factor” generally decreases with increasing bromide concentration.

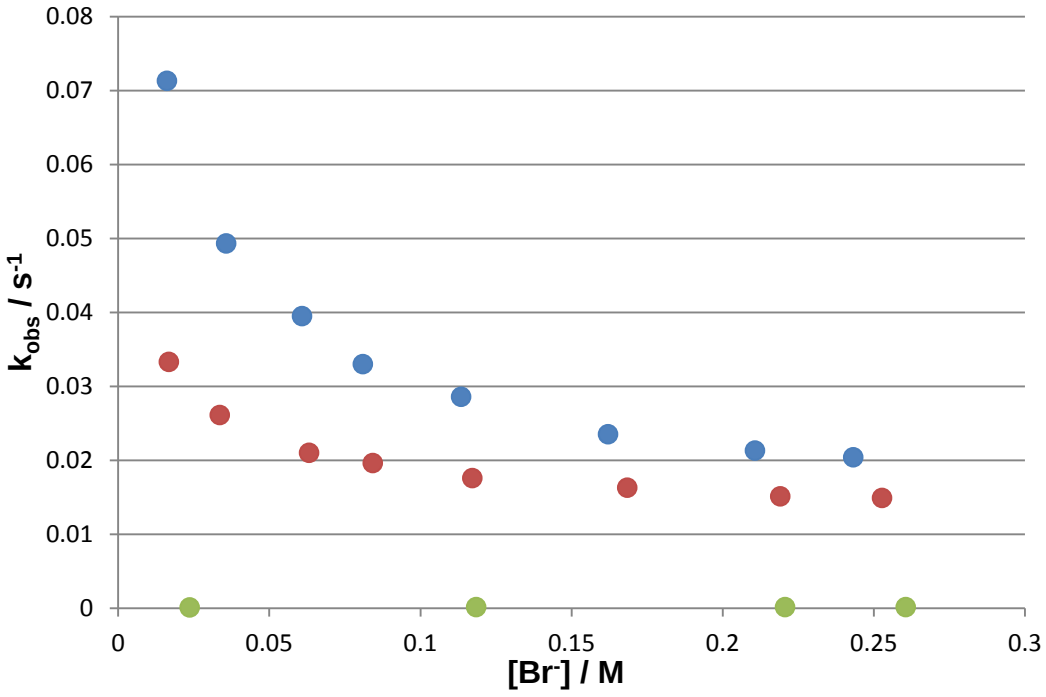

Figure 78 – The dependence of k_{obs} on the bromide concentration for the reactions with [*p*-$NO_2PhS(CH_3)_2$][NTf_2]in 100% 1,2-dichloroethane (blue), 1-butanol (light green) and 2.07 mol% benzyl alcohol / 97.93 mol% 1,2-dichloroethane (red)

Bromide concentration / M	Predicted k_{obs} / s^{-1}	Effective 1-butanol concentration / mol%	Rate retardation factor
0.017	0.0332	52.9	25.6
0.034	0.0260	49.4	23.9
0.065	0.0209	45.4	21.9
0.085	0.0196	39.9	19.3
0.12	0.0175	37.4	18.1
0.17	0.0163	29.9	14.4
0.22	0.0151	28.5	13.7

Table 40 – Predicted k_{obs}, effective 1-butanol concentrations and “rate retardation factor” for 2.07 mol% 1-butanol / 97.93 mol% 1,2-dichloroethane mixture

The kinetic results of reactions in these alcohol/1,2-dichloroethane mixtures further supported the hypothesis that rate retardation observed in $[C_4C_1pyrr][NTf_2]$/1,2-dichloroethane and $[C_4C_1pyrr][NTf_2]$/MeCN mixtures was mainly brought about by the strong hydrogen bonding interaction between the solvent ions/molecules and the bromide ions. The $[C_4C_1pyrr]^+$ cation, akin to benzyl alcohol and 1-butanol, is very capable of donating a hydrogen bond to the bromide nucleophile. The bromide preferentially interacted with the ionic liquid cation, which stabilized the starting material bromide to a greater extent than the transition state, and therefore increases the Gibbs energy of activation of the reaction. Consequently, even a small amount of ionic liquid is capable of reducing the reaction rate by a large amount. This result is reminiscence to the one reported by Humeres (**Section 1.4**), who demonstrated the reduction of nucleophilicity of 4-nitrophenoxide by addition of water that preferentially solvated the negatively charged nucleophile in water/aceotone solvent mixtures. [92]

One should note that the hydrogen bonding between the $[C_4C_1pyrr]^+$ and the bromide anion might not be the only factor that caused the huge rate retardation observed in $[C_4C_1pyrr][NTf_2]$/1,2-dichloroethane and $[C_4C_1pyrr][NTf_2]$/MeCN mixtures. Formation of ionic clusters[142-144] and the great size of $[C_4C_1pyrr]^+$ cation (compared to 1,2-dichloroethane and MeCN) might also contribute to the preferential solvation and hence the huge rate retardation. Solvent-solvent (ionic liquid-molecular solvent) interactions might also be important, but their effects on the rates of the reaction were difficult to envisage and quantify for these mixtures.

The most interesting focus of this investigation was that it might be possible to determine at what composition ionic liquid/molecular solvent mixture becomes “ionic liquid like” (i.e. when the plot of k_{obs} vs $[Br^-]$ is linear). From the kinetic results it can be observed that in 50.0 mol% $[C_4C_1pyrr][NTf_2]$ / 50.0 mol% 1,2-dichloroethane and

50.4 mol% $[C_4C_1pyrr][NTf_2]$ / 49.6 mol% MeCN the plots become linear. In other words, the solutes were not preferentially ion paired, and were "ionic liquid like" in these systems. In these systems, the ionic solutes (i.e. $[p\text{-}NO_2PhS(CH_3)_2]^+$, $[NTf_2]^-$, $[C_4C_1pyrr]^+$ and Br^-) were clustered to form large non-discriminating ionic aggregates. Microscopic heterogeneities were therefore created in these systems. Formation of ionic liquid aggregates in molecular liquids has been reported elsewhere,[142-144] and the degree of aggregation depends on the concentrations of ionic liquids as well as the dielectric constants of the molecular solvents. These ionic aggregates behaved similarly to bulk ionic liquids in the binary solvent mixtures, thus gave similar kinetic behaviour. In binary solvent mixtures of much lower ionic liquid concentrations (i.e. 19.80 mol% $[C_4C_1pyrr][NTf_2]$ / 80.20 mol% 1,2-dichloroethane), the degrees of aggregation were smaller and not all the solute ions could be incorporated into the non-discriminating ion clusters, therefore "ionic liquid like" behaviour were not observed in these systems. Note that ~50 mol% of $[C_4C_1pyrr][NTf_2]$ in 1,2-dichloroethane and MeCN account for more than 70% and 80% in volume respectively, meaning that quite a lot of ionic liquid was actually needed to force the binary solvent mixtures to become "ionic liquid like". The ionic liquid/molecular solvent mixtures possessed ionic liquid solvation behaviour only when the ionic liquid was the major component in these mixtures.

4.7 *Pseudo*-first order kinetics of reactions in mixtures of $[C_4C_1pyrr][NTf_2]$ and protic solvents

The *pseudo*-first order rate constants k_{obs} for the same reaction in benzyl alcohol were measured. The results are presented in **Figure 79**:

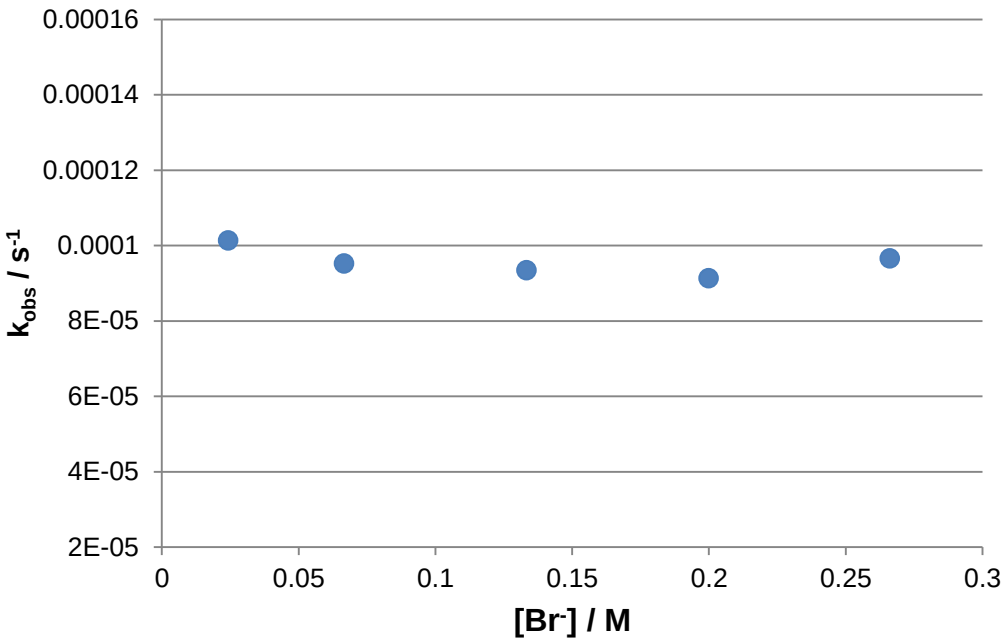

Figure 79 – The dependence of k_{obs} on the bromide concentration for the reactions with [*p*-$NO_2PhS(CH_3)_2$][NTf_2] in pure benzyl alcohol

The k_{obs} for reaction in benzyl alcohol varies little across different concentrations of [C_4C_1pyrr]Br; a flat line is produced when k_{obs} is plotted against Br^- concentration (**Figure 79**). In other words, when the reaction was carried out in benzyl alcohol, the reaction order with respect to concentration of Br^- became 0; and the total reaction order becomes 1. The results point toward a S_N1 reaction mechanism in which the rate is dependent only upon the concentration [*p*-$NO_2PhS(CH_3)_2$][NTf_2]; the rate-determining step of this reaction is unimolecular and dissociative (**Figure 80**):

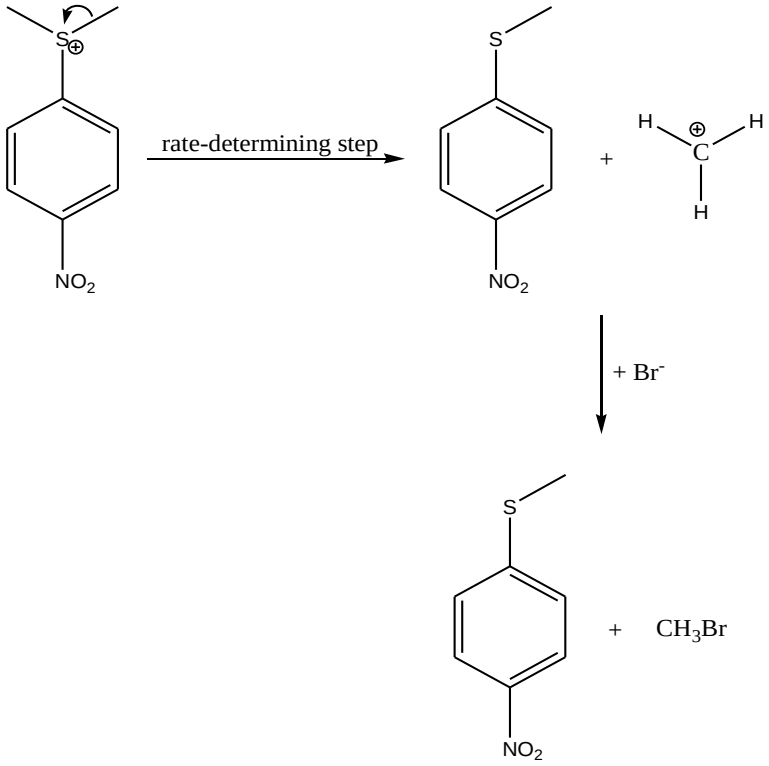

Figure 80 – Proposed S_N1 mechanism for the reaction carried out in benzyl alcohol

The rate constants of reaction in 1-butanol were also measured and are summarized in **Figure 81:**

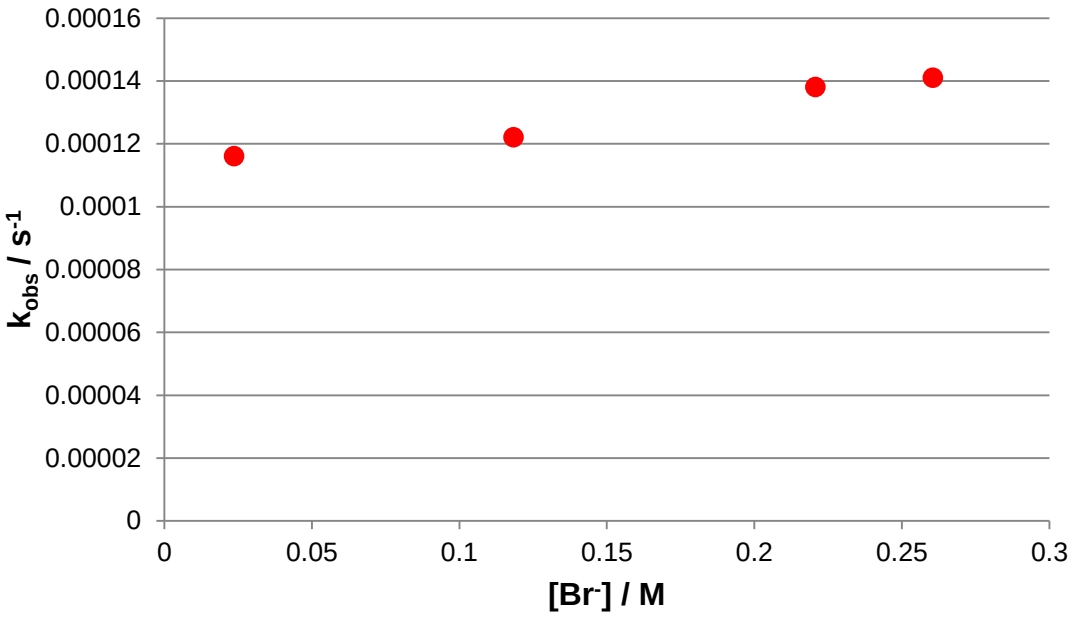

Figure 81 – The dependence of k_{obs} on the bromide concentration for the reactions with [*p*-$NO_2PhS(CH_3)_2$][NTf_2] in pure 1-butanol

Dissimilar to the behaviour in benzyl alcohol, k_{obs} did increase slowly with increasing concentration of Br^- in 1-butanol. The rates of reaction in 1-butanol is slower than in $[C_4C_1pyrr][NTf_2]$, 1,2-dichloroethane and MeCN; again, this was due its strong hydrogen bond donating effect, which stabilized the bromide anion to a greater extent to the transition state.

Before the reaction is carried out in mixtures of benzyl alcohol and $[C_4C_1pyrr][NTf_2]$, one would expect the k_{obs} measured in these mixtures to be somewhat between the values of pure benzyl alcohol and pure $[C_4C_1pyrr][NTf_2]$. However, the rates for the two mixtures (50 mol% $[C_4C_1pyrr][NTf_2]$ / 50 mol% benzyl alcohol and 2 mol% $[C_4C_1pyrr][NTf_2]$ / 98 mol% benzyl alcohol) were both lower than the rates for pure benzyl alcohol and pure $[C_4C_1pyrr][NTf_2]$ (**Figure 82** and **83**).

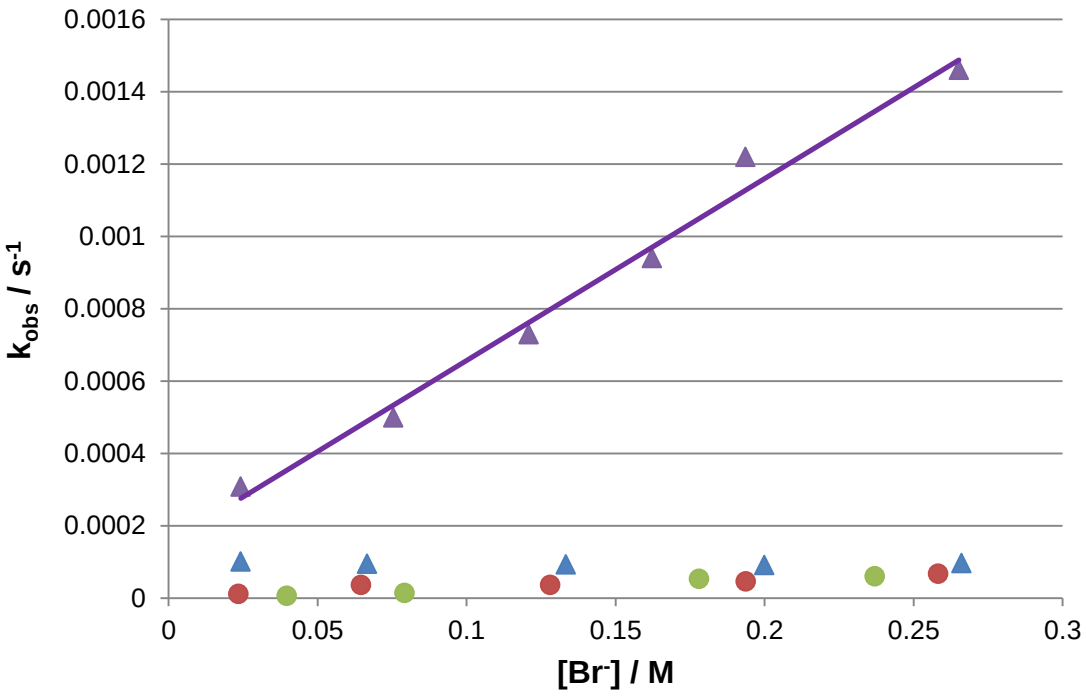

Figure 82 – The dependence of k_{obs} on the bromide concentration for the reactions with [*p*-$NO_2PhS(CH_3)_2$][NTf_2] in [C_4C_1pyrr][NTf_2]/benzyl alcohol mixtures (Purple: 100% [C_4C_1pyrr][NTf_2]; light blue: 100% benzyl alcohol; red: 2.01 mol% [C_4C_1pyrr][NTf_2]; light green: 50.1 mol% [C_4C_1pyrr][NTf_2]))

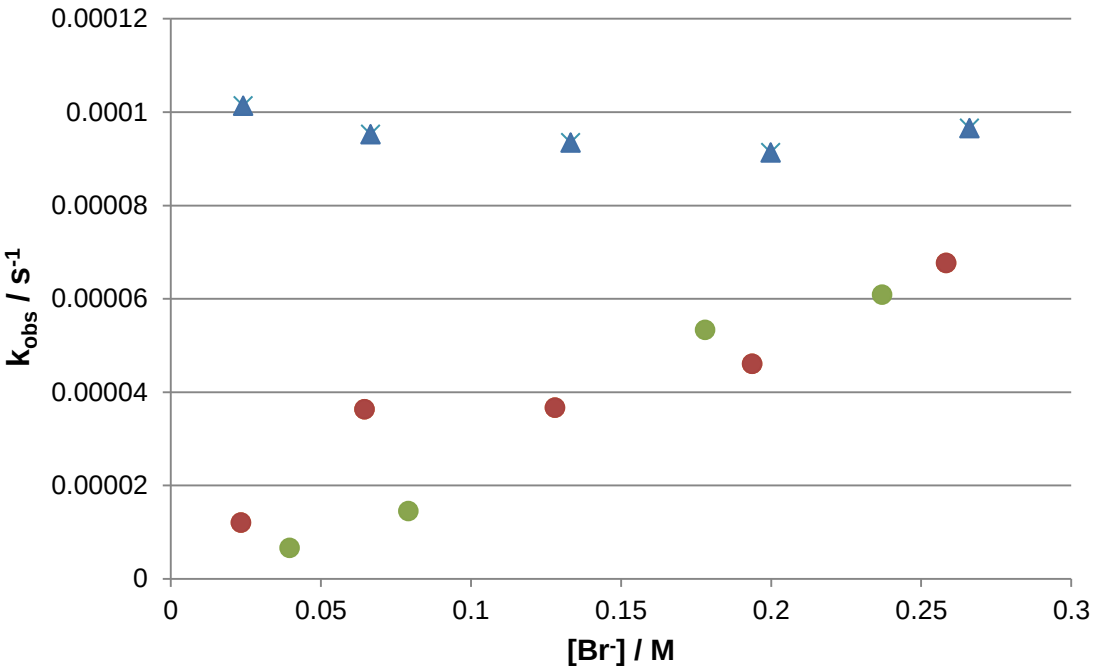

Figure 83 – Expansion of the bottom part of Figure 81 for clarity (Light blue: 100% benzyl alcohol; red: 2.01 mol% [C_4C_1pyrr][NTf_2]; light green: 50.1 mol% [C_4C_1pyrr][NTf_2])

This behaviour cannot be explained without further investigation. To understand whether this behaviour is general for ionic liquid and alcohol mixtures, kinetic measurements of the same reaction in solvent mixtures of 1-butanol and [C_4C_1pyrr][NTf_2] were carried out (**Figure 84** and **85**). Once again, the rate for the mixtures of ionic liquid and alcohol were found to be slower than the rates for both pure solvents.

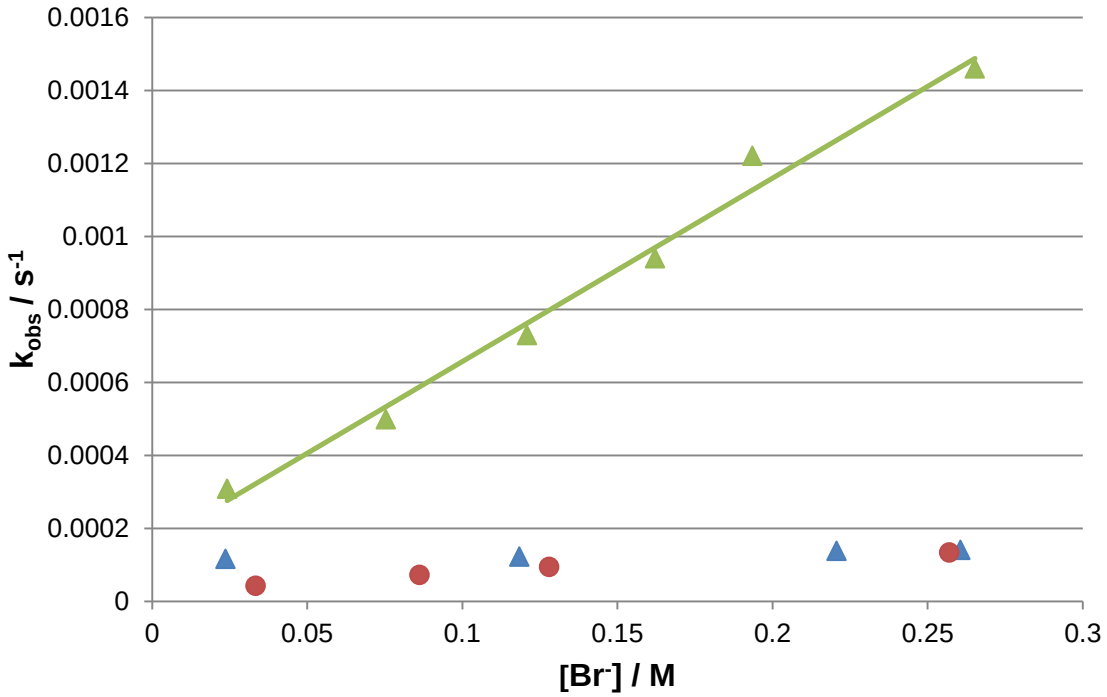

Figure 84 – The dependence of k_{obs} on the bromide concentration for the reactions with [*p*-$NO_2PhS(CH_3)_2$][NTf_2] in mixtures of [C_4C_1pyrr][NTf_2]/1-butanol (Light green: 100% [C_4C_1pyrr][NTf_2]; light blue: 100% 1-butanol; red: 2.01 mol% [C_4C_1pyrr][NTf_2])

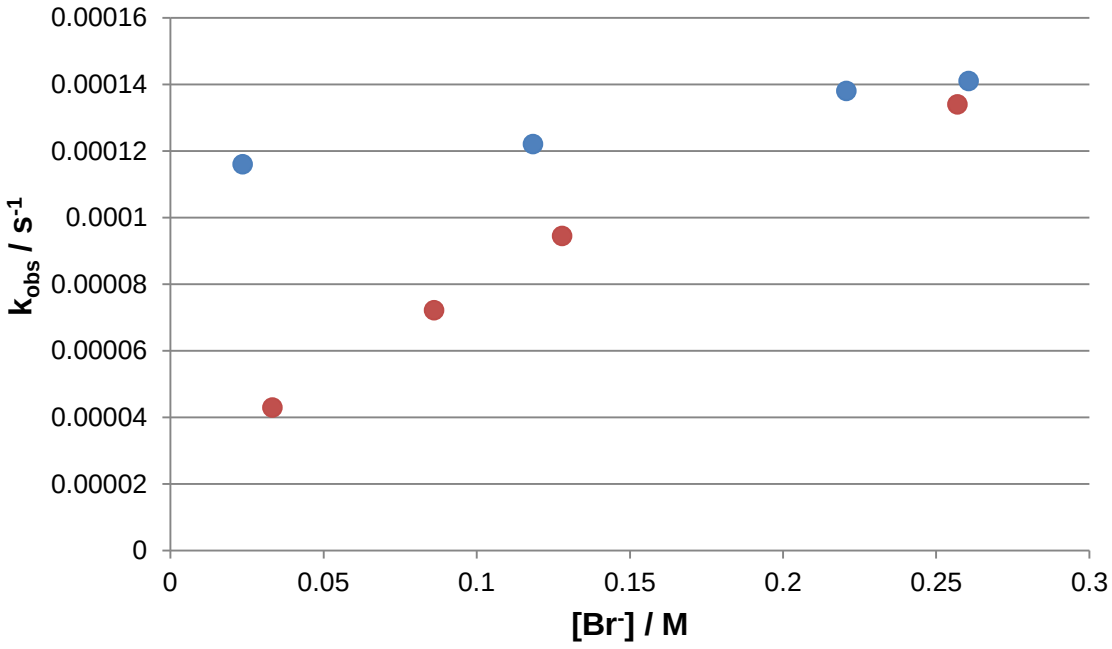

Figure 85 – Expansion of the bottom part of Figure 83 for clarity (Light blue: 100% 1-butanol; red: 2.01 mol% [C_4C_1pyrr][NTf_2])

As described earlier, the rates of reaction of [*p*-$NO_2PhS(CH_3)_2$][$N(Tf)_2$] and halides are inversely dependent upon the hydrogen bond acidity (α) of solvent. The decrease in k_{obs} might indicate an increase in α as a result of mixing alcohols and [C_4C_1pyrr][NTf_2]. The ideal solution to confirm this hypothesis would be measuring α of the mixtures of ionic liquid and alcohol, but α and β cannot be determined for solvent mixtures: Kamlet-Taft parameters are measured using solvatochromic comparison method that calculates the difference in solvent's stabilization of the two dyes. In a binary solvent mixture, the ratios of the two solvents in solvation shells of the two dyes would be different due to preferential solvation. Nevertheless, Kamlet-Taft solvatochromic comparison method was intended to measure polarity in terms of microscopic interactions between solvents and suitable solutes, and was not intended to measure the bulk, overall polarity of a solvent mixture. Although much research has been carried out in measuring Kamlet-Taft parameters for ionic liquid/molecular solvent mixtures, [89, 145] the α and β values obtained from these investigation have insignificant meaning. On the other hand, the π^* values of binary solvent mixtures can be taken more seriously (less error) since the values are based on one dye (e.g. *N,N*-diethyl-4-nitroaniline).

It was decided to measure the E_T^N, which is based on one dye, of two benzyl alcohol/[C_4C_1pyrr][NTf_2] mixtures, in the hope that the measurements would give some insights on the polarity of these solvent mixtures. The E_T^N values of these mixtures were found to be higher than those of pure benzyl alcohol and pure [C_4C_1pyrr][NTf_2] (**Table 41**). These results demonstrated that the overall solvent strength of the solution might be raised as a result of mixing an alcohol with ionic liquid [C_4C_1pyrr][NTf_2]. According to Hughes-Ingold rules (**Section 1.2.1**), this increase in solvent strength enhanced stabilization of the bromide anion (relative to

the transition state), and therefore decreased the rates. There have been other solvatochromic studies of preferential solvation that demonstrated similar "synergetic effect" between the binary solvent components – the solvent strength for the mixed solvents is greater than for the pure solvent components. Machado[146] reported an enhancement of $E_T(30)$ value by mixing protic solvent (e.g methanol) with an hydrogen bond accepting solvent (e.g. DMSO, MeCN), and suggested this synergetic effect might be resulted from an interaction through hydrogen bonding between the protic and the hydrogen bond accepting solvents, forming an even more polar solvent complex. Reichardt[25] and Rosés[147] both reported similar suggestions, but all of these claims lacked substantial experimental evidence and plausible explanations. Overall, the overall increase in solvent strength of $[C_4C_1pyrr][NTf_2]$/alcohol mixtures might be caused by some solvent-solvent interactions, but the mechanism of how these increase the overall solvent strength is unknown.

Liquid/Liquid mixture	$\boldsymbol{E_T^N}$
Benzyl alcohol	0.608
$[C_4C_1pyrr][NTf_2]$	0.544
2.0 mol% $[C_4C_1pyrr][NTf_2]$/98 mol% benzyl alcohol	0.664
50 mol% $[C_4C_1pyrr][NTf_2]$/50 mol% benzyl alcohol	0.713

Table 41 – E_T^N values of benzyl alcohol, $[C_4C_1pyrr][NTf_2]$ and their mixtures

4.8 Conclusion

In this investigation, the rates of reaction of dimethyl-4-nitrophenylsulfonium *bis*(trifluoromethanesulfonyl)imide salt with excess amounts of bromide in some $[C_4C_1pyrr][NTf_2]$/molecular solvent mixtures were measured. When the ionic liquid concentrations in the mixtures of $[C_4C_1pyrr][NTf_2]$/1,2-dichloroethane or MeCN were high enough, linear dependence of k_{obs} upon [Br-] and thus "ionic liquid like" behaviour were observed (i.e. in 50.0 mol% $[C_4C_1pyrr][NTf_2]$ / 50.0 mol% dichloroethane and 50.4 mol% $[C_4C_1pyrr][NTf_2]$ / 49.6 mol% MeCN). This happened because there was so much ionic liquid that nearly all the different ions clustered to form non-discriminating ionic aggregates in these mixtures. These ionic micro-domains behaved similarly to bulk ionic liquids, thus gave similar kinetic behaviour. At lower $[C_4C_1pyrr][NTf_2]$ concentrations in 1,2-dichloroethane or MeCN, the degree of aggregation was not great enough to form these micro-domains for most ions, hence "ionic liquid like" behaviour was not observed in such systems. Overall, ionic solutes would only stop being ion-paired if the amount of ionic liquid in ionic liquid/molecular liquid mixture is great enough.

It has also been found that only a small amount of ionic liquid is needed to heavily slow down the reactions in aprotic polar solvents, such as 1,2-dichloroethane or MeCN. This heavy slowing of rates might be caused by a strong hydrogen bond interaction between the $[C_4C_1pyrr]^+$ cation and the halide nucleophiles. A previous study by Ranieri[137] illustrated that the rate of reaction of this type of sulfonium salt and halide was governed by the hydrogen bond acidity of the solvent. To strengthen this hypothesis, the same reaction was carried out in mixtures of protic solvents (1-butanol and benzyl alcohol) and 1,2-dichloroethane. The results show that these

protic solvents (i.e. solvents which have high α) can also slow the down the reaction by huge amount in the solvent mixtures; this gave support to the speculation that the huge rate reduction in ionic liquid/aprotic solvents was mainly caused by the deactivation of halide by ionic liquid's hydrogen bond donation.

Since out of all the common ionic liquid cations, $[C_4C_1pyrr]^+$ is one of the weakest hydrogen bond donors, ionic liquids of other cations are predicted to form stronger hydrogen bond interaction with the halide nucleophiles. Hence, most common cations of ionic liquids are expected to make an even bigger impact in similar circumstances: stronger rate retardation. However, one must not forget the extent of preferential solvation does not only depend on the difference in polarity between the individual solvents, the difference in size matters as well. $[C_4C_1pyrr]^+$ is larger than 1,2-dichloroethane and MeCN, and this difference in sizes might also contribute to the extent of preferential solvation. Clustering of ions might also further promote preferential solvation in solution.

The kinetic behaviour of the same reaction in $[C_4C_1pyrr][NTf_2]$/1-butanol and $[C_4C_1pyrr][NTf_2]$/benzyl alcohol was also examined. Unexpectedly, the rates for these mixtures did not come in between those for the two pure liquids; k_{obs} recorded in the ionic liquid/alcohol mixtures were lower than rate constants recorded in both pure ionic liquid and pure alcohol. The exact reason for this behaviour is not known (possibly due to some sort of solvent-solvent interactions), but the E_T^N values suggested the solvent strength of $[C_4C_1pyrr][NTf_2]$/benzyl alcohol mixtures was higher than either pure $[C_4C_1pyrr][NTf_2]$ or benzyl alcohol. This pointed toward the possibility of enhanced stabilization of the bromide anion (relative to the transition state), as a result of mixing and therefore decreased the rates, according to Hughes-Ingold rules.

4.9 Full kinetic results

4.9.1 Full kinetic results for the reaction between [C_4C_1pyrr]Br and [*p*-$NO_2PhS(CH_3)_2$][NTf_2] in [C_4C_1pyrr][NTf_2]/1,2-dichloroethane mixtures

[Br^-] / M	[sulfonium] / M	k_{obs} / s^{-1}
0.0162	$1.41 \cdot 10^{-4}$	0.0713 ($1.14 \cdot 10^{-4}$)
0.0358	$1.41 \cdot 10^{-4}$	0.0493 ($2.94 \cdot 10^{-5}$)
0.0609	$1.41 \cdot 10^{-4}$	0.0395 ($9.02 \cdot 10^{-5}$)
0.0811	$1.41 \cdot 10^{-4}$	0.0330 ($4.69 \cdot 10^{-5}$)
0.114	$1.41 \cdot 10^{-4}$	0.0286 ($3.91 \cdot 10^{-5}$)
0.162	$1.41 \cdot 10^{-4}$	0.0235 ($2.09 \cdot 10^{-5}$)
0.211	$1.41 \cdot 10^{-4}$	0.0213 ($3.15 \cdot 10^{-5}$)
0.243	$1.41 \cdot 10^{-4}$	0.0204 ($2.73 \cdot 10^{-5}$)

Table 42 – *Pseudo*-first order rate constants of reactions in 100% 1,2-dichloroethane

[Br^-] / M	[sulfonium] / M	k_{obs} / s^{-1}
0.0167	$1.41 \cdot 10^{-4}$	0.0538 ($7.47 \cdot 10^{-5}$)
0.0334	$1.41 \cdot 10^{-4}$	0.0434 ($5.12 \cdot 10^{-5}$)
0.0626	$1.41 \cdot 10^{-4}$	0.0360 ($5.06 \cdot 10^{-5}$)
0.0835	$1.41 \cdot 10^{-4}$	0.0330 ($3.82 \cdot 10^{-5}$)
0.117	$1.41 \cdot 10^{-4}$	0.0273 ($2.63 \cdot 10^{-5}$)
0.170	$1.41 \cdot 10^{-4}$	0.0242 ($2.17 \cdot 10^{-5}$)
0.217	$1.41 \cdot 10^{-4}$	0.0209 ($1.59 \cdot 10^{-5}$)
0.250	$1.41 \cdot 10^{-4}$	0.0207 ($1.66 \cdot 10^{-5}$)

Table 43 – *Pseudo*-first order rate constants of reactions in 0.21 mol% [C_4C_1pyrr][NTf_2] / 99.79 mol% 1,2-dichloroethane

$[Br^-]$ / M	[sulfonium] / M	k_{obs} / s^{-1}
0.0173	$1.34 \cdot 10^{-4}$	0.0347 ($3.22 \cdot 10^{-5}$)
0.0346	$1.34 \cdot 10^{-4}$	0.0353 ($2.57 \cdot 10^{-5}$)
0.0650	$1.34 \cdot 10^{-4}$	0.0301 ($3.01 \cdot 10^{-5}$)
0.0866	$1.34 \cdot 10^{-4}$	0.0285 ($4.11 \cdot 10^{-5}$)
0.121	$1.34 \cdot 10^{-4}$	0.0238 ($8.58 \cdot 10^{-6}$)
0.173	$1.34 \cdot 10^{-4}$	0.0221 ($1.71 \cdot 10^{-5}$)
0.225	$1.34 \cdot 10^{-4}$	0.0195 ($1.99 \cdot 10^{-5}$)
0.260	$1.34 \cdot 10^{-4}$	0.0195 ($2.45 \cdot 10^{-5}$)

Table 44 – *Pseudo*-first order rate constants of reactions in 0.54 mol% $[C_4C_1pyrr][NTf_2]$ / 99.46 mol% 1,2-dichloroethane

$[Br^-]$ / M	[sulfonium] / M	k_{obs} / s^{-1}
0.0173	$1.45 \cdot 10^{-4}$	0.0223 ($2.76 \cdot 10^{-5}$)
0.0347	$1.45 \cdot 10^{-4}$	0.0252 ($3.78 \cdot 10^{-5}$)
0.0651	$1.45 \cdot 10^{-4}$	0.0257 ($4.23 \cdot 10^{-5}$)
0.0867	$1.45 \cdot 10^{-4}$	0.0247 ($3.61 \cdot 10^{-5}$)
0.121	$1.45 \cdot 10^{-4}$	0.0231 ($4.81 \cdot 10^{-5}$)
0.173	$1.45 \cdot 10^{-4}$	0.0213 ($3.47 \cdot 10^{-5}$)
0.225	$1.45 \cdot 10^{-4}$	0.0188 ($1.63 \cdot 10^{-5}$)
0.260	$1.45 \cdot 10^{-4}$	0.0182 ($3.90 \cdot 10^{-5}$)

Table 45 – *Pseudo*-first order rate constants of reactions in 1.09 mol% $[C_4C_1pyrr][NTf_2]$ / 98.91 mol% 1,2-dichloroethane

$[Br^-]$ / M	[sulfonium] / M	k_{obs} / s^{-1}
0.0168	$1.27 \cdot 10^{-4}$	0.0125 ($1.17 \cdot 10^{-5}$)
0.0340	$1.27 \cdot 10^{-4}$	0.0162 ($2.19 \cdot 10^{-5}$)
0.0638	$1.27 \cdot 10^{-4}$	0.0193 ($2.75 \cdot 10^{-5}$)
0.0850	$1.27 \cdot 10^{-4}$	0.0197 ($2.18 \cdot 10^{-5}$)
0.119	$1.27 \cdot 10^{-4}$	0.0194 ($3.36 \cdot 10^{-5}$)
0.170	$1.27 \cdot 10^{-4}$	0.0184 ($1.91 \cdot 10^{-5}$)
0.220	$1.27 \cdot 10^{-4}$	0.0173 ($2.60 \cdot 10^{-5}$)
0.255	$1.27 \cdot 10^{-4}$	0.0170 ($1.35 \cdot 10^{-5}$)

Table 46 – *Pseudo*-first order rate constants of reactions in 2.00 mol% $[C_4C_1pyrr][NTf_2]$ / 98.00 mol% 1,2-dichloroethane

$[Br^-]$ / M	[sulfonium] / M	k_{obs} / s^{-1}
0.0446	$1.76 \cdot 10^{-4}$	0.00151 ($7.03 \cdot 10^{-7}$)
0.0892	$1.76 \cdot 10^{-4}$	0.00257 ($2.35 \cdot 10^{-6}$)
0.134	$1.76 \cdot 10^{-4}$	0.00351 ($2.31 \cdot 10^{-6}$)
0.178	$1.76 \cdot 10^{-4}$	0.00403 ($6.61 \cdot 10^{-6}$)
0.223	$1.76 \cdot 10^{-4}$	0.00474 ($7.37 \cdot 10^{-6}$)
0.268	$1.76 \cdot 10^{-4}$	0.00510 ($3.87 \cdot 10^{-6}$)

Table 47 – *Pseudo*-first order rate constants of reactions in 19.8 mol% $[C_4C_1pyrr][NTf_2]$ / 80.2 mol% 1,2-dichloroethane

$[Br^-]$ / M	[sulfonium] / M	k_{obs} / s^{-1}	k_2 / $M^{-1}s^{-1}$
0.0220	$1.58 \cdot 10^{-4}$	2.14×10^{-4} ($1.78 \cdot 10^{-6}$)	0.00953 ($4.19 \cdot 10^{-4}$)
0.0879	$1.58 \cdot 10^{-4}$	0.00101 ($2.85 \cdot 10^{-6}$)	
0.132	$1.58 \cdot 10^{-4}$	0.00136 ($1.51 \cdot 10^{-6}$)	
0.176	$1.58 \cdot 10^{-4}$	0.00182 ($2.31 \cdot 10^{-6}$)	
0.220	$1.58 \cdot 10^{-4}$	0.00223 ($3.27 \cdot 10^{-6}$)	
0.264	$1.58 \cdot 10^{-4}$	0.00252 ($5.35 \cdot 10^{-6}$)	

Table 48 – *Pseudo*-first order and second order rate constants of reactions in 50.0 mol% $[C_4C_1pyrr][NTf_2]$ / 50.0 mol% 1,2-dichloroethane

$[Br^-]$ / M	[sulfonium] / M	k_{obs} / s^{-1}	k_2 / $M^{-1}s^{-1}$
0.0242	$1.67 \cdot 10^{-4}$	$3.08 \cdot 10^{-4}$ ($1.58 \cdot 10^{-7}$)	0.00503 ($3.02 \cdot 10^{-4}$)
0.0754	$1.67 \cdot 10^{-4}$	$4.99 \cdot 10^{-4}$ ($3.02 \cdot 10^{-7}$)	
0.121	$1.67 \cdot 10^{-4}$	$7.30 \cdot 10^{-4}$ ($1.11 \cdot 10^{-6}$)	
0.162	$1.67 \cdot 10^{-4}$	$9.40 \cdot 10^{-4}$ ($5.00 \cdot 10^{-7}$)	
0.194	$1.67 \cdot 10^{-4}$	0.00122 ($4.83 \cdot 10^{-6}$)	
0.265	$1.67 \cdot 10^{-4}$	0.00146 ($8.98 \cdot 10^{-7}$)	

Table 49 – *Pseudo*-first order and second order rate constants of reactions in 100% $[C_4C_1pyrr][NTf_2]$

4.9.2 Full kinetic results for the reaction between $[C_4C_1pyrr]Br$ and $[p\text{-}NO_2PhS(CH_3)_2][NTf_2]$ in $[C_4C_1pyrr][NTf_2]$/MeCN mixtures

$[Br^-]$ / M	[sulfonium] / M	k_{obs} / s^{-1}
0.0176	$1.31 \cdot 10^{-4}$	0.00469 ($5.34 \cdot 10^{-7}$)
0.0352	$1.31 \cdot 10^{-4}$	0.00543 ($1.34 \cdot 10^{-6}$)
0.0661	$1.31 \cdot 10^{-4}$	0.00599 ($1.87 \cdot 10^{-6}$)
0.088	$1.31 \cdot 10^{-4}$	0.00610 ($1.63 \cdot 10^{-6}$)
0.123	$1.31 \cdot 10^{-4}$	0.00616 ($2.25 \cdot 10^{-6}$)
0.176	$1.31 \cdot 10^{-4}$	0.00609 ($1.91 \cdot 10^{-6}$)
0.229	$1.31 \cdot 10^{-4}$	0.00598 ($2.40 \cdot 10^{-6}$)
0.264	$1.31 \cdot 10^{-4}$	0.00577 ($1.91 \cdot 10^{-6}$)

Table 50 – *Pseudo*-first order rate constants of reactions in 100% MeCN

$[Br^-]$ / M	[sulfonium] / M	k_{obs} / s^{-1}
0.0178	$1.38 \cdot 10^{-4}$	0.00320 ($2.31 \cdot 10^{-6}$)
0.0356	$1.38 \cdot 10^{-4}$	0.00439 ($1.42 \cdot 10^{-6}$)
0.0667	$1.38 \cdot 10^{-4}$	0.00524 ($1.51 \cdot 10^{-6}$)
0.0889	$1.38 \cdot 10^{-4}$	0.00552 ($2.34 \cdot 10^{-6}$)
0.124	$1.38 \cdot 10^{-4}$	0.00568 ($2.27 \cdot 10^{-6}$)
0.178	$1.38 \cdot 10^{-4}$	0.00572 ($1.58 \cdot 10^{-6}$)
0.231	$1.38 \cdot 10^{-4}$	0.00571 ($2.85 \cdot 10^{-6}$)
0.267	$1.38 \cdot 10^{-4}$	0.00564 ($2.67 \cdot 10^{-6}$)

Table 51 – *Pseudo*-first order rate constants of reactions in 0.21 mol% $[C_4C_1pyrr][NTf_2]$ / 99.79 mol% MeCN

$[Br^-]$ / M	[sulfonium] / M	k_{obs} / s^{-1}
0.0173	$1.50 \cdot 10^{-4}$	0.00249 ($9.02 \cdot 10^{-7}$)
0.0345	$1.50 \cdot 10^{-4}$	0.00367 ($1.05 \cdot 10^{-6}$)
0.0648	$1.50 \cdot 10^{-4}$	0.00456 ($8.81 \cdot 10^{-7}$)
0.0863	$1.50 \cdot 10^{-4}$	0.00501 ($2.14 \cdot 10^{-6}$)
0.121	$1.50 \cdot 10^{-4}$	0.00523 ($1.93 \cdot 10^{-6}$)
0.173	$1.50 \cdot 10^{-4}$	0.00547 ($2.38 \cdot 10^{-6}$)
0.224	$1.50 \cdot 10^{-4}$	0.00543 ($2.33 \cdot 10^{-6}$)
0.259	$1.50 \cdot 10^{-4}$	0.00548 ($4.02 \cdot 10^{-6}$)

Table 52 – *Pseudo*-first order rate constants of reactions in 0.50 mol% $[C_4C_1pyrr][NTf_2]$ / 99.50 mol% MeCN

$[Br^-]$ / M	[sulfonium] / M	k_{obs} / s^{-1}
0.0169	$1.46 \cdot 10^{-4}$	0.00189 ($1.13 \cdot 10^{-6}$)
0.0338	$1.46 \cdot 10^{-4}$	0.00310 ($1.13 \cdot 10^{-6}$)
0.0634	$1.46 \cdot 10^{-4}$	0.00390 ($1.47 \cdot 10^{-6}$)
0.0845	$1.46 \cdot 10^{-4}$	0.00423 ($1.56 \cdot 10^{-6}$)
0.118	$1.46 \cdot 10^{-4}$	0.00464 ($2.57 \cdot 10^{-6}$)
0.169	$1.46 \cdot 10^{-4}$	0.00511 ($7.72 \cdot 10^{-6}$)
0.220	$1.46 \cdot 10^{-4}$	0.00495 ($2.70 \cdot 10^{-6}$)
0.253	$1.46 \cdot 10^{-4}$	0.00511 ($4.56 \cdot 10^{-6}$)

Table 53 – *Pseudo*-first order rate constants of reactions in 1.03 mol% $[C_4C_1pyrr][NTf_2]$ / 98.97 mol% MeCN

$[Br^-]$ / M	[sulfonium] / M	k_{obs} / s^{-1}
0.0168	$1.37 \cdot 10^{-4}$	$9.98 \cdot 10^{-4}$ ($5.76 \cdot 10^{-8}$)
0.0336	$1.37 \cdot 10^{-4}$	0.00178 ($1.94 \cdot 10^{-7}$)
0.0631	$1.37 \cdot 10^{-4}$	0.00263 ($4.33 \cdot 10^{-7}$)
0.0841	$1.37 \cdot 10^{-4}$	0.00307 ($9.37 \cdot 10^{-7}$)
0.118	$1.37 \cdot 10^{-4}$	0.00353 ($5.62 \cdot 10^{-7}$)
0.168	$1.37 \cdot 10^{-4}$	0.00403 ($1.78 \cdot 10^{-6}$)
0.219	$1.37 \cdot 10^{-4}$	0.00428 ($1.85 \cdot 10^{-6}$)
0.252	$1.37 \cdot 10^{-4}$	0.00442 ($2.21 \cdot 10^{-6}$)

Table 54 – *Pseudo*-first order rate constants of reactions in 2.17 mol% $[C_4C_1pyrr][NTf_2]$ / 97.83 mol% MeCN

$[Br^-]$ / M	[sulfonium] / M	k_{obs} / s^{-1}
0.0443	$1.68 \cdot 10^{-4}$	$5.69 \cdot 10^{-4}$ ($2.65 \cdot 10^{-8}$)
0.0887	$1.68 \cdot 10^{-4}$	0.00104 ($1.52 \cdot 10^{-7}$)
0.133	$1.68 \cdot 10^{-4}$	0.00146 ($3.12 \cdot 10^{-7}$)
0.178	$1.68 \cdot 10^{-4}$	0.00179 ($5.96 \cdot 10^{-7}$)
0.222	$1.68 \cdot 10^{-4}$	0.00205 ($6.26 \cdot 10^{-7}$)
0.266	$1.68 \cdot 10^{-4}$	0.00222 ($1.10 \cdot 10^{-6}$)

Table 55 – *Pseudo*-first order and second order rate constants of reactions in 18.8 mol% $[C_4C_1pyrr][NTf_2]$ / 81.2 mol% MeCN

$[Br^-]$ / M	[sulfonium] / M	k_{obs} / s^{-1}	k_2 / $M^{-1}s^{-1}$
0.0442	$1.85 \cdot 10^{-4}$	$4.32 \cdot 10^{-4}$ ($1.02 \cdot 10^{-7}$)	0.00560 ($1.26 \cdot 10^{-4}$)
0.0894	$1.85 \cdot 10^{-4}$	$7.20 \cdot 10^{-4}$ ($1.17 \cdot 10^{-6}$)	
0.132	$1.85 \cdot 10^{-4}$	$9.06 \cdot 10^{-4}$ ($7.63 \cdot 10^{-7}$)	
0.177	$1.85 \cdot 10^{-4}$	0.00121 ($8.77 \cdot 10^{-7}$)	
0.221	$1.85 \cdot 10^{-4}$	0.00143 ($1.86 \cdot 10^{-6}$)	
0.265	$1.85 \cdot 10^{-4}$	0.00167 ($1.93 \cdot 10^{-5}$)	

Table 56 – *Pseudo*-first order and second order rate constants of reactions in 50.4 mol% $[C_4C_1pyrr][NTf_2]$ / 49.6 mol% MeCN

4.9.3 Full kinetic results for the reaction between $[C_4C_1pyrr]Br$ and $[p\text{-}NO_2PhS(CH_3)_2][NTf_2]$ reactions in alcohols/1,2-dichloroethane mixtures

$[Br^-]$ / M	[sulfonium] / M	k_{obs} / s^{-1}
0.0242	$1.71 \cdot 10^{-4}$	$1.01 \cdot 10^{-4}$ ($2.25 \cdot 10^{-7}$)
0.0666	$1.71 \cdot 10^{-4}$	$9.64 \cdot 10^{-5}$ ($8.47 \cdot 10^{-7}$)
0.133	$1.71 \cdot 10^{-4}$	$9.35 \cdot 10^{-5}$ ($8.57 \cdot 10^{-7}$)
0.200	$1.71 \cdot 10^{-4}$	$9.13 \cdot 10^{-5}$ ($5.25 \cdot 10^{-7}$)
0.266	$1.71 \cdot 10^{-4}$	$9.66 \cdot 10^{-5}$ ($9.43 \cdot 10^{-7}$)

Table 57 – *Pseudo*-first order rate constants of reactions in 100% benzyl alcohol

$[Br^-]$ / M	[sulfonium] / M	k_{obs} / s^{-1}
0.0170	$1.70 \cdot 10^{-4}$	0.0183 ($1.07 \cdot 10^{-5}$)
0.0341	$1.70 \cdot 10^{-4}$	0.0155 ($1.02 \cdot 10^{-5}$)
0.0640	$1.70 \cdot 10^{-4}$	0.0145 ($1.01 \cdot 10^{-5}$)
0.0852	$1.70 \cdot 10^{-4}$	0.0140 ($9.00 \cdot 10^{-6}$)
0.119	$1.70 \cdot 10^{-4}$	0.0137 ($9.20 \cdot 10^{-6}$)
0.170	$1.70 \cdot 10^{-4}$	0.0136 ($7.84 \cdot 10^{-6}$)
0.222	$1.70 \cdot 10^{-4}$	0.0136 ($7.73 \cdot 10^{-6}$)
0.256	$1.70 \cdot 10^{-4}$	0.0139 ($1.03 \cdot 10^{-5}$)

Table 58 – *Pseudo*-first order rate constants of reactions in 2.15 mol% benzyl alcohol / 97.85 mol% 1,2-dichloroethane

$[Br^-]$ / M	[sulfonium] / M	k_{obs} / s^{-1}
0.0237	$1.81 \cdot 10^{-4}$	$1.16 \cdot 10^{-4}$ ($2.62 \cdot 10^{-7}$)
0.118	$1.81 \cdot 10^{-4}$	$1.22 \cdot 10^{-4}$ ($1.27 \cdot 10^{-6}$)
0.221	$1.81 \cdot 10^{-4}$	$1.38 \cdot 10^{-4}$ ($1.53 \cdot 10^{-6}$)
0.261	$1.81 \cdot 10^{-4}$	$1.41 \cdot 10^{-4}$ ($2.02 \cdot 10^{-6}$)

Table 59 – *Pseudo*-first order rate constants of reactions in 100% 1-butanol

$[Br^-]$ / M	[sulfonium] / M	k_{obs} / s^{-1}
0.0169	$1.45 \cdot 10^{-4}$	0.0333 ($2.10 \cdot 10^{-5}$)
0.0337	$1.45 \cdot 10^{-4}$	0.0261 ($1.42 \cdot 10^{-5}$)
0.0633	$1.45 \cdot 10^{-4}$	0.0210 ($7.94 \cdot 10^{-6}$)
0.0843	$1.45 \cdot 10^{-4}$	0.0196 ($9.68 \cdot 10^{-6}$)
0.117	$1.45 \cdot 10^{-4}$	0.0176 ($7.63 \cdot 10^{-6}$)
0.169	$1.45 \cdot 10^{-4}$	0.0163 ($7.68 \cdot 10^{-6}$)
0.219	$1.45 \cdot 10^{-4}$	0.0151 ($6.57 \cdot 10^{-6}$)
0.253	$1.45 \cdot 10^{-4}$	0.0149 ($6.17 \cdot 10^{-6}$)

Table 60 – *Pseudo*-first order rate constants of reactions in 2.07 mol% 1-butanol / 97.93 mol% 1,2-dichloroethane

4.10.4 Full kinetic results for the reactions in between $[C_4C_1pyrr]Br$ and $[p\text{-}NO_2PhS(CH_3)_2][NTf_2]$ in $[C_4C_1pyrr][NTf_2]$/ alcohols mixtures

$[Br^-]$ / M	[sulfonium] / M	k_{obs} / s^{-1}
0.0234	$1.84 \cdot 10^{-4}$	$1.20 \cdot 10^{-5}$ ($3.19 \cdot 10^{-7}$)
0.0646	$1.84 \cdot 10^{-4}$	$3.63 \cdot 10^{-5}$ ($4.54 \cdot 10^{-7}$)
0.128	$1.84 \cdot 10^{-4}$	$3.67 \cdot 10^{-5}$ ($1.03 \cdot 10^{-6}$)
0.194	$1.84 \cdot 10^{-4}$	$4.60 \cdot 10^{-5}$ ($7.69 \cdot 10^{-7}$)
0.258	$1.84 \cdot 10^{-4}$	$6.77 \cdot 10^{-5}$ ($7.87 \cdot 10^{-7}$)

Table 61– *Pseudo*-first order rate constants of reactions in 2.01 mol% $[C_4C_1pyrr][NTf_2]$ / 97.99 mol% benzyl alcohol

$[Br^-]$ / M	[sulfonium] / M	k_{obs} / s^{-1}
0.0396	$2.01 \cdot 10^{-4}$	$6.63 \cdot 10^{-6}$ ($1.05 \cdot 10^{-6}$)
0.0792	$2.01 \cdot 10^{-4}$	$1.46 \cdot 10^{-5}$ ($2.24 \cdot 10^{-7}$)
0.178	$2.01 \cdot 10^{-4}$	$5.33 \cdot 10^{-5}$ ($1.03 \cdot 10^{-6}$)
0.237	$2.01 \cdot 10^{-4}$	$6.09 \cdot 10^{-5}$ ($7.00 \cdot 10^{-7}$)

Table 62 – *Pseudo*-first order rate constants of reactions in 50.1 mol% $[C_4C_1pyrr][NTf_2]$ / 49.9 mol% benzyl alcohol

$[Br^-]$ / M	[sulfonium] / M	k_{obs} / s^{-1}
0.0334	$3.74 \cdot 10^{-4}$	$4.31 \cdot 10^{-5}$ ($8.53 \cdot 10^{-8}$)
0.0862	$3.74 \cdot 10^{-4}$	$7.55 \cdot 10^{-5}$ ($7.41 \cdot 10^{-7}$)
0.128	$3.74 \cdot 10^{-4}$	$9.47 \cdot 10^{-5}$ ($3.89 \cdot 10^{-7}$)
0.193	$3.74 \cdot 10^{-4}$	$1.14 \cdot 10^{-4}$ ($3.73 \cdot 10^{-7}$)
0.257	$3.74 \cdot 10^{-4}$	$1.34 \cdot 10^{-4}$ ($2.14 \cdot 10^{-7}$)

Table 63 – *Pseudo*-first order rate constants of reactions in 1.00 mol% $[C_4C_1pyrr][NTf_2]$ / 99.00 mol% 1-butanol

$[Br^-]$ / M	[sulfonium] / M	k_{obs} / s^{-1}
0.0334	$2.88 \cdot 10^{-4}$	$4.29 \cdot 10^{-5}$ ($8.11 \cdot 10^{-8}$)
0.0862	$2.88 \cdot 10^{-4}$	$7.22 \cdot 10^{-5}$ ($8.00 \cdot 10^{-7}$)
0.128	$2.88 \cdot 10^{-4}$	$9.45 \cdot 10^{-5}$ ($5.66 \cdot 10^{-7}$)
0.257	$2.88 \cdot 10^{-4}$	$1.34 \cdot 10^{-4}$ ($9.19 \cdot 10^{-7}$)

Table 64 – *Pseudo*-first order rate constants of reactions in 2.01 mol% $[C_4C_1pyrr][NTf_2]$ / 97.99 mol% 1-butanol

5. Summary

In the previous kinetic study of a nucleophilic substitution reaction between a charged nucleophile and a charged electrophile, the Welton group demonstrated that ionic liquids were “super-dissociated” toward solute ions and that no solute ion pairs were present in these ionic solutions.[1] In this investigation, it was demonstrated that the term “super-dissociated” solvent might not be a suitable term to describe an ionic liquid. This is because ionic solutes neither associate nor dissociate in an ionic liquid. On the contrary, they form a non-discriminating ideal mixture with the ionic liquid, with no preferential ion pairing involved. In this investigation, the Kosower’s charge-transfer complex 1-ethyl-4-(methoxycarbonyl)pyridinium iodide was combined with ionic liquids of three different cations and four different anions – all of these mixtures were found to be non-discriminating. In molecular solvents, the Kosower’s complex existed as different types of ion pairs, aggregates and free ions, and the solute ions of opposite charges were required to be close in proximity in order to preserve charge neutrality. Ionic liquids, conversely, can solvate individual ions completely as they are capable of preserving charge neutrality.

In the second part of this investigation, the kinetic study of a S_N2 reaction between $[C_4C_1pyrr]Br$ and $[p\text{-}NO_2PhS(CH_3)_2][NTf_2]$ in some ionic liquid/molecular solvent mixtures was carried out. At high ionic liquid concentrations in these solvent mixture (i.e. 50.0 mol% $[C_4C_1pyrr][NTf_2]$ / 50.0 mol% dichloroethane and 50.4 mol% $[C_4C_1pyrr][NTf_2]$ / 49.6 mol% MeCN), there were so much ionic liquid that nearly all the different ions (solvents, electrophiles and nucleophiles) clustered to form non-discriminating ionic aggregates in these mixtures. These ionic micro-domains behaved similarly to bulk ionic liquids (i.e. lack of preferential ion pairing), thus gave similar kinetic behaviour. However, at lower ionic liquid concentrations, the ionic

liquid/molecular liquid mixtures gave kinetic behaviour as that in pure organic solvents. These results indicated that at low ionic liquid concentrations, a certain amount of solutes were still preferentially ion paired to each other.

In this investigation, it was also found the ionic liquid deactivated the nucleophilicity of bromide ion in aprotic solvents (e.g. 1,2-dichloroethane and MeCN) very strongly. The huge slowing of reaction rates by ionic liquids might be caused by the strong hydrogen bond interaction between the cation and the electron lone pairs on the halide. This interaction led to the preferential solvation of the bromide by the ionic liquid, which slowed down this reaction in an ionic liquid/aprotic solvent mixture. Size disparity between the ionic liquid (cation) and the molecular solvents and ion clustering might also contribute to the strong preferential solvation.

6. References

1. J. P. Hallett, C. L. Liotta, G. Ranieri and T. Welton, *J. Org. Chem.*, **2009**, 74 (5), 1864-1868.
2. E. M. Kosower, *J. Am. Chem. Soc.*, **1958**, 80 (13), 3253-3260.
3. J. M. DeSimone, *Science*, **2002**, 297, 799-803.
4. M. Poliakoff, J. M. Fitzpatrick, T. R. Farren and P. T. Anastas, *Science*, **2002**, 297, 807-810.
5. J. B. McClain, D. E. Betts, D. A. Canelas, E. T. Samulski, J. M. DeSimone, J. D. Londono, H. D. Cochran, G. D. Wignall, D. Chillura-Martino and R. Triolo, *Science*, **1996**, 274, 2049-2052.
6. T. Welton, *Chem. Rev.*, **1999**, 99, 2071-2083.
7. R. D. Rogers and K. R. Seddon, *Science*, **2003**, 32 (5646), 792-793.
8. X. Li, D. Zhao, Z. Fei and L. Wang, *Science in China Series B: Chemistry*, **2006**, 49 (5), 385-401.
9. J. D. Holbrey, M. B. Turner, M. Reichert and R. D. Rogers, *Green Chem.*, **2003**, 5, 731-736.
10. H. Niedermeyer, M. A. Ab Rani, P. D. Lickiss, J. P. Hallett, T. Welton, A. J. P. White and P. A. Hunt, *Phys. Chem. Chem. Phys.*, **2010**, 12, 2018-2029.
11. M. Freemantle, *Chem. Eng. News*, **2003**, 81, 9.
12. V. Stegmann and K. Massonne, U.S. Patent 0055084, **2007**.
13. B. Weyershausen and K. Lehmann, *Green Chem.*, **2005**, 7, 15-19.
14. M. J. Earle, J. M. S. S. Esperança, M. A. Gilea, J. N. Canongia Lopes, L. P. N. Rebelo, J. W. Magee, K. R. Seddon and J. A. Widegren, *Nature*, **439**, 831-834.
15. J. P. Armstrong, C. Hurst, R. G. Jones, P. Licence, K. R. J. Lovelock, C. J. Satterley and I. J. Villar-Garcia, *Phys. Chem. Chem. Phys.*, **2007**, 9, 982-990.
16. D. M. Fox, W. H. Awad, J. W. Gilman, P. H. Maupin, H. C. De Long and P. C. Trulove, *Green Chem.*, **2003**, 5, 724-727.
17. M. Smiglak, W. M. Reichert, J. D. Holbrey, J. S. Wilkes, L. Sun, J. S. Thrasher, K. Kirichenko, S. Singh, A. R. Katritzky and R. D. Rogers, *Chem. Commun.*, **2006,** 2554-2556.
18. M. A. Haidekker, T. P. Brady, D. Lichlyter and E. A. Theodorakis, *Bioinorg. Chem.*, **2005**, 33, 415-425.

19. P. Wasserschied and T. Welton, *Ionic liquids in synthesis*, VCH-Wiley, Weinheim, **2002**.

20. M. Matzke, S. Stolte, K. Thiele, T. Juffernholz, J. Arning, J. Ranke, U. Welz-Biermann and B. Jastorff, *Green Chem.*, **2007**, 9, 1198-1207.

21. D. J. Couling, R. J. Bernot, K. M. Docherty, J. K. Dixon and E. J. Maginn, *Green. Chem*, **2006**, 8, 82-90.

22. D. M. Eike, J. F. Brennecke and E. J. Maginn, *Green Chem.*, **2003**, 5, 323-328.

23. M. C. Kroon, W. Buijs, C. J. Peters and G-J. Witkamp, *Thermochim. Acta*, **2007**, 465, 40-47.

24. P. M. Mancini; G. G. Fortunato; C. G. Adam and L. R. Vottero, *J. Phys. Org. Chem.*, 2008, **21**, 87-95.

25. D. W. Kim; C. E. Song and D. Y. Chi, *J. Org. Chem.*, 2003, **68**, 4281-4285.

26. J. D. Holbrey and K. R. Seddon, *J. Chem. Soc., Dalton Trans.*, **1999,** 2133-2140.

27. L. Ropel, L. S. Belvèze, S. N. V. K. Aki, M. A. Stadtherr, J. F. Brennecke, *Green Chem.*, **2005**, 7, 83-90.

28. A. Heintz, D. V. Kulikov and S. P. Verevkin, *J. Chem. Eng. Data*, **2002**, *47*, 894-899.

29. D. B. Trampe, *Ph. D Thesis, University of Illinois at Urbana-Champaign*, **1993**.

30. J. Wisniak, E. Magen, M. Shachar, I. Zeroni, R. Reich and H. Segura, *J. Chem. Eng. Data*, **1997**, 42, 458-462.

31. H. Weingärtner, *Z. Phys. Chem.*, **2006**, 220, 1395-1405.

32. C. Wakai, A. Oleinikova, M. Ott, H. Weingärtner, *J. Phys. Chem. B*, **2005**, 105, 17028-17030.

33. E. Grunwald and S. Winstein, *J. Am. Chem. Soc.*, **1948**, 70(2), 846–854.

34. C. Reichardt, *Chem. Rev.*, **1994**, 94, 2319-2358.

35. L. Crowhurst, P. R. Mawdsley. J. M. Perez-Arlandis, P. A. Salter and T. Welton, *Phys. Chem. Chem. Phys.*, **2003**, 5, 2790-2794.

36. M. J. Kamlet and R. W. Taft, *J. Am. Chem. Soc.*, **1976**, 98 (2), 377-383.

37. R. W. Taft and M. J. Kamlet, *J. Am. Chem. Soc.*, **1976**, 98 (10), 2886-2894.

38. M. J. Kamlet, J. L. Abboud and R. W. Kamlet, *J. Am. Chem. Soc.*, **1977**, 99 (18), 6027-6038.

39. A. Piatek, C. Chapuis and J. Jurczak, *J. Phys. Org. Chem.*, **2003**, 16, 700-708.

40. B. Chawla, S. K. Pollack, C. B. Lebrilla, M. J. Kamlet and R. W. Taft, *J. Am. Chem. Soc.*, **1981**, 103, 6924-6929.

41. H. Svith, H. Jensen, J. Almstredt, P. Andersson, T. Lundbäck, K. Daasbjerg, M. J. Jonsson, *J. Phys. Chem. A.*, **2004**, 108, 4805-4811.

42. C. Reichardt, *Solvents and solvent effects in organic chemistry*, VCH, Weinheim, **1990**.

43. R. F. Nystrom and W. G. Brown, *J. Am. Chem. Soc.*, **1947**, 69 (5), 1197-1199.

44. E. D. Hughes and C. K. Ingold, *J. Chem. Soc.*, **1935**, 244-255.

45. J. L. Gleave, E. D. Hughes and C. K. Ingold, *J. Chem. Soc.*, **1935**, 236-241.

46. S. G. Smith, A.H. Fainberg and S. Winstein, *J. Am. Chem. Soc.*, **1961,** 83, 618-625.

47. C. Wheeler, K. N .West, C. L. Liotta and C. A. Eckert, *Chem. Commun.*, **2001**, 887-888.

48. M. Makosza, *Pure Appl. Chem.*, **2000**, 72 (7), 1399-1403.

49. N. M. T. Lourenço and C. A. M. Alfonso, *Tetrahedron*, **2003**, 59, 789-794.

50. J. P. Hallett and T. Welton, *Chem. Rev.*, **2011**, 111 (5), 3508-1876.

51. J. S. Yadav, B. V. S. Reddy, A. K. Basak and A. V. Narsaiah, *Tetrahedron Lett.*, **2003**, 44, 1047-1050.

52. Z. Liu, Z-C Chen and Q-G Zheng, *Synthesis*, **2004**, 1, 33-36.

53. N. L. Lancaster, T. Welton and G. B. Young, *J. Chem. Soc., Perkin 2*, **2001**, 2267-2270.

54. N. L. Lancaster, P. A. Salter, T. Welton and G. B. Young, *J. Org. Chem.*, **2002**, 67, 8855-8861.

55. L. Crowhurst, N. L. Lancaster, J. M. Perez-Arlandis and T. Welton, *J. Am. Chem. Soc.*, **2004**, 126 (37), 11549-11555.

56. L. Crowhurst, R. Falcone, N. L. Lancaster, V. Llopis-Mestre and T. Welton, *J. Org. Chem.*, **2006**, 71 (23), 8847-8853.

57. I. Newington, J. M. Perez-Arlandis and T. Welton, *Org. Lett.*, **2007**, 9 (25), 5247-5250.

58. G. Ranieri, J. P. Hallett and T. Welton, *Ind. Eng. Chem. Res.*, **2008**, 47, 638-644.

59. P. M. Mancini, G. G. Fortunato, C. G. Adam and L. R. Vottero, *J. Phys. Org. Chem.*, **2008**, 21, 87-95.

60. D. W. Kim, C. E. Song and D. Y. Chi, *J. Org. Chem.*, **2003**, 68, 4281-4285.

61. K. R. Seddon, A. Stark and M-J Torres, *Pure Appl. Chem.*, **2000**, 72 (12), 2275-2287.

62. J. Wang, Y. Tian, Y. Zhao and K. Zhuo, *Green Chem.*, **2003**, 5, 618-622.

63. A. Arce, E. Rodil and A. Soto, *J. Solution Chem.*, **2006**, 35 (1), 63-78.

64. D. W. Kim, C. E. Song and D. Y. Chi, *J. Am. Chem. Soc.*, **2002**, 124, 10278-10279.

65. D. W. Kim, D. J. Hong, J. W. Seo, H. S. Kim, H. K. Kim, C. E. Song and D. Y. Chi, *J. Org. Chem.*, **2004**, 69, 3186-3189.

66. M. R. Gerstenberger and A. Haas, *Angew. Chem. Int. Ed. Engl.*, **1981**, 20, 647-667.

67. A. R. Harifi-Mood, A. Habibi-Yangjeh and M. R. Gholami, *Int. J. Chem. Kinet.*, **2007**, 39, 681-687.

68. Y. Marcus and G. Hefter, *Chem. Rev.*, **2006**, 106 (11), 4585-4621.

69. R. Buchner, F. Samani, P. M. May, P. Sturm and G. Hefter, *ChemPhysChem*, **2003**, 4, 373-378.

70. G. Makov and A. Nitzan, *J. Phys. Chem.*, **1992**, 96, 2965-2967.

71. Y. Marcus, *Ion solvation*, Wiley-Interscience, **1985**.

72. E. Grunwald, *Anal. Chem.*, **1954**, 26 (11), 1696-1701.

73. S. Winstein and G. C. Robinson, **1958**, 80, 169-181.

74. T. E. Hogen-Esch and J. Smid, *J. Am. Chem. Soc.*, **1965**, 87, 669-670.

75. T. E. Hogen-Esch and J. Smid, *J. Am. Chem. Soc.*, **1966**, 88, 307-318.

76. R. M. Fuoss and C. A. Kraus, *J. Am. Chem. Soc.*, **1933**, 55, 1019-1028.

77. C. Guha, J. M. Chakraborty, S. Karanjai and B. Das, *J. Phys. Chem. B*, **2003**, 107, 12814-12819.

78. N. M. Atherton and S. I. Weissman, *J. Am. Chem. Soc.*, **1961**, 83, 1330-1334.

79. N. Hirota, *J. Phys. Chem.*, **1967**, 71, 127-138.

80. A. Ben-Naim, *Pure & Appl. Chem.*, **1990**, 62 (1), 25-34.

81. E. Grunwald, G. Baughman and G. Kohnstam, *J. Am. Chem. Soc.*, **1960**, 82, 5801-5811.

82. Y. Marcus, *J. Chem. Soc. Faraday Trans. 1*, **1988**, 84, 1465-1473.

83. H. Ohtaki, *Monatshefte fur Chemie*, **2001**, 132, 1237-1268.

84. P. Chatterjee and S. Bagchi, *J. Chem. Soc. Faraday Trans.*, **1990**, 1785-1789.

85. P. Chatterjee and S. Bagchi, *J. Phys. Chem.*, **1991**, 95, 3311-3314.

86. P. Chatterjee, A. K. Laha and S. Bagchi, *J. Chem. Soc. Faraday Trans.*, **1992**, 88, 1675-1678.

87. P. Chatterjee and S. Bagchi, *J. Chem. Soc. Faraday Trans.*, **1991**, 87 (4), 587-589.

88. A. J. Parker, *Chem. Rev.*, **1969**, 69, 1-32.

89. B. R. Mellein, N. V. K. Aki, R. L. Ladewski and J. F. Brennecke, *J. Phys. Chem. B*, **2007**, 111, 131-138.

90. L. S. Frankel, C. H. Langford and T. R. Stengle, *J. Phys. Chem.*, **1970**, 74 (6), 1376-1381.

91. H. Krienke, G. Ahn-Ercan and J. Barthel, *J. Mol Liq.*, **2004**, 109, 115-124.

92. E. Humeres, R. J. Nunes, V. G. Machado, M. D. G. Gasques and C. Machado, *J. Org. Chem.*, **2001**, 66 (4), 1163-1170.

93. J. W. Larson and T. B. McMahon, *J. Am. Chem. Soc.*, **1984**, 106 (3), 517-521.

94. G. T. Hefter, *Pure & Appl. Chem.*, **1991**, 63 (12), 1749-1758.

95. J. Zielkiewicz, *Phys. Chem. Chem. Phys.*, **2000**, 2, 2925-2932.

96. J. C. Schleicher and A. M. Scurto, *Green Chem.*, **2009**, 11, 694-703.

97. R. S. Varma and V. V. Namboodiri, *Chem. Commun.*, **2001**, 643-644.

98. V. V. Namboodiri and R. S. Varma, *Org. Lett*, **2002**, 4 (18), 3161-3163.

99. C. W. Davies and A. L. Jones, *Trans. Faraday. Soc.*, **1955**, 51, 812-817.

100. J. D. Holbrey, W. M. Reichert, R. P. Swatloski, G. A. Broker, W. R. Pitner, K.R. Seddon and R. D. Rogers, *Green Chem.*, **2002**, 4, 407-413.

101. K. Fukumoto, M. Yoshizawa and H. Ohno, *J. Am. Chem. Soc.*, **2005**, 127 (6), 2398-2399.

102. J. Kagimoto, K. Noguchi, K. Murata, K. Fukumoto, N. Nakamura and H. Ohno, *Chem. Lett.*, **2008**, 37 (10), 1026-1027.

103. W. Ogihara, M. Yoshizawa and H. Ohno, *Chem. Lett*, **2004**, 33 (8), 1022-1023.

104. M. Smiglak, C. C. Hines and R. D. Rogers, *Green Chem.*, **2010**, 12, 491-501.

105. N. J. Bridges, C. C. Hines, M. Smiglak and R. D. Rogers, *Chem. Eur. J.*, **2007**, 13 (18), 5207-5212.

106. R. Kalb, W. Staber, M. Schelch, M. Kotschan, R. Hermann and W. Wesner, US Patent 0251759, **2008**.

107. M. Smiglak, J. D. Holbrey, S. T. Griffin, W. M. Reichert, R. P. Swatloski, A. R. Katritzky, H. F. Yang, D. Z. Zhang, K. Kirichenko and R. D. Rogers, *Green Chem.*, **2007**, 9, 90-98.

108. H. H. Bosamia, *MSci Research Report, Imperial College London*, **2010**.

109. V. Farmer and T. Welton, *Green Chem.*, **2002**, 4, 97-102.

110. M. J. Earle, C. M. Gordon, N. V. Plechkova, K. R. Seddon and T. Welton, *Anal. Chem.*, **2007**, 79, 758-764.

111. M. J. Earle, J. M. S. S. Esperança, M. A. Gilea, J. N. Canongia Lopes, L. P. N. Rebelo J. W. Magee, K. R. Seddon and J. A. Widegren, *Nature,* **2006**, 439, 831-834.

112. M. J. Earle, S. P. Katdare and K. R. Seddon, *Org. Lett.*, **2004**, 6 (5), 707-710.

113. R. M. Lynden-Bell, *Phys. Chem. Chem. Phys.*, **2010**, 12, 1733-1740.

114. K. J. Fraser, E. I. Izgorodina, M. Forsyth, J. L. Scott and D. R. MacFarlane, *Chem. Commun.*, **2007**, 3817-3819.

115. D. R. MacFarlane, M. Forsyth, E. I. Izgorodina, A. P. Abbott, G. Annat and K. Fraser, *Phys. Chem. Chem. Phys.*, **2009**, 11, 4962-4967.

116. H. Tokuda, K. Hayamizu, K. Ishii, M. A. B. H. Susan and M. Watanabe, *J. Phys. Chem. B*, **2004**, 108, 16593-16600.

117. H. Tokuda, K. Hayamizu, K. Ishii, M. A. B. H. Susan and M. Watanabe, *J. Phys Chem. B,* **2005**, 109, 6103-6110.

118. H. Tokuda, K. Ishii, M. A. B. H. Susan, S. Tsuzuki, K. Hayamizu and M. Watanabe, *J. Phys. Chem. B.*, **2006**, 110, 2833-2839.

119. S. Tsuzuki, H. Tokuda, K. Hayamizu and M. Watanabe, *J. Phys. Chem. B*, **2005**, 109, 16474-16481.

120. T. R. Griffiths, D. C. Pugh, *Coord. Chem. Rev.*, **1979**, 29, 129-211.

121. G. J. Janz and R. P. T. Tomkins, *The non-aqueous electrolytes handbook,* **1972**, Academic Press, New York.

122. L. G. S. Brooker, G. H. Keyes, R. H. Sprague, R. H. VanDyke, E. VanLare, G. VanZandt and F. L. White, *J. Am. Chem. Soc.*, **1951**, 73 (11), 5326-5332.

123. S. J. Davidson and W. P. Jencks, *J. Am. Chem. Soc.*, **1969**, 91 (2), 225-234.

124. L. I. Katzin and E. Gebert, *J. Am. Chem. Soc.*, **1954**, 76 (8), 2049-2094.

125. www.gbcscientific.com/appnotes/uv_app_note_003.pdf

126. D. A. Binder and M. M. Kreevoy, *J. Phys. Chem. A*, **1997**, 101, 1774-1781.

127. S. N. V. K. Aki, B. R. Mellein, B. R. Saurer and J. F. Brennecke, **2004**, 108 (52), 20355-20365.

128. Calculated using density of $[C_4C_1pyrr][N(Tf)_2]$ reported in: R. L. Gardas, H. F. Costa, M. G. Freire, P. J. Carvalho, I. M. Marrucho, I. M. A. Fonseca, A. G. M. Ferreira, J. A. P. J. Coutinho, *Chem. Eng. Data*, **2008**, 53 (1), 805-811.

129. M. Y. Lui, L. Crowhurst, J. P. Hallett, P. A. Hunt, H. Niedermeyer and T. Welton, *Chem. Sci.*, **2011**, 2, 1491-1496.

130. M. Pal and S. Bagchi, *J. Chem. Soc. Faraday Trans. 1*, **1985**, 81, 2323-2331.

131. P. Hemmes, J. N. Costanzo and F. Jordan, *J. Phys. Chem.*, **1978**, 82 (4), 387-391.

132. P. Hemmes, J. Costanzo and F. Jordan, *J. Chem. Soc., Chem. Commun.*, **1973**, 18, 696-697.

133. Y Marcus, *Chem. Rev.*, **1993**, 22 (6), 409-416.

134. A. Arce, M. J. Earle, S. P. Katdare, H. Rodríguez and K. R. Seddon, *Chem. Comm.*, **2006**, 2548-2550.

135. A. P. Abbott, R. C. Harris and K. S. Ryder, *J. Phys. Chem. B*, **2007**, 111 (18), 4910-4913.

136. C. Chiappe, D. Pieraccini and P. Saullo, *J. Org. Chem.*, **2003**, 68 (17), 6710-6715.

137. G. Ranieri, *Ph. D Thesis, University of London*, **2009**.

138. www.blueleafsoftware.com/Products/Dagra/LinearInterpolationExcel.php

139. E. A. S. Cavell, *J. Chem. Soc.*, **1958**, 4217-4222.

140. E. A. S. Cavell and J. A. Speed, *J. Chem. Soc.*, **1960**, 1453-1457.

141. J. A. Leary and M. Kahn, *J. Am. Chem. Soc.*, **1959**, 81 (16), 4173-4176.

142. T. Takamuku, Y. Honda, K. Fujii and S. Kittaka, *Analyt. Sci.*, **2008**, 24, 1285-1290.

143. W. Li, Z. Zhang, J. Zhang, B. Han, B. Wang, M. Hou and Y. Xie, *Fluid Phase Equilib.*, **2006**, 248, 211-216.

144. S. Dorbritz, W. Ruth and U. Kragl, *Adv. Synth. Catal.*, **2005**, 347, 1273-1279.

145. J. N. Canongia Lopes, M. F. Costa Gomes, P. Husson, A. A. H. Pádua, L. P. N. Rebelo, S. Sarraute and M. Tariq, *J. Phys. Chem. B*, **2011**, 115, 6088-6099.

146. D. C. da Silva, I. Ricken, M. A. Do. R. Silva and V. G. Machado, *J. Phys. Org. Chem.*, **2002**, 15, 420-427.

147. K. Herodes, I. Leito, I. Koppel and M. Rosés, *J. Phys. Org. Chem.*, **1999**, 2, 109-115.